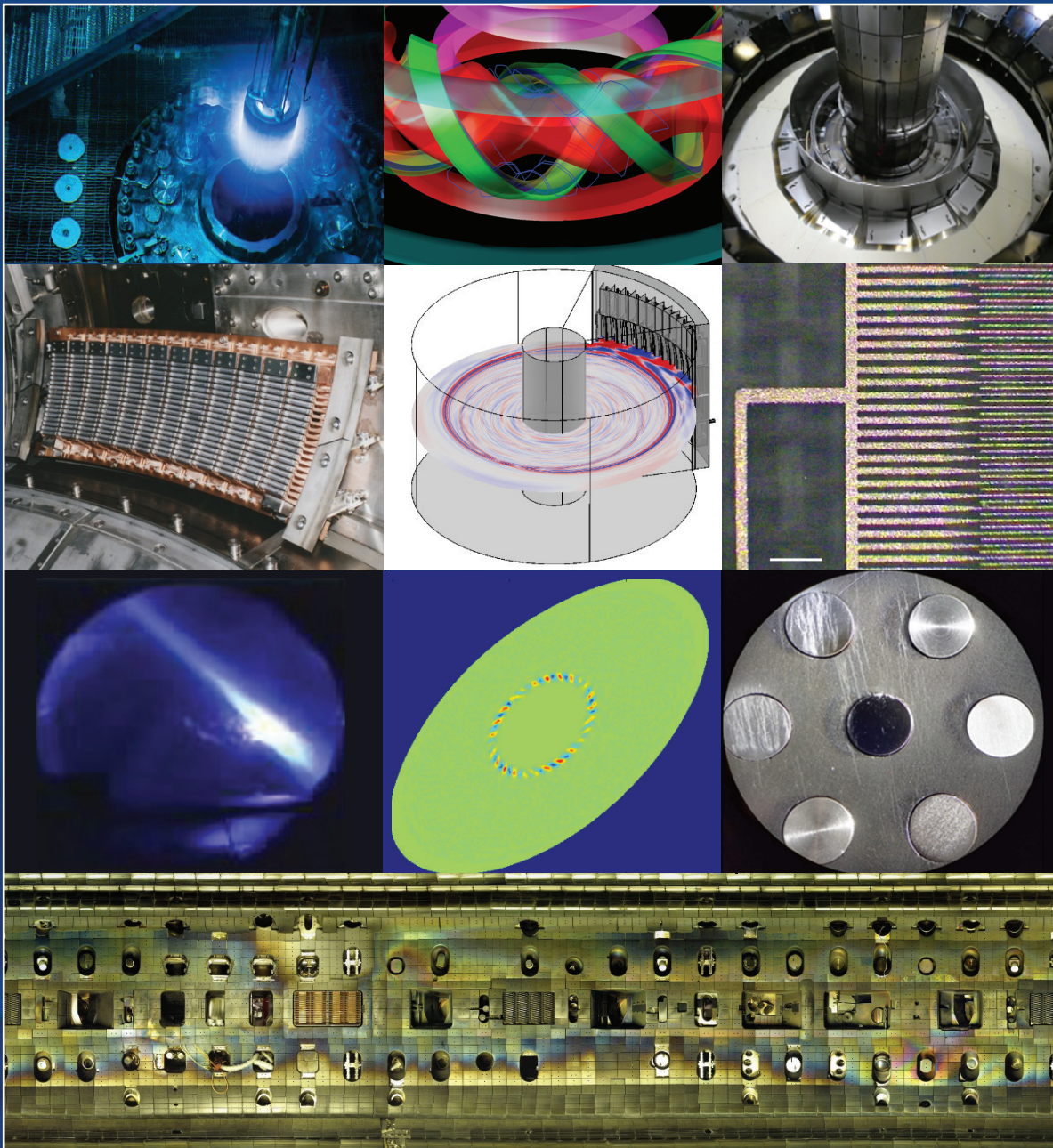


SPECIAL REPORT ON THE OCCASION OF THE 40TH ANNIVERSARY OF THE JAPAN/U.S. FUSION RESEARCH COLLABORATION

Summary Report for the Period 2011-2020
Japan/U.S. Coordinating Committee on Fusion Energy



Under Agreement between the Government of Japan and the Government of the United States of America on Cooperation in Research and Development in Energy and Related Fields

PREFACE

For forty years, Japan and the United States of America have worked together to pursue research and development of fusion energy science and technology. Fusion energy R&D is a multi-disciplinary field focused on the science and technology needed to develop an energy source based on a controlled thermonuclear fusion reaction. Fusion occurs when two nuclei combine to form a new nucleus. It is a fundamental source of energy in the universe and one that occurs in our Sun and other stars. Creating conditions for fusion on Earth involves generating and sustaining a plasma at sufficiently high temperatures so that ions can overcome repulsive electrostatic forces, fuse together, and release energy. Since fusion can be an attractive source of green energy for the world, Japan and the US have maintained productive collaborations dating back to discussions between Prime Minister Fukuda and President Carter held in 1977. These discussions led to a governmental agreement and the formation of the Coordinating Committee for Fusion Energy (CCFE) in 1979.

This 40th Anniversary report is being published to commemorate another decade of successful cooperation under the CCFE. Two previous reports were published to celebrate the 20th and 30th anniversaries. As before, this report contains many summaries of the activities and scientific results produced during the last decade. This progress has only been possible because of the strong alliance between the governments of Japan and the US, the continued support for fusion energy R&D from both sides, and because of the combined efforts of innovative and hard-working researchers from both countries.

This type of multi-level cooperation is an exceptional example of the mutually beneficial relationship that can be sustained when two of the world's most successful democracies work together to address a grand challenge for humankind. The value and importance of strong US-Japan cooperation is evident not only in ongoing bilateral activities, but also in the multi-lateral activities both parties participate in with other international partners, such as the ITER Project that is being pursued together with the European Union, China, India, Korea, and Russia, and the JT-60 Super Advanced Facility supported under the Broader Approach Agreement.

We hope this report will convey the breadth of ongoing activities managed under the CCFE, the value these collaborations bring to the worldwide pursuit of fusion energy, and the importance of continuing this long-standing collaboration as the world endeavors to establish sustainable sources of energy.

Contents

CHAPTER 1 Introduction	1
1.1 Overview of the Program	1
1.2 Executive Summary of the Categories	1
1.2.1 Fusion Technology Planning Committee (FTPC)	1
1.2.2 Fusion Physics Planning Committee (FPPC)	1
1.2.3 Joint Institute for Fusion Theory (JIFT).....	1
1.2.4 DIII-D	2
1.2.5 TITAN/PHENIX/FRONTIER.....	2
1.2.6 HFIR	2
1.3 Statistics.....	2
CHAPTER 2 Fusion Technology Planning Committee (FTPC)	5
2.1 Objectives.....	5
2.2 Activities	5
2.3 Administration	5
CHAPTER 3 Fusion Physics Planning Committee (FPPC)	19
3.1 Objectives.....	19
3.2 Activities	19
3.3 Administration	19
3.4 Accomplishments and Highlights	20
3.4.1 Steady-State Operation.....	20
3.4.2 MHD and High Beta	26
3.4.3 Confinement.....	33
3.4.4 Diagnostic Collaborations	48
3.4.5 High Energy Density Science (HEDS)	55
CHAPTER 4 Joint Institute for Fusion Theory (JIFT).....	67
4.1 Objectives	67
4.2 Activities	67
4.3 Administration	68
4.4 Accomplishments and Highlights	69

CHAPTER 5 DIII-D.....	82
5.1 Objectives	82
5.2 Activities	82
5.3 Administration	82
5.4 Accomplishments and Highlights	82
CHAPTER 6 US-Japan Joint Research Projects Overview.....	88
6.1 Objectives, Research Subjects, and Facilities.....	88
6.2 Administration and Operations Management.....	91
CHAPTER 7 HFIR Collaborative Research	106
7.1 Objectives	106
7.2 Accomplishments and Highlights	106

CHAPTER 1 Introduction

1.1 Overview of the Program

The Japan/US Fusion Research Collaboration is coordinated by Coordination Committee for Fusion Energy (CCFE). The CCFE meetings have been held annually via web meetings, where current status of Japanese and the US fusion programs, technical highlights of cooperative activities for the categories of Fusion Technology Planning Committee (FTPC), Fusion Physics Planning Committee (FPPC), Joint Institute for Fusion Theory (JIFT), DIII-D, Joint Research Project (presently FRONTIER), and HFIR, and other activities were reported and reviewed, and the activities of the next fiscal year were proposed and approved. The activities of the six categories from 2010 to 2019 are summarized as follows.

1.2 Executive Summary of the Categories

1.2.1 Fusion Technology Planning Committee (FTPC)

The FTPC (Fusion Technology Planning Committee) is responsible for organizing US-Japan collaboration on the research of fusion technology aiming at realization of fusion energy. The topical areas represented are: 1) Superconducting Magnets, 2) Structural Materials, 3) Plasma Heating Related Technologies, 4) Blankets, 5) In-Vessel/High Heat Flux Materials and Components, and 6) Others, which includes Power Plant Studies and Related Technologies. During the Japan Fiscal Years (JFY) of 2010-2019, which concluded in 2020, 32 workshop events were held: 15 in the US and 17 in Japan. During these events, there were 128 personnel exchanges: 69 to the US and 59 to Japan. There were 75 exchanges performed to pursue R&D: 36 to the US and 39 to Japan.

1.2.2 Fusion Physics Planning Committee (FPPC)

The FPPC (Fusion Physics Planning Committee) is responsible for organizing US-Japan collaboration on the experimental research of fusion plasma physics. The topical areas represented are: 1) Planning, 2) Steady-state Operation, 3) MHD and High Beta, 4) Confinement, 5) Diagnostics, and 6) High Energy Density Science. During JFY 2010-2019, 67 workshop events were held: 37 in the US and 30 in Japan. During these events, there were 361 personnel exchanges: 159 to the US and 202 to Japan. There were 195 exchanges performed to pursue R&D: 126 to the US and 69 to Japan.

1.2.3 Joint Institute for Fusion Theory (JIFT)

The Joint Institute for Fusion Theory (JIFT) is responsible for: (1) advancing the theoretical understanding of plasmas with special emphasis on stability, equilibrium, heating, and transport in magnetic fusion systems; and (2) developing fundamental theoretical and computational tools and concepts for predicting nonlinear plasma evolution. During JFY 2010-2019, 38 workshop events were held: 18 in the US and 20 in Japan. During these events, there were 200 personnel exchanges: 90 to the US and 110 to Japan. There were 87 exchanges performed to pursue R&D: 47 to the US and 40 to Japan.

1.2.4 DIII-D

Collaborative activities on the DIII-D program are focused on establishing the scientific basis for the optimization of the tokamak for fusion energy, using a non-circular cross-section plasma with high triangularity, double-null divertor configuration, and various current drive systems. Research has focused on several areas including advanced tokamak physics, divertor properties, ELM-free operation, high beta physics and control, electron cyclotron heating and current drive, diagnostics development, and tokamak stability. These collaborations provided input for planning the research programs on JT-60SA. During JFY 2010-2019, the DIII-D Steering Committee met annually to review past exchange and develop a proposal for the next fiscal year. The collaboration included 20 exchanges to the US.

1.2.5 TITAN/PHENIX/FRONTIER

The US-Japan Joint Research Projects have decades of rich and successful history contributing to advancing fusion materials science and enabling technologies. These include a series of six-year projects such as the Tritium, Irradiation and Thermofluid for America and Nippon (TITAN) project that concluded in JFY-2012, the PFC Evaluation by Tritium Plasma, Heat and Neutron Irradiation Experiments (PHENIX) project that concluded in JFY-2018, and the on-going FRONTIER project, which address the scientific questions related to the neutron and hydrogen isotope interactions with the interfacial and transition elements in advanced PFCs. During JFY 2010-2019, 37 workshop events were held: 26 in the US and 11 in Japan. During these events, there were 180 personnel exchanges: 135 to the US and 45 to Japan. There were 146 exchanges performed to pursue R&D: 93 to the US and 53 to Japan.

1.2.6 HFIR

The goal of this collaboration is to jointly design, conduct, and evaluate irradiation experiments in the High Flux Isotope Reactor (HFIR) at Oak Ridge National Laboratory to investigate the irradiation response of structural materials that are of interest to Japan and U.S. During JFY 2010-2019, the HFIR Steering Committee met annually to review past exchange and develop a proposal for the next fiscal year. The collaboration included 24 exchanges to the US.

1.3 Statistics

The number of workshops and assignments by workshop participation and collaboration are summarized for the cases from Japan to the US (Figure 1) and from the US to Japan (Figure 2).

1.4 Publications

All the publications identified in this document are compiled in electronic format and are available at the following web address: <https://science.osti.gov/fes/community-resources>

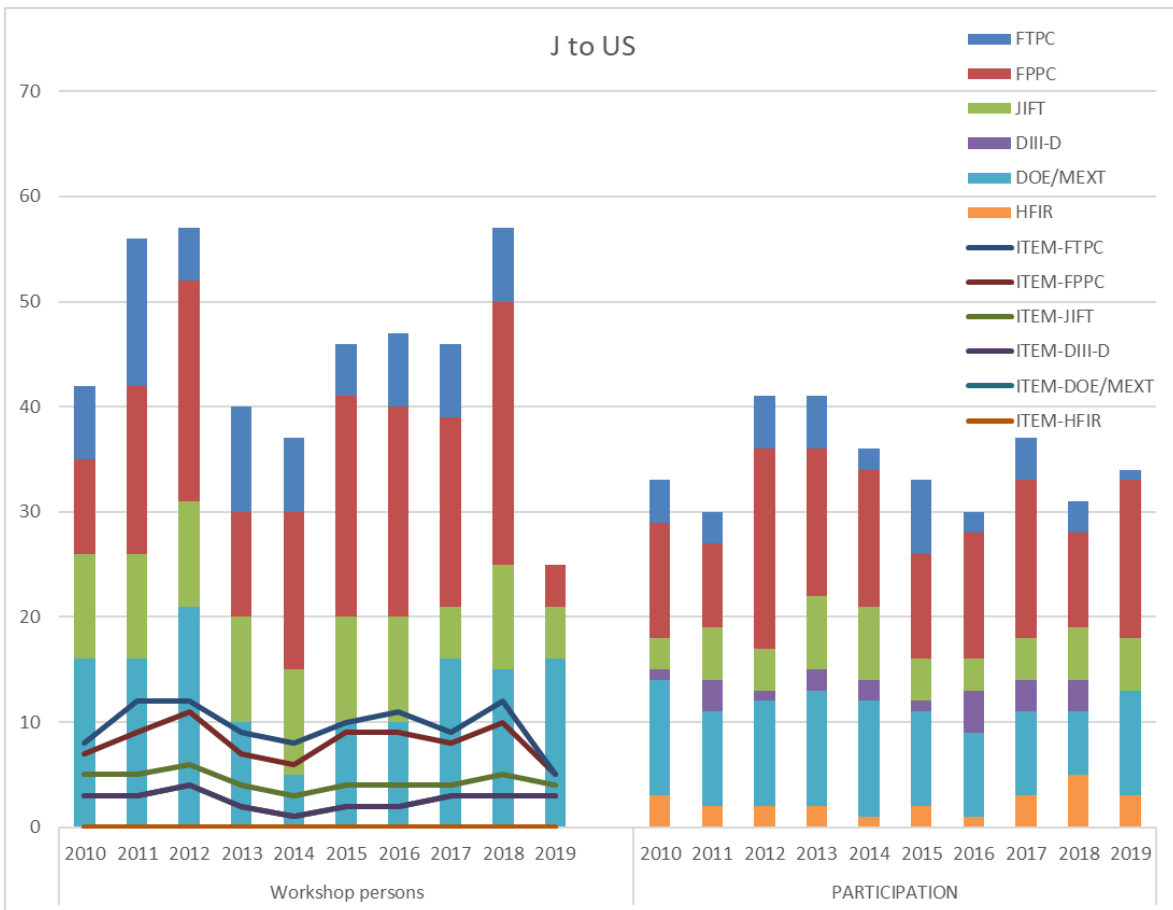


Figure 1. Annual changes in the number of workshops held in the US, number of assignments for the workshop participation and collaboration from the US to Japan for the six categories.

ITEM : workshop held in the US

Workshop persons : assignment for workshop participation

PARTICIPATION : assignment for collaboration

DOE/MEXT : TITAN (FY2010-2012), PHENIX (FY2013-FY2018), FRONTIER (FY2019)

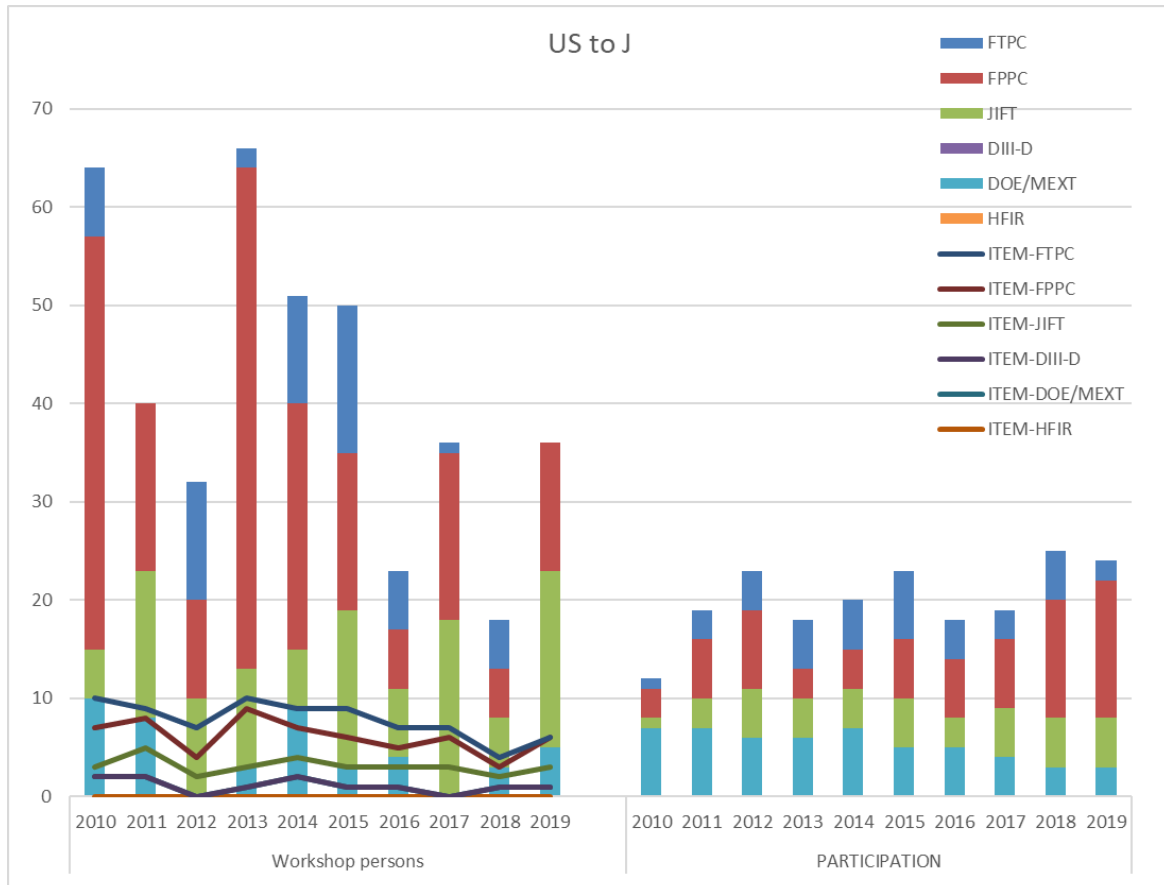


Figure 2. Annual changes in the number of workshops held in Japan, number of assignments for the workshop participation and collaboration from the US to Japan for the six categories.

ITEM : workshop held in Japan

Workshop persons : assignment for workshop participation

PARTICIPATION : assignment for collaboration

DOE/MEXT : TITAN (FY2010-2012), PHENIX (FY2013-FY2018), FRONTIER (FY2019)

CHAPTER 2 Fusion Technology Planning Committee (FTPC)

2.1 Objectives

The FTPC (Fusion Technology Planning Committee) is responsible for organizing US-Japan collaboration on the research of fusion technology aiming at realization of fusion energy. After the separation of the FTPC and FPPC (Fusion Physics Planning Committee) in 1991, the topics represented in FTPC are 1) Superconducting Magnets, 2) Structural Materials, 3) Plasma Heating Related Technologies, 4) Blankets, 5) In-Vessel/High Heat Flux Materials and Components, and 6) Others, which includes Power Plant Studies and Related Technologies. The FTPC also includes two formal Annexes on fusion materials research, one under the MEXT/DOE agreement and another under the QST/DOE agreement. The important and diverse technologies required to enable fusion energy deployment are discussed together in these subsections.

2.2 Activities

The collaborations are carried out by workshops and exchange visits of researchers, keeping in mind that the number of the collaboration places should be balanced in US and Japan as much as possible. There were also several remote collaboration activities using tele-video system and e-mail as necessary, although the focus remained on in-person collaboration where possible. During the Japan fiscal years of 2010-2019 under US-Japan collaboration, 32 workshop events were held: 15 in the US and 17 in Japan. During these events, there were 128 personnel exchanges: 69 to the US and 59 to Japan. Across the themes related to FTPC, there were 75 exchanges performed to pursue R&D: 36 to the US and 39 to Japan.

2.3 Administration

The present steering committee of FTPC consists of a key-person from the US representing the DOE, and two key-persons from Japan, representing QST and NIFS respectively. The steering committee of FTPC is also attended by the key-persons of the joint materials projects and the few relevant observers from universities and institutes both in US and Japan, according to necessity. The steering committee meeting of FTPC is usually held by a tele-video system with complementary e-mails once a year.

US/JA Collaboration on Electron Cyclotron Heating and Current Drive Technology

Category: FTPC – Plasma Heating

Name: R. Temkin / K. Sakamoto

Affiliation: MIT / QST

Summary: Japan and the United States have had an extremely productive collaboration on the technology needed for electron cyclotron heating (ECH) and current drive (ECCD) of plasmas. Joint technology activities have included research on the gyrotrons, transmission lines and launchers. Major accomplishments include joint work on the early design of the ECH/ECCD system for ITER; theoretical analysis of transmission line components; and testing of losses in transmission line components at both low and high microwave power levels. These important advances have been discussed and analyzed in the very useful US/JA annual coordination meetings. Results of joint work are well documented in journal articles and conference publications. In this short report, we can include only a few representative examples of the important joint research.

Examples: The ITER project requires a system of 24 170 GHz gyrotrons operating in pulses of up to one hour. The QST gyrotron laboratory was the first in the world to develop a true 1 MW gyrotron at 170 GHz and generously provided time on the gyrotron test transmission line for testing of components made in the US. Figure 1 shows the test at QST of transmission line components built in the US by General Atomics, such as waveguides, miter bends and polarizers¹⁾. Such testing was critical to progress in the US ITER program.



Figure 1. Transmission Line test set-up at QST, where a 1MW, 170 GHz gyrotron, located in the large enclosure at the back wall, is used to test components on the transmission line

Joint work between the US and JA teams also included research on novel concepts for transmission line components for application in ITER and in the US and JA domestic

programs. Figure 2 shows the testing of novel components at NIFS in Japan using a 154 GHz gyrotron.²⁾

Fruitful collaborations have also occurred in basic research on transmission lines, including theory and experiment of higher order modes and the losses at miter bends. The set-up for low power testing of transmission line components at MIT is shown in Figure 3.³⁾

Many additional, important results can be found in the extensive list of joint publications.

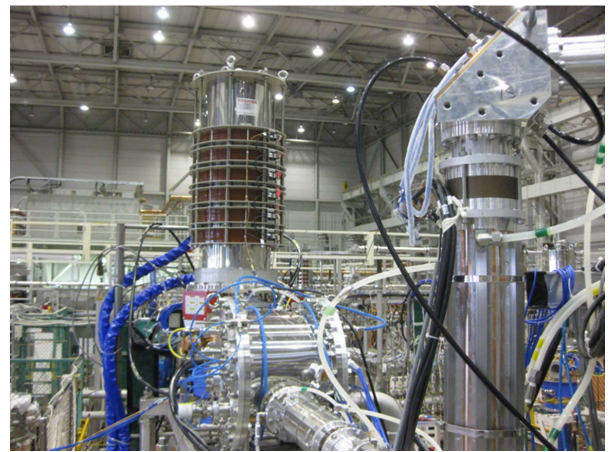


Figure 2. Innovative beam position monitor in a miter bend (upper right) under test with a 154 GHz gyrotron (center) at LHD²⁾.

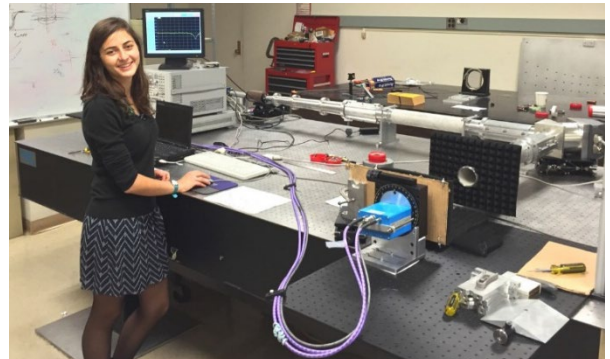


Figure 3. A miter bend polarizer for the ITER ECH transmission line under test with a vector network analyzer at MIT³⁾.

¹⁾ Y. Oda, K. Kajiwara, K. Takahashi et al., J. IR MM THz Waves Vol. 31, pp. 949–957 (2010).

²⁾ T. Shimozuma, S. Kubo, Y. Yoshimura, et al., J. Micr. Power & Electr. Energy Vol. 43, No. 1, pp. 60 70 (2009).

³⁾ S. K. Jawla, M. A. Shapiro, H. Idei et al., IEEE Trans. Plasma Sci. Vol. 42, pp. 3358 3364 (2014)

Collaboration Work on RF Technology

General Atomics (GA) and the National Institutes for Quantum and Radiological Science and Technology (QST) have worked together for over a decade under the US-Japan Fusion Collaboration Program (Figure 1). The organizations have jointly conducted a number of experiments to help advance microwave transmission line technology for electron cyclotron heating (ECH) systems in fusion devices. The collaborative testing campaigns have produced a number of important discoveries in the area of high power microwave transmission. Advanced microwave components such as waveguides, polarizers, a power monitor and an expansion joint have been tested and verified at QST's gyrotron facility, as well as novel diagnostics used to determine the power in a transmission line.

A built polarizer miter bends for 170 GHz (Figure 2a) is to use transforming the polarization of an incoming signal to any desired output polarization. In 2010 and 2014, the performance of these polarizers was tested using the QST transmission line and gyrotron. The results showed that the components can be used to effectively change the polarization of the signal, and furthermore that the heating of the polarizer mirror depends on the orientation of the grooves with respect to the incoming polarization. Power monitors in high-power waveguide transmission lines have been used for three main purposes: (1) monitoring the performance of the microwave source, (2) protecting the microwave source by turning it off when significant amounts of power traveling back toward the source are detected; and (3) determining the delivered power. In 2014, two types of a bend, a power monitor miter

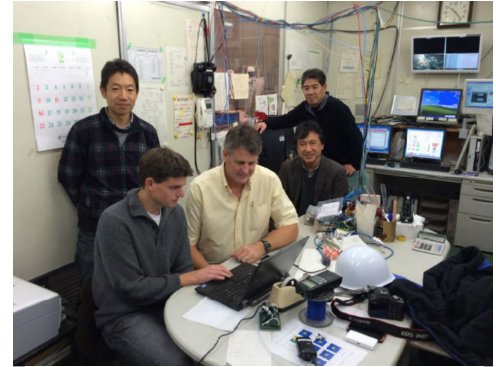


Figure 1. Control room of the QST gyrotron testing facility during a collaborative campaign in 2014. Pictured in the photo are Ken Kajiwara, Koji Takahashi, and Keishi Sakamoto from QST, and James Anderson and Howard Grunloh from GA.

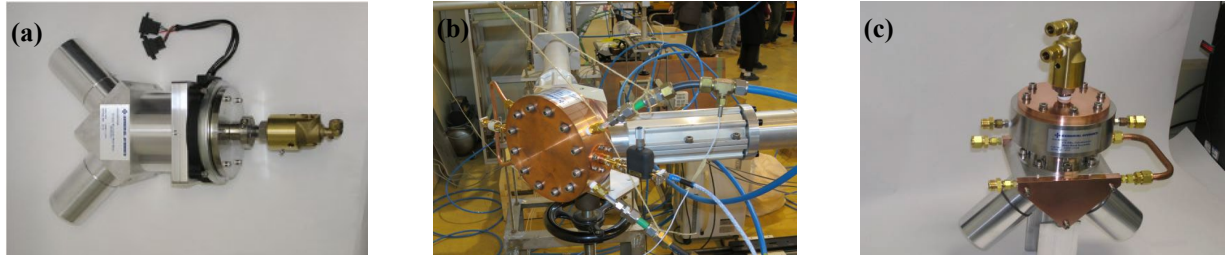


Figure 2. 170-GHz polarizing rotator miter bend (a), PMMB installed in the test line at QST's Naka facility in 2014 (b) and CMB showing separate cooling lines for the miter bend housing, the stainless steel isolation, and the mirror (c).

bend (PMMB) and a calorimetric miter bend (CMB) were installed and tested in the QST transmission line with the ITER prototype gyrotron (Figure 2b~c). The results showed the expected directivity of the PMMB and surface resistance of the copper mirror.

Waveguide components such as a single 4.2-m waveguide assembly and an expansion joint, which is necessary to account for thermal expansion in a transmission line, are installed in QST's gyrotron facility as shown in Figure 3. Calorimetric measurements were taken of the part, which is water cooled. The measurements were used to provide key information to ITER on realistic power absorption in transmission lines. This information was used to help create the technical requirements for ITER's ECH transmission system.



Figure 3. The arrangement of water-cooled waveguides, including the 4.2-m waveguide assembly and the expansion joint, in the transmission line.

Non-inductive Current Drive on TST-2: Personnel and Technology Exchange from US to Japan

Category: FTPC – Plasma Heating

Names: C. Moeller/Y. Takase

Affiliations: General Atomics/University of Tokyo

For the realization of a spherical tokamak, a method of non-inductive start up is essential, since there is no room for a solenoid on the center post. The TST-2 spherical tokamak was built for the purpose of testing startup current drive schemes in the lower hybrid (LH) range of frequencies

The first experiments used a 400 kW, 200 MHz RF source and the Comb Line Antenna, originally used on the JFT2-M tokamak for fast wave current drive. The antenna, shown in Figure 1, was developed by GA as part of an earlier collaboration. It did drive significant current, but indirectly through mode conversion to the LH wave, an inefficient process.

Therefore, a new antenna, the Capacitively Coupled Comb Line antenna (CCCL), shown in Figure 2, was developed at GA that launched LH waves directly and drove current more efficiently than the JFT2-M antenna. It was also much more effective than a 4 waveguide “Grill” that was tried.

Ray tracing analysis suggested that rays launched from the outside do not reach the center directly, whereas rays launched from above the plasma might reach the center, so a top version was designed and built at GA, shown in Figure 3. There is evidence of improved efficiency once a plasma is established.



Figure 3. The radial top launch CCCL antenna, inverted.

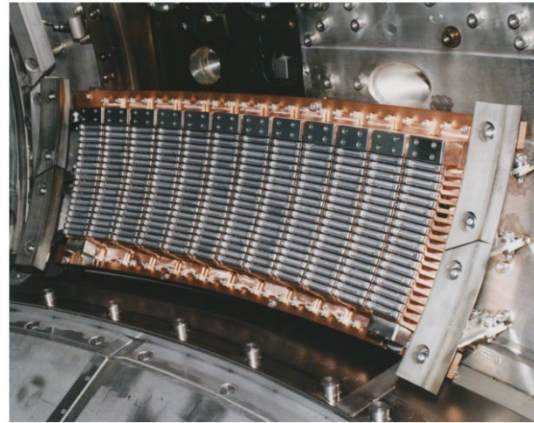


Figure 1. The antenna, used for the first experiments.

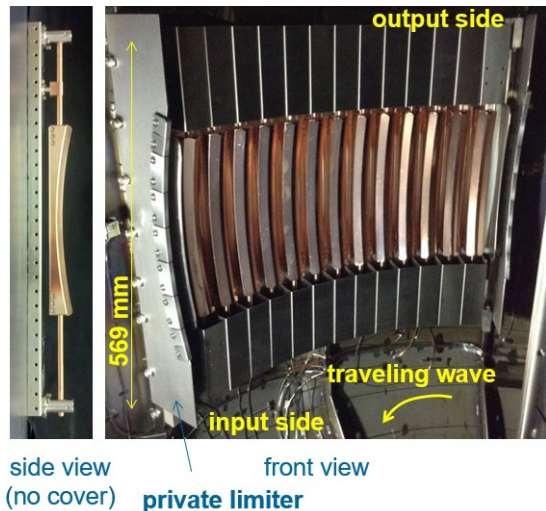


Figure 2. The CCCL antenna, with a side view of a fed element with inductive shields removed.

The antennas have contributed a great deal to the experimental program at TST-2. Below is a list of publications of research performed using those antennas.

For references, see the compiled list of publications.

Plasma-Material Interaction I: Personnel Exchanges From Japan To US

Category: FTPC- Materials

Name: R. Doerner/M. Miyamoto

Affiliation: UCSD/Shimane Univ.

A critical plasma-material interaction (PMI) issue is the retention of fuel atoms within the surrounding materials. If this value is too large, achieving tritium self-sufficiency in a future reactor may be compromised. To better understand this issue, the collaboration focused on the effects of mixed-species (D & He) plasma on retention in tungsten plasma-facing surfaces. With an eye towards ITER, the influence of Be impurities seeded into the plasma was also investigated.

The addition of He to D plasma was known to dramatically reduce the uptake of D in W. The reason for this reduction was examined using TEM cross-section analysis¹⁾ of samples exposed in PISCES-A. A dense network of nano-bubbles was seen to form in the near surface (~ 40 nm), Figure 1, when the He was present in the plasma and was not observed in the absence of He. The nano-bubbles formed interconnected pathways to the surface (Figure 2) which could account for the reduced D migration into the bulk W. W samples exposed to similar (D/5%He) plasma, however containing 0.8% Be impurities, in PISCES-B, did not show any reduction in D retention¹⁾, but did show the formation of thin (few nm) Be surface layers which prevented the nano-bubble formation.

TEM was also used to examine the microstructure of W exposed at higher temperature, 1123 K, to mixed plasma (D/2%He/0.2%Be). In this case, the Be concentration was small enough to allow the He to interact with the W surface and nano-scale structures formed in the surface²⁾ (so-called W fuzz).

The microstructure of deposits formed during D/He/Be plasma exposure of W were also investigated³⁾. There appeared to be little impact on the D content in the deposits, whether or not, He was included. Small nano-bubbles were observed scattered throughout the depth of the deposits when He was present, but since the formation included the co-deposition with D, and not the diffusion of D through the deposit, they were not beneficial effects from the nano-bubble formation.

Other topics, centered around the use of the PISCES laser systems, were also included in the collaborations. One involved using a laser to vaporize the surface of plasma exposed samples, simulating the effects of vapor shielding during transient power loads to PFMs. The results showed low-Z (Be) vapor clouds led to significant plasma cooling, whereas high-Z (W or Mo) clouds did not⁴⁾. LIBS measurements were also performed where small amount of Re (0.5 at.%) and Ta (2 at.%) in W were detected. These LIBS measurements aimed at providing proof-of-principle experiments showing the usefulness of LIBS as a diagnostic for determining the level of transmutation

elements in activated tungsten used in burning plasma environments

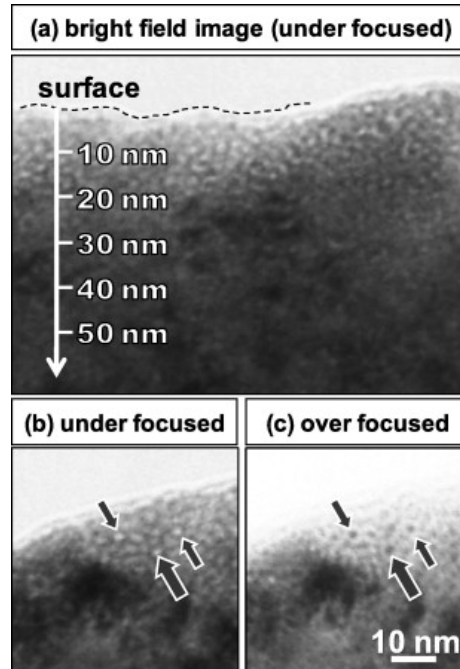


Figure 1. TEM image of the cross-section of the He nano-bubble network formed at the surface of a W sample exposed at 573 K to a mixed D/5% He plasma.

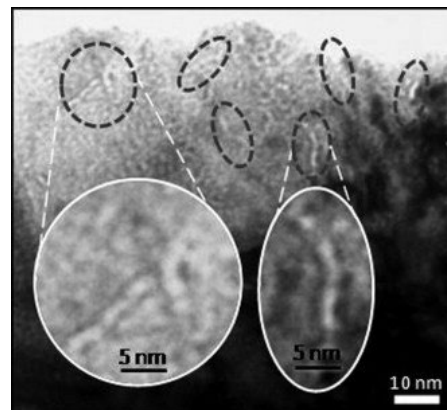


Figure 2. TEM cross-sections show He nano-bubbles forming inter-connected pathways back toward the surface in W samples exposed at 773 K during D/5% He plasma.

¹⁾ M. Miyamoto, D. Nishijima, et al., J. Nucl. Mater. 415 (2011) S657.

²⁾ K. Tokunaga, M.J. Baldwin et al., J. Nucl. Mater. 442 (2013) S313.

³⁾ M. Miyamoto, D. Nishijima, et al., Nucl. Mat. and Energy 12 (2017) 633.

⁴⁾ K. Isono, D. Nishijima et al., Nucl. Mat. and Energy 12 (2017) 278.

Plasma-Material Interaction II: Personnel Exchanges From US To Japan

Category: FTPC- Materials

Name: D. Nishijima/M. Tokitani

Affiliation: UCSD/NIFS

Plasma-material interaction (PMI) is a key factor to determine the performance of a nuclear fusion device. Thus, the following PMI-related issues were mainly addressed through personnel exchanges from US (the PISCES group at UCSD) to Japan: (1) response of tungsten (W) surfaces to ELM (edge localized mode)-like pulsed plasma bombardment, (2) in-situ LIBS (laser-induced breakdown spectroscopy) analysis of plasma-facing surfaces, and (3) hydrogen isotope (deuterium: D) retention in RAFM (reduced-activation ferritic/martensitic) steels.

Since W is the primary candidate for plasma-facing materials (PFMs), in particular, in the divertor, response of W to ELM-like pulsed plasma bombardment was investigated. Sequential exposures of W samples to steady-state and then pulsed (~0.5 ms) plasmas were performed in the PISCES-A linear plasma device at UCSD and a magnetized coaxial plasma gun at University of Hyogo¹⁾. Surface cracks appeared on samples containing D blisters or nano-sized He bubbles following 10 shots at ~0.5 MJ/m² per shot, while a mirror-polished sample with no pre-plasma exposure did not show cracks after similar transient exposures. This means that the energy density threshold for surface cracking is lowered by the existence of D blisters and He bubbles. On the other hand, He-induced fuzzy surfaces were found to exhibit a better resistance to surface cracking, while arcing was prone to occur (Figure 1).

An in-situ LIBS system was developed on the Heliotron-DR helical device in Kanazawa University based on expertise in PISCES. The temperature dependence of the D retention in W co-deposits (D/W), measured with the developed system, agreed well with available literature data. It was also found that D/W increased with N₂ injection, which was caused by the increased surface blistering.

For the possible use of RAFM steels as PFM in future fusion devices, D retention properties of various RAFM steels (CLF-1, Eurofer, F82H, and Rusfer) were explored. First, the RAFM steels were exposed to pure D plasma in PISCES-A²⁾. It was found that there was a large difference (up to ~30x) in the D retention between the RAFM steels. The incident ion fluence, ϕ_D , dependence of the D retention exhibited a peculiar, counterintuitive feature: the D retention decreases with an increase in ϕ_D from $2 \times 10^{23} \text{ m}^{-2}$ to $1 \times 10^{25} \text{ m}^{-2}$. Surface analyses were conducted at UCSD and NIFS, and revealed that a Cr-rich surface layer (Figure 2) was formed during outgassing at 773 K

for 1 h before plasma exposure. The D retention in the RAFM steels was then found to depend on the Cr concentration in the surface layer.

Subsequently, impact of seeded plasma impurities (He, Ar, and N₂) on the D retention in the RAFM steels was studied³⁾. It was found that He and Ar seeding to D plasma reduced the D retention, while N₂ seeding resulted in a significant increase of the D retention. This can be caused by the formation of a N-rich surface layer observed with surface analyses, overriding the effect of a Cr-rich surface layer.

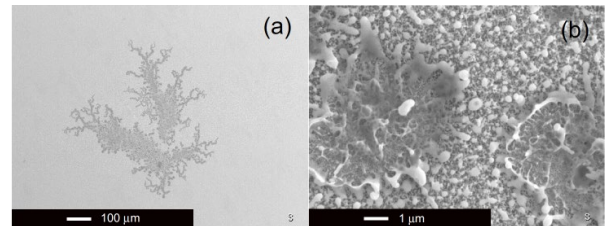


Figure 1. (a) Arc tracks on a W fuzzy surface, and (b) a magnified image of (a) clearly shows the melting of W fuzz.

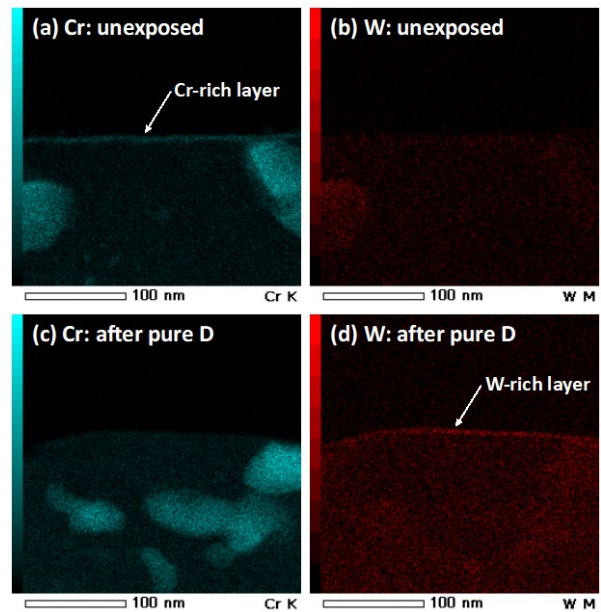


Figure 2. Cross-sectional EDX elemental mapping images of CLF-1 samples: (a), (c) Cr and (b), (d) W. (a), (b) an unexposed surface and (c), (d) a surface after pure D plasma exposure.

¹⁾ D. Nishijima, Y. Kikuchi et al., Fusion Science and Technology 60 (2011) 1447

²⁾ D. Nishijima, M. Tokitani et al., Phys. Scr. T171 (2020) 014005

³⁾ D. Nishijima, M. Tokitani et al., Nuclear Materials and Energy 23 (2020) 100740

US/JA 40th anniversary Collaborations to be reported at the 2020 IAEA FEC meeting

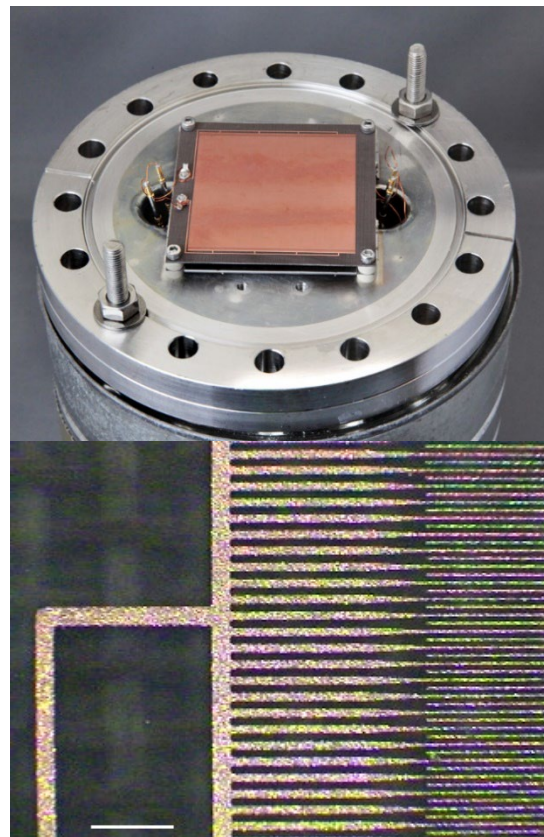
Category: FTPC – Materials/Dust

Name: C. Skinner

Affiliation: PPPL retired

Dust in fusion reactors has important safety and operational consequences and in-vessel monitoring of dust generated by plasma wall interactions will be essential for compliance with dust safety limits. The experimental detection of surface dust in fusion devices was the subject of a US/JA collaboration. Charles Skinner (PPPL) visited the Large Helical Device (LHD) at National Institute for Fusion Science (NIFS), Toki, Japan from 4 Oct 2013 – 25 Oct 2013 with Dr. Ashikawa of NIFS as the host.

A novel dust detector system, originally developed for NSTX¹⁾, was shipped to NIFS. The detector and custom-built counting electronics were first tested in the laboratory with an electronic dust simulator. After passing the tests, it was installed at LHD lower port 3.5 and again tested with an electronic simulator and artificially introduced dust. The detector was first exposed to plasmas on 10/16/13 and preliminary results showed the first dust signals from LHD. In one example LHD shot #118829, there was a transient spike in radiated power at 4.85 seconds likely due to an influx of dust particles, and the detector registered a dust signal at 5.1 s. This delay is normal for the instrument. The dust levels on LHD so far appear to be low- of order ~ng/cm²/discharge and dust signals are detected only on some discharges. The low dust level is encouraging news for fusion machines with metal PFCs.



Close up of dust detector grid with 500 micron scale bar) and 5 x 5 cm dual grid dust

¹⁾“First real-time detection of surface dust in a tokamak” C. H. Skinner, et al., Rev. Sci. Instrum., 81, (2010) 10E102

Development of HTS-TSTC Conductor

Category: FTPC- Magnets

Name: M. Takayasu / N. Yanagi

Affiliation: MIT / NIFS

Developments of High-Temperature Superconductor (HTS) cable for a high field, high current fusion magnet has been carried out under a collaboration between NIFS and MIT.

MIT fabricated an HTS cable based on a Twisted Stacked-Tape Cabling (TSTC) method for REBCO superconducting tapes. The MIT TSTC sample composing of 48 REBCO-tapes of SuperOx 6 mm width was a single-turn coil of about 650 mm in diameter. The coil was a dodecagon-shape with a half-turn twist-pitch of 180 mm. Total conductor length was 3.79 m, including the terminations and the vertical current leads. The flat one-turn coil section of 1.65 m was in the high-field plane at the center of a background field magnet. NIFS tested the MIT TSTC sample using the NIFS test facility of a 13 T, 700 mm cold bore superconducting magnet with a 50 kA DC current supply. The experimental setup is shown in Figure 1a.

The sample was preliminarily charged without a background field at NIFS in September 2018. During this test, the charge current was limited to about 19 kA due to the heat generation of the facility's current lead extensions.

The high field test was performed at NIFS in January 2019. The background field was increased up to 5 T at temperatures between 12 and 19 K. Unfortunately, the sample showed quenches at much lower currents than expected, even if taking into account the uncertainty of the sample temperatures.

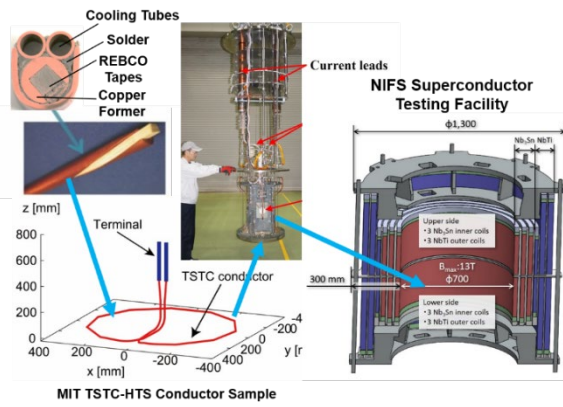


Figure 1a. Experimental setup of the MIT's TSTC-HTS conductor sample into the NIFS superconductor testing facility.

The quench current was detected by the total voltage tap VT that covered the entire cable. The quench currents gradually decreased from 19 kA without the background field to about 9 kA at 5 T. Only the voltage tap VT showed the quench, but other voltage tapes did not show any voltage increases.

It indicates that the TSTC sample quenched near the terminations. The high field sections were superconductive and did not show any quench signs.

By charging the TSTC sample with various rates of the currents, the current distribution in the TSTC conductor was investigated. Self-fields of a single turn coil around the TSTC conductor were measured with Hall sensors. The analytical results indicated that the current distribution of the TSTC conductor was uniform for a constant current of 10 kA. In contrast, the current distribution was not uniform during the ramp up and down with a ramp rate of 50 A/s.

1) T. Obana, Y. Terazaki, N. Yanagi, S. Hamaguchi, H. Chikaraishi, and M. Takayasu, "Self-field measurements of an HTS twisted stacked-tape cable conductor", Cryogenics 105 (2019) 103012.

Electromagnetic Stress Analysis on HTS Conductor Experiment

Category: FTPC- Magnets

Name: Y. Zhai / N. Yanagi

Affiliation: PPPL / NIFS

Developments of a large scale 100-kA current capacity High-Temperature Superconducting (HTS) conductor has been carried out at NIFS to apply to the helical fusion reactor, FFHR-d1. A prototype conductor sample is designed and its testing will be carried out using a 13-T magnetic field, 700-mm bore solenoid magnet at NIFS. The electromagnetic stress analysis has been carried out by PPPL for this sample using a FEM calculation code. PPPL will be involved in the joint HTS conductor test in the NIFS new test facility. PPPL contribution included EM / Stress analysis of test conductor samples in the new test facility. Long term interests include develop PPPL HTS conductors for the FNSF-ST and testing it in NIFS facility.

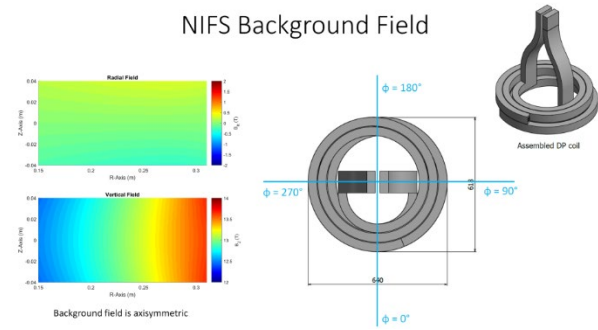


Figure 1b. SolidWorks CAD model of the NIFS HTS-STARS conductor testing sample.

Flow measurements in MTOR under the US-JA TITAN Program

Category: FTPC- Materials

Name: S. Smolentsev, T. Yokomine

Affiliation: Univ. of Calif. Los Angeles, Kyoto Univ.

Task 1-3 “*Flow Control and Thermofluid Modeling*” of the US-JAPAN “TITAN” Program (2007-2012) included experimental and computational studies of magnetohydrodynamic (MHD) flows and heat and mass transfer of electrically conducting fluids under conditions relevant to fusion blankets to support development of key blanket concepts in the US and Japan, such as Molten Salt (MS) and Dual Coolant Lead Lithium (DCLL) blankets. The US team was presented by S. Smolentsev (Task Coordinator), F-C Li, K. Messadek, N. Morley, M. Abdou, T. Sketchley, V. Naveen, J. Young, and D. Sutevski. The key participants from Japan included: T. Kunugi (Task Coordinator), T. Yokomine, Y. Ueki, K. Yuki, J. Takeuchi, M. Aoyagi, S. Satake, Y. Yamamoto, S. Ebara, and H. Hashizume.

From 2007 to 2009, the main research focus was on low electrical conductivity molten salts, such as Flibe and Flinabe, and their simulants (KOH). The experimental studies utilized MTOR (Magneto-Thermofluid Omnibus Research Facility) facility at UCLA. The experiments in MTOR addressed the most critical to all MS blankets phenomena of suppression of turbulence and degradation of heat transfer in a strong magnetic field, using advanced flow diagnostics, such as Particle Image Velocimetry and Ultrasonic Velocimetry. The theoretical efforts included DNS studies under the experimental and MS blanket conditions and development of turbulent closures for high Prandtl number MHD flows.

Starting from 2009, the research was reoriented to liquid metals, culminating in the construction of MaPLE (Magnetohydrodynamic PbLi Experiment) facility in 2011 and several pioneering experiments, in which eutectic alloy PbLi was used as a working fluid. Over the period from 2009 to the end of the program in 2012, major efforts were taken to design, construct and test the MHD lead-lithium loop, including testing and calibration of its components (EM pump, EM flow-meter, high-temperature pressure sensors) as well as development and testing of the most important loop operation procedures, such as melting PbLi, removing trapped oxygen from the melt, filling and draining the loop, pumping the liquid metal throughout the loop, and temperature control. Following the construction period, the next experimental efforts included development of high-temperature ultrasound Doppler velocimeter (HT-UDV) and addressed the most critical material compatibility issues and reduction of MHD pressure drop by insulating flow channel inserts. Other liquid metal experiments utilized the mercury loop at UCLA to study transitional phenomena from the 3D to 2D state in rectangular duct MHD flows. All experimental efforts for liquid metals were accompanied with the numerical MHD/thermofluid

computations using DNS-type codes developed during the program.

- 1) J. Doe, A. Author *et al.*, Fusion Eng. & Des., 83 (2008) 771
- 2) T. Yokomine, J. Takeuchi, H. Nakaharai, S. Satake, T. Kunugi, N. Morley, M. Abdou, “Experimental investigation of turbulent heat transfer of high Prandtl number fluid flow under strong magnetic field”, Fusion Science and Technology, 52, 625-629 (2007).
- 3) J. Takeuchi, S. Satake, T. Kunugi, T. Yokomine, N. Morley, M. Abdou, “Development of PIV technique under magnetic fields and measurement of turbulent pipe flow of Flibe simulant fluid”, Fusion Science and Technology, 52, 860-864 (2007).
- 4) J. Takeuchi, S. Satake, N. Morley, T. Kunugi, T. Yokomine, M. Abdou, “Experimental study of MHD effects on turbulent flow of Flibe simulant fluid in circular pipe”, Fusion Engineering and Design, 83, 1082–1086 (2008).
- 5) Y. Yamamoto, T. Kunugi, S. Satake, S. Smolentsev , “DNS and k- model simulation of MHD turbulent channel flows with heat transfer”, Fusion Engineering and Design, 83, 1309-1312 (2008).
- 6) Y. Ueki, T., Kunugi, N.B., Morley, M.A. Abdou, “Electrical insulation test of alumina coating fabricated by sol-gel method in molten PbLi pool”, Fusion Engineering and Design, 85, 1824-1828 (2010).
- 7) Y. Ueki, M. Hirabayashi, T. Kunugi, K. Nagai, J. Saito, K. Ara, N.B. Morley, “Velocity profile measurement of lead-lithium flows by high-temperature ultrasonic doppler velocimetry”, Fusion Science and Technology, 60, 506-510 (2011).
- 8) M. Aoyagi, Y. Inage, S. Ito, S. Ebara, Y. Ueki, K. Yuki, F.-C. Li, S. Smolentsev, T. Yokomine, T., Kunugi, T. Sketchley, M. Abdou, “Verification test of a three-surface-multi-layered channel to reduce MHD pressure drop”, Proceedings of the 8th Japan-Korea Symposium on Nuclear Thermal Hydraulics and Safety (NTHAS8), December 9-12, 2012, Beppu, Japan, N8P1089 (2012).
- 9) T. Kunugi, S. Smolentsev, T. Yokomine, F.-C. Li, Y. Ueki, K. Yuki, M. Aoyagi, T. Sketchley, M. Abdou, “Current status of TITAN Task 1-3 Flow Control and Thermofluid Modeling,” Journal of Applied Nuclear Science and Technology 5, 72-75 (2012).
- 10) S. Smolentsev, T. Kunugi, K. Messadek, T. Yokomine, J. Young, K. Yuki, Y. Ueki, T. Sketchley, F.-C. Li, N. Morley, M. Abdou, Status of TITAN Task 1-3 Flow Control and Thermofluid Modeling, Fusion Engineering and Design, 87, 777-781 (2012).
- 11) S. Smolentsev, F.-C. Li, N. Morley, Y. Ueki, M. Abdou, T. Sketchley, “Construction and initial operation of MHD PbLi facility at UCLA”, Fusion Engineering and Design, 88, 317-326 (2013).

PPPL Contribution to Japan-US Research Collaboration on Liquid Metals for Fusion Reactors

Category: FTPC – High Heat Flux Materials

Name: E. Kolemen / T. Kunugi, T. Yokomine

Affiliation: Princeton Univ. / Kyoto University

The efficiency of thermal mixing dictates the heat flux carrying capability of a free-surface liquid metal (LM). Collaborations between PPPL and Kyoto University have focused on improving thermal mixing efficiency by engineering techniques using vortex generators. Stationary vortex generators placed in the LM can enhance heat transfer. This can reduce the flow speed requirements. Mr. Koji Kusumi, a graduate student of Kyoto University under supervision of Profs. Tomoaki Kunugi and Takehiko Yokomine, visited LMX at PPPL for two separate summers during which a large number of experiments were performed over a wide range of parameters. Mr. Shoki Nakamura, a graduate student of Kyoto University under supervision of Profs. Tomoaki Kunugi and Takehiko Yokomine, also visited LMX to study thermal mixing enhancement of LM flow. They used various vortex generator array configurations to optimize the shape and configuration under varying magnetic fields, showing that a high level of mixing can be achieved. Non-dimensional scaling studies identified the parameters of importance and showed the scaling of heat transport enhancement to a reactor. The results are reported in three joint papers⁽¹⁻³⁾. Based on the experiences obtained on LMX, Mr. Kusumi has built a smaller version of LMX, called Liquid Metal FRee-surface EXperiment, at Kyoto University where he obtained further experimental data needed for his graduation as a Ph.D. of Nuclear Engineering.

With magnetic fields, LM currents can lead to MHD drag, slowing the flow and enhancing LM evaporation. Introducing electrodes to the walls and running currents through the LM can overcome this effect. To test the idea, Dr. Adam Fisher, a graduate student of Princeton University under supervision of Prof. Egemen Kolemen experimentally studied the stability of the surface waves under various MHD conditions in facilities that have unique capabilities in Japan. Dr. Fisher visited National Institute of Fusion Science (NIFS), Toki, Japan, for an extended period of time in 2019. He upgraded the Liquid Metal FRee-surface EXperiment, which he placed in the Operational Recovery Of Separated Hydrogen and Heat Inquiry-2 (Oroshhi2) facility, that allows LM experiments at 3 Tesla magnetic field, with laser diagnostics and electric current injection systems. He showed that, by injecting electrical currents into the flow, the effects of MHD drag may be eliminated and reversed, increasing the velocity by an order of magnitude. These results were presented in an invited talk and poster at the International Symposium on Liquid Metals Applications for Fusion (ISLA) in Urbana-Champaign, IL, and an oral talk at the IEEE Symposium on Fusion Engineering in Jacksonville, FL, both in 2019.

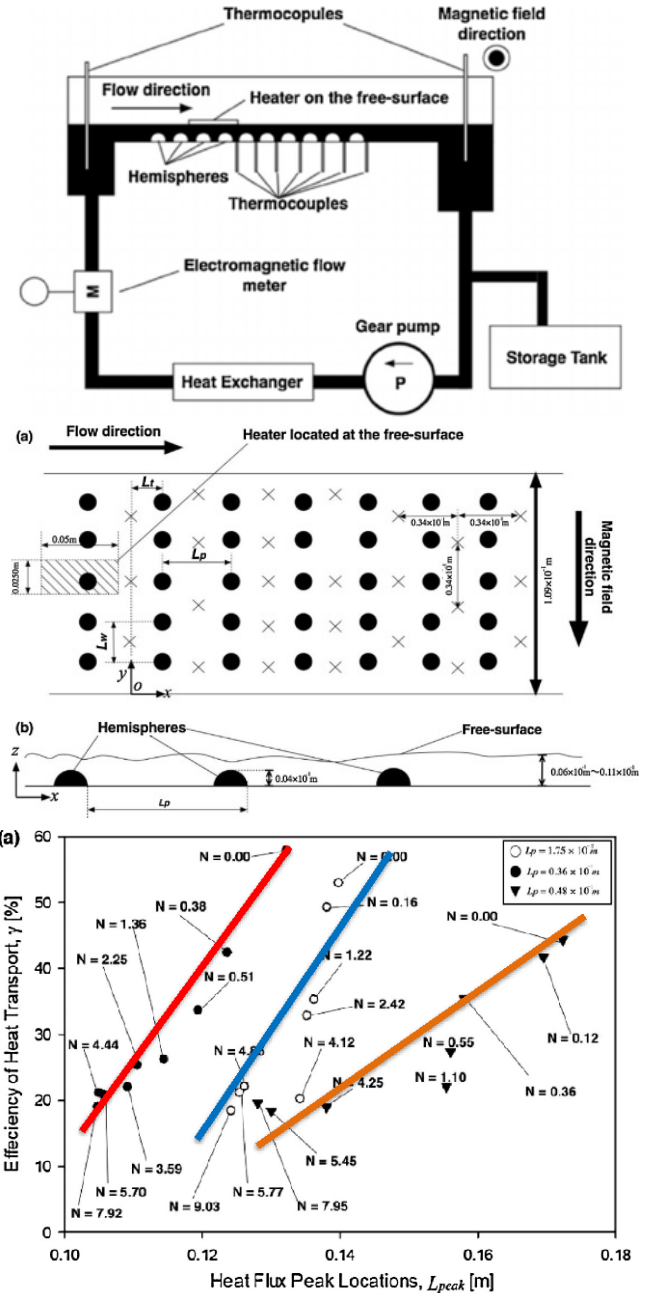


Figure 1. Top: Side view of vortex generators installed on LMX; Middle: Top view of the vortex generators; Bottom: Efficiency of heat transport as a function of obstacle size and interaction parameter.

¹⁾ Kusumi, et al., Fusion Eng. Design 109 111, 1193 (2016).

²⁾ K. Kusumi, et al., Fusion Sci. Tech. 72, 796 (2017).

³⁾ K. Kusumi, et al., Fusion Eng. Design 136, 223 (2018).

Plasma-Material Interaction: Personnel Exchanges between Japan and US

Category: FTPC- Materials

Name: N. Ashikawa /H.Y. Guo, D.Rudakov

Affiliation: NIFS/GA, UCSD

Control of plasma-material interactions (PMI) is one of the main challenges facing ITER and future magnetic fusion devices. Tungsten (W) will be used for plasma facing components (PFCs) in the ITER divertor and is a leading candidate material for PFCs in DEMO. Both bulk W and W coatings are under investigation for DEMO. The present collaboration effort involved exposures of W-on-W coatings prepared in Japan (K. Katayama, Kyushu University) and China (ASIPP). The samples were pre-characterized locally and brought to US by N. Ashikawa (NIFS) for exposure to divertor plasmas in the DIII-D tokamak operated by General Atomics (GA).

The exposures were performed in the lower divertor of the DIII-D tokamak using the Divertor Material Evaluation System (DiMES)¹⁾ with H.Y. Guo being the DiMES program manager and D. Rudakov (UCSD) serving as the DiMES experimental coordinator. Seven W button samples including two from Kyushu and two from ASIPP were loaded in a graphite holder (Figure 1) and exposed in 14 high-power ELMing H-mode discharges with up to 11 MW of Neutral Beam Injection (NBI) and 4 MW of Electron Cyclotron Heating (ECH). Three bulk W button samples were exposed alongside the W coated ones for comparison.

While the original aim of this experiment was to compare deuterium retention in the coatings versus bulk W, the most interesting results were associated with unipolar arcing and were reported at the PSI-23 conference²⁾. Arcs cause erosion of PFCs and release of impurities into plasma, they can also be a source of dust production. In Figure 1 arc traces are clearly visible on samples #1 and #2 with W coatings from ASIPP, while none were found on samples #3 and #4 with W coatings from Kyushu. Figure 2 shows Scanning Electron Microscopy (SEM) images of the arc traces on samples #1 and #2. The arc traces that look scratch-like in Figure 1 under larger magnification appear as chains of pits up to ~30 µm in diameter with W coating removed completely within the pits. Micron-size droplets are observed along the pit edges and some cracking of the underlying solid W is observed too.

Arc traces were also observed near the edge of the solid W sample #5. This sample was studied in more detail with SEM cross-section imaging, treated by the Focused Ion Beam (FIB). Figure 3 shows a SEM image of the surface with arc spots (a) and some sub-surface features like pores and evidence of re-crystallization obtained by FIB (b, c). Blisters were observed on both the surface and the sample measured by FIB.

In particular, large pores of 1 micron were observed, especially inside the significantly melted surface, as shown in Figure 3(c).

As a result, this leads to different properties between bulk W and coated-W samples.

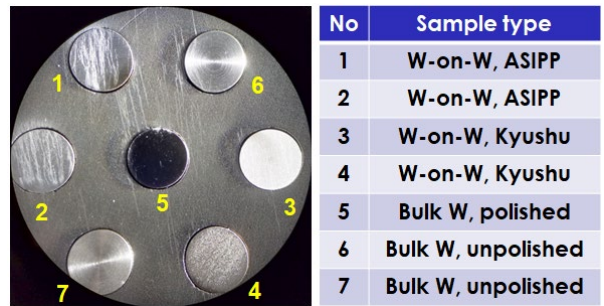


Figure 1. Post-exposure photograph of the DiMES head with sample buttons showing evidence of arcing

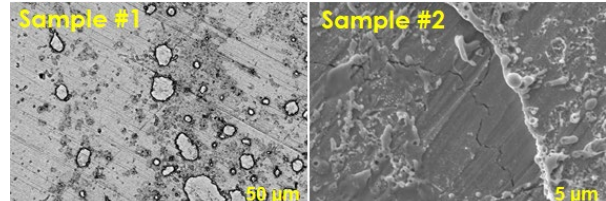


Figure 2. SEM images of the arc traces on W-coated samples

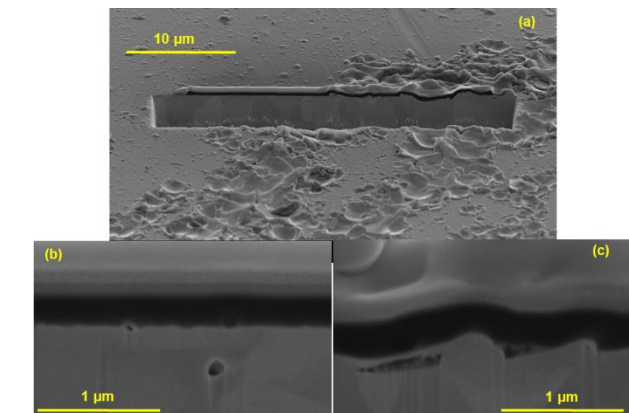


Figure 3. FIB SEM images of the arc traces and sub-surface features on solid W sample #5

¹⁾ C.P.C. Wong, et al., J. Nucl. Mater. 196–198 (1992) 871

²⁾ D.L. Rudakov et al., “Impact of unipolar arcing on PFC surfaces in DIII-D divertor.” 23rd PSI Conference, Princeton, NJ, USA, June 18–22, 2018

Fusion Safety Studies

Category: FTPC- Safety

Name: P. Humrickhouse/Y. Someya

Affiliation: INL/QST

The prospect of enhanced safety and reduced environmental impact compared to other nuclear systems is a primary motivation to pursue fusion energy. Ensuring that is so requires design choices informed by consideration of off-normal and accident scenarios, and their impact on decay heat management and radionuclide inventories. To that end, INL has long developed of a version of the MELCOR code customized for fusion safety analysis. MELCOR models thermal hydraulics, heat transfer, aerosol and radionuclide transport, and other phenomena important in off-normal and accident scenarios. Modifications originally made to MELCOR 1.8.2 for ITER included oxidation models for C, Be, and W, an HTO aerosol transport model, and condensation models for cryogenic surfaces.

In recent years, efforts have focused on migrating the original ITER modifications to a more recent version of the code (1.8.6)¹⁾, and continuing to add to its capabilities to facilitate modeling of a wide variety of DEMO and other reactor designs. Extensions include the ability to model multiple, multi-phase fluids in single analysis (e.g., for PbLi/H₂O designs or intermediate coolant loops)²⁾, revision and expansion of the fluid property libraries to improve code execution and accuracy and add additional fusion-relevant fluids³⁾, and full integration of the tritium transport models from the TMAP code⁴⁾. Preliminary verification activities for MELCOR-TMAP have been completed (Figure 1).

MELCOR is widely used for fusion safety analyses internationally, and INL hosted user Makoto Nakamura to receive training in use of the code for application to Japanese DEMO design efforts. A wide variety of accident scenarios in the Japanese water-cooled ceramic breeder DEMO design were subsequently analyzed⁵⁾⁻⁹⁾, including 1) an ex-vessel LOCA involving a double-ended break of the primary cooling water pipe; 2) an in-vessel LOCA involving a break in first wall coolant channels into the vacuum vessel; 3) an “in-box” LOCA involving a water coolant leak into the pebble bed regions of the breeder blanket; and 4) loss of vacuum (LOVA), and subsequent tritium and dust transport.

Regarding both the in-vessel and ex-vessel LOCAs, a significant early finding⁷⁾ was that the resultant generation of

steam would create overpressure sufficient to breach the primary (vacuum vessel) and secondary (tokamak hall) confinement boundaries, respectively, which would lead to a release of tritium and/or activated dust. The result prompted subsequent evaluation of design options to mitigate this, including a pressure suppression system for the tokamak cooling water system vault (Figure 2) and use of the upper tokamak hall as a large expansion volume.⁸⁾

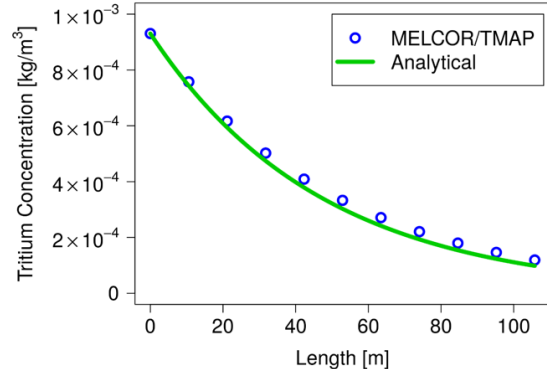


Figure 1. MELCOR/TMAP verification problem: tritium concentration evolution in a molten salt vacuum permeator²⁾.

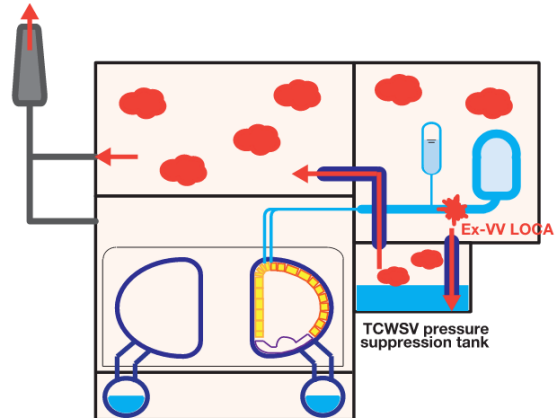


Figure 2. JA DEMO with Tokamak Cooling Water System Vault (TCWSV) pressure suppression tank, an option evaluated for managing overpressure in loss-of-coolant accidents⁸⁾.

¹⁾ B. Merrill, P. Humrickhouse, and R. L. Moore, Fusion Engineering and Design 85 (2010) 1479–1483.

²⁾ B. Merrill, P. Humrickhouse, and S. J. Yoon, Fusion Engineering and Design 146 (2019) 289–292.

³⁾ P. Humrickhouse and B. Merrill, Fusion Engineering and Design 146 (2019) 2519–2522.

⁴⁾ B. Merrill, P. Humrickhouse, and M. Shimada, Fusion Engineering and Design 109 111 (2016) 970–974.

⁵⁾ M. Nakamura, K. Tobita, Y. Someya et al., Plasma and Fusion Research 9 (2014) 1405139.

⁶⁾ M. Nakamura, K. Watanabe, K. Tobita et al., Proceedings 26th SOFE (2015).

⁷⁾ M. Nakamura, K. Tobita, Y. Someya et al., Nuclear Fusion 55 n. 12 (2015) 123008.

⁸⁾ M. Nakamura, K. Watanabe, K. Tobita et al., IEEE Transactions on Plasma Science 44 n. 9 (2016) 1689–1699.

⁹⁾ M. Nakamura, K. Tobita, Y. Someya et al., Fusion Engineering and Design 109 111 (2016) 1417–1421.

Workshop on RF Heating Technology

Category: FTPC – Plasma Heating

Name: J. Anderson, R. Olstad

/ T. Shimozuma, T. Mutoh

Affiliation: General Atomics / NIFS

Workshops on RF heating technology have been held annually, including contributions from the EU. The goal of the workshops is to promote RF heating research for fusion through stimulated discussions and resulting collaborations. Many researchers from US, Japanese and European institutions and

Universities have participated in the workshops and held discussions on the latest technologies for plasma heating and control methods using high power electro-magnetic waves. Recently the workshop participants have expanded to include members from the ITER Organization. Arrangement of future collaboration are also discussed, arranged and determined on the final day of the workshop. These collaborations result in the establishment of cooperative research for the next year and lay the groundwork for such work in the future.

History of the US-EU-Japan RF Heating Technology Workshop

Year	Date	Country	Venue	The number of participants	The number of presentations
2010	Sept.13-15	Italy	Como		
2011	Oct. 10-12	USA	Austin	USA:25, JPN:10, EUR:7, KOR:2, etc:2	ECH: 13, Gyrotron: 6, ICH etc: 6
2012	Dec. 11-13	Japan	Nara	USA:12, JPN:28, EUR:7, KOR:3	ECH: 18, Gyrotron: 6, LHCD: 3, ICH etc: 5
2013	Sept.9-11	Germany	Speyer		
2014	Sept.21-26	USA	Sedona	USA:11, JPN:6, EUR:10	ECH:19, LHCD: 2, ICH: 4
2015	Aug.31-Sept.2	Japan	Tokyo	USA:7, JPN:25, EUR:11	ECH: 25, LHCD: 2, ICH: 4
2016	Sept. 21-23	Germany	Leinsweiler		
2017	Sept. 5-8	USA	Santa Monica	USA: 11, JPN: 12, EUR: 12	ECH: 25, LHCD: 3, ICH: 3, etc: 1
2018	Sept. 5-7	Japan	Shizuoka	USA: 14, JPN: 25, EUR: 10	ECH: 24, LHCD: 3, ICH: 4, etc: 1
2019	Sept. 9-12	Germany	Freiburg		



US-EU-JPN Workshop on RF Heating Technology, Sept. 5- 7, 2017, Santa Monica, CA

Workshop on Fusion Power Plant Design, Next Steps and Related Advanced Technologies

Category: FTPC – Other

Name: C. Kessel / N. Yanagi, Y. Sakamoto

Affiliation: ORNL / NIFS, QST

Workshops on “Fusion Power Plant Design, Next Steps and Related Advanced Technologies” have been held as one of the important activities for the US-Japan collaborations in the

category of FTPC. Researchers from the US and Japanese universities and institutes have participated in the workshops and made active discussions on the latest reactor designs together with technological developments on the numerical design integration code, superconducting magnet, plasma facing component, blanket, materials and tritium handling. During the ten years of 2010-2020, seven workshops (four times in US and three times in Japan) were held as shown in Table 1.

Table 1. List of workshops on “Fusion Power Plant Design, Next Steps and Related Advanced Technologies”

Fiscal Year	Date	Country	Place	Number of participants	Number of presentations
FY2010	February 22-24, 2011	JA	NIFS (Toki)	26	22
FY2011	March 8-9, 2012	US	UCSD (San Diego)	13	14
FY2012	February 26-28, 2013	JA	Kyoto University (Uji)	32	27
FY2013	March 13-14, 2014	US	UCSD (San Diego)	13	15
FY2015	October 28-30, 2015	US	Denver	21	23
FY2016	March 27-29, 2017	JA	NIFS (Toki)	32	26
FY2018	December 13-15, 2018	US	ORNL (Oak Ridge)	21	23

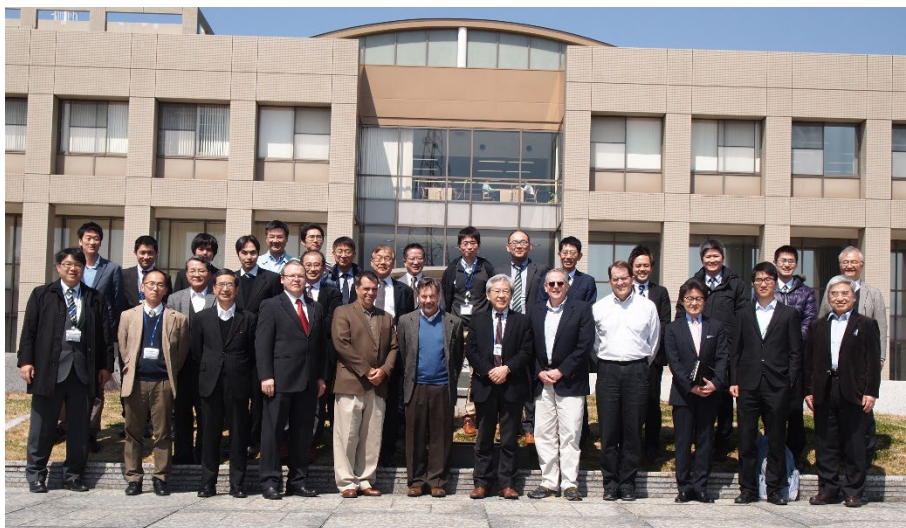


Figure 1. Group photo from the workshop on “Fusion Power Plant Design, Next Steps and Related Advanced Technologies” held at NIFS in March, 2017.

CHAPTER 3 Fusion Physics Planning Committee (FPPC)

3.1 Objectives

The FPPC (Fusion Physics Planning Committee) is responsible for organizing US-Japan collaboration on the experimental research of fusion plasma physics. In the initial phase of the US-Japan collaboration, the experimental collaboration was planned and conducted to promote various concepts of fusion including fusion technology. The separation of the FPPC and FTPC (Fusion Technology Planning Committee) was established in 1991. In order to study more common physics among different machines, since 1992, the collaboration was conducted to promote plasma core phenomena, plasma edge behavior and control, heating and current drive, and new approaches and diagnostics development. This was revised in 2007 to the present structure. The present subsections are now 1) Planning, 2) Steady-state Operation, 3) MHD and High Beta, 4) Confinement, 5) Diagnostics, and 6) High Energy Density Science. The physics of various concepts of magnetic and inertial confinement can be discussed together by these subsections, which allows us to deepen the understanding of complex behaviors of confined plasmas.

3.2 Activities

The collaborations are carried out by workshops and personal exchanges of researchers, being mindful that the locations of the collaborations should be balanced between US and Japan as much as possible. There were also collaboration activities using remote tools such as videoconferencing and e-mail, although the focus remained on in-person collaboration where possible. During the Japan fiscal years of 2010-2019 under US-Japan collaboration, 67 workshop events were held: 37 in the US and 30 in Japan. During these events, there were 361 personnel exchanges: 159 to the US and 202 to Japan. Across the themes related to FPPC, there were 195 exchanges performed to pursue R&D: 126 to the US and 69 to Japan. The highlights of these activities are described in this chapter.

3.3 Administration

The present steering committee of FPPC consists of US DoE key-persons and a person in charge from universities including National Institute for Fusion Science (NIFS) and 5 key-persons for 5 subsections from Japanese universities. Two high-level planning meetings are held annually: one for the FPPC itself and another for the NSTX-U Program Advisory Committee.

3.4 Accomplishments and Highlights

3.4.1 Steady-State Operation

In the ITER era, one of the important research areas in fusion programs is steady state operation of the fusion plasma. The mutual collaboration of steady state operation covers the following subjects; 1) plasma heating and current drive in tokamaks by RF waves, 2) physics of plasma current start-up method using ECH/EBW and CHI, especially in spherical tokamaks, 3) liquid metal for controlling divertor heat flux while improving plasma confinement. The US-Japan Workshop on the Physics of RF Heating of Fusion Plasmas has been held each year from 2011-2019 while the exchanges did not take place in 2020 due to COVID-19. Topics covered at the workshops included (i) RF heating and start-up/current drive in spherical tokamak; (ii) Lower hybrid current drive in tokamak; (iii) Electron cyclotron current drive (ECCD) in tokamak; (iv) RF heating in the LHD Device; (v) Innovative applications of RF; and (vi) Advances in RF simulation. Collaboration with “Wave physics” including current start-up has been carried out from 2010 to 2019 by QUEST (Kyushu University), TST-2 (University of Tokyo), JT-60SA (QST), NSTX-U (PPPL), C-Mod (MIT PSFC), DIII-D (GA). Simulations of LHCD experiments on TST-2 were carried out using Petra-M, a simulation code developed in the US. Additionally, the current drive performance of HFS LHCD on JT-60SA was assessed as a part of broad survey of HFS LHCD on various tokamak experiments utilizing various codes including GENRAY/CQL3D. As collaboration between the University of Tokyo and the MIT Plasma Science and Fusion Center, study of parametric decay instability of lower hybrid waves propagation and its interaction with boundary plasmas on the Alcator C-Mod tokamak have been also investigated. In the spherical tokamak plasma start-up area, US-Japan collaboration on RF and coaxial helicity injection (CHI) start-up experiments were carried out on the QUEST spherical tokamak at Kyushu University. The HFS launched x-mode can mode convert to electron Bernstein wave (EBW) which can propagate as an electrostatic wave in the over-dense regime and be strongly damped near the electron cyclotron resonance (ECR) layers where GENRAY code was used to simulate the experiments. Using a high-field-side (HFS) waveguide injection, a feasibility study of HFS RF injection for EBW was carried out in QUEST. For the development of plasma start-up using CHI in QUEST, the experiments were performed using a CHI electrode configuration which can be more readily incorporated into a reactor design. In the recent CHI experiment, discharges from the high-field side, were successfully generated with some indications of the toroidal current persisting after the CHI discharge is over, an indication of closed flux surface. In the area of liquid metal plasma facing component collaboration, the first US-Japan workshop on “Power and Particle Control in a Steady-State Magnetic Fusion DEMO Reactor by Liquid Metal Plasma-Facing Components” was held at PPPL for Mar. 3rd through Mar. 5th, 2019. This series of US-Japan workshop was initiated owing to the active US-Japan collaboration activities on liquid metal PFCs spanning over the last two decades to resolve technical issues with the tungsten divertor design and investigate the utilization of liquid metals as a possible solution.

US-Japan Workshop on the Physics of RF Heating of Fusion Plasmas

Category: FPPC – Steady-State Operation

Year-Number: 2011-FP-2, 2012-FP2-4, 2013-FP-2, 2014-FP2-2, 2015-FP2-1, 2016-FP2-, 2017-FP2-1, 2018-FP2-4, 2019-FP2-1,

Name: ¹Shin Kubo, ²J. Hosea, ³Paul T. Bonoli, ⁴R. Pinsker, ²M. Ono

Affiliation: ¹Chubu University, ²PPPL, ³MIT, ⁴GeneralAtomics

This document summarizes the US-Japan Workshop on the Physics of RF Heating of Fusion Plasmas for the US-Japan Fusion Collaboration 40th Anniversary Report covering the 10-year period from 2011 to 2020. This series of workshops was part of an historical ongoing series on RF heating physics, contributing to the understanding of RF heating in fusion research through active discussion and collaboration between the US and Japan. The workshop location was altered between Japan and the US locations: 2011 – Newport, USA; 2012 – Nara, Japan; 2013 – Boston, USA; 2014 – Kyoto, Japan; 2015 – Lake Arrowhead, USA; 2016 – Toyama, Japan; 2017 – Santa Monica, USA; 2018 – Gotemba, Japan; 2019 – Princeton, USA. A group photo of the most recent workshop held in Gotemba, Japan 2018 is shown in Figure 1. The workshop is typically enjoyed about 50 participants from Japan and the USA.

The topics of interest at the US-Japan workshops covered the ion cyclotron, lower hybrid, and electron cyclotron range of frequencies for RF heating and current drive, in the areas of experiment, theory, and simulation. Topics covered at the workshops included (i) RF heating and start-up/current drive in spherical tokamak; (ii) Lower hybrid current drive in tokamak; (iii) Electron cyclotron current drive (ECCD) in tokamak; (iv) RF heating in the LHD Device; (v) Innovative applications of RF; and (vi) Advances in RF simulation.

In the area of RF heating in Spherical Tokamaks, results were presented on spherical tokamak startup by electron Bernstein wave (EBW) heating on the LATE device, non-inductive driven plasma start-up and investigation of electron Bernstein wave current drive (EBWCD) in QUEST, and high harmonic fast wave operation in NSTX-U. Results were presented on lower-hybrid startup scenarios on the TST-2 spherical tokamak, and performance of various types of antennas (capacitively-coupled combline, inductively-coupled combline, and dielectric loaded waveguide) at the mid-plane and top were reviewed for TST-2.

In the area of ICRF and HHFW antenna physics and design, results were presented on the Alcator C-Mod field aligned antenna and its implications for future RF antenna design and development, studies were presented on field-aligned edge-loss of HHFW power on NSTX, and investigations were reported on possible HHFW edge power

deposition processes with Langmuir probes intercepting the lower divertor HHFW RF power deposition spiral on NSTX.

Progress towards steady state regimes with lower hybrid current drive, and the effects of edge turbulence on lower current drive efficiency in Alcator C-Mod were reported. Steady progress on ECCD in DIII-D has been reported including use of the top-launcher which showed improved current drive efficiency compared to the mid-plane launcher. Helicon antenna design and preparation on DIII-D was also presented.

In the area of RF heating in the LHD device, recent electron cyclotron resonance heating (ECRH) results were presented and the use of ion cyclotron heating (ICH) in steady-state discharges was discussed.

In the area of innovative applications of RF, a number of interesting studies were reported that covered topics such as using high field side LHCD in advanced reactor concepts, full-wave modeling in the ECRF, with application to a novel safety factor profile diagnostic by oblique reflectometry imaging, high efficiency off-axis current drive by high frequency (helicon) fast waves, ICRF-related experiments on the GAMMA 10 tandem mirror, and metamaterial applications to electron cyclotron emission and heating at multiple frequencies.

Significant progress in the area of RF simulation has been reported including innovative full-wave simulations for ICRF, LHCD in C-Mod, HHFW in NSTX and NSTX-U, and Helicon in DIII-D particularly the antenna and edge scrape-off layer region have been reported. Also reported were a configuration space algorithm for the linear kinetic plasma response to RF power, and integrated modeling of RF physics in tokamaks.



Figure 1. A group photo of the US-Japan Workshop in RF Physics held in Gotemba, Japan in September, 2018.

Simulations of LHCD experiments on TST-2 and comparison with experiment / High field side LHCD studies including antenna analysis

Category: FPPC – Steady-State Operation

Year-Number: 2017-FP2-2, 2017, 2018-FP2-5

Name: S. Shiraiwa^{1,3}, S. Yajima², Y. Takase², S. Ide⁴, P. Bonoli¹, R. Parker¹

Affiliation: ¹MIT PSFC, ²Univ. Tokyo, ³PPPL, ⁴QST

Lower hybrid current drive (LHCD) requires to locate an antenna structure closed to a plasma to excite the slow wave. A various novel lower hybrid launchers have been developed in University of Tokyo for LHCD on the spherical tokamak. Traditionally, for the standard grill-type LHCD antenna, a semi-analytic approach was used¹⁾, where the plasma response computed using a linearized density profile is used. However, this approach restricts the antenna structure to a periodic bundle of waveguides and more computationally expensive finite element method (FEM) based analysis is required for the antennas being studied in Univ. of Tokyo. While a commercial code is available for such a FEM analysis even with the cold plasma load¹⁾, it demands a lot bigger computational resources and analyzing the wave field in the entire TST-2 tokamak plasma is prohibitive.

In this collaboration, we used the Petra-M framework developed at MIT for analyzing the LH wave excitation and propagation in TST-2. Petra-M is based on the scalable modular finite element method (MFEM) library and it allows for solving the Maxwell equation with much bigger simulation volume, while including an arbitrary 3D antenna structure. We used Petra-M to analyze a capacitively coupled combline (CCC) antenna located on the low field side of TST-2. The computed LH wave electric field is shown in Figure 1. The entire TST-2 plasma is included in the simulation. An RF power at 200MHz was fed from the left side port of the antenna. The RF power propagates through the antenna via the mutual coupling between antenna elements, which resulting in a traveling wave and the LH wave excitation in the plasma as seen in the Figure.

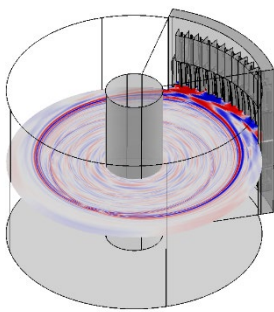


Figure 1. Petra-M simulation of LH waves excited by CCC antenna on TST-2

Another important issue of LHCD is to improve the wave accessibility. The limited accessibility restricts the role of LHCD in a reactor in far off-axis regions, although it has a large current drive efficiency and has been used for long pulse steady state tokamak operations. Furthermore, the long-standing spectrum gap issue makes it difficult to extrapolate the present-day experiment to reactors.

The high field side (HFS) LHCD⁴⁻⁵⁾ was proposed to address the accessibility and potentially spectrum gap issues. At MIT, we assessed the potential of HFS LHCD using a wide range of tokamak configurations based on various existing and proposed/future tokamak experiments including ADX, DIII-D, and WEST⁴⁾. As a part of survey, through the US-Japan collaboration, the current drive performance of a hypothetical HFS LHCD experiment on JT-60SA was studied. An example of GENRAY/CQL3D (raytracing/Fokker Planck) calculation is shown in Figure 2, showing driving 50kA/MW near $r/a = 0.7$ for this target plasma scenario.

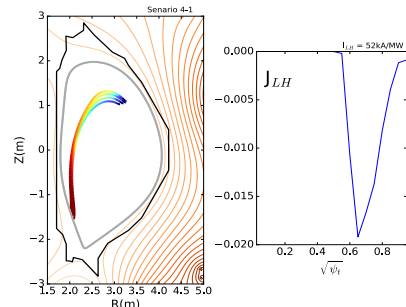


Figure 2: GENRAY/CQL3D prediction of HFS LHCD on JT-60SA. The target plasma is based on Scenario 4-1 in Ref. [7].

In summary, LHCD modeling collaborations have made progress in improving our capability to analyze LHCD to include an arbitrarily shaped antenna structure with a large target plasma volume. Additionally, the current drive performance of HFS LHCD on JT-60SA was assessed as a part of broad survey of HFS LHCD on various tokamak experiments.

Acknowledgement: Provision of Alcator C-Mod data sets was supported under DOE Award number DE-FC02-99ER5451.

¹⁾J. Hillairet et. al., Nucl. Fusion 50, 125010 (2010)

²⁾S. Shiraiwa et. al., Physics of Plasmas 17, 056119 (2010).

³⁾S. Shiraiwa et. al., EPJ Web of Conferences 157, 03048 (2017).

⁴⁾G. Wallace, et. al., AIP Conference Proceedings 1689, 030017 (2015).

⁵⁾P.T. Bonoli et. al., Nucl. Fusion 58, 126032 (2018).

Developments in Plasma Startup Using Transient Coaxial Helicity Injection

Category: FPPC – Steady-State Operation

Year-Number: 2018-FP2-4, 2019-FP2-3

Name: ¹K. Kuroda, ²R. Raman, ¹K. Hanada, ³M. Ono

Affiliation: ¹Kyushu University, Kyushu, Japan

²University of Washington, Seattle, WA, USA,

³Princeton Plasma Physics Laboratory, Princeton, NJ, USA

The first application of transient CHI startup on QUEST, aimed at developing solenoid-free plasma startup capability, biased the CHI electrode to the outer vessel (low-field side injection). While the CHI discharges could be easily generated without spurious arcing¹⁾ it is found that as the discharge filled the vessel, the separation between the injector flux footprints widened, a condition that is not favorable for the generation of closed flux surfaces. Biasing to the inner wall (high-field side injection) takes advantage of the higher toroidal field on the inboard side. It is a configuration similar to that successfully used on HIT-II and NSTX. Initial tests in the high-field injection cases were prone to spurious arcing, and no reliable discharge initiation or evolution scenario could be developed. As a first step to solving this issue, an improved gas injection manifold was installed in the high-field injection location. This configuration, which was tested during the February 2021 CHI run campaign on QUEST, successfully generated discharges

from the high-field side, with some indications of the toroidal current persisting after the CHI discharge is over. Figure 1 shows the location of the new gas manifolds with respect to a steel cylinder electrode. The injector current traces show that an injector current of just 10 kA can grow the plasma to a toroidal current level of 35 kA. However, as the CHI-produced toroidal current starts to decrease, a spurious arc (referred to as an absorber arc) is initiated, which causes the injector current to increase to 25 kA. The absorber arc later diminishes and becomes very low, while the toroidal current continues to be present. The fast camera image (last frame) shows the plasma to be present and the presence of CHI-produced toroidal current.

These results encourage a planned upgrade, which involves lowering the divertor plate closer to the CHI injector coil, allowing improved injector flux coupling to the CHI electrodes and the greater separation between the CHI electrode and the outer wall, which would further reduce spurious arcing.

CHI on QUEST uses a reactor-relevant electrode configuration. Unlike most STs and tokamaks, QUEST does not use routine central solenoid capability for plasma current initiation. The goals on QUEST are to develop a transient CHI start-up scenario that could be used to routinely couple to ECH to study full non-inductive current drive.

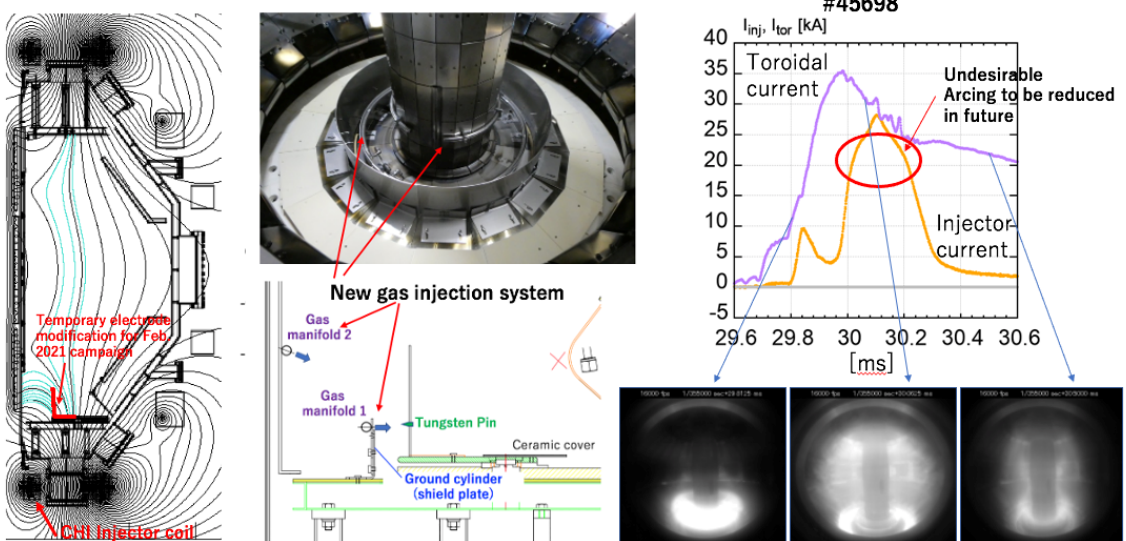


Figure 1. QUEST high-field side injection configuration. Left – injector vacuum flux configuration. Middle – photo and drawing showing the new gas injection manifolds and tungsten pins used to aid gas breakdown for discharge initiation inside the cylindrical region. Right – Injector current and CHI produced toroidal current and fast camera images. Note that in the first image, the discharge begins inside the cylindrical region. The spike in the injector current at 30.1ms is an absorber arc, and this can be seen in the middle camera image that shows that the discharge has moved outside the cylinder. In the third camera image, the absorber arc is mostly gone, and the region inside the cylinder once again shows brighter light emission.

¹⁾ K. Kuroda, et al., Plasma. Phys. Control. Fusion 60, 115001 (2018)

The first US Japan workshop on “Power and Particle Control in a Steady State Magnetic Fusion DEMO Reactor by Liquid Metal Plasma Facing Components”

Category: FPPC – Steady-State Operation

Year-Number: 2019-FP2-1

Name: Y. Hirooka (JP-PI) and M. Ono (US-PI)

Affiliations: Chubu University and PPPL

Due to its high thermal resistance and low sputtering characteristics, tungsten is employed as the divertor surface material in many of the existing plasma confinement devices as well as magnetic fusion power reactor designs. In addition, the International Thermonuclear Experimental Reactor (ITER) is envisaged to use tungsten as the divertor surface material. In these current divertor design, tungsten backed with an actively cooled heat sink made of a material with a high thermal conductivity, such as copper alloys, is expected to handle heat fluxes up to 10MW/m^2 , which may be sufficient for the heating power expected in ITER.

However, these conditions may not apply for the first steady state magnetic fusion DEMO reactor and the following commercial reactors to which the heating power can easily exceed that of ITER. It is also true that to meet the radiation safety requirement these reactors must employ reduced activation ferritic steel alloys, the thermal conductivities of which are significantly lower, compared with those of copper alloys. In addition, the ductile-brittle transition temperature (DBTT) for commercially available tungsten materials is typically around 400°C , either prepared by powder metallurgy or chemical vapor deposition. Because the ITER divertor will be operated at around 1000°C , temperature cycles associated with reactor start-up and shutdown would cross the DBTT repeatedly, which could then induce thermo-mechanical cracking.

To resolve these technical issues with the tungsten divertor design, the use of liquid metals has been proposed and discussed over the past two decades. A series of conferences, referred to as the International Symposia on the Liquid Applications for fusion devices (ISLA), have been held first in Japan (2010), in the U.S. (2011), in Italy (2013), in Spain (2015), in Russia (2017) and most recently in the U.S. (2019). The next one is planned to be held in China for 2021. Following this historical process, as part of the US-Japan bi-lateral collaboration program, a new series of workshops have been inaugurated in the Japanese fiscal year of 2018 on the subject of “Power and Particle Control by Liquid Metal. This series of US-Japan workshops will be organized by Y. Hirooka of Chubu Univ. as the Principal Investigator (PI) on the Japanese side and M. Ono of the Princeton Plasma Physics Laboratory (PPPL) as the PI on the U.S. side. It has been agreed by both sides that these

workshops will be held once every Japanese fiscal year and hosted alternately by the U.S. and Japan.

The first workshop was held at PPPL for Mar. 3rd through Mar. 5th, 2019. All the details on this workshop have already been published as a Conference Report in the Nuclear Fusion journal¹. Unfortunately, however, no workshop has been held ever since due to the worldwide COVID-19 situation.

The participants for the first US-Japan workshop are:

1. From Japan (Last name alphabetical order)
 1. Hanada, K. (Kyushu Univ.)
 2. Hirooka, Y. (Chubu Univ.)
 3. Kondo, M (Tokyo Inst. Tech.)
 4. Miyazawa, J. (NIFS)
 5. Shimada, M. (retired from QST)
2. From the U.S.
 1. Allain, J. P. (Univ. Illinois)
 2. Andruszyk, D. (Univ. Illinois)
 3. Brown, T. (PPPL)
 4. de Castro, A. (Univ. Illinois)
 5. Goldston, R. (PPPL)
 6. Kessel, C. E. (ORNL)
 7. Kaganovich, I. (PPPL)
 8. Khodak, A. (PPPL)
 9. Koel, B. (Princeton Univ.)
 10. Maingi, R. (PPPL)
 11. Majeski, R. (PPPL)
 12. Menard, J. (PPPL)
 13. Ono, M. (PPPL)
 14. del Rio, G. (PPPL)
 15. Zarnstorff, M. (PPPL)



Figure 1. A photo of the first US-Japan workshop participants, taken at a local restaurant in Princeton.

¹ Y. Hirooka et al. Nucl. Fusion 60(2020)017001(6pp).

Study of Parametric Decay Instability of Lower Hybrid Wave

Category: FPPC – Steady-State Operation

Year-Number: 2015-FP2-2, 2017-FP2-5

Name: S. G. Baek¹, G. M. Wallace¹, R. Parker¹,

T. Shinya², Y. Takase², S. Shiraiwa³

Affiliation: ¹MIT PSFC, ²Univ. Tokyo, ³PPPL

Lower hybrid wave propagation and its interaction with boundary plasmas on the Alcator C-Mod tokamak have been investigated under the collaboration between the University of Tokyo and the MIT Plasma Science and Fusion Center. In the lower hybrid current drive (LHCD) experiments, a challenge remains to understand and control the anomalous loss of current drive efficiency at high density, which are thought to be associated with parasitic interactions of the injected RF waves with the edge and scrape-off-layer plasmas. In this collaboration, direct measurements of LH wavefields on Alcator C-Mod provided invaluable information on wave characteristics such as wave polarization and frequency spectrum. Two collaborative research activities are highlighted.

First, parametric decay instabilities (PDIs) of lower hybrid waves are characterized on a diverted tokamak. A numerical code for a growth analysis is provided by the Univ. of Tokyo. A notable observation made on C-Mod is the onset of instabilities at the high-field-side edge in the magnetic equilibrium with $\vec{B} \times \nabla B$ pointing toward the active divertor¹⁾. Such a magnetic-configuration-dependent PDI onset was attributed to the SOL density profiles that are poloidal asymmetric in the presence of the SOL $E \times B$ flow. The model analysis shows that a relevant PDI process is a decay into ion cyclotron quasi-mode due to a weaker radial penetration of the LH wave in the high-density plasma. Later experiments show that parasitic interactions are suppressed by operating at a low Greenwald fraction with a decreased level of the SOL turbulence and density. In those plasmas, improved LHCD performance is observed, which has important implications for future LHCD experiments.

Second, an array of RF magnetic probe array had been designed, fabricated, and installed on C-Mod for measurements of the dominant wave parallel refractive index $n_{\parallel} = ck_{\parallel}/\omega$. The wave n_{\parallel} is a key physics parameter that determines wave propagation and absorption. Here, c is the speed of light, k_{\parallel} is the parallel (to the background magnetic field) wavenumber, and ω is the wave frequency. Two probe arrays were installed at 36° and 108° toroidally away from the launcher. An RF magnetic probe that is sensitive to 4.6 GHz was developed. An RF circuitry was also developed for direct digitization of the LH wave signals collected.

With this diagnostic, information on wave accessibility, wave branch, and wave propagation in the SOL are obtained by analyzing the measured n_{\parallel} , polarization, and radial profile²⁾. The wave branch associated with the oscillating wave magnetic field that is parallel (perpendicular) to the background magnetic field is identified to be the slow (fast) wave. The latter is identified as the LH fast wave generated by slow-fast wave mode conversion. At moderate densities, the observed power and n_{\parallel} of the slow-wave branch corresponds to the applied power spectrum. The measured wave propagation is consistent with a ray-tracing analysis, suggesting that the probes dominantly measure the wavefield leaving the launcher

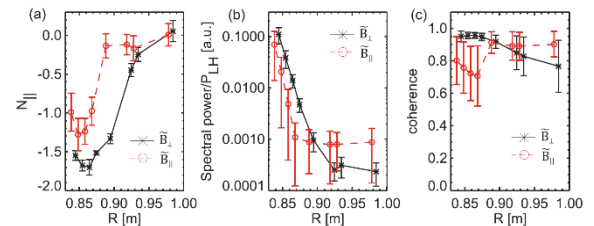


Figure 1. Radial profiles of (a) the wave n_{\parallel} , (b) spectral power, and (c) coherence measured with the RF magnetic probe array. Figure from Ref.²⁾

However, at high density, coherence decreases below 90%. The measured wave power also rapidly decreases, which indicates the roles of the accessibility condition and parasitic loss mechanisms. No substantial modification in the dominant n_{\parallel} of the ion cyclotron sideband is observed, which is likely due to (1) the limited n_{\parallel} resolution in the diagnostic and (2) the measurement location being away from the PDI excitation location. Thus, in this experiment, no clear causality was identified between the observed ion cyclotron parametric instabilities and spectral broadening in the wavenumber space, while frequency spectral broadening was apparent. Nevertheless, the experiments demonstrated a usefulness of the RF probe measurement to understand wave properties.

In summary, a modeling and experimental collaboration have made progress in understanding how lower hybrid waves interact with the edge/SOL plasma on C-Mod, which operated LHCD at a reactor-relevant condition in terms of magnetic field and density with respect to the LHCD frequency.

Acknowledgement: Provision of Alcator C-Mod data sets was supported under DOE Award number DE-FC02-99ER5451.

¹⁾ S. G. Baek et al., Phys. Plasmas, 21 (2014) 061511

²⁾ T. Shinya et al., Nucl. Fusion, 57 (2017) 036005

³⁾ S. G. Baek et al., Phys. Plasmas, 23 (2016) 050701

3.4.2 MHD and High Beta

Collaborative exchanges in Magnetohydrodynamics (MHD) and High Beta include joint workshops and personnel exchanges. There were 58 workshop exchanges, and 159 personnel exchanges to complete planned R&D. An important workshop exchange includes the US-Japan MHD workshop on Active Control of MHD Modes in Toroidal Plasmas, the first one held in San Diego in conjunction with the 3rd US MHD meeting in November 1998. Since then, the US-Japan MHD workshop has been held annually except in 2019 and 2020 due to travel restrictions related to the pandemic. The workshop provides a venue for the dissemination of key results in MHD mode control and the impact of non-axisymmetric magnetic fields. These advancements enable tokamak operation at high plasma beta, which supports the steady-state objectives of the U.S. and Japan programs.

Highlights from the last decade include:

- a comparison of experimental and computational MHD phenomena in the reversed field pinch experiments MST and RELAX aiming at improved validation of MHD simulation of fluctuations due to tearing mode instabilities;
- a study of the relation between current decay time and MHD dynamics in mitigated disruptions and verification of the halo current model during disruption;
- validation of 3D equilibrium modeling using the HINT code and applied 3D magnetic fields in DIII-D and LHD facilities;
- an experimental study of power loss of high harmonic fast waves in the scrape-off layer of NSTX spherical tokamak plasmas; and
- a series of highlights from the US-Japan MHD Workshops conducted annually.

This collection of results and workshop highlights demonstrate steady progress made by US and Japan collaborations aimed at achieving stable operation in high beta plasmas, which will provide important input to operation of future facilities including the JT-60SA facility currently being commissioned in Naka, Japan, and in long-pulse, ITER steady-state scenarios.

Comparison of experimental and computational MHD phenomena in MST and RELAX: toward Validation of MHD simulation

Category: FPPC - MHD

Name: D. J. Den Hartog, K. J. McCollam/S. Masamune*

Affiliation: University of Wisconsin–Madison/Kyoto Institute of Technology

The Reversed-Field Pinch (RFP) toroidal magnetic plasma confinement configuration provides potential fusion reactor advantages of high $\beta \propto p/B^2$ and a path to Ohmic ignition. An RFP plasma relaxes to a minimum energy state while holding magnetic helicity approximately constant. During this relaxation process, multiple magnetic tearing modes are active and exhibit complex nonlinear MHD interactions. Thus, the RFP is an excellent platform for validation via comparison of experimental results to extended MHD simulation with the NIMROD code.¹⁾

The RELAX RFP experiment at the Kyoto Institute of Technology produced plasmas in which both the Lundquist (S) and magnetic Prandtl (P_m) numbers were accessible to simulation using NIMROD. RELAX is a low-aspect-ratio ($R_0/a \approx 2$) RFP which exhibits quasi-single-helicity (QSH) behavior with a large plasma core region inside the innermost $m = 1$ resonant surface.²⁾

For this collaboration, computation of MHD dynamics was carried out for a variety of distinctive equilibria in RELAX, varying from low- q non-reversed to deeply reversed RFP plasmas (Figure 1). Initial equilibria were modelled appropriately, and resistive MHD simulations were performed using both cylindrical and toroidal geometry.

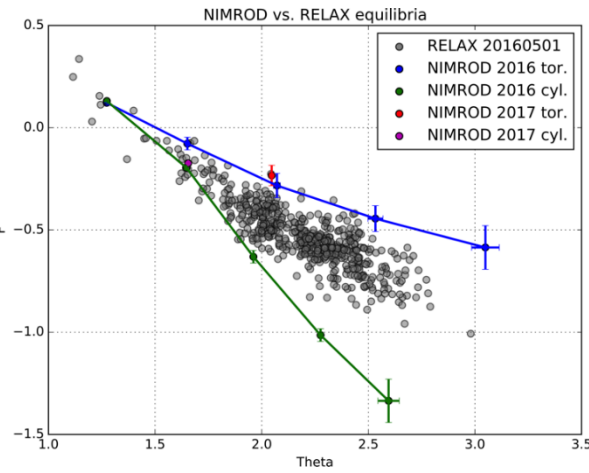


Figure 1. The equilibria simulated with NIMROD are close to the equilibria produced in RELAX.

Comparisons of magnetic tearing fluctuation activity in simulation and experiment were also performed. Toroidal NIMROD simulations of RELAX plasmas show magnetic fluctuation behavior similar to experiment, but amplitudes did not match, and QSH observed in the experiment has not been identified clearly in the simulations (Figure 2). Focused studies were also done on how the spatiotemporal dynamics of the fluctuations vary with RFP equilibrium parameters. Interestingly, at shallow reversal, cylindrical simulations show a relatively uncoupled spectrum of nearly quiescent modes periodically varying in time, whereas the corresponding toroidal cases show a fully chaotic spectrum of strongly nonlinearly interacting modes. We ascribe this to the geometric $m = 1$ coupling present in the toroidal but not the cylindrical case.

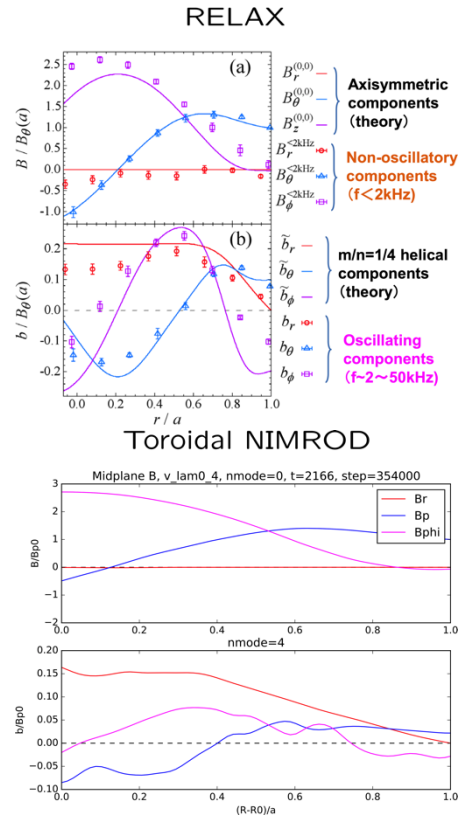


Figure 2. Toroidal NIMROD simulations show similar magnetic profiles to probe measurements made in RELAX.

* Now at Chubu University.

¹ C. Sovinec et al., J. Comput. Phys. 195, 355 (2004), J. Comput. Phys. 229, 5803 (2010).

² K. Oki et al., Plasma Fusion Res. 7, 1402028 (2012).

Disruption issues on DIII-D: Study of the relation between current decay time and MHD dynamics in mitigated disruptions and verification of the halo current model during disruption

Category: FPPC - MHD

Name: Y. Shibata /N.W. Eidietis

Affiliation: NIT Gifu college/General Atomics

Disruption is one of the most important issues to resolve for realization of the ITER and DEMO reactors. The plasma current (I_p) decays rapidly because of the sudden increase in plasma resistance following the thermal quench (TQ). The rapid current decay generates potentially damaging eddy currents and electromagnetic force in conducting materials around plasma. In our previous study, it was found that there was fast current decay during the initial phase of the current quench (CQ) in high electron temperature (T_e) disruptions (T_e at the plasma center: over 100eV) on JT-60U and the I_p decay rate increased with the change in plasma inductance L_p during the CQ, especially internal plasma inductance L_i ¹⁾. It was found from analysis of disruption simulations that the existence of a T_e profile during CQ was important to increase the L_i ²⁾. However, verification of the current decay model using experimental data from other tokamak devices beyond JT-60U is necessary for understanding the current decay physics during a disruption.

In this study, we analyzed the CQ in three types of DIII-D disruptions (low-q, error field and shell pellet injection) to confirm the effect of the time evolution of the L_i on the decay time during the initial phase of the CQ in DIII-D. Typical plasma parameters are as follows; Low-q: $I_p = 1.89\text{--}2.11\text{ MA}$, $B_t = 1.98\text{ T}$, $R_0 = 1.73\text{ m}$, $a = 0.59\text{ m}$, $\kappa = 1.81$, Error field: $I_p = 1.63\text{ MA}$, $B_t = 1.97\text{ T}$, $R_0 = 1.73\text{ m}$, $a = 0.59\text{ m}$, $\kappa = 1.81$, Shell pellet injection (6 shots): $I_p = 1.6\text{ MA}$, $B_t = 2.15\text{ T}$, $R_0 = 1.72\text{ m}$, $a = 0.6\text{ m}$, $\kappa = 1.8$. The experimental plasma current decay time was evaluated by using the following equation:

$$\tau_{100-80} = I_{p0}/(\Delta I_p/\Delta t)$$

Here, I_{p0} is the plasma current just after the TQ, ΔI_p is 20% of I_{p0} , and Δt is the time interval between I_{p0} and $0.8I_{p0}$, respectively. Evaluations of plasma resistance R_p and L_p are necessary to verify the current quench model during the initial phase of CQ in DIII-D tokamak. To evaluate L_p during the initial phase of the CQ, we used the CCS code. The CCS code can only evaluate magnetic flux outside the plasma boundary, and the shape of last closed flux surface and Shafranov shift can be evaluated from that evaluated magnetic flux. For evaluation of L_p , the following equation was used;

$$L_p = L_i + L_e = \mu_0 R_0 (\Lambda - \beta_p) + \mu_0 R_0 (\ln(8R_0/a) - 2)$$

Here, Λ is Shafranov lambda and β_p is the poloidal beta. In this study, $\beta_p = 0$ after the TQ was assumed. Figure 1 shows the time evolution of plasma parameters evaluated by CCS code. In this discharge, the experimentally current decay time τ_{100-80} is 9.4 ms. as shown in Figure 1 (b), it was found that L_p , especially L_i ,

increased during the initial phase of CQ. Figure 2 shows the relationship between the time change rate of L_i and CQ time during the initial phase of the CQ in the three types of DIII-D disruptions. It was found that dL_i/dt was increased with decrease of CQ time like JT-60U results.

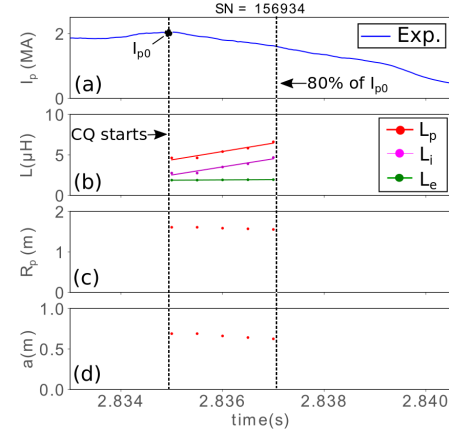


Figure 1. Time evolutions of (a) the plasma current I_p , (b) the plasma inductance L , (c) the major radius R_p , and (d) minor radius a evaluated by CCS code during CQ.

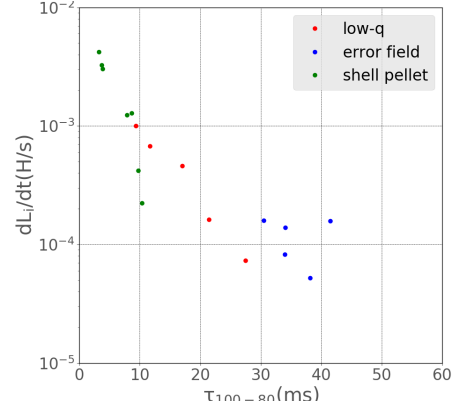


Figure 2. The relationship between time change rate of L_i and CQ time during the initial phase of the CQ.

In summary, current quenches in three types of DIII-D disruptions were analyzed to investigate the determination mechanism responsible for the initial phase of current quench in DIII-D. It was found that dL_i/dt during the initial phase of CQ increased with a decrease of CQ time, identical to JT-60U results. This material is based upon work supported by the US Department of Energy under Award Number(s) DE-FC02-04ER54698 and Japan/U.S. Cooperation in Fusion Research and Development.

¹ Y. Shibata, et. al., Nucl. Fusion 50, 025015 (2010).

² Y. Shibata, et. al., Plasma Phys. Cont. Fusion 56 045008 (2014).

Confirmation of 3D MHD modeling using SX imaging and Comparison of RMP transport in tokamaks and stellarators

Category: FPPC - MHD

Name: Y. Suzuki, S. Ohdachi/T. E. Evans

Affiliation: NIFS/GA

In recent tokamak experiments, it is noted that stochastic field lines reduce strong heat load driven by the edge localized mode (ELM) to the divertor plate. Stochastic field lines are produced by the external perturbed field, and it is called the Resonant Magnetic Perturbation (RMP). From the viewpoint of high-beta stellarator equilibrium, 3D equilibrium responses on the stochastic magnetic field are very important because the pressure-induced perturbed field by the plasma leads further stochasticization in the peripheral region. However, in the present analysis of RMP fields, a vacuum helical perturbed field superimposed on a 2D MHD equilibrium, a so-called vacuum approximation, is widely used. Since the vacuum approximation does not include the 3D equilibrium response, considerations including the 3D equilibrium response and its impact are critical and urgent issue.

An important plasma response is the shielding effect of the external field. If the plasma rotates, the RMP field is shielded by the plasma response. Modeling and simulation of the shielding are done in the vacuum approximation. However, if the RMP field is superposed and the magnetic field is stochasticized, the pressure and current density profiles might be changed. Therefore, the plasma boundary and geometry might be changed.

In this study, as a first step of 3D MHD modeling, the fully 3D equilibrium of non-axisymmetric tokamak is solved numerically, and the 3D equilibrium responses are studied. For this study, we use a 3D equilibrium code, HINT, which is widely used to analyze the 3D equilibrium of helical system plasmas. Since HINT uses the cylindrical coordinate system, it is independent to the magnetic topology. Thus, HINT can treat magnetic island and stochastic field in the computational domain.

The 3D equilibrium of a DIII-D plasma, which includes the effect of the RMP fields by the C-coil (Error Field Correction Coil), was studied. A strong nonlinearity in the 3D equilibrium response to an RMP field is found in the DIII-D plasma. In $n=1$ RMP field phase-flip experiments, differences in the $n=1$ plasma response are observed in each phase, although the RMP field is periodically symmetric. To understand this plasma response nonlinearity, a 3D equilibrium including the

error field, which breaks the field periodicity is studied. Figure 1 shows a comparison of the 3D equilibrium for different phases ($\phi_{RMP}=5$ or 185) of the RMP field. The island width at $\phi_{RMP}=185$ is larger than the width at $\phi_{RMP}=5$. Because, the error field amplifies an $m/n = 1/1$ island, the island redistributes the toroidal current density. Thus, the redistributed toroidal current density amplifies the further nonlinear evolution of the $m/n = 1/1$ island. This is the reason for the strong nonlinearity that appears after the phase flip of the RMP field.

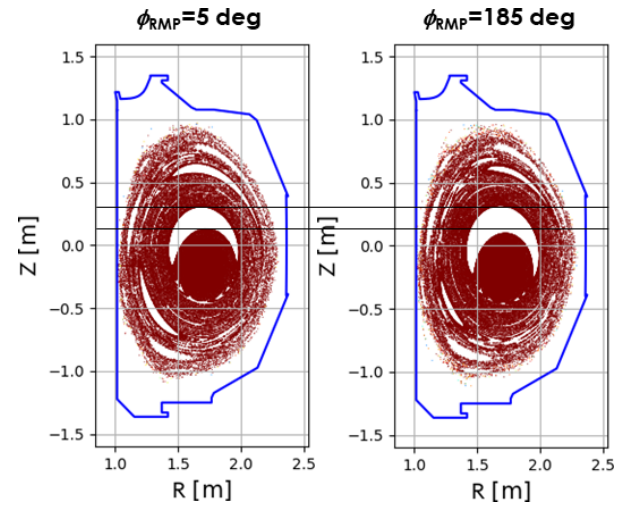


Figure 1. a comparison of the 3D equilibrium for different phases ($\phi_{RMP}=5$ or 185) of the RMP field.

In stellarator studies, the RMP experiment was conducted in the LHD. This experiment was done as part of a collaboration between DIII-D and LHD to expand our physics basis for the effects of the magnetic topology on transport, stability and plasma-surfaces interactions. In DIII-D it is found that locked $m/n=2/1$ core magnetic islands cause a non-axisymmetric distribution of the heat and particle flux on the divertor target plates. It has been hypothesized that a helical current in the $2/1$ island perturbs the axisymmetric separatrix resulting in the toroidally asymmetric distribution. If this is the case, the $2/1$ helical magnetic field from the current in the locked mode acts on the separatrix in the same way as the 3D field from external magnetic perturbation coils used to suppress ELMs and correct field-errors.

Power Loss of High Harmonic Fast Wave in SOL

Category: FPPC – MHD

Year-Number: 2011-FP3-3

Name: ¹T. Oosako, ²J. Hosea

Affiliation: ¹Univ. Tokyo, ²PPPL

Plasma heating and current drive using RF waves are important issues for the realization of a tokamak fusion reactor. Losses of wave power in the scrape-off layer (SOL) in the ion-cyclotron and lower hybrid frequency ranges have been reported from many tokamaks worldwide. In addition to degrading the effectiveness of heating and current drive in the plasma core, the electrons accelerated by the waves in the SOL can strike the antenna or vacuum vessel wall and cause hot spots or damage to internal hardware. Although many mechanisms have been proposed, the details of the mechanism have not been determined. This personnel exchange was performed to analyze data at PPPL in order to clarify the mechanisms responsible for these phenomena.

Electron heating and current drive experiments using the high harmonic fast wave (HHFW) are being performed on NSTX at PPPL. In these experiments, visible light emission localized in a spiral structure in the SOL has been observed during HHFW injection. This is most likely related to the RF power loss in the SOL. However, the exact mechanism has not

been identified. There are efforts to understand the SOL power loss mechanism by RF simulation codes such as TORIC, AORSA, and GENRAY. The present work can provide feedback from experimental observations and analyses to the simulation results and future experiments. At the University of Tokyo, HHFW experiments are being carried out on the UTST spherical tokamak device. Comparison of analysis results between the two devices may lead to advancing the understanding of common physics.

During the present personnel exchange, data from probes and reflectometer installed on NSTX were analyzed to understand the cause of RF power loss in the SOL. These data were digitized by AD convertors at a sampling frequency of 100 MHz. These data were analyzed by performing fast Fourier transform (FFT) on the data viewer based on LabVIEW. The frequency spectra were compared under different conditions. Differences in the frequency spectra were observed for different wavenumbers of the launched HHFW. In particular, when lower wavenumbers are excited, pronounced decay wave components due to the parametric instability were observed. In addition, from the time evolution of these data, it was found that these instabilities occur intermittently in bursts. These new findings will contribute to the understanding of the physical mechanism responsible for RF power losses in the SOL.

3-D magnetic field effects on MHD control

Category: FPPC - MHD

Name: S. Masamune/ M. Okabayashi

Affiliation: Kyoto Institute of Technology (Now Chubu University)/PPPL

In the last decades magnetic perturbation with 3-D structure, either resonant or non-resonant, has attracted much attention because of its effect on MHD equilibrium and stability in toroidal fusion devices. Even in axisymmetric toroidal configuration such as tokamak and RFP, 3-D structure arising from external magnetic perturbation, i.e., magnetic island, stochastic region and self-organized core structure has been recognized, and extensive studies have been performed. In toroidal configuration without symmetry, i.e., helical fusion devices, has advanced with new important results, has revealed commonality and difference in MHD physics between axisymmetric and asymmetric toroidal fusion devices. ITER operation scenario requires deep understanding of the core helical field structure, and that is also the case with RFP for confinement improvement in otherwise stochastic core region.

Under these circumstances, a series of US-Japan MHD Workshops (US-J MHD WS for short) were held every year in turn in Japan and the United States. When held in Japan, it was organized as a joint meeting with ITPA MHD and Disruption Control Topical Group meeting (ITPA MHD TG) and ITPA Energetic Particles Topical Group meeting (ITPA EP TG), and in the US, it was a joint meeting with the US MHD Control Workshop (US NHD WS).

There follows a list of the Workshops with the numbers of participants and presentations, and with some topics.

FY2011(FP3-6): Joint meeting of US-J MHD WS, ITPA MHD TG and ITPA EP TG, “Effect of 3-D magnetic field on MHD equilibrium and stability: toward optimum control of toroidal plasmas”, March 5-7 2012, NIFS, with 83 participants and 33 presentations (for US-J WS part). Overview presentations from LHD, DIII-D, MST and AUP were presented. The topics were roles of magnetic islands and stochastic region in the interaction between energetic particles and 3-D field, roles of plasma flow in 3-D MHD stability, 3-D equilibrium and its stability, reconstruction of 3-D equilibrium, RWM control in high-beta regime, islands and sawteeth in tokamak, and neoclassical toroidal viscosity (NTV) issues.

FY2013(FP3-4): Joint meeting of US-J MHD WS and ITPA MHD TG, “3-D effect on MHD control: the roles of magnetic island and stochasticity in optimum MHD control”, March 10-12 2014, NIFS, with 65 participants and 30 presentations. Overview from LHD and DIII-D were presented. Round table discussion session on “RMP issues – present understanding and prospect” was set for information exchange among tokamak, helical system, RFP and ITER.

FY2014(FP3-1): Joint meeting of US-J MHD WS and US MHD WS, “Fundamental understanding of 3-D magnetic field effects in various toroidal fusion devices”, November 3-5 2014, Auburn University, with 50 participants and 38 presentations. Special session on “Using internal coils for MHD control” was set, where historical review, status in the operating machines, and design and analysis in tokamaks under construction including ITER were reported.

FY2015(FP3-7): Joint meeting of the US-J MHD WS and ITPA MHD TG, “Fundamental Understanding of 3-D magnetic field effects for further optimization of operating scenarios for fusion devices”, March 7-9 2016, NIFS, with 67 participants and 44 presentations. Overview from LHD, including first results from Deuterium experiment, and DIII-D were presented. Round table discussion session on “MHD issues for operation and control in DEMO” was set to clarify the MHD control issues in DEMO.

FY2016(FP3-1): Joint meeting of US-J MHD WS and US MHD WS, “3-D equilibrium and control for optimization of fusion devices”, November 7-9 2016, GA, with 47 participants and 37 presentations.

FY2017(FP3-5): Joint meeting of US-J MHD WS and ITPA MHD TG, “Toward development of integrated studies of 3-D magnetic field effect in fusion devices”, March 5-7 2018, Naka Fusion Institute, QST, with 63 participants and 25 presentations. In the discussion session for the future of the US-J MHD WS, the following points were raised; (i) Joint meeting (with ITPA MHD TG and US MHD WS) is favored by the attendees because of the wider topics of the US-J MHD WS. (ii) Efforts should be made to encourage EU colleagues (from W7-X and other devices) to attend the US-J MHD WS. (iii) MHD issues associated with DEMO could be important topics in a longer time scope. At a special session for JT-60SA, status of the Broader Approach (BA) project was reported. MHD research plans on JT-60SA were also reported from both Japan and EU teams.

FY2018(FP3-2): Joint meeting of US-J MHD WS and US MHD WS, “Toward development of integrated studies of 3-D magnetic field effect in fusion devices”, November 12-14 2018, UCLA, with 50 participants and 34 presentations. Special session on “MHD challenges across devices” was set as an outcome of the discussion in the previous Workshop at QST. Machine learning was one of the emerging topics.

Although the US-J MHD WS proposals for FY 2019 and 2020 were approved, the meetings were canceled because of the COVID-19 pandemic. The US-J MHD WS has played, and will play also in the future, its unique roles in fertilizing 3-D MHD physics among various fusion devices.

US-Japan Workshop on the Physics of Spherical Tokamak Plasmas (2011)

Category: FPPC - MHD

Year-Number: 2011-FP3-5

Name: ¹Y. Takase, ²M. Peng

Affiliation: ¹Univ. Tokyo, ²ORNL

This workshop was held jointly with the 16th International ST Workshop under the IEA Implementing Agreement on ST and the 5th IAEA Technical Meeting on ST for four days (September 27-30, 2011) at NIFS. For this reason, there were 67 participants representing 21 organizations from nine countries (including 26 graduate students), among which there were 10 participants from the US and 42 participants from Japan. Out of the 56 presentations, there were 11 oral and six poster presentations from the US, and 15 oral and nine poster presentations from Japan. Because the workshop was held at NIFS, there were many observers from outside the ST research community. There were also three presentations related to LHD research, before the LHD tour.

NSTX (PPPL) reported improvement of H-mode, reduction of C impurity, and improvement of operation efficiency by the use of liquid Li divertor. Li concentration in the core was low. It was shown that the snowflake divertor is useful for reducing the divertor heat flux. Successful current drive by HHFW and 300 kA Ip formation by CHI were reported. Using an advanced control algorithm, high elongation ($\kappa = 2.7$) and high shape factor ($S = 40$) operation became possible, allowing reliable simultaneous achievement of high normalized beta ($\beta_N = 6$), high noninductive current fraction, and high confinement. LTX (PPPL) reported a large

confinement improvement by the use of liquid Li at high wall temperature. Pegasus (U. Wisconsin) reported plasma startup to $I_p = 170$ kA using local helicity injection.

QUEST (Kyushu U.) has achieved $I_p = 100$ kA by OH and 20 kA by ECCD. It aims for steady-stat operation and particle control by high temperature W wall. LATE (Kyoto U.) has achieved $I_p = 20$ kA. Because the density is 10 times the cutoff density, CD is attributed to EBW. Ion beam probe is being prepared for potential profile measurement. HIST (U. Hyogo) has achieved I_p increase by double-pulse CHI, and its mechanism is identified as MHD dynamo and Hall dynamo. On TS-3, TS-4 and UTST (U. Tokyo) mechanisms of ion heating and electron heating are being investigated in detail. On TST-2 (U. Tokyo) plasma startup to $I_p = 15$ kA has been achieved by LHCD. The formation process of energetic electrons is being studied using X-ray diagnostics. Initial experiment has begun on Tokastar-2 (Nagoya U.) which is an ST with outboard helical coils. A conceptual study of an ST reactor with superconducting coils was presented.

In the afternoon of the final day, we held a special session on US-Japan collaboration, where possible future collaborative activities were discussed. The US has a special situation that NSTX will not operate for about two years because of its major upgrade to NSTX-U. During this period, some NSTX researchers will work at other labs including overseas. To facilitate discussion of collaboration possibilities using Japanese ST devices, it is agreed that Japan will provide information on research activities and immediate future plans of various ST groups to the US.

	Sep. 27 (Tue.)	Sep. 28 (Wed.)	Sep. 29 (Thu.)	Sep. 30 (Fri.)				
9:00	9:00 Opening 3 speeches 9:30 Group Photo	Nagayama	Session 28-1 9:00 Yono 28-1-1i 9:40 Fonck 28-1-2i	Peng	Session 29-1 9:00 Menard 29-1-1i 9:40 Yamada 29-1-2 10:05 Maingi 29-1-3	Lloyd	Session 30-1 9:00 Peng 30-1-1i 9:40 Majeski 30-1-2 10:05 Gates 30-1-3	M.Ono
10:00	10:00 Registration	Takase	10:20 Coffee Break	Tan	10:30 Coffee Break	Yamazaki	10:30 Coffee Break	Hanada
11:00	Session 27-1 11:10 MOOno 27-1-1i 11:50 Lloyd 27-1-2i	Fonck	Session 28-2 10:50 Nishino 28-2-1 11:15 Tanaka 28-2-2 11:40 Wakatsuki 28-2-4	13:00	Session 29-2 11:00 Tritz 29-2-1 11:25 McClements 29-2-2 11:50 Nagashima 29-2-3 12:15 Garzotti 29-2-4	Menard	Session 30-2 11:00 Nagayama 30-2-1i 11:40 Yamazaki 30-2-2 12:05 Ban 30-2-3	Peng
12:00	12:30 Lunch		12:05 Lunch	13:00	12:40 Lunch		12:30 Lunch	
13:00					Session 29-3 13:40 Tan 29-3-1i 14:20 Hasegawa 29-3-2 14:45 Hwang 29-3-3 15:10 Chung 29-3-4 15:35 Coffee Break	Sato	13:30 Session 30-3 (ST Review Paper Disc) (Summary & Closing) 15:00 90	Takase
14:00	13:30 Hanada 27-2-1i 14:10 Idei 27-2-2 14:35 Uchida 27-2-3 15:00 Watanabe 27-2-4		13:30 Session 28-3P poster 28-3P-1~21 15:45	16:00	Session 29-4 16:05 Mutoh 29-4-1 16:40 Suzuki 29-4-2 17:05 Kobayashi 29-4-3 17:30 Dinner		15:00 US-J collaboration discussion 16:00 60	
15:00	15:25 Coffee Break	McClements						
16:00	Session 27-3 15:55 Raman 27-3-1 16:20 Nagata 27-3-2 16:45 Victor 27-3-3		Excursion hot spring	18:00	18:30 LHD Tour IEA IA ExCo 20:00		18:00	
17:00	17:10		19:00 Banquet	21:00			20:00	LHD Tour
18:00	17:30 Japan ST Committee 20:00							

Figure 1. Program of the US-J ST Workshop, held jointly with IEA International ST Workshop and IEA ST Technical Meeting.

3.4.3 Confinement

Collaborative exchanges in the area of Confinement includes joint workshops and personnel exchanges. This includes 21 workshop exchanges, and 67 personnel exchanges to complete planned R&D. During 2009-2019, a key focus of U.S.-Japan collaborations has been in the area of compact toroids (CT), a field with a primary objective is to generate and sustain high temperature plasmas within magnetic configurations that do not utilize an externally generated toroidal magnetic field. These configurations include the field reversed configuration (FRC), reversed field pinch (RFP), and spheromak. A centerpiece of the joint collaboration has been the U.S.-Japan Compact Toroid Workshop, held annually and alternating between Japan and the U.S. This report describes aspects of the workshops held during the last decade. The workshop has encouraged continued interactions between CT advocates from educational institutions, national laboratories, and private companies from the U.S. and Canada. Other relevant activities in this area are focused on detailed confinement and transport studies in 3D magnetic configurations including studies in LHD and HSX. The summaries in this section mention notable scientific highlights including:

- suppression of the $n=2$ rotational instability using a saddle coil in the C-2 facility;
- active density control in C-2U/2W using spheromak-like CT injection;
- successful merging of super-Alfvénic FRCs in the FAT-CM device;
- generation of fast electrons by reconnection electric fields during the merging process;
- establishment of an advanced divertor operation in C-2W;
- partial penetration of the CT into plasmas in the JFT-2M tokamak;
- advanced plasma diagnostic development in RELAX RFP;
- comparison of fluctuation amplitudes computed with NIMROD to MST and RELAX;
- comparisons of non-local transport in TFTR and LHD plasmas;
- benchmarking of turbulence growth rates in LHD plasmas with transport barriers;
- comparison of impurity confinement times using a laser blow off system in HSX;
- demonstration of toroidal flow generation by ECH in HSX;
- reduced turbulent fluctuations and increased plasma temperature, stored energy and energy confinement time in LHD using an impurity powder dropper;
- demonstration of superior recycling control and improved density control across many configurations using a closed divertor in LHD; and
- the application of the XGC code, which has been extended to stellarator/heliotron geometries, to study improved confinement regimes in LHD.

High-Field-Side Injection of RF to Excite Electron Bernstein Waves

Category: FPPC - Confinement

Name: ¹R. Yoneda, ¹H. Elserafy, ¹S. Kojima, ²N.

Bertelli, ¹K. Hanada, ²M. Ono

Affiliation: ¹Kyushu University, Kyushu, Japan ,

²Princeton Plasma Physics Laboratory, Princeton, NJ, USA

Excitation of electron Bernstein wave (EBW) is expected to result in highly efficient heating of magnetized plasmas. The EBW can propagate as an electrostatic wave in the over-dense regime and be strongly damped near the electron cyclotron resonance (ECR) layers. The significance of EBW is often referred in the context of over-dense plasmas, where the electron plasma frequency ω_{pe} is larger than the electron cyclotron frequency Ω_{ce} ($\omega_{pe} / \Omega_{ce} > 1$) but also in the initial phase of the discharge where efficient collisional damping of the EBW is expected since the group velocity of the EBW is comparable with electron thermal velocity.

In Q-shu University Experiments with Stead-state Spherical Tokamak (QUEST), we have demonstrated a feasibility study of High Field Side (HFS) RF injection for EBW by GENRAY ray tracing code and a fundamental experiment for EBW excitation. To excite EBW, delivering eXtraordinary-mode (X-mode) to

upper hybrid resonance (UHR) from HFS is necessary. By GENRAY, mode conversion of X-mode to EBW and absorption and current drive have been analyzed¹⁾. The results showed that in the early stage of plasma start-up, when ECR and UHR layers are close to each other, efficient and localized heating by EBW is attainable. Secondly, for increased n_e , we showed that the HFS scenario spontaneously shifts to current drive as T_e increases. This shift can be explained by the transition of heating mechanism from collisional to electron cyclotron damping.

The direct X-mode injection from HFS has a technical difficulty that the RF must pass through the ECR layer located inside the waveguide. The detailed design of RF waveguide can be found in Ref. 2²⁾. We have successfully delivered RF power of 40kW from HFS without breakdown inside the waveguide. The produced plasma by HFS injection was compared to Low Field Side (LFS) one. Our experimental results showed that HFS injection of X-mode via waveguides gives a much higher EBW absorption efficiency than that of the multi-reflection effect of LFS O-mode one, evidenced by the camera image brightness, the interferometer measurement, and RF leakage monitors.

Future work includes further wall regulation to reduce the impurity level and increase the plasma current, which would then allow for testing of EBW current drive.

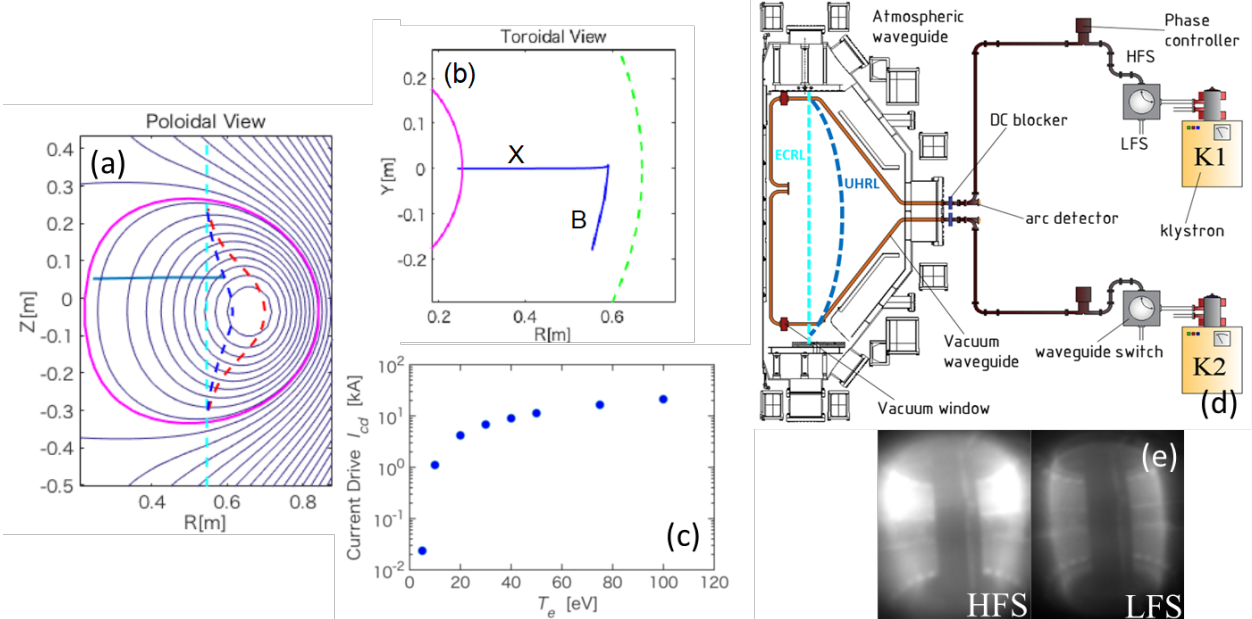


Figure 1. Low-density regime. (a) Poloidal view of raytracing. Light blue dotted line is 1st ECR, red dotted line is R-cut off, blue dotted line is UHR, and magenta line is last closed flux surface. 1st ECR and UHR are located close to each other. (b) Toroidal view of raytracing. Green dotted line is the magnetic axis. (c) Dependence of the net current drive I_{cd} with different T_e by GENRAY. (d) Setup for power delivery from LFS to HFS in QUEST, where K1 and K2 are the two klystrons, each having a maximum input power of 25kW. (e) Fast camera brightness comparison of HFS and LFS RF injection.

¹⁾R. Yoneda et al., Plasma. Fusion. Res. 13 (2018) 3402115

²⁾H. Elserafy et al., Plasma Phys. Control. Fusion 62 (2020) 03501

Innovative technologies for high-beta confinements

Category: FPPC - Confinement

Name: T. Takahashi / B. A. Nelson (retired)

Affiliation: Gunma University / University of Washington

The US-Japan Workshop was held jointly with ICC (Innovative Confinement Concepts Workshop), hosted by the University of Washington from August 15th to 20th, 2011. The HIT-SI supplies world-leading data in helicity-injection experiments, and the Plasma Science Innovation center has collaborated with multiple experimental facilities in the United States in theoretical simulation research. For this reason, many CT researchers participated in the workshop, and the laboratory tours conducted during the workshop were also meaningful.

The research results reported at the workshop are shown below.

The feature of merging FRCs is that they can maintain a relatively high magnetic flux, which is attractive as an NBI target. There is a simulation result by a US researcher that the density ratio of high-energy ions to thermal ions needs to exceed the threshold for stabilization of NB injected FRCs, and this verification is necessary. Inomoto reported the results of the tangential NBI experiment introduced in the TS-4 device of the University of Tokyo. From the temporal variation of the two-dimensional magnetic field structure, stabilization by tangential NBI and extension of configuration lifetime were observed. Ono of the University of Tokyo also reported on the results of magnetic reconnection heating experiments on TS-3, TS-4, and UTST devices. Ion temperature measurement was performed by the two-dimensional Doppler imaging method, and it was clarified that two high-ion-temperature regions were observed on the downstream side of the magnetic reconnection region.

Nagata of the University of Hyogo reported on a multi-pulse coaxial helicity injection (CHI) experiment aimed at amplifying and maintaining the magnetic flux of a spherical torus (ST). Observation results on helicity transport from the central open magnetic flux region to the closed magnetic flux region with a diamagnetic structure were reported, and it was shown that the two-fluid Hall dynamo effect contributed to CHI.

Asai of Nihon University reported on some control methods in the theta pinch FRC experimental device NUCTE. Of particular note is the report on the magnetic helicity injection experiment using a magnetized coaxial plasma gun. In the absence of helicity injection, the temporal change in bremsstrahlung intensity shows oscillations with a period of 25 μ s to about 5 μ s after formation. This reflects the rotation of the elliptically-deformed FRC. However, it was found that the onset of oscillation was delayed to about 50 μ s after formation when helicity was injected. It was also shown that the magnetic flux decay becomes gentle due to helicity injection.

Takahashi of Gunma University proposes the direct conversion of poloidal magnetic flux to the angular momentum

of plasma as a mechanism of spontaneous toroidal rotation of FRC. In this theory, the angular momentum obtained by the electronic fluid is lost by some anomalous loss mechanism, and only the rotation of the net ion fluid is observed. To elucidate the mechanism of anomalous loss of electron angular momentum, the relationship between the fluctuation of the frequency band, which is about 1/10 of the electron cyclotron frequency, and electron transport was reported. As a result of totaling the electron orbits in the fluctuating field, it was shown that a sudden collapse of the configuration was observed.

Gota reported the results of a C-2 experiment (Tri Alpha Energy) conducted by gathering together US researchers from FRCs. It was reported that when two compact tori (CT) accelerated in the axial direction to about 250 km/s were collided and merged, the merged FRC had a configuration lifetime of more than 1 ms, which is more than twice that of the conventional one without driving the current after formation and performing additional heat. Furthermore, the introduction of a quadrupole saddle coil to suppress $n = 2$ rotational instability and wall conditioning aimed at reducing neutral particles was reported. It was reported that the introduction of these technologies can be expected to further extend the lifetime from the two points of suppressing instability and suppressing high-energy ion loss due to the charge exchange reaction with neutral particles.

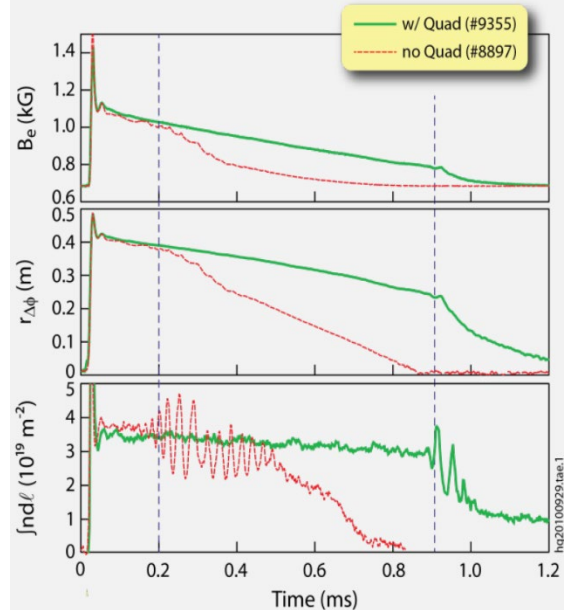


Figure 1. Effect of quadrupole stabilization against the $n = 2$ mode, which can be clearly seen from the amplitude oscillations on the line integrated density. Onset of the $n = 2$ mode is indicated in vertical-dashed-lines.

Advanced control and confinement improvement of innovative compact toroidal configurations

Category: FPPC - Confinement
Name: T. Asai/T. Tajima/B. Victor
Affiliation: e.g., Nihon U/UCI/LLNL

Compact torus (CT) research has been led by Japan and the United States. The U.S.-Japan Science Cooperation Program has provided a framework leading to a cross-sectional understanding of the torus and the contribution of the results in this field to fusion development. Annual U.S.-Japan CT workshops are being held alternately in Japan and the U.S. in the framework.

The field-reversed configuration (FRC), which has the highest beta value of about unity among toroidal confinement systems, is studied under the close cooperation between TAE Technologies and Nihon University¹⁻³⁾. In 2015 and 2016, the U.S.-Japan CT workshop was hosted by Professor Tajima (TAE/UCI) and Professor Asai (Nihon University) in Tokyo (2015) and Irvine (2016). The Workshop in Irvine (Figure1) was held with approximately 70 participants from both Japan and the U.S., and 34 oral presentations were given. This was the same scale as the Exploratory Plasma Research (EPR) workshop (formerly structured as Innovative Confinement Concepts workshop) held every 1.5 years in the U.S.



Figure 1. 2016 U.S.-Japan CT workshop in Irvine, CA.

The most successful US-Japan collaboration in FRC research so far is the active density control of large FRCs in C-2U/C-2W by spheromak-like CT injection. In this research, CT injectors developed by Nihon University were brought to TAE, and particle and magnetic-flux injection experiments have been performed.

The developed CT injectors can fuel $0.5\text{--}1.0 \times 10^{19}$ particles with a 1 kHz repetition frequency. The injection velocity evaluated on a test stand remains in the range of 100 km/s while in a transverse magnetic field even after passing through the 1 m long drift tube. This speed is high enough (in other words, high enough kinetic energy) to penetrate the

external magnetic field of the C-2U FRC. CTs injected perpendicularly to the geometrical axis of the C-2U (Figure 2) demonstrated successful fueling with significant density build-up of 20–30% of the total particle inventory per single CT injection without any serious deleterious effects on FRCs. The global wobble motion driven by the CT injection can be suppressed by counter CT injection⁴⁾. An effective technique of particle fueling is a common development issue in any magnetically confined fusion reactor. This work would provide an effective fueling technique for magnetically confined plasmas.

The developed CT injector is expanding the U.S.-Japan collaborative research to other CT experiments. The 1st generation injector was transferred to the University of Wisconsin-Madison after the initial series of C-2U experiments, and installed on the Big Red Ball facility for shock wave excitation experiments. UW-Madison group has constructed two brand-new CT injectors based on the design of the loaned original injector and further explored their experiments.

Furthermore, a high-flux FRC generation via compact-toroid merging using the developed CT injectors has been proposed as a collaboration among TAE, Princeton Plasma Physics Lab and Nihon University. To reach plasma parameter levels required for successful energy generation the FRC must maintain high particle density and large trapped-magnetic-flux density. Generation of the high-flux FRC core is essential to the operation and sustainment of a fusion power plant with a cylindrical geometry. Development of these technologies under the U.S.-Japan cooperation will contribute to realizing a CT based fusion reactor.

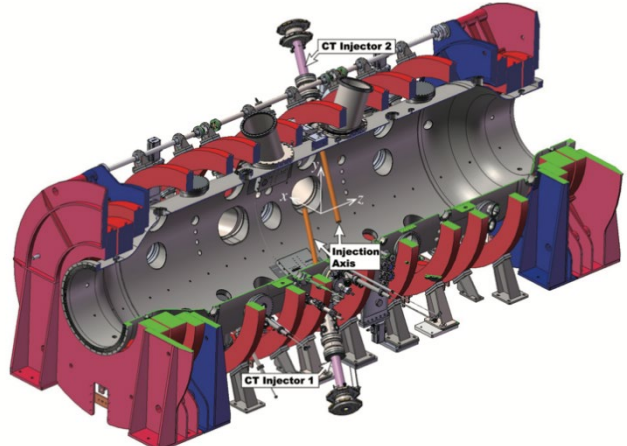


Figure 2. Schematic drawing of CT injector arrangement on the C-2U device at TAE.

¹⁾ H. Goto et al., Nuclear Fusion, 59 (2019) 112009

²⁾ T. Asai et al., Nuclear Fusion, 59 (2019) 056024

³⁾ H. Goto et al., Nuclear Fusion, 57 (2017) 116021

⁴⁾ T. Asai et al., Nuclear Fusion, 57 (2017) 076018

2018 US-Japan CT Workshop- Improved confinement and novel applications of compact tori

Category: FPPC - Confinement

Name: A. C. Hossack, M. Inomoto*

Affiliation: CTfusion, Inc., *Graduate School of Frontier Sciences, The University of Tokyo

This workshop was held in Portland, Oregon from November 2nd to 4th of 2018, the weekend before and co-located with the American Physical Society – Division of Plasma Physics annual meeting. The annual workshop, which alternates between the US and Japan, brings together researchers focusing on compact tori (CTs) since the two countries are world leaders and collaborators on CT research.

The first session covered CT injection, Field-Reversed Configurations (FRCs), and two fluid physics. T. Asai of Nihon University reported on the successful merging of super-Alfvénic FRCs in the FAT-CM device. A greater than two-fold increase in excluded flux and confinement was observed over the single-translation case. T. Takahashi of Gunma University presented results from ion particle / electron fluid hybrid simulations of FRCs with a low frequency wave applied externally. The simulations showed a remarkable reduction in wave amplitude inside the separatrix and anisotropic ion temperature. Retired researcher R. Bourque presented a novel fusion reactor concept based on the RACE program from Lawrence Livermore National Laboratory (LLNL) wherein kinetic energy from highly accelerated, low-beta CTs is converted to thermal energy. H. Gota from TAE Technologies, Inc. presented an overview of recent results from the C-2W device which had recently started up and was already exceeding the performance of the previous C-2U device. L. Steinhauer presented a fast equilibrium solver which can accommodate fully-kinetic ions and finite-beta electrons which is particularly useful for beam-driven FRCs. Finally, H. Himura reported on direct observation of a two-fluid plasma state by extending the ion skin depth in the BX-U linear trap.

The second session included magnetic reconnection, helicity, spherical tokamaks (STs), and the Compact Fusion Reactor (CFR). M. Nagata from the University of Hyogo presented experimental results from plasmoid reconnection and relaxation studies in the HIST device. M. Inomoto from The University of Tokyo showed soft x-ray results from ST merging startup which demonstrate the generation of fast electrons by reconnection electric fields during the merging process. Next, measurements of canonical flux tubes including their helicity and transport in a gyrating plasma kink were presented by J. von der Linden of LLNL. M. Kaur of Swarthmore College presented work on the characterization of turbulence in a magnetized plasma using density and magnetic field fluctuation correlations. Initial results showed a negative correlation between density and magnetic field, much like the solar wind. The final presentation, from J. Heinrich of Lockheed Martin Corporation, was an overview of the CFR project which comprised plasma heating in the T4B and T5 devices.

The concept uses diamagnetic, high-beta, magnetically encapsulated, linear ring cusp plasma confinement.

The next session included the HIT-SI research group, General Fusion, and space propulsion. D. Sutherland of the University of Washington (UW) showed results from his recent addition of an interacting, monatomic neutral fluid into the PSI-Tet 3D, extended-MHD code and validation using two-photon absorption laser induced fluorescence (TALIF) measurements. A. Hossack, presenting results from work at UW, showed the design and initial measurements from a tomography system which observed two neutral helium emission lines to deduce electron density profiles. K. Morgan, also from UW, showed extended-MHD simulation results from a 2.5x scaled-up version of the HIT-SI device where closed-flux volumes persist for up to 20 helicity injector periods (1.3 ms) and undergo a sawtooth cycle. The final presentation from UW was by J. Penna who showed NIMROD MHD simulation results of the HIT-SI3 device compared with experimental data. Next, J. Thomas presented novel concepts for space propulsion using CT ejection from spacecraft. The last talk was by M. Laberge of General Fusion. He gave an overview of General Fusion's concept wherein an ST plasma is compressed by a liquid metal wall which is driven by pistons.

All presenters displayed their slides in a poster session along with five poster-only presentations. D. Schaffner from Bryn Mawr College showed initial results from the Bryn Mawr Magnetohydrodynamic Experiment (BMX) which studies turbulence in a coaxial plasma gun discharge. S. Kawai of Nihon University presented a three-phase rotating magnetic field system for compact plasma sources. T. Seki showed initial results from a tracer-contained compact toroid (TCCT) injection system which is used to study impurity transport from the core of target plasmas. T. Jarboe from UW presented theoretical work on self-organization of kink-stable equilibria including the Taylor minimum energy principle, imposed-dynamo current drive, dynamic stabilization, velocity gradient stabilization, and pressure-driven current penetration. Finally, C. Everson, also from UW, detailed the upgraded Thomson scattering diagnostic on HIT-SI3 which involves new band-pass filters enabling lower temperature measurements and avoidance of impurity lines.

A banquet dinner was held during which plans for the next CT workshop were discussed. The following day, an open discussion was held on the future of CT research and the US-Japan workshop. A general theme of the discussion was the desire to have increased engagement with the tokamak and stellarator communities for the benefit of all involved.

Frontiers of Physics in High Performance Compact Tori

Category: FPPC – Confinement

Name: L. Steinhauer / T. Takahashi

Affiliation: TAE Technologies / Gunma University

The US-Japan Compact Toroid (CT) workshop is held annually, alternating between Japan and the US. The title of the 2019 workshop was “Frontiers of Physics in High Performance Compact Tori” and it focused on key challenges in CT R&D including the self-organizing process observed in high-beta CT plasmas, two-fluid relaxation, and kinetic effects. Predictive modeling of CTs was called out as a high priority research frontier. The workshop was motivated by the recent improvement in confinement in the Field Reversed Pinch (FRC) mainly pursued by U.S. companies such as TAE Technologies.

During the workshop, a total of 22 results from experimental / theoretical / simulation research were presented orally, including a review lecture on the theory of two-fluid equilibrium and relaxation, and a memorial lecture on the self-organization phenomenon of the high-beta torus plasma reversed field pinch (RFP). Overview talks, delivered in the first half of the workshop, facilitated understanding of the detailed technical talks, scheduled in the latter half of the agenda. A poster session with 10 contributions centered on early career participants.

Several topics were of general interest during the event. A primary point of discussion during the workshop was TAE Technologies' latest experimental device C-2W, which is the world's largest compact torus. The facility is capable of high-powered neutral beam injection (NBI) up to 21 MW, an end-bias system for internal and external divertors, and high-speed external magnetic field control for plasma ramp-up and sustainment. Recent breakthroughs in improving the performance of FRC include 1) establishment of an advanced divertor operation method with end magnetic-field control and end-bias control functions, 2) significant reduction of convective electron energy loss, and 3) steady maintenance up to 30 ms, 4) realization of high-temperature plasma operating

regimes over 3 keV, 5) confirmation of “TAE confinement scaling” under high-electron temperature conditions above 400 eV.

Another main workshop topic involved the coaxial helicity injection experiment at the University of Hyogo's HIST device, where multiple small plasmoid formations were observed on the elongated toroidal current sheet. At Nihon University, the development of tracer-containing CT (TCCT) injection technology is in progress for impurity transport research. The impurities sputtered from the cylindrical electrode are contained in a CT, generated and accelerated by the magnetized coaxial plasma gun. They are accelerated and ejected up to 100 km/s. Translation of impurity-containing CT has been confirmed in both the test equipment of Nihon University and TAE Technologies.

Similar to previous workshops, the 2019 event prompted a vigorous interaction, including contributions by several young scientists and graduate students. The workshop reported significant advances, especially in FRC research. Several institutions participated at a significant level including The University of Tokyo, Nihon and Gunma Universities (Japan), General Fusion (Canada), the University of Washington and TAE Technologies (US).

Long-time participants of US-Japan CT workshop strongly encourage increased participation in the workshop from CT-relevant R&D programs including new programs under ARPA-E, and the INFUSE program supported by the Fusion Energy Sciences program within the DOE Office of Science. It is hoped that the emerging thrust for PPP (public-private partnerships) will strengthen CT research, better connect private and public connections, and perhaps stabilize public investment.

Study of Improvement in Plasma Confinement with Compact Toroid Injector

Category: FPPC - Confinement

Name: ¹R. Raman, ²N. Tamura

Affiliation: ¹University of Washington, Seattle, USA

²National Institute for Fusion Science, Toki-shi, Japan.

The Compact Toroid (CT) injection concept was first proposed by Perkins and Hammer of the Lawrence Livermore National Laboratory in the USA ¹⁾. In this approach, a small (few liters in volume) spheromak plasma is formed and accelerated to very high velocities of the order of 300 to 1000 km/s using a coaxial rail-gun accelerator. At these velocities, the kinetic energy density ($0.5\rho v^2$) of the high-velocity spheromak plasmoid can exceed the magnetic field line pressure of the target plasma ($B^2/2\mu_0$), and allow the CT to push aside the target magnetic field lines and propagate deep into the tokamak plasma. Here ρ is the plasma density inside the CT, v is the directed CT velocity, and \mathbf{B} is tokamak toroidal field. Inside the tokamak plasma, the CT would deposit the fuel it contained. The need for deep core fueling is also essential for reactors based on the stellarator concept.

Since the CT has high velocity, it also has high momentum. A significant added benefit is that if the CT were to be injected tangentially, it would impart a toroidal momentum to the target plasma and induce toroidal plasma rotation. This feature is significant, perhaps more critical than the fueling aspect itself, because present high-performance tokamak plasmas rely on the tangential momentum injected by neutral beams to induce toroidal rotation and generate rotation shear to improve plasma stability limits. As the fusion generated isotropic alpha particles in a burning plasma reactor provide the needed heating power, there is no need for neutral beam injection to heat the plasma, so alternate methods may need to be developed to induce rotation and rotation shear. The CT has the potential benefit that it can provide both density profile control (required for maximizing the bootstrap current drive and thus reduce auxiliary current drive power) and toroidal momentum injection at the same time.

Initial results on CT injection were encouraging, including plasma confinement improvement on TdeV ²⁾ and discharge transition to an H-Mode on STOR-M ³⁾. Through collaborative efforts, this led to an active program in Japan. First, an experiment was built for the JFT-2M tokamak. Results obtained on JFT-2M produced results similar to the other results showing partial penetration of the CT into the plasma discharge ⁴⁾. A conceptual design study for the JT-60U tokamak was also conducted ⁵⁾. Shown in Figure 1 is an injector that was also built for the LHD device at NIFS ⁶⁾. More recently, the first stage of a CT injector was used for low-velocity CT fueling of the FRC

plasma ⁷⁾ at TAE Technologies in the USA. CT injection experiments were also carried out on the QUEST ST.

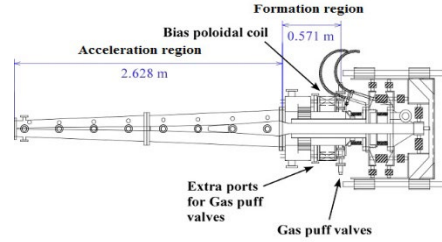


Figure 1. SPICA CT injector for LHD⁸⁾.

An important technical difficulty with these CT experiments was the lack of sufficient CT kinetic energy for penetrating the 2T magnetic fields. The second difficulty was the large relative size of the CT with respect to the target tokamak's poloidal cross-section. Finally, spheromak plasma generated by the early injectors tended to be long in length and were accompanied by plasma and gas load that exceeded the mass of the CT itself. These issues can be rectified through the proper design of a CT injector so that a short-length CT is the dominant plasma that exits the injector and through careful design of the second stage accelerator to permit higher CT velocities.

Conceptual design studies for ITER indicate that a CT injector for ITER does have the potential for fueling and adequate toroidal momentum injection ⁹⁾. It also suggests that as the tokamak plasma's size increases, it is much easier to reduce the size of the CT in relation to the tokamak plasma cross-section, permitting localized fueling.

Since the promising early work, this research area has been largely stagnant because the CT technology is perceived as being much more complicated than frozen pellet injection. But frozen pellets cannot inject momentum. Their capability for core fueling reactors while ensuring that the optimized pressure profiles needed to maintain a high bootstrap current fraction are yet to be adequately demonstrated. This is mainly because present tokamaks use neutral beams for both imparting the needed toroidal momentum and for core fueling. While this is adequate for present physics studies, it remains to be seen how all this translates to sustain reactor tokamak plasmas, as neutral beams, at present, are not a reactor-relevant technology largely because of the very large fusion neutron shine-through through the large neutral beam ducts. If suitable low-torque plasmas with good stability properties and confinement are not developed within the next decade, it is quite likely that concepts such as CT injection will see a resurgence to support tokamak reactor designs.

¹⁾ L.J. Perkins, S.K. Ho, J.H. Hammer, Nucl. Fusion 28, 1365 (1988)

²⁾ R. Raman, et al., Nuclear Fusion. 37, 967 (1997)

³⁾ C. Xiao, et al., Physics of Plasmas 11, 4041 (2004)

⁴⁾ N. Fukumoto et al., Nucl. Fusion 44, 982 (2004)

⁵⁾ R. Raman and K. Itami, Plasma and Fusion Research, 76, 1079 (2000)

⁶⁾ J. Miyazawa, H. Yamada, O. Motojima, Jpn. J. Appl. Phys. 37, 6620 (1998)

⁷⁾ T. Asai, et al., Nucl. Fusion 57, 076018 (2017)

⁸⁾ D. Liu, et al., J. Plasma Fusion Res. SERIES 8, 999 (2009)

⁹⁾ R. Raman, Fusion Engin. Design, 83, 1368 (2008)

Studies of Neoclassical Effect on Particle Confinement in the RFP

Category: FPPC - Confinement
 Name: S. Masamune, A. Sanpei / J.S. Sarff,
 D.J. Den Hartog, K.J. McCollam
 Affiliation: KIT / Univ. Wisconsin-Madison

The reversed field pinch (RFP) is a high beta, weak external field magnetic confinement system having a potential of attractive Ohmic ignition. Progress in RFP research is described in a major new review paper¹⁾. RELAX at KIT (Kyoto Institute of Technology) is a low-aspect-ratio (low-A) machine whose research aims are focused on the geometrical issues such as MHD relaxation to a helical equilibrium and neoclassical effects in low-A RFP configuration. Collaboration with the MST group at the University of Wisconsin-Madison has been undertaken to boost the research goals on RELAX and MST through diagnostic development and MHD modeling.

Most of the collaboration activities during the period 2010-2020 were devoted to development of temperature diagnostics in RELAX, and implementation of the NIMROD code for nonlinear 3D MHD simulation.

A Thomson scattering diagnostic system was developed to measure the central electron temperature and density on RELAX²⁾. The electron temperature T_{e0} was confirmed to be in the 100-eV range for plasmas with current $I_p = 60\text{-}80\text{ kA}$, reaching $\sim 200\text{ eV}$ in optimized discharges. The density is around $10^{18}\text{-}10^{19}\text{ m}^{-3}$. The central electron beta, defined as the ratio of central electron pressure to edge magnetic pressure, reached $\sim 10\%$ in the optimized conditions, as shown in Figure 1. It is thus confirmed that high-temperature RFP plasmas are obtained in RELAX, with the estimated value of the Lundquist number $10^4\text{-}10^5$.

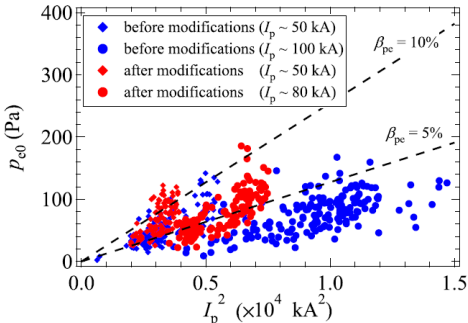


Figure 1. Central electron pressure vs. plasma current squared.

A 2D soft-X ray imaging system was also developed for 2D electron temperature measurements³⁾. As shown in Figure 2, the system consists of two pinholes with thin foils of different

thickness in the SXR camera to record two pinhole images simultaneously on a MCP. Since the viewing areas of these two images are almost the same, and the spatial resolution for each image on the phosphor plate is good, it is straightforward to calculate the ratio of SXR signals and convert them to a line-of-sight estimate of the electron temperature. A change of the 2D electron temperature profile associated with relaxation from axisymmetric to helical RFP state was identified using this imaging diagnostic.

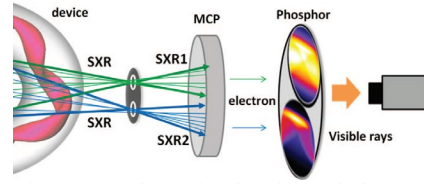


Figure 2. Schematic drawing of the 2D electron temperature measurement system using soft-X ray imaging.

To extend the range of validation of extended MHD models, nonlinear 3D MHD computation for RELAX plasmas was initiated using the NIMROD code. One goal is to compare with NIMROD modeling done for MST as well⁴⁾. As shown in Figure 3, the Lundquist number range of the experimental RELAX plasma is appropriate for direct comparison with NIMROD simulation in low-S regime. RELAX studies allow assessing the effects of extreme toroidal geometry at low A. Initial NIMROD RELAX runs show reasonable agreement of radial profiles of magnetic fluctuation amplitudes. The importance of toroidal mode coupling to RFP dynamics is also shown.

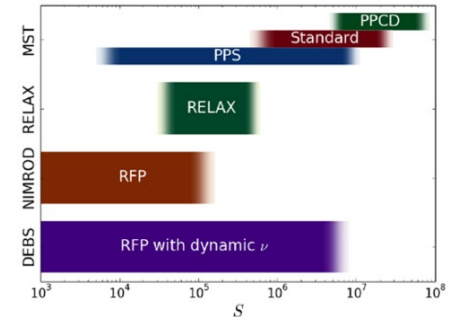


Figure 3. Lundquist number range of MST and RELAX experiments, and NIMROD and DEBS codes.

Following the successful collaboration activities, new topics are emerging for continuing collaboration, such as canonical helicity issues or neoclassical transport studies in helical RFP by global gyro-kinetic simulation. The RFP continues to contribute valuable fusion science studies.

¹⁾ L. Marrelli et al., Nucl. Fusion 61, 023001 (2021)
²⁾ R. Ueba et al., Plasma Fusion Res. 9, 1302009 (2014)
³⁾ K. Nishimura et al., Rev. Sci. Instrum. 85, 033502 (2014)
⁴⁾ K.J. McCollam, Seminar at NIFS, Sep.14, 2017

Comparison Study of a nonlocal transport focused on the spatio-temporal response of local electron temperature gradients

Category: FPPC – Confinement

Year-Number: 2015-FP4-1

Name: N. Tamura/M. Ono

Affiliation: NIFS/PPPL

In magnetically-confined high-temperature plasmas, an abrupt increase in electron temperature of the core plasma has been observed in response to an edge plasma cooling induced by the injection of materials or gas-puffing. This phenomenon, called as “nonlocal transport phenomenon,” is one of the long-standing problems to be clarified in magnetically-confined high-temperature plasmas. The nonlocal transport phenomenon was firstly discovered in the TEXT tokamak¹⁾ in 1995, and then such a phenomenon has been widely observed in many tokamaks. At that time, since there was no observation of the nonlocal transport phenomenon in stellarators^{e.g.2)}, the nonlocal transport phenomenon was considered to be a problem unique to tokamak. However, a discovery of the nonlocal transport phenomenon in the stellarator, Large Helical Device³⁾ in 2005 have made the nonlocal transport phenomenon a common problem in magnetically-confined toroidal plasmas. The experimental study of nonlocal transport phenomenon in LHD has revealed some new features of the nonlocal transport phenomenon, such as a unique spatio-temporal response of local electron temperature gradients.

The discovery of similar mysterious phenomena in toroidal plasmas with different magnetic configurations may lead to a breakthrough in elucidating the physical mechanism of nonlocal transport phenomena through a detailed comparison of the similarities and differences of nonlocal transport phenomenon between tokamaks and stellarators. Therefore, we decided to compare the nonlocal transport phenomena observed in TFTR and LHD under the Japan-US collaboration auspices.

The TFTR was already shut down in 1997. Therefore, in order to perform the detailed comparison, the collection of non-digitized information regarding the experiments is firstly necessary. The collected information, such as timing of intentional or unintentional perturbation at the edge region and TFTR port arrangement, that has been not recorded in the published paper allow us to understand which discharges might have the nonlocal transport phenomenon, and a positional relationship of diagnostics and edge perturbators, such as a laser blow-off, in TFTR. And I have also learned how to use the tools for viewing the experimental data of the TFTR directly from the researcher, Dr. E.D. Fredrickson, who was participated the TFTR experiment at that time. Finally, a research base for comparing the nonlocal transport phenomena observed in TFTR and LHD had been established.

Figure 1 shows the temporal evolution of electron temperature and its gradient at different radii around the time of edge perturbation (drop of a carbon flake in TFTR and injection of a Tracer Encapsulated Solid pellet (TESPEL) in LHD, respectively). As can be seen clearly from Figure 1(a, b), the core electron temperature was similarly increased after the edge cooling in both TFTR and LHD. However, the spatio-temporal evolution of local electron temperature gradient in TFTR is different from that obtained in LHD. In LHD, the elevated electron temperature gradient at the edge region was sustained for a certain time (~ 20 ms). On the other hand, in TFTR, the electron temperature gradient at the edge region was rapidly increased in response to the edge perturbation, but quickly decreased. And then the electron temperature gradient at the edge region was increased again and the second round of increase in electron temperature gradient was propagated from the edge to the core. Therefore, this result clearly indicated that the nonlocal transport phenomena in stellarator, LHD, is qualitatively different from that observed in tokamak, TFTR. The findings in this comparison study provided a useful clue to understand the nonlocal transport phenomena.

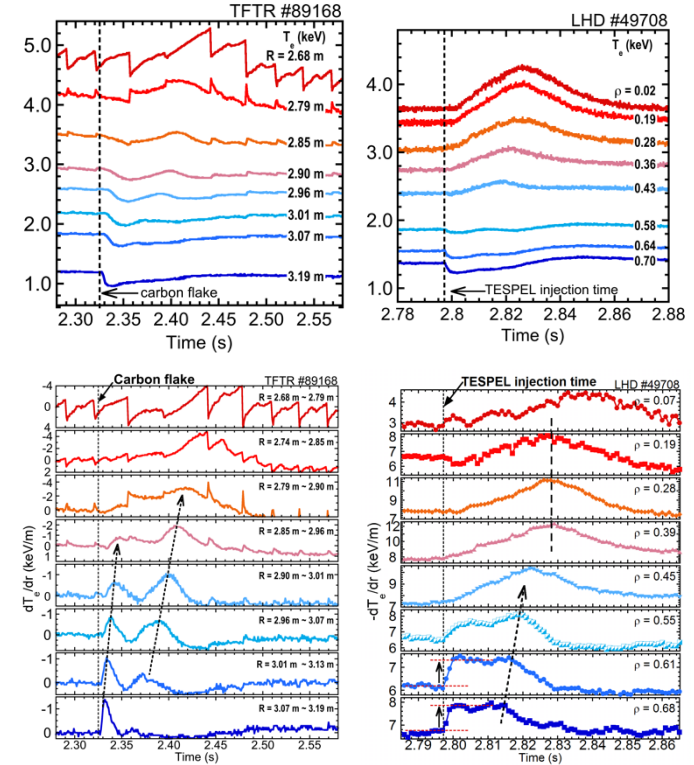


Figure 1. Spatio-temporal evolutions of the electron temperature and its gradient at different radii in (a, c) TFTR and (b, d) LHD

¹⁾ K.W. Gentle et al., Phys. Plasmas, 2 (1995) 2292

²⁾ H. Walter et al., Plasma Phys. Control. Fusion, 40 (1998) 1661

³⁾ N. Tamura et al., Phys. Plasmas, 12 (2005) 110705

Gyrokinetic investigations for helical plasmas using GS2

Category: FPPC - Confinement
 Name: K. Tanaka /D. R. Mikkelsen
 Affiliation: NIFS/PPPL

The gyrokinetic investigations provide essential knowledge to understand the turbulence driven transport physics in toroidal devices. Plenty of the works have been performed in tokamaks, however, much less works are carried out in stellarator/helical devices. The difficulties of gyrokinetic analyses in stellarator/helical devices are due to the complexity of three dimensional magnetic structure. In order to take into account the effects of helical magnetic ripples, much larger number of the resolutions along the magnetic field are required compared with tokamaks. The gyrokinetic investigations in helical plasmas have been carried out by the framework of the Japan/US fusion research collaboration.

The bench marking between two gyrokinetic codes GS2 and GKV were carried out. Both codes are local flux tube codes. GS2 was developed by PPPL/IFS Univ. Texas¹⁾ and GKV was developed by NIFS²⁾. Excellent agreements are found in linear growth rate and real frequency for the ion ITB plasma in LHD³⁾.

The impurity transport in ion ITB of LHD was investigated. Three ion species (H^+ , He^{2+} , C^{6+}) and the electrons are treated kinetically, including collisions. Figure 1 was time trace of ion ITB plasma. At $t=4.56$ sec, a carbon pellet was injected. During decay of electron density, T_i increased and C^{6+} profile became hollow. The C^{6+} profiles became hollower at later timing as shown in Figure 2.

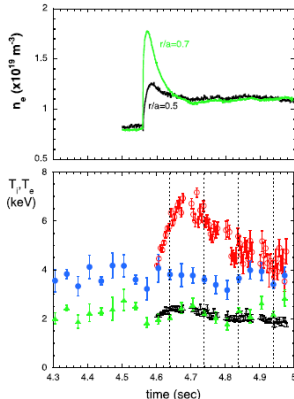


Figure 1. Electron density at $r/a=0.5$ and 0.7 ; temperature at $r/a=0$ (circles) and 0.7 (triangles), filled symbols for electrons, outline symbols for ions. The four vertical dashed lines denote the simulation times⁴.

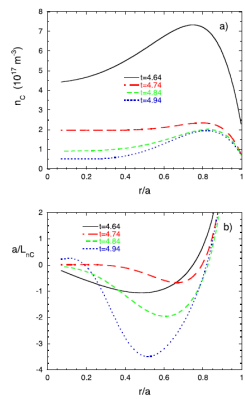


Figure 2. At four simulation times, profiles of (a) carbon density and (b) carbon density gradient parameter⁴.

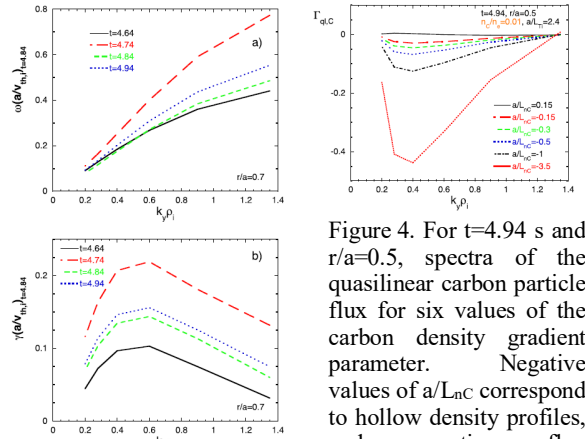


Figure 3. Normalized frequency spectra and growth rate spectra for $r/a=0.7$ at $t=4.64$ s (solid), 4.74 s (long dashes), 4.84 s (short dashes), and 4.94 s (very short dashes). The normalizing rate for $t=4.84$ s is used for all times.

Figure 3 shows growth rate and real frequency at for different timings at $r/a=0.7$. The dominant instabilities were ion temperature gradient mode. At $t=4.94$ sec, when C^{6+} profile becomes the hollowest, quasi-linear carbon particle fluxes were estimated as shown in Figure 4. With experimental value of C^{6+} normalized gradient, C^{6+} particle flux directs inward. With scan of C^{6+} normalized gradient, zero flux, which is realized in the steady state, required peaked C^{6+} profile. These result does not account for the hollow C^{6+} profile in steady state at $t=4.94$ sec. Additional outwardly directed C^{6+} flux, which is possibly due to the neoclassical effects, are necessary to account for the observations.

Linear analyses were performed for the comparison between H and D plasma in Compact Helical System (CHS) and for the comparison between H and He plasma in LHD. In CHS, lower linear growth rate of the trapped electron mode in D plasma, than in H plasma qualitatively agreed with the reduced particle transport in the D dominant plasma of the low density regime⁵⁾. In LHD, higher T_i in ion ITB in He plasma than in H plasma are consistent to the lower ITG stiffness in He plasma⁶⁾

¹⁾ M. Kotschenreuther, et al, G. Rewoldt, and W. M. Tang, Comp. Phys. Comm. 88, 128 (1995).

²⁾ M. Nunami et al, Plasma Fusion Res. 5, 016 (2010)

³⁾ D. R. Mikkelsen, K. Tanaka et al, Physics of Plasmas 21, 112305 (2014)

⁴⁾ D. R. Mikkelsen, K. Tanaka et al, Physics of Plasmas 21, 082302 (2014)

⁵⁾ K. Tanaka, D. R. Mikkelsen et al, Plasma Phys. Control. Fusion 58 (2016) 055011

⁶⁾ K. Tanaka, D. R. Mikkelsen et al, Nucl. Fusion 57 (2017) 116005

Comparison Study of the impact of magnetic configurations on impurity transport in helical plasmas

Category: FPPC - Confinement
 Name: N. Tamura/S.T.A. Kumar
 Affiliation: NIFS/UW. Madison

In magnetically-confined fusion plasmas, an effective removal of helium ash and other impurities in the core plasma is very important issue to keep a fusion burning process. Especially in stellarator plasmas, since the impact of a radial electric field on neoclassical transport is significant, the problem of impurity control is more important in stellarator than in tokamaks. Therefore, a more precise understanding of impurity transport in stellarator plasmas is highly necessary. Unlike tokamak, there are many variations of magnetic configuration in stellarator devices. This is the reasons why there are many different types of stellarator devices in the world, and why a fundamental optimization of the magnetic configurations in the stellarator concept is still ongoing. In this regard, it is significantly important to understand the impact of magnetic configurations on impurity transport in stellarator plasmas. Therefore, we decided to perform a comparison study of the impact of magnetic configurations on impurity transport in stellarators, Large Helical Device (LHD) and Helically Symmetric eXperiment (HSX) under the Japan-US collaboration auspices. Figure 1 shows the radial profiles of effective ripple in stellarators (LHD, HSX, and TJ-II). As a reference, the radial profile of effective ripple in the spherical tokamak, NSTX is also shown. As can be clearly seen from Figure 1, the radial profile of effective ripple in LHD is quite different from that in HSX. And HSX can change the radial profile of effective ripple drastically. Therefore, such a comparison of the impact of magnetic configurations on impurity transport between LHD and HSX could provide a useful clue to understand the impact of magnetic configurations on impurity transport.

Figure 2 shows a typical temporal evolution of the bolometer signal from the channel looking into the center of HSX plasma. In this case, the magnetic configuration is set to Quasi-Helically Symmetric (QHS) mode and a centrally focused ECH (50 kW) is applied to produce a hydrogen plasma. Here, aluminum (Al) is injected into the plasma by a laser blow-off (LBO). A line-averaged electron density at the time of Al injection is $4.0 \times 10^{18} \text{ m}^{-3}$. In the previous analysis, the impurity confinement time was estimated as 0.3946 ms by fitting the decay of the bolometer signal immediately after the Al-LBO. However, when there are two decay processes in the bolometer signal after the impurity injection, the first decay time can be considered to reflect mainly the ionization process, rather than the impurity transport process. This is because the bolometer measures the emissions from various charge states of impurities ions. I proposed to focus on the second decay process in the temporal evolution of the bolometer signal for estimating the impurity confinement time. As shown in Figure 2, the

impurity confinement time based on the second decay process is estimated as 2.3762 ms, which is comparable to the energy confinement time in similar plasmas.

We had discussed the future experiment for the systematic comparison of impurity transport between HSX and LHD. Then high priorities were given to the study of dependence of impurity transport on background ions, such as hydrogen or helium, and on ECH deposition location. As a diagnostic, in order to estimate the impurity confinement time, the measurement of the temporal evolution of the line emission from the highest charge state impurity ions, which are expected to be existed in the core plasma was proposed.

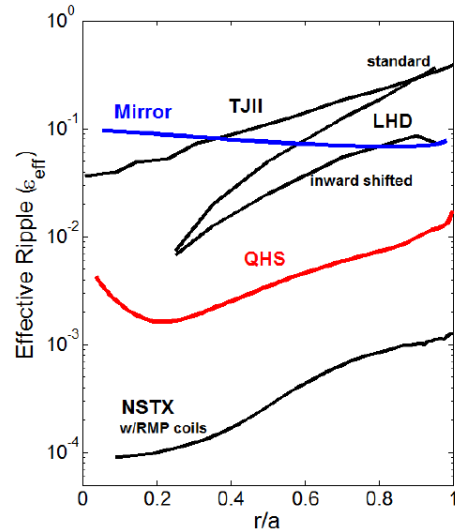


Figure 1. Radial profiles of effective ripple in HSX and HSX with different magnetic configurations. The radial profile of effective ripple in NSTX spherical tokamak is also shown.

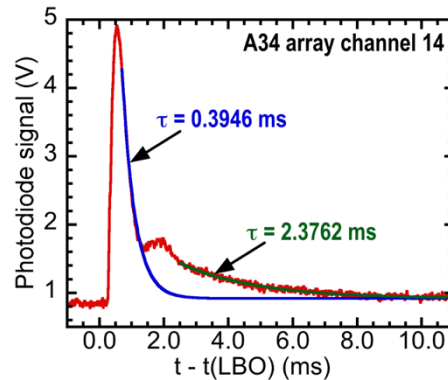


Figure 2. Temporal evolution of the signal of bolometer channel looking into the central region of HSX plasma

Study of toroidal flow generation by ECH in HSX plasma

Category: FPPC - Confinement

Year-Number: 2019-FP4-1

Name: Y. Yamamoto, S. Murakami, S.T.A. Kumar*,

J.N. Talmadge*, K.M. Likin*, D.T. Anderson*

Affiliation: Dpt. of Nuclear Eng., Kyoto Univ.,

* HSX Plasma Laboratory, Univ. of Wisconsin

Recently, spontaneous toroidal flows have been observed in electron cyclotron heating (ECH) plasmas in many tokamak and helical devices. Also, the effects of the magnetic configuration on plasma flow are intensively investigated in HSX. HSX has two typical magnetic configurations: the Quasi-Helically Symmetric (QHS) configuration and the Mirror configuration. The QHS configuration has a quasi-helical symmetry of the $(m, n) = (1, 4)$ mode in the magnetic field strength. The Mirror configuration has additional toroidal mirror terms, the $(m, n) = (0, 4)$ and $(0, 8)$ modes, to break the helical symmetry. The parallel neoclassical viscosity of the QHS configuration is smaller than that of the Mirror configuration, so we expected that the toroidal flow velocity in the QHS configuration would be more significant than that of the Mirror configuration. However, a smaller toroidal flow was observed in the QHS configuration.

ECH can drive the radial electron current j_e due to the radial diffusion of supra-thermal electrons^{1,2)}. The net radial current in the steady state should vanish to maintain the quasi-neutrality, so the return current, j_r ($= -j_e$), flows in the bulk plasma by ambipolar condition. Therefore, the bulk plasma feels the $j_r \times B$ force due to the return current. On the other hand, during the slowing down of the supra-thermal electrons, they transfer their momenta to the bulk plasma due to collisions, which is referred to as the collisional force. To evaluate the forces, we apply the GNET code, which can solve a linearized drift kinetic equation for δf by ECH in 5-D phase space¹⁾. Also, we solve the momentum balance equation to evaluate the toroidal flow velocity driven by the $j_r \times B$ force effect³⁾.

In the perfectly symmetric configuration, the forces in the symmetry direction almost cancel each other. As seen in Figure 1, the $j_r \times B$ force and the collisional force cancel each other, and the component parallel to the helical symmetry direction is quite small in the perfectly helically symmetric configuration. However, non-symmetric magnetic modes enhance the radial current j_e . Even in the QHS configuration the $j_r \times B$ force is dominant, and there is a net force in the symmetry direction due to other small non-symmetric modes. The peak value of the force in Mirror configuration is more than twice as large as that in QHS configuration with the same input power. The collisional force is so small as being negligible in both QHS and Mirror configurations, and we do not include the

collisional force in the momentum balance equation for simplicity. Solving the momentum balance equations, we obtain the flow velocity as shown in Figure 2. Here, we use the absorption power calculated by ray-tracing code, 24kW in QHS configuration and 16kW in Mirror configuration. The evaluated toroidal flow in Mirror configuration is larger than that in QHS configuration except for the peaking around the heating location. The obtained flows have relatively good agreements with the experiments.

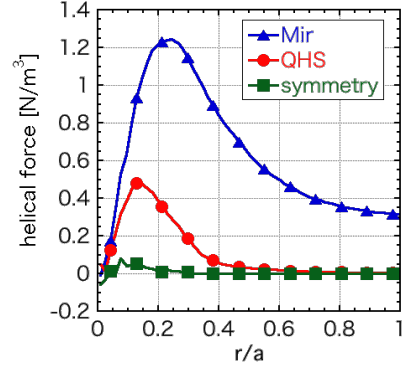


Figure 1. The total helical forces including $j_r \times B$ and collisional forces by 100kW ECH in three configurations.

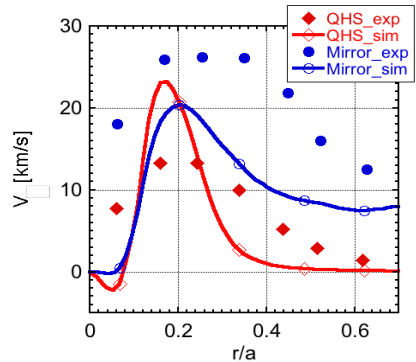


Figure 2. The obtained toroidal flow in QHS (24kW) and Mirror (16kW) configurations. The lines are simulation results and the dots are experimental ones.

¹⁾ S. Murakami, et al., Nucl. Fusion 40 (2000) 693.

²⁾ Y. Yamamoto, et al., Plasma Fusion Res. 14 (2019) 3403105.

³⁾ M. Coronado and J. N. Talmadge, Phys. Fluids B 5, 1200 (1993).

LHD Plasma Performance Improvement With The Impurity Powder Dropper

Category: FPPC - Confinement

Name: N. Ashikawa, S. Masuzaki, M. Shoji, G. Kawamura, A. Nagy*, R. Lunsford*, E. Gilson*, F. Nespoli*, D. Gates*

Affiliation: National Institute for Fusion Science (NIFS), *Princeton Plasma Physics Laboratory (PPPL)

The Impurity Powder Dropper (IPD) is a device designed and built by PPPL for injecting sub-millimeter powder grains into the plasma¹⁾. Its main application is to perform a real-time boronization by injecting boron powder into the plasma, improving wall conditions. To test the viability of this technique in steady-state operation, the IPD was installed on LHD, capable of one-hour long plasma discharge.

The installation took place in September 2019 and was supported by predictive simulations of the penetration of powder grains trajectory into the plasma with the EMC3-EIRENE and DUSTT codes²⁾.

The IPD was used for the first time on LHD in the following experimental campaign (October 2019- February 2020) to inject boron and boron nitride powder into the plasma, demonstrating the successful injection of the powder in the peculiar LHD magnetic geometry, and characterizing the plasma response to the impurity injection³⁾. The evaporation of the boron powder into the plasma was confirmed, among other diagnostics, by UV spectroscopy⁴⁾.

Positive results such as decrease in impurity concentration and wall recycling, both on a shot-to-shot basis and in real time, were observed as a result of the deposition of boron on the plasma facing components due to the powder injection⁵⁾. Modeling of the experiments with the codes EMC3-EIRENE, DUSTT and ERO2.0 suggested that injection of boron powder into low density plasmas results in a more uniformly distributed boron coating, while toroidal asymmetries increase with plasma density⁶⁾.

Further experiments were performed in the 2020-2021 campaign, where the IPD was operated by the NIFS collaborators while the PPPL team participated to the experiments remotely due to the pandemic situation.

To date, the most notable result is the observation of a novel regime characterized by reduced turbulent fluctuations and increased plasma temperature, stored energy and energy

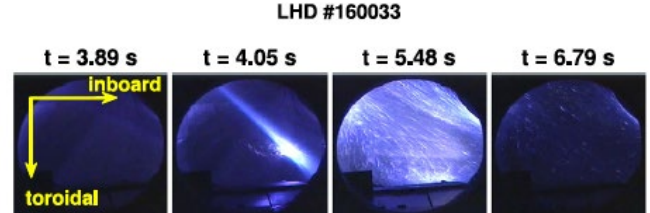


Figure 1. Visible imaging of boron powder injection into the LHD plasma³⁾.

confinement time⁷⁾. The transition to the new regime occurs at constant plasma density and input power, and is triggered by boron powder injection into the plasma. The transition is observed for different plasma heating schemes, working gas isotopes, and both directions of the magnetic field.

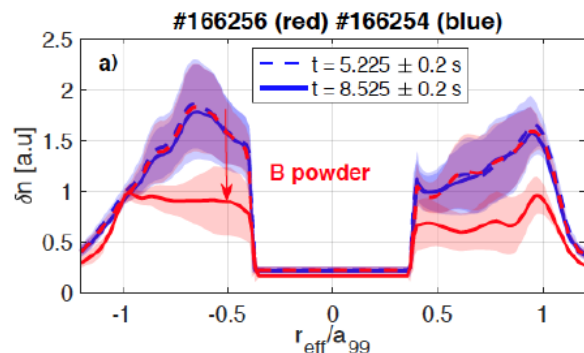


Figure 2: Reduction of turbulent density fluctuations during boron powder injection, measured by 2D Phase Contrast Imaging⁷⁾.

¹⁾ A. Nagy et al., Review of Sci. Instr. 2018

²⁾ M. Shoji et al., Contributions to Plasma Phys. 2019

³⁾ F. Nespoli et al., Nucl. Mater. and Energy 2020

⁴⁾ T. Oishi et al., Plasma Sci. Technol. 2021

⁵⁾ F. Nespoli et al., APS-DPP conference 2020

⁶⁾ M. Shoji et al., Nucl. Mater. and Energy 2020

⁷⁾ F. Nespoli et al., submitted to Nature Physics, 2021

Exploration of particle and helium exhaust with the closed helical divertor at LHD

Category: FPPC - Confinement

Name: O. Schmitz^a, A. Bader^a, S. Sereda^a, M. Kobayashi^b, K. Ida^b, H. Funaba^b, G. Motojima^b
Affiliation: a) University of Wisconsin-Madison,
b) National Institute for Fusion Science

UW-Madison researchers contributed to the exploration of the closed helical divertor that has been gradually implemented since 2015. This major device upgrade entailed equipping the so far open divertor target areas of the helical divertor with baffling structures. These plasma facing components are arranged around the divertor strike line to reduce the likelihood of plasma ions that are neutralized to stream back towards the main plasma. This allows to build up a high neutral gas pressure, which facilitates neutral particle pumping, including impurity exhaust. Also, the condensed neutral gas inside of the divertor chamber in front of the target plates consumes incoming plasma energy flux and hence protects the target surface material from heat loading.

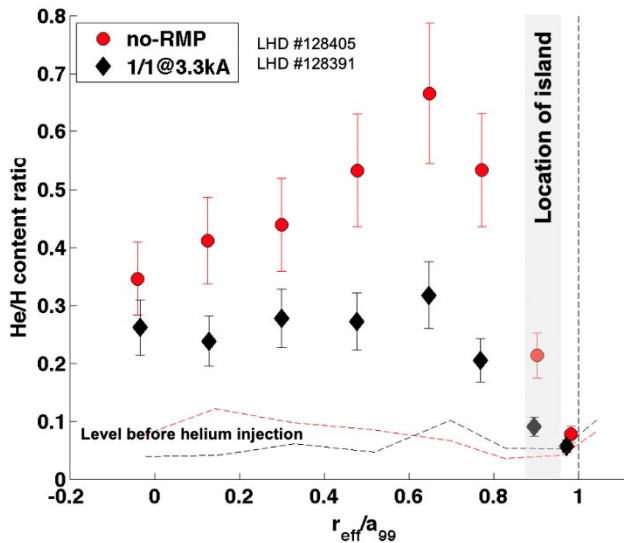


Figure 1. Demonstration of improved helium exhaust characteristics with the closed helical divertor at LHD. Aided by the $m/n=1/1$ resonant magnetic control field, a magnetic island is seeded in the plasma edge that reduces the helium confinement time by 35%. At the same time divertor helium neutral gas increases which facilitates the complete exhaust of this gas, which is the ash of the D-T fusion process

A specific focus of UW students and researchers was to study the impact of this new divertor structure on the recycling properties of the divertor and the access to detachment under the impact of this increased neutral condensation effect. It was demonstrated in collaboration with the NIFS study leads that the closed divertor features a superior recycling control that

provides access to a regime of improved density control across many configurations. A central effort was to shed light into the helium exhaust properties under these conditions. He exhaust is necessary in a fusion device if D-T fusion is used as He is the product of this fusion cycle. It needs to be exhausted in order to keep the hydrogen plasma clean and in a continuous burning plasma regime. It was shown that the application of resonant magnetic fields can aid the helium exhaust substantially with helium confinement times decreased by up to 35%. The high neutral pressure for well recycling discharges is seen to aid this state of improved helium exhaust. New experiments with a larger number of divertor elements closed have been performed recently to disentangle these effects further. Very recently, a U.S. developed neutral gas measurement system, the Wisconsin In-Situ Penning (WISP) gauge, was implemented into one of the divertor pumping ducts to study the local He gas concentration during this promising aspect of the closed helical divertor.

-
- 1) O. Schmitz et al. "Enhancement of helium exhaust by resonant magnetic perturbation fields at LHD and TEXTOR-DED", NF 56 (2016) 106011
 - 2) K. Ida et al. "Helium transport in the core and stochastic edge at LHD" PPCF 58 (2016) 074010
 - 3) A. Bader et al. "Modeling of helium transport and exhaust in the LHD edge", Plasma Phys, Controlled Fusion 58 (2016) 124006

Global gyrokinetic modelling of an improved confinement regime in LHD

Category: FPPC - Confinement

Name: M. D. J. Cole^{a)}, T. Moritaka^{b)}, D. Gates^{a)},
F. Nespoli^{a)}, R. Hager^{a)}, C. S. Chang^{a)}

Affiliation: ^{a)}Princeton Plasma Physics Laboratory
(PPPL), ^{b)}National Institute for Fusion Science (NIFS)

The global gyrokinetic code XGC has been extended for stellarator/heliotron geometries. In other work, the numerical schemes have been described and verification studies performed. These demonstrate the code's capacity to simulate microinstabilities in the linear and nonlinear (turbulent) regimes. This code can then be applied to a variety of problems in fusion physics. One such problem is understanding and predicting the behaviour of impurities in stellarators and, for example, their effect on turbulent transport. This topic is an area of active research and connects with a recent experimental programme at LHD, during which a PPPL powder dropper was installed on the machine and used to introduce boron nitrite during device operation. It was found that this significantly improved plasma performance and led to a higher measured neutron rate. This experimental finding described in greater detail elsewhere, but the effect is briefly illustrated in Figure 1 where we show significantly increased electron temperature with the same heating power after the introduction of boron powder.

It is of interest to understand the mechanism behind this improvement in plasma performance. One possibility, in analogy to low atomic number impurity studies on other machines including tokamaks, is that turbulent transport is reduced. This can be investigated using global gyrokinetic tools such as the XGC stellarator version. It has already been shown that the XGC code can simulate LHD geometry and this capability has been applied to investigate the isotope effect using a quasilinear model (Moritaka *et al.*, FEC 2020).

In order to investigate the impurity performance improvement observed experimentally with our numerical tool, we have set up a series of exploratory electrostatic gyrokinetic turbulence runs with a range of parameterised temperature and density profiles, as well as the experimentally measured profiles. In Figure 2, we show the calculated Ion Temperature Gradient-driven (ITG) mode eigenfunction calculated with a localised temperature gradient parameterised by scale length $a/L_T = 3.0$.

In ongoing work, we are performing large simulations with the experimentally measured temperature and density profiles into the nonlinear regime, which the aim of comparing the steady state heat flux due to electrostatic ITG turbulence in each case and at each radial location. In the outlook, we will extend this work to include kinetic electrons and electromagnetic effects, introducing trapped electron mode-driven turbulence, and consider the possibility of extending the simulations to the first wall with self-consistent treatment of the boron impurities. The XGC self-consistent impurity and kinetic electron/electromagnetic capabilities have

recently been introduced and benchmarked with tokamak cases and are actively being incorporated into the stellarator version. This case is envisioned to eventually profile the first opportunity to rigorously verify a stellarator gyrokinetic code directly against an experiment.

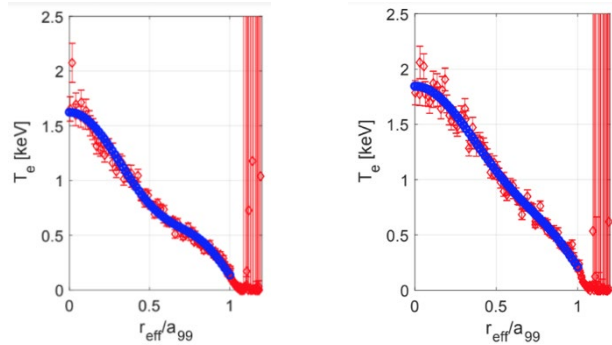


Figure 1. Comparison of the electron temperature, T_e , before (left) and after (right) boron powder is introduced into LHD in shot #166256. A significant increase is seen with otherwise similar density profiles, for an increase in overall plasma pressure

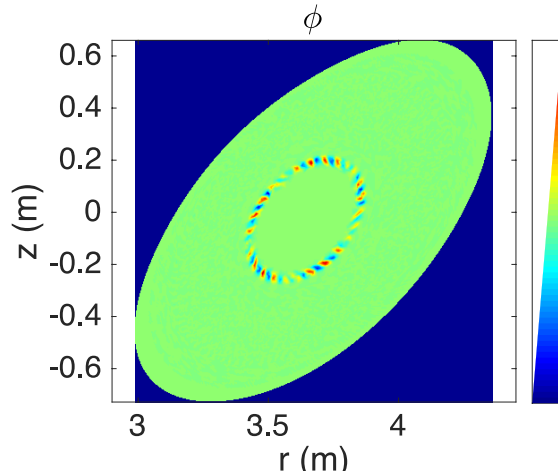


Figure 2. Cross-section of the perturbed electrostatic potential (V) for an electrostatic ITG mode during the linear phase in the experimental magnetic geometry of LHD used for the powder dropper experiments.

-
- 1) T. Moritaka, R. Hager, M. Cole *et al.*, Plasma, 2 (2019) 179-200
 - 2) M. D. J. Cole, R. Hager, T. Moritaka *et al.*, Phys. Plasmas, 26 (2019) 082501
 - 3) M. D. J. Cole, T. Moritaka, R. Hager *et al.*, Phys. Plasmas, 27 (2020) 044501

3.4.4 Diagnostic Collaborations

We often picture diagnostics as the window to the science, but they are also the window or the door to collaborations. Over the last 10 years, many collaborations have taken place between Japan and the US with exchanges of ideas, personnel and instruments, covering a wide range of topics, areas and facilities. Many state-of-the-art techniques have been extended in range, accuracy and applications through these exchanges and in some cases, have gained in acceptance by being applied in different facilities and used in different configurations or conditions. These diagnostics have covered many different areas of measurement, going from visible spectroscopy, to soft X-rays, microwave, plasma radiation and much more.

In terms of developing microwave diagnostics (N. Luhmann- UCDavis, A. Mase – Kyushu Univ.) have studied extending electron cyclotron emission and reflectometry to imaging approaches. Work has been also done in further developing Doppler reflectometry at NSTX (R. Kaita – PPPL, T. Tokuzawa- NIFS) to measure rotation and flows. Advanced microwave-based diagnostics have also developed to study turbulent fields in tokamaks such as DIII-D (T. Rhodes – UCLA, T. Tokuzawa- NIFS).

The development of imaging bolometers has reached a level of maturity which enables reliable 2D measurements of radiation patterns within core and edge plasmas. Further developments have enabled this measurement to be now performed in a variety of configurations (M. Reinke – PPPL/ORNL, B. Peterson – NIFS, L. Delgado-Aparicio- PPPL).

Techniques associated with measuring beam emission fluctuations (in the visible range) have matured considerably and have been extended to measure turbulent flows though velocimetry (McKee- U. Wisconsin-Madison, T. Kobayashi- NIFS) and density fluctuations through Beam Emission Spectroscopy in DIII-D (McKee- U. Wisconsin-Madison, Ohno- NIFS) and in Advanced Stellarator/Heliotron Configuration (Anderson, U. Wisconsin-Madison, S. Kobayashi- Kyoto Univ.).

Many collaborations were the focus on advancing the state of the art in Thomson Scattering techniques, both in Japan and in the US, in all confinement configurations (S. Masamune- KIT, D. Den Hartog – UW. Madison, T. Carlstrom- GA, B. Stratton-PPPL, R. Yasuhara- NIFS)



Figure 1. Top: Manfred Bitter (PPPL), Ken Hill (PPPL), Morita Shigeru (NIFS), Novimir Pablant (PPPL); Bottom: Motoshi Goto (NIFS) reviewing implementation of Crystal Spectrometer at LHD- NIFS



Figure 2. Dr. Den Hartog giving a lecture on Plasma Diagnostics at the PLADyS workshop in summer 2019 at Kyoto University

Comprehensive tests of a Dispersion Interferometer have been performed on DIII-D after development on LHD (see attached full report). X-ray spectroscopy techniques of measuring ion temperatures and plasma rotation have been extended at LHD and other facilities (see attached report and Figure 1), including new techniques extending to Imaging approaches (L. Delgado-Aparicio – PPPL , H. Yamazaki – Univ. of Tokyo) for MST, DIII-D, NSTX-U, and TST2. Advanced spectroscopic techniques based on line emission in the visible range have been greatly improved in RFP devices in Japan and US to better diagnose plasma rotation and flows (see attached report).

In addition to the diagnostic exchanges described above, Dr. D. J. Den Hartog (U. of Wisconsin – Madison) participated in the 2019 PLADyS Summer School* which was sponsored by the Japan Society for the Promotion of Science. He gave a lecture entitled “Overview of Plasma Diagnostics,” describing principles and implementation of many of the diagnostics in common use on fusion research experiments (see Figure 2). The students responded to this lecture with many insightful questions, illustrating that the future of the field of plasma diagnostic development is in good hands.

* www.iae.kyoto-u.ac.jp/plasma/pladys/activity/summerschool/2019/SS2019.html

Development of Electromagnetic-Wave Imaging Diagnostics

Category: FPPC - Diagnostics

Year: 2011-2016

Name: Neville C. Luhmann, Jr.^{a)}, Atsushi Mase^{b)}

Affiliation: ^{a)}UCD, ^{b)}Kyushu University

This collaboration program originates in the importance of electromagnetic wave diagnostics in magnetically confined plasmas in the early 1980's. Since various specific frequencies such as the cutoffs and resonances in plasmas determined by confining magnetic fields and electron densities are in the range of 10-300 GHz, the optimum wavelengths are in the range of micro-to-millimeter-waves. In the initial stage, the transmission and scattering as well as the radiation processes have been utilized as diagnostic tools. As the electron density increases the reflection process, so called reflectometry began to be used in the 1990's. Reflectometry and radiometry share a common feature in that they provide good spatial resolution and temporal resolution while requiring a single viewing chord and minimal vacuum access in contrast to interferometry and scattering. The recent advances in microwave technology together with computer technology have enabled the development of a new generation of diagnostics for visualization of 2D and 3D plasma structures, such as, electron cyclotron emission imaging (ECEI) and microwave imaging reflectometry (MIR).

The cooperation programs include execution of workshop and personnel exchanges. The main subjects are the study of advanced microwave to millimeter-wave plasma diagnostics, so called, electromagnetic wave imaging diagnostics composed of system development, imaging processing techniques, and physics understanding of the results.

The optics design is one of the important subjects for the imaging diagnostics. The position of transmitting and receiving points and distance between lenses/mirrors are determined from the accessibility condition to the machine. The focusing point or the wavefront at the cutoff layer is determined from the plasma shape. It has been concluded that an optical design code, such as, Code V can be applied to tokamak plasmas, however, the simulation using FDTD has to be utilized to the LHD plasma due to the complexity of the plasma shape.¹⁻³⁾

As for the development studies of the imaging arrays, it is extremely important to note that epoch-making technical progress has arisen from this cooperation, so called, local-integrated imaging arrays as shown in Figure 1 (a),⁴⁾ which uses the technology to combine waveguide and microstrip lines for heterodyne detection radiometers and provides sufficient LO power for the receiver array.⁵⁾ The UCD group performs advanced SoC (system-on-chip) receiver arrays as shown in Figure 1 (b), and makes progress to W-band (75-110 GHz) and F-band (110-140 GHz) SoC detector arrays for application to large plasma devices.⁶⁻⁷⁾

There have also been discussions concerning another type of imaging, synthetic aperture (SA) imaging. The signal reflected at a local point arrives at each of the antennas at a different time depending on the direction of the source equivalent to SAR imaging for remote sensing. This SA imaging technique has been developed for various industrial applications by the Kyushu University group.⁸⁾

Physics understandings of the obtained results have led to a new approach in physics study of tokamak plasmas. They are model based on a helically symmetric crash zone, 3D local connection model. A high-confinement discharge on DIII-D with edge localized modes (ELMs) is presented to demonstrate some of MIR's capabilities. Inter-ELM density fluctuations, such as the upward sweeping modes, were clearly seen from interferometry as well as with the MIR system. The imaging systems (ECEI and MIR) have been installed in magnetically confinement systems all over the world as shown in Figure 2.^{7,9)}

The exchanges from Japan to the US have given priority to the dispatch of young researchers, since the device fabrication and characterizations have been the main research subjects. The period of stay is usually in the range of 2-3 weeks. A longer stay is desirable for the collaborative experiment using the diagnostic system installed in the magnetic confinement devices. Also, the dispatch of young researchers from US to Japan is also important for the buildup of a new strong cooperation group.

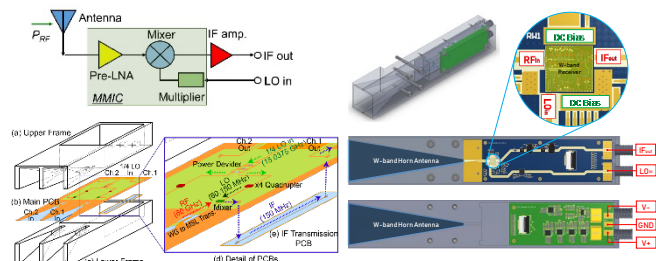


Figure 1. Advancement of MMIC design of imaging receiver

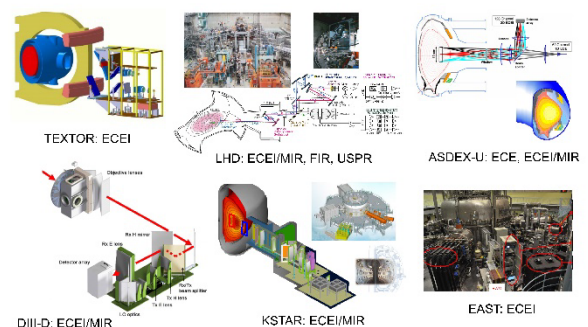


Figure 2. Microwave imaging applied to various magnetic confinement devices.

- ¹⁾ B. Tobias et al., Plasma Fusion Res. 6 (2011) 2106042.
- ²⁾ A. Mase et al., J. Instrum. 7 (2012) C01089.
- ³⁾ G. S. Yun et al., Rev. Sci. Instrum. 85 (2014) 11D820.
- ⁴⁾ D. Kuwahara et al., Rev. Sci. Instrum. 85 (2014) 11D805.
- ⁵⁾ D. Kuwahara et al., J. Instrum. 10 (2015) C12031.
- ⁶⁾ X. Ren et al., J. Instrum. 10 (2015) C10036.
- ⁷⁾ Y. Wang et al., Nucl. Fusion 57 (2017) 072007.
- ⁸⁾ A. Mase et al., Adv. Phys. X: 3, 1 (2018) 1472529.
- ⁹⁾ Y. Zhu et al., IEEE Trans. Plasma Sci. 47 (2019) 2110.

Energetic particle confinement studies in LHD and NSTX/NSTX-U

Category: FPPC - Diagnostics

Name: K. Ogawa, M. Isobe, D. S. Darrow*,

A.L. Roquemore*

Affiliation: NIFS, *PPPL

Energetic particle confinement is one of the issues for realizing a future fusion reactor because a fusion burning plasma is heated by energetic alpha particles born due to deuterium-tritium reactions. To understand/predict the energetic particle confinement in a fusion burning plasma, the study of transport and loss of energetic particles such as beam ions and ion cyclotron resonance frequency heated tail ions has been performed in existing devices.

We have been performed a corroborative study of energetic ion transport/loss using the fast-ion loss detector (FILD) in LHD and NSTX/NSTX-U. FILD was originated in PPPL and is now widely used to measure escaping energetic particles in many toroidal devices. In the measurement of beam ion loss, the so-called self-shadow effect, beam ions reaching the FILD position are blocked by the finite size of FILD head, should be considered in LHD and NSTX/NSTX-U where relatively large FILD head is adopted. NIFS developed a calculation code with the support of PPPL and evaluated the self-shadow effect of FILD. We found why the FILD installed on NSTX could not measure the relatively low-energy beam ion loss. The design of the FILD head for NSTX-U was modified based on this analysis. Also, a faraday-cup-type FILD was designed by NIFS with the support of PPPL for Heliotron-J¹⁾ to obtain the knowledge of installing Faraday-cup-type FILD in LHD.

LHD deuterium experiment was initiated in March 2017. One of the targets in the LHD deuterium experiment is the enhancement of energetic particle confinement in helical systems using comprehensive neutron diagnostics. In the deuterium plasma discharges of LHD, neutrons are mainly created by so-called beam-thermal reactions because LHD is equipped with high-energy intensive neutral beams. A study of energetic particle confinement has been largely advanced using comprehensive neutron diagnostics^{2,3)}.

One of the most critical diagnostics for LHD deuterium operation is the neutron flux monitor (NFM) used to manage the neutron budget⁴⁾. Therefore, absolute calibration of the NFM with high accuracy is crucial for LHD deuterium experiment management. M. I. and K. O. joined the absolute calibration of NFM in NSTX and NSTX-U, respectively, in order to learn the

method and procedure of the absolute calibration. In these calibrations, a standard ²⁵²Cf neutron source was loaded on the train, which runs along the ring track installed on the midplane of the vacuum vessel to simulate the ring-shaped neutron source (Figure 1). NIFS successfully performed the absolute calibration experiment in LHD based on the knowledge of joining the absolute calibration in NSTX/NSTX-U⁵⁾.



Figure 1. Absolute calibration of the neutron flux monitor in NSTX-U.

Neutron camera is a powerful tool to study the energetic particle transport caused by energetic-particle-driven magnetohydrodynamic (MHD) instabilities. Shot-integrated neutron emission profile measurement using nuclear emulsion was performed in NSTX in order to obtain the knowledge of neutron profile diagnostics⁷⁾ (Figure 2 left). Based on this knowledge and the neutron camera for TFTR⁸⁾ and NSTX⁹⁾, the LHD vertical neutron camera (Figure 2 right) was designed. Energetic particle transport due to the energetic-particle-driven MHD instability has been studied using the NFM and vertical neutron camera in LHD¹⁰⁾.



Figure 2. (left) Neutron collimator installed in NSTX (right) Neutron camera in LHD. Reproduced with permission from K. Ogawa et al., Rev. Sci. Instrum. **89** (2018) 113509.

¹⁾ K. Ogawa et al., Plasma Fusion Res. **8** (2013) 2402128.

²⁾ M. Isobe et al., Nucl. Fusion **58** (2018) 082004.

³⁾ K. Ogawa et al., Nucl. Fusion **59** (2019) 076017.

⁴⁾ M. Isobe et al., Rev. Sci. Instrum. **85** (2014) 11E114.

⁵⁾ M. Isobe et al., IEEE Trans. Plasma Sci. **46** (2018) 2050.

⁶⁾ K. Ogawa et al., Rev. Sci. Instrum. **89** (2018) 113509.

⁷⁾ M. Isobe et al., Plasma Fusion Res. **8** (2013) 2402068.

⁸⁾ A. L. Roquemore et al., Rev. Sci. Instrum. **61** (1990) 3163.

⁹⁾ A. L. Roquemore, D. Darrow, A. Herr, S. S. Medley, M. J. Loghlim, M. Isobe, "Feasibility Study for a Neutron Profile monitor on NSTX", American Physical Society, 45th Annual Meeting of the Division of Plasma Physics, October 27-31, 2003, Albuquerque, New Mexico, MEETING ID: DPP03, abstract id. LP1.032.

¹⁰⁾ K. Ogawa et al., Nucl. Fusion **60** (2020) 112011.

An X-Ray Imaging Crystal Spectrometer for the Large Helical Device

Category: FPPC - Diagnostics

Name: N.A. Pablant^{a)}, M. Bitter^{a)}, K.W. Hill^{a)}, S. Morita^{b)},
S. Satake^{b,c)}, M. Yokoyama^{b,c)}

Affiliation: ^{a)}PPPL, ^{b)}NIFS, ^{c)}SOKENDAI

The Large Helical Device (LHD), an advanced superconducting heliotron/stellarator experiment at the National Institute for Fusion Science (NIFS), is one of the key international experiments to study stellarator performance. One of the key issues for stellarator physics is the understanding of core neoclassical transport (NC) and the validation of neoclassical transport models. Understanding experimental core transport requires a suite of core plasma profiles, namely the ion/electron temperature and density and the radial electric field. These measurements are desired across the broadest range of plasma conditions accessible in LHD experiments. For neoclassical validation studies one particularly interesting plasma regime to study is the Core Electron-Root Confinement (CERC) in which high core electron temperatures are achieved through central ECRH heating. These low-density high electron temperature plasmas are important for NC validation in a reactor relevant low collisionality condition, and are relatively simple to analyze due to the localized ECRH heat deposition profiles.

With these measurement goals in mind a collaboration between PPPL and NIFS to install an X-Ray Imaging Crystal Spectrometer (XICS) on LHD was formed in 2010 between M.Bitter (PPPL), K.W. Hill (PPPL) and S. Morita (NIFS)¹⁾. The goal was to complement the existing Charge Exchange Spectroscopy (CXS) diagnostic and provide core profile measurements when neutral beam injection was not available in the experiment, or when the neutral beams were unable to penetrate fully into the plasma core.

The XICS diagnostic was installed on LHD in 2011²⁾ and was routinely operational for the 2012-2015 experimental campaigns. This installation was the first time that an XICS system had been installed on a heliotron/stellarator, and required a completely new diagnostic analysis suite to be developed that was compatible with fully 3D stellarator equilibria such as those provided by the VMEC code. The installation of this diagnostic on LHD validated the use of XICS in stellarator geometry including demonstration of high-quality tomographic inversions of XICS line-integrated measurements in stellarator geometry³⁾. In addition, with this installation XICS was used to measure the perpendicular plasma flow (or poloidal rotation) in a heliotron/stellarator.

With the new availability of radial electric field measurements in pure ECRH plasmas, a first NC validation exercise was completed by comparing experimental measurements of the radial electric field (E_r) from the XICS

diagnostic to both non-local (FORTEC-3D, S. Satake) and local (GSRAKE, C.D. Beidler) neoclassical transport calculations. This offered not only experimental validation of NC codes in a low collisionality regime but also provided a first detailed comparison between the local and non-local NC profile calculations.⁴⁾

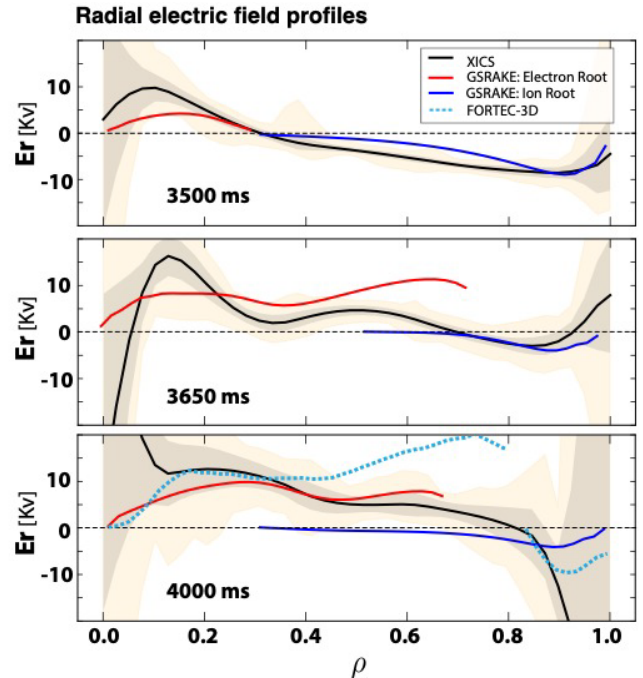


Figure 1. Radial electric field at three different times during an ECRH heated CERC discharge at LHD. Experimental profiles from the XICS diagnostic show an expansion of the core electron-root region as the electron temperature is increased. The experimental profiles are compared to predictions from neoclassical codes, GSRAKE and FORTEC-3D.

In addition, the measurements from the XICS diagnostic were successfully integrated into the transport code TASK-3D⁵⁾ and were subsequently used to study experimental energy fluxes and effective diffusion coefficients along with comparisons to NC predictions⁴⁾.

Measurements from XICS have contributed to several other physics studies on LHD. The data collected during the operational period of the diagnostic is still being used to this day in ongoing physics studies.

The XICS diagnostic was removed from LHD in 2015 in preparation for the LHD deuterium campaigns. The collaborations that were formed from this project are enduring and include continued data analysis, joint studies using data from W7-X, and new collaborative activities at LHD.

¹⁾ M.Bitter, K.W. Hill et al., Rev. Sci. Instrum. 81 (2010) 10E328

²⁾ N. Pablant, M. Bitter et al., Rev. Sci. Instrum., 83 (2012)

³⁾ N. Pablant, R.E. Bell et al., Rev. Sci. Instrum. 85 (2014) 11E424

⁴⁾ N. Pablant, S. Satake et al., Plas. Phys. And Contr. Fusion 58 (2016) 045004

⁵⁾ M. Yokoyama, R. Seki, et al., Nuc. Fusion, 57 (2017) 126016

Demonstration of high temporal resolution heterodyne dispersion interferometry on DIII-D

Category: FPPC - Diagnostics

Name: T. Akiyama^{1,2)}, M.A. Van Zeeland¹⁾,

D. Finkenthal³⁾, and R. Boivin¹⁾

Affiliation: ¹⁾General Atomics (GA), ²⁾National Institute of Fusion Science (NIFS), ³⁾Palomar College

Dispersion interferometry (DI) can measure line-integrated electron density while suppressing unwanted phase shifts caused by the mechanical vibrations, which is one of drawbacks of conventional interferometers. This is accomplished through a variation of the two-color interferometer approach where the second color is produced by a nonlinear frequency doubling crystal. The feasibility of dispersion interferometry on large fusion devices was demonstrated on LHD and elsewhere. Due to advantages of the DI, it has been adopted as one of the electron density diagnostics on ITER. Through the Japan-US collaboration described here, heterodyne techniques were introduced for the first time to the DI approach, creating both a more reliable phase measurement, as well as significantly increasing the measurement bandwidth allowing resolution of high frequency density fluctuations as well fast density monitoring.

A DI heterodyne scheme is implemented by shifting the frequency of the second harmonic component of 10.6 μm CO₂ laser with an acousto-optic (AO) cell. The upper limit of the bandwidth is determined by the frequency of the beat signal, which is the same as the drive frequency of the AO cell, 40 MHz. Hence the heterodyne DI (HDI) can cover the frequency range of most instabilities typically observed in magnetically confined plasmas. On the other hand, the fundamental and the second harmonic beams need to be physically separated in order to shift frequency of the second harmonic component only – destroying the intrinsic co-linearity (an advantage of the DI). Mechanical vibrations and disturbances by air along the uncommon beam paths between the two wavelengths can lead to unwanted phase shifts. Bench testing was conducted as proof-of-principle of this approach and a relative insensitivity to mechanical vibrations was demonstrated along with wide bandwidth¹⁾ using a modern real-time digital demodulation developed at GA. The unwanted phase shifts generated as a result of beam separation were found to be acceptable and were minimized by compact design of the optical system and coverage of the optical table to avoid air flow.

After the demonstration of the feasibility of HDI and improvement of the phase resolution through bench testing, the HDI system was installed on DIII-D. The DIII-D HDI tests used a ~100m long beam transmission line, which was originally prepared for the ITER Toroidal Interferometer and Polarimeter (TIP) prototype²⁾. Figure 1 shows the line densities measured by the radial DI and the standard DIII-D two-color laser

interferometer. Although the pulsed central solenoid coil on DIII-D combined with the toroidal field, causes displacements of mirrors installed on DIII-D, the active beam alignment system, which was also developed for TIP²⁾, maintained beam alignment back to detection system. Hence the HDI system could keep tracking the phase shift without loss of signal and fringe jump errors³⁾, including during a disruption phase. The HDI measured line density shows good agreement with the existing interferometer. The line density resolution, which is defined as standard deviation for 1 s, was $9 \times 10^{17} \text{ m}^{-2}$. If the same performance were obtained on ITER, this resolution would correspond to $1 \times 10^{17} \text{ m}^{-3}$, which is 0.1% of a standard H-mode discharge. Figure 2 shows the density fluctuations measured with HDI. In addition to coherent fluctuations with harmonics up to 75 kHz, relatively broadband fluctuations up to 150 kHz were measured in this discharge, thus demonstrating HDI fluctuation measurement capability.

Through this collaboration, DI technology was advanced as a tool for both fast density monitoring and physics studies. Demonstration on DIII-D also offered an ITER-relevant diagnostic conditions, and HDI is now one of the specified electron density measurements on ITER as well as KSTAR and DTT.

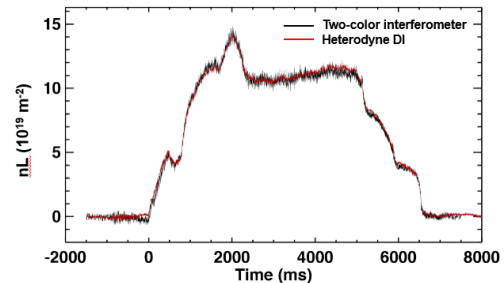


Figure 1. Measured line densities along radial chords with HDI and the two-color interferometer on DIII-D.

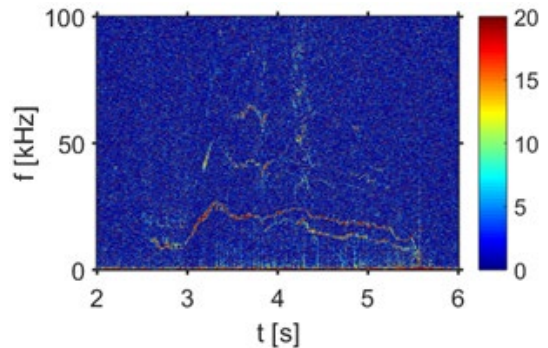


Figure 2. The density fluctuations measured with HDI

¹⁾T. Akiyama et al., Rev. Sci. Instrum. 87 (2016) 123502

²⁾M.A. Van Zeeland et al., Rev. Sci. Instrum. 89 (2018) 10B102

³⁾T. Akiyama et al., Rev. Sci. Instrum. 89 (2018) 10B105

Reversed-Field Pinch Diagnostic Exchanges

Category: FPPC - Diagnostics

Name: D. J. Den Hartog

Affiliation: UW-Madison

The Reversed-Field Pinch (RFP) diagnostic exchanges that took place during the last decade involved the MST experiment at the University of Wisconsin-Madison (UW-Madison) and the RELAX experiment at the Kyoto Institute of Technology (KIT). An important outgrowth of the US-Japan Fusion Collaborations during this period was a formal Agreement for Academic Exchange between UW-Madison and KIT. The first five-year agreement was signed in 2015, and then renewed for another five years in 2020. This agreement facilitates exchange of students, faculty, and researchers, joint research projects, and internships. Several KIT students have visited UW-Madison to work on spectroscopy, diagnostic development, and data analysis. Faculty and researchers from both institutions have made complementary visits to pursue joint research projects on both MST and RELAX. The latest of these projects is the development of a capacitive probe to measure the flux of canonical helicity in both MST and RELAX.

One of the highlights of the collaboration between KIT and UW-Madison was the development of a Thomson scattering diagnostic to measure electron temperature in RELAX¹⁾. Figure 1 shows a schematic of the Thomson scattering diagnostic system for RELAX. The main components are a high-power Nd:YAG laser and associated optical elements for beam injection, scattered-light collection optics, and a polychromator for spectrum measurements. The polychromator was loaned to RELAX by the MST group. In addition, MST personnel provided design assistance for this diagnostic system. Installation and operation of this complex diagnostic was overseen by Prof. S. Masamune, and was done primarily by undergraduate and graduate students. The high-quality results are a testament to their ability and dedication.

Referring again to Figure 1, the beamline for the RELAX Thomson scattering system incorporates two adjustable mirrors to enable precise alignment of the laser beam through the plasma and into the beam dump. The beam focus is at the center of the plasma, where scattered light is collected and focused onto a fiber. The fiber transports the light to a remote polychromator, where it is divided into four wavelength regions (four channels), with an avalanche photodiode to measure the light intensity for each channel. As configured, the system is able to make measurements down to an electron density of $3 \times 10^{18} \text{ m}^{-3}$, which confirms the soundness of the design and construction of the system. For the range of plasma current 50-80 kA in RELAX RFP plasmas, the typical central electron temperature was $\sim 100 \text{ eV}$, and demonstrated a weakly increasing trend with plasma current.

Another important US-Japan diagnostic exchange completed in the last decade was development and construction of a high-repetition-rate laser for the Thomson scattering diagnostic on the Large Helical Device (LHD) at NIFS-Toki. This collaboration project was the direct outgrowth of development of high-rep-rate Thomson scattering on the MST RFP. The laser built for LHD has two operating scenarios, a fast-burst sequence at 20 kHz rep rate, and a slow-burst sequence at 1 kHz. There is substantial flexibility in burst sequences for tailoring to experimental requirements. This new laser system operates alongside the existing lasers in the LHD Thomson scattering diagnostic, and uses the same beamline. The increase in temporal resolution provided by this new laser capability complements the high spatial resolution (144 points) of the LHD Thomson scattering diagnostic, providing unique measurement capability unmatched on any other fusion experiment. Burst operation of this laser system is being used to capture fast time evolution of the electron temperature and density profiles during pellet injection and events such as ELMs, RMP perturbations, and various MHD modes.

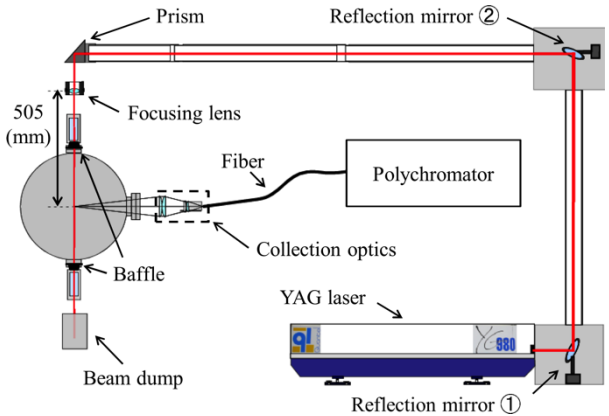


Figure 1. Layout of the Thomson scattering diagnostic system on RELAX¹⁾.

¹⁾ R. Ueba et al., Plasma Fusion Res. 9, 1302009 (2014); doi: 10.1585/pfr.9.1302009.

3.4.5 High Energy Density Science (HEDS)

High-energy-density (HED) science is the study of matter and radiation at conditions of high pressure or temperature or under the influence of a strong external perturbation, such as an intense laser, particle beam, pulsed power, or radiation source. A multidisciplinary field, HED originated from the pursuit of controlled fusion energy, and the interpretation of astrophysical observations. HED science has been a strong area of collaboration between Japan and the United States for over three decades.

Japan and the U.S. have a long and mutually beneficial history, working together and the larger global community in high energy density science (HEDS) and the science and technology of high-power lasers. The Japan-U.S. collaboration in HED science offers several dividends to both countries. There is a great deal of interest in the study of materials at extreme conditions and understanding the physics basis toward attaining fusion. Excellent experimental and computational facilities exist in Japan and the U.S. for the pursuit of these studies. From a strategic perspective, the technical ties that bind the two countries offers strategic benefits for both nations. The U.S. has long had interests in the Pacific rim and strengthening an ally in HEDS, benefits both countries strategically.

The first decade of the collaboration (1999-2009) focused on laboratory astrophysics, fast ignition, and plasma photonics. Experiments were conducted at the GEKKO-XII and Vulcan laser facilities. The second decade (2010-2019) saw continued growth in the collaboration through work in laboratory astrophysics and magnetic high-field laser fusion. At this point in time, several facilities several facilities became integral to the collaboration. This included large scale lasers such as NIF at LLNL and LFEX at ILE, as well as high power lasers coupled to x-ray free electron lasers (XFELs) at LCLS and SACLAC. In January of 2019, a new start to the relationship began when, High Energy Density (HED) and laser scientists from Japan and the U.S. met in Washington DC to discuss areas of mutual interest in HED. The 2019 Symposium, “Perspective of High Energy Density Science and Technology by High Power Lasers” built upon 20 years of past collaboration between Japan and the U.S. The 2019 Symposium opened a new decade by looking for continued expansion in the collaboration and the establishment of a framework that would oversee the relationship between the two countries. A Project Arrangement, signed between MEXT (Ministry of Education, Culture, Sports, Science and Technology) and the Department of Energy, at the 2019 Symposium, outlines the framework for the expansion in the collaboration.

What lies ahead in the relationship between Japan and the US in HED science? First, forming a LaserNetJapan based on the European (LaserLab Europe) and U.S. models. Currently, ILE-Osaka, SACLAC-RIKEN and KPSI-QST collaborate. A LaserNetJapan that links Japanese facilities and supports the network with a budget in the manner of the U.S. and European models is needed. LaserNetJapan and LaserNetUS facilities could then be linked under the current Project Arrangement. Second, Japan is proposing a paradigm shift in HED science through the building of high repetition rate, MW-average power laser facilities, J-EPoCH. An exciting new facility that will significantly advance HEDS and greatly enhance research cooperation and increase opportunities to access the laser experiments for Japan-U.S. students and scientist exchanges. Third, since the NIF has demonstrated the condition close to the ignition, an area of mutual interest is burn physics. The study of thermonuclear burn or “burn physics”, has continued to be of intense interest internationally for many decades. It is an area of interest to many students studying HED science. This is not surprising since burn is the mechanism which powers stars, but it also holds the hope for clean limitless energy. The pursuit of controlled burn is at the heart of the inertial confinement fusion (ICF) and magnetic fusion energy (MFE) programs. Within this context, the Japan-U.S. collaborations would be focused on ICF.

Progress on Alternative Ignition Experiments

Category: FPPC - HEDS

Name: Shinsuke Fujioka, Hiroshi Sawada*

Affiliation: Institute of Laser Engineering,
Osaka University, *University of Nevada, Reno

Fast Ignition (FI) is an alternative approach of the inertial confinement fusion to achieve a high fusion gain. In the electron-based FI scheme, a fuel target pre-compressed by nanosecond lasers is rapidly heated to the ignition temperature by a relativistic electron beam (REB) generated by an additional high-intensity, short-pulse laser. The separation of the fuel assembly and ignition processes enables lower required driver energies and less constraint on the target symmetry compared to the conventional hot spot ignition.

Over the last decade, significant progresses have been made specifically on dense core formation, the transport of a REB, enhancement of electron-to-core coupling efficiency by controlling a diverging REB and the creation of petapascal ultra-high-energy-density state by diffusive heating. This section highlights those experimental investigations using the GEKKO-XII and the kilo-joule petawatt LFEX laser at the Institute of Laser Engineering, Osaka University.

As a baseline target design, a target consisted of a solid density deuterated carbon (CD) ball attached to a hollow gold cone was introduced in order to stably assemble a high-density core with a high degree of reproducibility¹⁾. The areal density of a compressed cone-in-ball target was measured using flash K α radiography that was originally developed on the Omega laser²⁾. In the GXII-LFEX experiment, a spherically bent crystal and LFEX-laser-produced 4.5 keV Ti K α x-rays were deployed. A cone-in-ball target was compressed by nine GXII beams, while the 1.6 ps, 1 kJ LFEX laser was used to produce spatially uniform K α backscatter x-rays [Figure 1(a)]. A time history of the experimentally inferred areal density agrees with a 2D hydrodynamics simulation as shown in Figure 1(b)³⁾. The

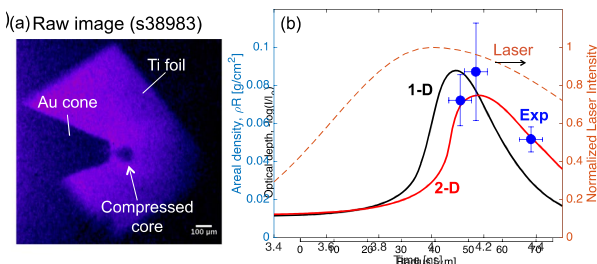


Figure 1. (a) A monochromatic radiographic image of the compressed cone-in-ball target (b) A comparison of experimental areal density against 1D and 2D hydrodynamics simulation

monochromatic x-ray imager developed for this study was also applied to visualization of an electron transport region in integrated FI experiments and to aids to evaluation of an electron-to-core coupling efficiency⁴⁾.

Control of the large divergence of a REB is key in the FI. To guide REB to the core for a better energy coupling, a novel experimental platform was developed using a laser-driven capacitor coil target to generate a magnetic field of hundreds of Tesla. As shown in Figure 2(a), three infrared GXII beams irradiated a Nickel-made capacitor coil target to impose a magnetic field along the REB path and six beams were used for compression of a cone-in-Cu-oleate ball target. The four LFEX beams with the total beam energies ranging from 630 to 1520 J in 1.8 ps pulse duration was injected into the cone to generate a REB for core heating. The transport of the REB produced Cu K α x-rays that was recorded with an absolutely calibrated x-ray spectrometer and imaged with a spherical crystal imager⁵⁾. The application of the magnetic field clearly enhances K α emission in the compressed core as shown in Figure 2(b). Together with an open-tip cone target, the laser-to-core energy coupling was enhanced by a factor of two from the shot with no applied magnetic field.

(a)

Figure 2. (a) A schematic of the magnetized FI experiment. Measured Cu K α emission distribution (b) with and (c) without externally applied magnetic fields.

An ultrahigh-energy-density (UHED) state was produced with the LFEX laser using the same platform shown in Figure 2(a). It was found that thermal diffusion plays an important role in isochoric heating of a solid density foil⁶⁾ and a compressed dense plasma core⁷⁾. With the application of an external magnetic field for electron beam guiding, a UHED state of 2.2 petapascal was achieved experimentally with 4.6 kJ of total laser energy that is one order of magnitude lower than the energy used in the conventional implosion scheme⁶⁾. This scheme with the multi-picoseconds LEFX laser having a large beam spot has a potential to produce a large volume of dense keV plasmas for fast isochoric heating and high energy density science.

¹⁾ S. Fujioka et al., Phys. Plasmas **23**, 056308 (2016)

²⁾ W. Theobald et al., Nat. Commun. **5**, 5785 (2014).

³⁾ H. Sawada et al., Appl. Phys. Lett. **108**, 254101 (2016)

⁴⁾ L.C. Jarrott et al., Nat. Phys. **12**, 499 (2016).

⁵⁾ S. Sakata et al., Nat. Commun. **9**, 3937 (2018)

⁶⁾ H. Sawada et al., Phys. Rev. Lett. **122**, 155002 (2019)

⁷⁾ K. Matsuo et al., Phys. Rev. Lett. **124**, 035001 (2020)

Collaboration on research of kJ-class laser-plasma interactions

Category: FPPC - HEDS

Name: N. Iwata, Y. Sentoku, S. C. Wilks*, A. J. Kemp*

Affiliation: Institute of Laser Engineering (ILE), Osaka University, *Lawrence Livermore National Laboratory (LLNL)

The recent development of kJ-class lasers opens up access to a new regime of high energy density (HED) plasma physics. Owing to the large laser energy, tens to hundreds of Joules of relativistic electrons are generated in less than a billionth of a second. This enables a host of applications such as intense x-ray and proton beam generation, and fast ignition-based laser fusion. Our collaboration aims to elucidate the theory behind the physics of HED plasma creation under strong light irradiation, using continually evolving state-of-the-art plasma simulations codes as our tools.

Experimental studies using kJ-class lasers have been performed in both Japan using the LFEX laser at ILE, and in the US using the NIF-ARC laser at LLNL. Kilojoule laser-produced plasmas show very efficient laser absorption, and the resulting maximum proton energies exceed the conventional scaling for short pulse lasers. Our collaboration clarified the dynamics of high flux proton beam acceleration in ARC experiments² [2] and presented the results at the 2017 APS-DPP meeting [“Proton and Ion Acceleration using Multi-kJ Lasers” LLNL-PRES-740481 (2017)]. Simulation of kJ-class laser-plasma interactions is challenging, since both kinetic and fluid behaviors of the plasma are important in the long time scale interaction. Our hybrid simulation made it possible to study the dynamics of this complex interaction, as shown in Figure 1.

The particle-in-cell (PIC) simulation is an essential tool for investigating the non-equilibrium physics of the intense laser-produced plasmas. We have developed the PICLS code³[3] in Japan-US collaborations. The PICLS code is capable of simulating laser isochoric heating in a wide range of densities and temperatures including collisional, ionization, and radiation processes. Results from PICLS can be found in over 200 journal articles.

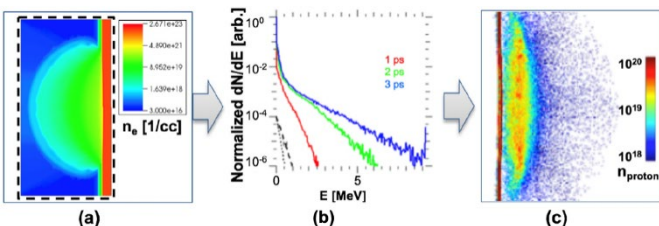


Figure 1. Hybrid simulation of the ARC proton acceleration. ARC-driven electron source calculated by PIC (b) is injected into a LSP simulation to study the proton dynamics (c)².

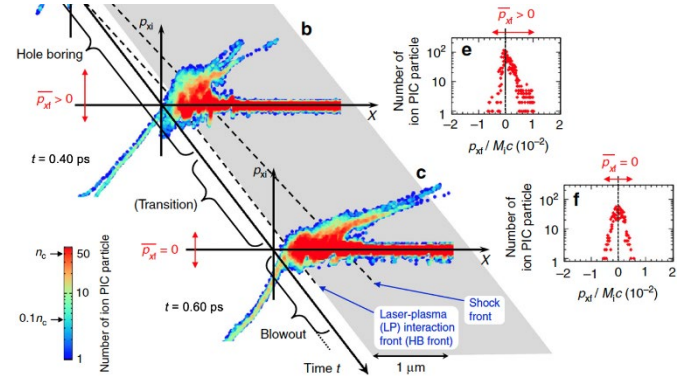


Figure 2. Dynamics of the interface between a relativistic laser light and a solid density plasma in a PIC simulation. The hole boring seen in the ion phase plot (b) stops at the limit density in (c) where the ion momentum p_{xi} at the interface is zero on average as shown in (f)⁴.

In the creation of HED plasmas by kJ laser light, the pressure balance between laser light and plasma is important. When the laser light pressure is higher than the plasma pressure, the light pushes the dense plasma by the hole boring process. Originally proposed by Wilks [Phys. Rev. Lett. (1992)], and later followed by a modified theory by Sentoku [Fusion Sci. Technol. (2006)], Iwata⁴ built on these results to derive the limiting plasma density for hole boring (Figure 2). Our collaboration is quite fruitful to advance the theoretical understanding.

Our collaboration is not limited to theory, but also involves planning of experiments. Through discussions in conferences/meetings, e.g., HEDS 2017 (LLNL), APS-DPP Meetings, and the LDRD team meetings, we have contributed to several publications [Kim, Phys. Plasmas (2018); Kemp, Phys. Plasmas (2020); Nishiuchi, Phys. Rev. Res. (2020)].

Japan scientists (Iwata and Sentoku) visited LLNL in January 2020 and started a new study, on kJ laser interactions resulting in a confinement mechanism of laser-accelerated electrons, that was completed via our ongoing web-based meetings (Figure 3), and resulted in a journal submission in 2021.



Figure 3. Snapshot of a web meeting for the theoretical study.

¹⁾ A. J. Kemp et al., Nucl. Fusion 54 (2014) 054002

²⁾ D. Mariscal et al., Phys. Plasmas 26 (2019) 143110

³⁾ Y. Sentoku et al., J. Comput. Phys. 227 (2008) 6846

⁴⁾ N. Iwata et al., Nat. Commun. 9 (2018) 623

Ion acceleration with kJ-class laser systems

Category: FPPC - HEDS

Name: A.J. Kemp, A.Morace*, N. Iwata*, Y. Sentoku*, D. Mariscal, T. Ma, S.C. Wilks
Affiliation: LLNL Livermore, *ILE Osaka.

The last decade has seen the arrival of multi-kiloJoule laser systems delivering picosecond scale pulses at relativistic intensities. One application of such laser pulses is the acceleration of ions to MeV energies via target-normal sheath field acceleration (TNSA), where laser-driven hot electrons create a sudden and strong electric field on the non-irradiated surface of a target, which then accelerates a thin layer of ions off the surface¹⁾. While TNSA has been around for years, the use of kJ pulses opens new doors to applications like ion fast-ignition of inertial confinement fusion targets²⁾, and Figure 2, cancer therapy, pulsed neutron generation and warm-dense matter research via isochoric heating of secondary targets²⁻³⁾. Our collaboration benefits from the fact that both ARC and LFEX deliver similar pulse energy into \sim 100um diameter focal spots.

A recent highlight of the US-Japan collaboration was the first demonstration of ARC-accelerated proton beams at the National Ignition Facility¹⁾. Our experiment not only achieved record doses of multi-MeV protons, but we also were able to predict maximum ion energies with a combination of hydro- with explicit and implicit particle-in-cell modeling, see Figure 1; the success of this campaign was thanks to a joint effort of our US/Japan team, see Figure 3. Our collaboration has also been studying the dynamics of ion beam in focusing plasma devices using set-ups like the ones shown in Figure 2, where an intense laser pulse interacts with a hemi-spherical foil embedded in a cone target; hot electrons generate electrostatic

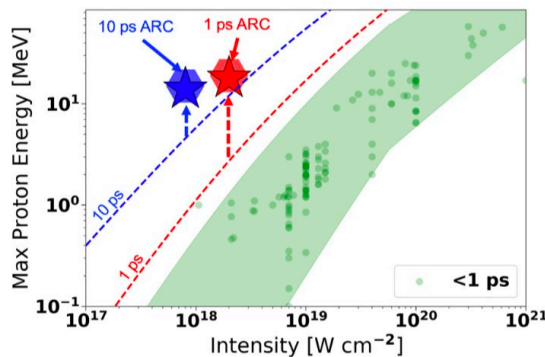


Figure 1. Maximum proton energy vs. intensity for sub-picosecond experiments with small f-number (green) and large f-number NIF-ARC experiments (blue, red), all at 1um laser wavelength. Shaded area behind stars refers to PIC/LSP modeling

fields that accelerate and focus protons to the cone tip where they are used to heat solid matter to multi-eV temperatures.

We have performed a detailed investigation of large-scale, kilojoule-class laser-generated ion beam dynamics in a

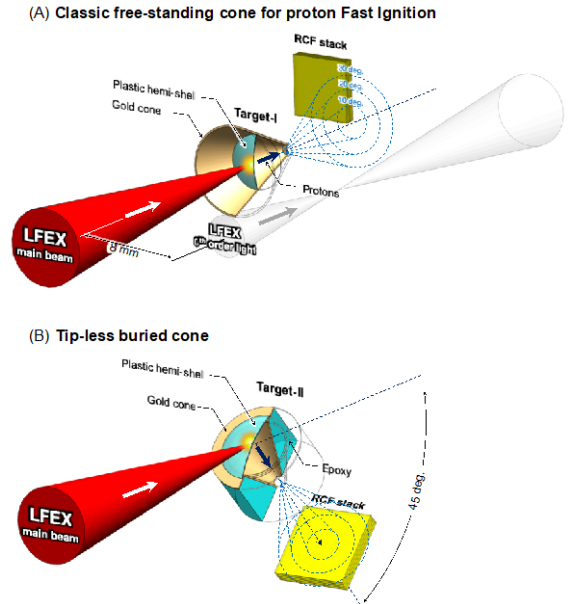


Figure 2. Setup for a proton fast-ignition experiment on the LFEX laser. A focusing geometry is used with free-standing / embedded cones and hemi-spherical foils that serve as a source of MeV protons²⁾.

cone-target geometry and demonstrate that magnetic fields play an important role, with free-standing cone target yielding a highly divergent proton beam with ring-like shape spatial distribution, while tip-less buried cone target yield highly collimated proton beams.

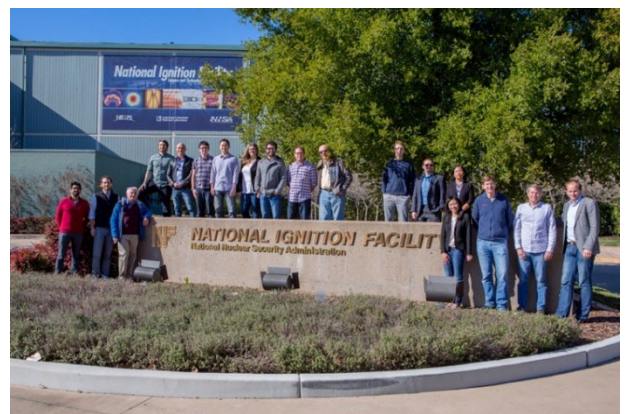


Figure 3. Team photo of first NIF-ARC proton shot. Lead PI at LLNL is T. Ma (4th from right) and A. Morace (LLE, 5th from left).

¹⁾ D.Mariscal et al., "First demonstration of ARC-accelerated proton beams at the National Ignition Facility", Phys.Plasmas 26 (2019).

²⁾ A.Morace et al., "Ion beam dynamics in focusing plasma devices", in preparation (2021).

³⁾ N.Iwata et al., "Fast ion acceleration in a foil plasma heated by a multi-ps high intensity laser", Phys.Plasmas 24 (2017).

Astrophysical Collisionless Shock Experiments with Lasers

Category: FPPC - HEDS

Name: Hye-Sook Park / Youichi Sakawa

Affiliation: LLNL/Osaka University

Interaction of high Mach-number plasma flows occur frequently in astrophysics, and the resulting shock waves are responsible for the properties of many astrophysical phenomena including cosmic ray particle acceleration. A US-Japan collaboration has been conducting high-energy-density laboratory astrophysics experiments to study the microphysics related to the formation of collisionless shocks and particle acceleration at Omega and NIF since 2010. Highlights from these experiments follow.

The first set of experiments were conducted at the Omega laser facility to see whether the Weibel instability¹⁾, which is a mechanism for converting high-velocity plasma flow kinetic energy into magnetic field formation, can enable shocks to be formed under non-magnetized conditions. The experimental configuration is shown in Figure 1 where two face-on plastic foils were illuminated by 4 kJ of laser energy on each foil. The measured plasma flow velocity was >1000 km/s indicating that the plasma flow was completely collisionless. The inter-penetrating plasma interaction was probed by imploding a nearby capsule filled with deuterium & helium gases that produced a stream of protons to probe the magnetic field. The characteristic signature of Weibel instability formation is a filamentary magnetic field structure. The results are displayed in the bottom panel of Figure 1 that clearly show the evolution of filamentary structures proving that magnetic fields are created by Weibel instabilities in high Mach-number plasma flows^{1),2)}.

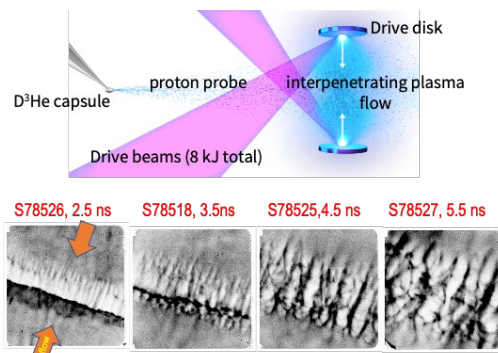


Figure 1. Experimental configuration to study astrophysical collisionless shocks on Omega. Two plastic targets were illuminated by 4 kJ lasers creating high velocity interpenetrating plasma flows. The bottom panels show the evolution of filamentary magnetic fields created by the Weibel instability.

The Omega experiments were important for demonstrating that the collisionless regime can be created by high-power lasers and that Weibel-mediated magnetic fields can be created by high Mach-number plasma flows. Nevertheless, these experiments did not form true collisionless shocks where a jump in density and temperature is expected. The Thomson scattering measurements indicated that the density pile-up in the interacting region never exceeded two times the single-flow plasma density. To form shocks bigger system size and higher density flows are required. The team proposed experiments on the NIF to achieve these conditions.

To increase the system sizes and the plasma density the NIF experiments used 900 kJ of laser energy and the separation was enlarged to 25 mm, compared to 8 mm for the Omega experiment, as shown in Figure 2 on the left panel. The plasma pile-up for the interpenetrating plasma flows was diagnosed by optical Thomson scattering which measures the electron density in the plasma. The result is shown on the right-top of Figure 2 where the interpenetrating double-flow shows greater than four times the density of the single flow indicating that a collisionless shock has truly been formed³⁾.

In addition, the NIF experiments also looked for evidence of electron acceleration using an electron spectrometer. A collisionless shock is expected to be the site of particle acceleration that happens by diffusive shock acceleration called the first-order Fermi acceleration process. The measured electron spectrum from the interacting double-flow clearly shows an enhancement of the flux in the high energy band.

Future work includes measuring ion acceleration and magnetized collisionless shocks.

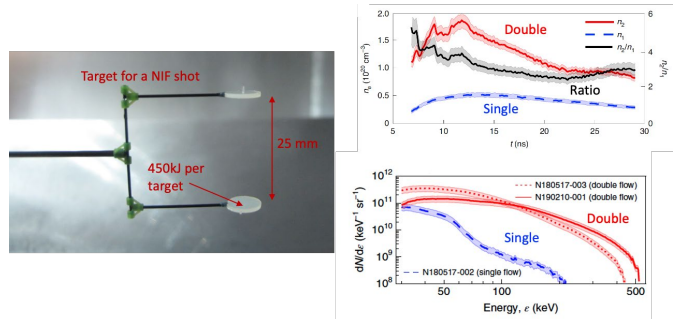


Figure 2. The left panel is the target used in the NIF experiments. The white deuterated foils are each illuminated by 450 kJ of laser energy. The interacting plasma flows were diagnosed by optical Thomson scattering showing the plasma pile-up is 4 times greater than for a single-flow (right-top panel) which is clear evidence of collisionless shock formation. In addition, the electron particle spectrometer measured a non-thermal distribution (right-bottom panel) indicating that the particles are accelerated within the shock front by a diffusive shock acceleration mechanism.

¹⁾C. Huntington et al., Nature Physics, 11, (2015), 173

²⁾H. -S. Park et al., Phys. Plasmas, 22, (2015), 056311

³⁾F. Fiúza et al., Nature Physics, 16 (2020), 916

The 2015 Symposium on Status and Prospects of High Energy Density Science by Giant Lasers

Category: FPPC - HEDS

Name: Keisuke Shigemori, Terry Land

Affiliation: Osaka University, Lawrence Livermore National Laboratory

Approximately 119 scientist and dignitaries attended the meeting which provided a forum to foster relationships, share cultures and exchange ideas. The meeting was held at Lawrence Livermore National Laboratory on September 28-29, 2015. It was organized by the Science Council of Japan (SCJ), Japan Society for Promotion of Science and held at SLAC National Accelerator Laboratory on September 30. The meeting was co-organized by Osaka University, Lawrence Livermore National Laboratory, RIKEN SPring-8, and SLAC National Accelerator Laboratory. Lead contacts for organizing the meeting were: Dr. Keisuke Shigemori, Osaka University, Technical Contact, shige@ile.osaka-u.ac.jp and Dr. Terry Land, LLNL, Technical Contact, land1@llnl.gov.

Scope of the Symposium:

High power lasers can heat matter to conditions that would otherwise only exist at the center of a planet or within a star. They can reproduce the phenomena that drive supernovae, and that accelerate particles to the highest energies in the universe. Most recently, a new scale of “giant lasers” has emerged – including the *National Ignition Facility* (NIF) in the United States (U.S.); the *Linac Coherent Light Source* (LCLS) and SPring-8 Angstrom Compact Free Electron Laser (SACLA) x-ray lasers in the U.S. and Japan; and the emerging *Extreme Light Infrastructure* (ELI) laser and *European-XFEL* x-ray laser in Europe. These are complemented by other advanced laser systems such as the GEKKO-XII and Laser for Fast Ignition Experiments (LFEX) lasers in Japan and Omega/Omega Extended Performance (EP) in the U.S.

These lasers have opened new fields of science known as “laboratory astrophysics” and “high energy density science”, as well as providing important new tools for the study of advanced materials, photonic devices, and the pursuit of fusion energy. This symposium will explore the science and technology frontiers of this field and identify areas for future international cooperation in the intersection of giant optical and x-ray lasers.

Overview talks describing the current capabilities of the various facilities and state of the art technology were presented followed by breakout sessions to discuss mutual areas of interest and collaboration as well as Identify requirements for laser, diagnostics and target development in 3-5-year time frame. Discussion also included Pump-Probe Systems, Seeding and Multi-pulse System Development for studying extreme material science.

Scientists in the breakout sessions discussed the themes listed below and talked about where the next frontier lies, what are the compelling questions to answer, can they be addressed with current facilities, if not, what advancements it would take to achieve these goals. Collaborations and areas of mutual interest were identified and presented by the groups.

Session #1: Laser Fusion, Plasma Physics and Neutron Sources

Chair: Takayoshi Norimatsu (ILE, Osaka University)

Co-chair: Nino Landen (LLNL)

Session #2: Laboratory Astrophysics

Chair: Youichi Sakawa (ILE, Osaka University)

Co-chair: Frederico Fiuzza (SLAC)

Session #3: Extreme Material Science

Chair: Ryosuke Kodama (Osaka University)

Co-chair: Arianna Gleason-Holbrook (LANL)

Session #4: High Power Optical, X-ray Photon Sources

Chair: Ken-ichi Ueda (UEC)

Co-chair: Felicie Albert (LLNL)

Based on the 2015 Symposium on HEDS, we had expanded the US-Japan collaborations, which comes to fruition as the 2019 Symposium and the Project Arrangement signed by DOE and MEXT in Jan. 2019.

2017 US-Japan Technical Meeting on HED Sciences with High-Power Lasers

Category: FPPC - HEDS

Name: Shinsuke Fujioka, Tammy Ma

Affiliation: ILE Osaka University, LLNL

Twelve Japanese scientists and fifteen Lawrence Livermore National Laboratory scientists gathered for a two-day technical meeting to share and discuss recent work and progress on experiments and simulations of a variety of HED topics including intense laser-plasma interactions, particle acceleration, plasma photonics, fast ignition, and magnetic field generation and dynamics. (See below for full agenda)

There was much interest from the Japanese side in the ARC laser and related NIF experiments. From the US side, there was considerable interest in their J-KAREN laser at the Kansai Photon Science Institute at the National Institutes for Quantum and Radiological Science and Technology (QST) (Ti-Sapphire, 10 J, 300 TW, ~20 fs pulse for typical experimental intensities of $3\text{-}5\text{e}21 \text{ W/cm}^2$) to explore proton and heavy ion acceleration for development of a compact accelerator source. New results (presented by M. Nishiuchi) include measurements of electron temperatures that scale with laser energy rather than intensity (likely due to very small focal spot of $\sim 1 \mu\text{m}$), and a very high electric field strength generated in thin targets that can ionize higher Z materials up to extremely high ionization states. A. Pirozhkov presented a talk on the upgrade, called J_KAREN-P that will be a 1 PW, 0.1 Hz, 10^{22} W/cm^2 intensity diffraction-limited, bandwidth-limited laser for extreme high field physics.

Osaka University, Kyoto University, and Tohoku University brought many young scientists (students, postdocs) that presented new theory on limits of the hole boring, the temporal evolution of energetic electron distributions in short-pulse interactions, and enhanced acceleration via self-generated magnetic fields; and experiments in magnetic reconnection on LFEX, and recent progress in Fast Ignition. Also of note, efforts are starting to apply machine learning to radiation hydrodynamics simulations of implosions.

As commented by Yasuhiko Sentoku of Osaka University, he “hopes that many more friendly interactions/ meetings can be held in the future between US and Japan, especially involving our young scientists.” He was “stimulated by the interactions with LLNL people.”

New collaborations are now forming to possibly use J-KAREN for positron studies, strengthen the collaboration between us and Osaka to work more closely together on simulations of our long pulse-length, high energy experiments (LFEX & ARC), develop future Discovery Science proposals, compare proton acceleration results spanning ARC scales to J-KAREN scales, and share knowledge on short pulse HED experimental diagnostics (SpecFROG for measurement of hydrodynamics of plasma interaction regions; framing cameras; scintillator ion detection technologies).

An invitation was extended to several physicists (Ma, Chen, Mariscal, & Williams) to visit J-KAREN. In return, an invitation to make a more extended visit to LLNL & see ARC was made to our Japanese colleagues (Nishiuchi & group).

The meeting was organized by Shinsuke Fujioka (ILE, Osaka University) and Yasuhiko Sentoku (ILE, Osaka University), and sponsored by the Japan Society for Promotion Sciences (JSPS).



The 2019 Symposium, Project Arrangement, and the Science Committee

Category: FPPC - HEDS

Name: R. Kodama, Y. Sentoku, F. Graziani

Affiliation: ILE Osaka University and Lawrence Livermore National Laboratory

The 2019 Symposium established a new start to the Japan-U.S. collaboration. Scientists from both countries met to discuss high power lasers, HED science with high power lasers and XFEL, computational HED science, and HED science with large scale laser facilities. The Symposium focused on four major goals.

- Identify focus areas of R&D for potential long-term and sustainable collaborations
- Identify opportunities for each country to host experiments by leveraging each country's unique facilities
- Identify lead scientists for the various research areas
- Define concrete steps and goals to carry this process forward



Figure 1. Photo in the signing ceremony of Project Arrangement.

A new framework to assist with describing the needs and goals of the collaboration was described by the Project Arrangement document. This document was signed by representatives from MEXT and DOE and arranged by the Embassy of Japan in Washington DC. The Project Arrangement functions as an umbrella that fosters Japan-U.S. HED activities. It also established the Science Committee made up of Japan and U.S. leaders in HED science. The Science committee functions to:

- Alleviate barriers to facilitate and encourage collaborations and education
- Identify and drive the formation of specific scientific collaborations
- Advocate for government funding
- Should funding become available, form a vision for these endeavors and ensure timely selection and delivery of projects

The Project Arrangement and Science Committee define a framework to strengthen and support research collaborations between Japan and the U.S. HED science communities. Two focused, follow-up meetings occurred in August of 2019 and January of 2020 between professors Kodama and Sentoku and LLNL scientists and management.

The August meeting was devoted to setting the path forward for research collaborations and defining the roles and responsibilities of the Science Committee. In January, a follow-up discussion with LLNL Director Bill Goldstein and LLNL scientists focused on concrete steps moving forward in the collaboration. By the end of the January meeting, it was agreed that, depending on the level of support between the two countries, Japan-U.S. collaborations have three options:

1. Japan and the U.S. can continue in this mode with no additional investment.
2. Modest investment would yield support for on-going collaborations, education, sabbaticals, and the exchange of students.
3. Larger investment could mean extension of the LaserNetUS idea to Japan and the investment by Japan in the building of high repetition rate, MW-average power laser facilities.



Figure 2. Participants photo in The 2019 Japan-US Symposium on "Perspective of High Energy Density Science and Technology by High Power Lasers"

A novel fusion-reaction-history detector with picosecond time resolution

Category: FPPC - HEDS

Name: Yasunobu Arikawa/Johan Frenje

Affiliation: Institute of laser engineering, Osaka University/ Massachusetts Institute of Technology

Inertial Confinement Fusion (ICF) experiments at the National Ignition Facility (NIF) have made significant strides towards achieving ignition in a laboratory. Significant alpha heating has been observed in recent experiments, which resulted in significantly enhanced neutron yields and shorter nuclear-burn durations. The nuclear burn history provides critical information about the dynamics of the hot-spot formation and high-density fuel-shell assembly of an ICF implosion, as well as information on the impact of alpha heating, and a multitude of implosion failure mechanisms. As the confinement time of an ICF implosion is a few 10's ps, ps time resolution is required for an accurate measurement of the nuclear burn history. To that end, Prof. Y. Arikawa (ILE-Osaka) and Dr. J. Frenje (MIT) have been collaborating on developing a novel neutron detector for detailed measurements of the nuclear burn history. Prof. Arikawa spent three months at MIT working with Dr. Frenje on developing a new detector concept with ps time resolution by means of ultra-short pulse laser and electro-optical mechanism.

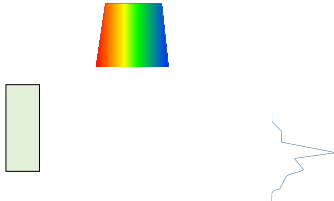


Figure 1. Conceptual design of the ultra-fast neutron detector. See text for more details.

To date, this collaboration has resulted in one paper published in Review of Scientific Instruments [Y. Arikawa, et al., Rev. Sci. Instrum., 91(6) 063304 Jun 1, 2020]. Figure 1 shows the conceptual design of the neutron detector. A chirped probe laser is injected and reflected by an Electro Optical material (EO material). The EO polymer is positioned at a small distance to an implosion (~5 mm) and is attached to the tip of an optical fiber (not shown in the Figure). At this distance, the temporal broadening of the Doppler-broadened neutron signal is negligibly small. The EO polymer and part of fiber are disposable and will be replaced after every shot. The fusion neutrons that interact with the EO material generate

absorption-rate changes of the chirped probe laser and these changes are observed with a wave-length spectrometer.

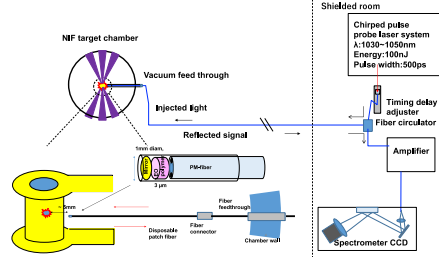


Figure 2. Conceptual description of the detector set up on the NIF. The neutron-sensitive EO material is positioned at 5 mm from the implosion center of NIF target and it is connected to the detection system by an optical fiber. More detail is described in the text.

Due to the nature of the chirped probe laser, the wavelength spectrum is subsequently converted into a temporal signal distribution. Figure 2 schematically shows the detector setup for the NIF. A proof-of-principle experiment was conducted with the LFEX laser at ILE-Osaka University. The experimental set up of the detector was similar to the one shown in Figure 2 except for the EO material was placed at 65 mm from a target. The LFEX laser (500J/1.5ps) was used to irradiate a Tantalum target for generation of electrons, and these were used instead of neutrons in this experiment. Figure 3 shows the observed signal from that experiment. The red curve shows the LFEX laser pulse, while the black curve illustrates the 4-ps temporal history of the detected electrons. This test demonstrates for the first time a 4-ps temporal response of the detector, which is adequate for measurements of higher moments in the nuclear burn history. The result will have important implications not only for ICF but also for the entire field of HEDS.

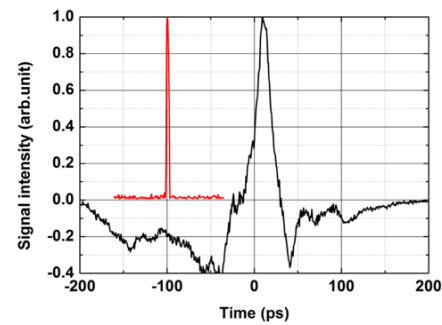


Figure 3. Results from the proof-of-principle test of the detector concept. This detector test used electrons generated by LFEX laser at ILE-Osaka University. See text for further details.

Development of laser ion source for heavy ion inertial fusion

Category: FPPC - HEDS

Name: M. Okamura/K. Takahashi

Affiliation: BNL/NUT

An ion source to supply a large number of heavy ions such as Pb and Bi with low charge state is one of the most important components for a heavy ion inertial fusion (HIF) system. We have studied high brightness ion beam production using laser ablation plasma in the framework of US-Japan collaboration. In the past decade, we have developed techniques to control ion beams provided from a laser ion source and many aspects of the ion source, such as beam current, pulse width, and emittance with a solenoid magnetic field, have significantly improved. The achieved performance of the laser ion source can satisfy the requirements for the HIF¹⁻²⁾.

Many accelerator systems have been considered to irradiate substantial current beams over 1 kA with a target fuel for fusion durations of the order of 10 ns. To avoid transporting too high current beams during acceleration, all schemes of the systems adopt a technique for longitudinal compression of the beam during acceleration, which allows us to supply smaller beam current and longer pulse duration from the ion source. However, still the ion source has to supply a large current beam with a low emittance.

Laser ion sources can generate large current ion beams with sufficient pulsed duration for various heavy ions with singly charge-state. Furthermore, the ablation plasma can be controlled with a magnetic field, and it can allow us to realize the large current ion beam required for HIF. Therefore far, we have shown that the solenoid magnetic field increases the current of the laser ion source. Figure 1 shows the change in the beam current waveform when the magnetic field is applied to a laser ablation plasma. This result suggests that the solenoid can

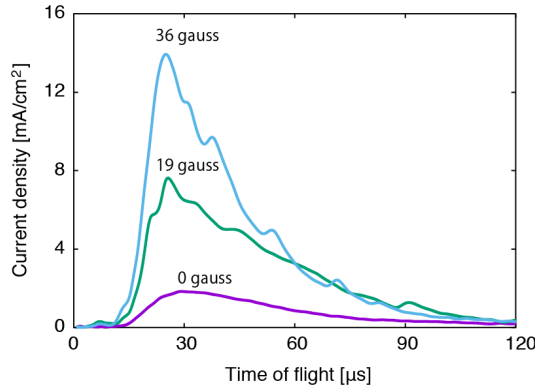


Figure 1. Ion beam current enhancement of a laser ion source using a solenoid magnetic field.

increase the ion current of the plasma even with relatively low magnetic field. When ion beams with a long pulse duration are required, a long distance for the plasma transport needs to extend the duration of plasma, which leads to decreasing the ion current drastically due to the three-dimensional expansion of the plasma. In such a case, applying a solenoid magnetic field to the plasma is more effective for the amplification of ion beam current.

Not only high beam current but also low emittance, which means good convergence property, is required for the HIF ion source because the ion beam should be irradiated on a small fuel target. The laser ion source can supply low emittance ion beams because an ion beam is extracted from a small part of ablation plasma in which the directions of the ions are oriented the same propagating direction. To obtain a much lower emittance beam from a laser ion source, it is necessary to suppress the density fluctuation of the plasma during the pulse. It has been confirmed that the beam current waveform can be modulated by applying a pulsed magnetic field as shown in Figure 2. When the beam current waveform is changed by the magnetic field, the α value of Twiss parameter, which indicates the degree of convergence and divergence of the beam, changes in response to the current waveform. This indicates that the pulsed magnetic field reduces the time evolution of the plasma density and suppresses the change in the meniscus of the ion emission surface during the pulse. Therefore, the behavior of the beams extracted from the plasma can be controlled by the pulsed magnetic field, and we can obtain a higher brightness ion beam.

Our US-Japan research collaboration has continued for the past decade without interruption. This collaboration has greatly encouraged the research and the development of the ion source for HIF.

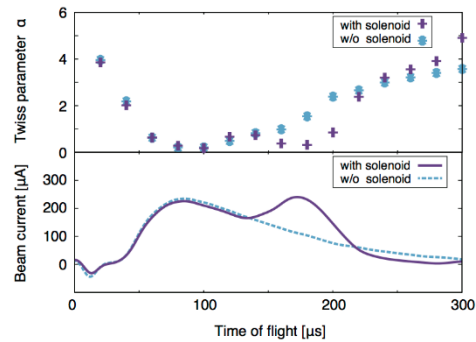


Figure 2. The variation of beam current waveforms and Twiss parameter α modulated by pulsed magnetic field.

¹⁾ 1) M. Okamura *et al.*, Nucl. Instrum. Meth. Phys. Res. A 733 (2014) 97

²⁾ 2) M. Okamura, Matter Radiat. at Extremes 3 (2018) 61

Study of relativistic electron-positron pair jet interactions using LFEX lasers

Category: FPPC - HEDS

Year-Number:2013-FP6-11, 2014-FP6-9, 2017-FP6-12

Name: Hui Chen and Mitsu Nakai

Affiliation: Lawrence Livermore National Laboratory, USA, *Institute of Laser Engineering, Osaka University, Japan

US-Japan joint team performed the experiments using LFEX laser at ILE, Osaka University to investigate the capability of laser-produced relativistic pair jets as a platform for laboratory astrophysical experiments. Through the effective collaboration, the joint team was successful obtaining exciting results from the three experimental campaigns. This data advanced our understanding of electron acceleration and further the quest of producing astrophysical relevant pair plasma at relativistic regime.

Relativistic pair plasmas and jets are believed to exist in many astrophysical objects and are invoked to explain energetic phenomena related to Gamma Ray Bursts, Black Holes and the heating of intergalactic medium(IGM). Although short lived, a laboratory source of relativistic pair plasma jets can be used as a surrogate to study the dynamics of pair jet-plasma interactions, such as the evolution of instabilities induced by relativistic pair slowing down in a neutral electron-ion plasma. This is directly applicable to quantifying the heating of the IGM by blazar-produced relativistic pairs and can test the theory that these “pair (jets) are expected to trigger *collective* plasma instabilities”

Electron-positron plasmas are generated using ultra-intense lasers as follows: when an intense laser is incident on a solid target, the laser electric and magnetic fields (via the JxB force) interact with free electrons in a coronal plasma, which was generated by the laser pre-pulse. For relativistic laser intensities ($> 10^{18} \text{ W/cm}^2$), the majority of the absorbed laser energy goes into creating $>\text{MeV}$ electrons, on the order of the ponderomotive potential. *These MeV electrons are the power source of pair generation.* Two positron production processes dominate depending on target conditions: the Bethe-Heitler (BH) process for thick high-Z targets, while the Trident process that plays a more important role for thin targets($<100 \text{ um}$).

In the BH process, the laser-accelerated hot electrons make high-energy bremsstrahlung photons that produce electron-positron pairs upon interacting with the nuclei, whereas in the Trident process the hot electrons produce pairs by directly interacting with the nuclei.

LFEX lasers have the unique capabilities, namely the high intensity with long focal length, to significantly increase positron emission by enhancing the conversion efficiency to relativistic electrons. Leveraging such capabilities, we performed a set of experiments on this laser to producing relativistic pairs. On the first LFEX experiment in 2012, laser to electron energy transfer, referred using x-ray and neutron measurements, was found to be consistent with measured positron yield¹⁾, although the yield was far below the previous scaling which US team compiled at other facilities²⁾.

In the FY2017 experiment, the goal was set to increase the laser-target coupling and increase the positron yield using the LFEX’s unique capabilities such as the contrast control, large laser energy, long focal length and the ability to setup a pulse-train. We performed series of shots on the LFEX laser to systematically study the energy conversion from laser to relativistic electrons. This includes 1) the scaling of pair creation at various pre-plasma conditions via controlling laser contrast level; 2) the effect of electron acceleration at various target geometry and laser focal conditions; and 3) the effect of double pulse train on the electron acceleration. Enhanced laser coupling to MeV electrons were observed using 1D cone targets and tailoring the pre-plasma conditions. It was also found that an optimized preplasma condition dramatically increases electron conversion and pair generation³⁾. Our Discovery Science pair experiments (2018-2019) on NIF ARC laser has benefited greatly from these LFEX experiments⁴⁾.

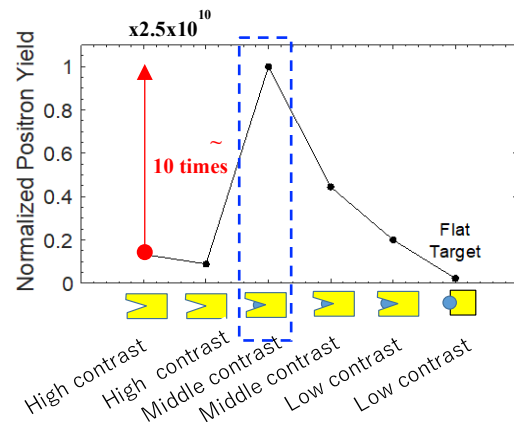


Figure 1. Six data shots were performed changing the target and laser setup at FY2017 experiment. Positron yield was dramatically increased by optimizing pre-plasma conditions.

¹⁾ H. Chen, et al., New Journal of Physics **15**, 065010(2013).

²⁾ H. Chen, et al., Phy. Plasmas **22**, 056705 (2015).

³⁾ Y. Arikawa, et al., APS DPP (2018).

⁴⁾ G. Williams, et al., Phy. Rev. E (2020).

Japan-United States Educational, Sabbatical, and Internship Opportunities

Category: FPPC - HEDS

Name: R. Kodama, Y. Sentoku, F. Graziani

Affiliation: ILE Osaka, LLNL

A new and growing area for collaboration is education. For minimal financial investment, this area will have far reaching impact-bringing students and faculty from Japan together with their counterparts in the U.S. HEDS is a rapidly growing interdisciplinary subject, that used to be the sole purview of the national laboratories. That situation has changed rapidly in the last decade. An ever-growing number of universities are now offering graduate programs in HED science and laser technology. One challenge facing education in HEDS is that HED science is offered in mechanical, electrical, and nuclear engineering or in physics departments. This fact implies that undergraduate students are entering with very different backgrounds. Engineering students wanting to study HED science might have very little background in quantum mechanics but a solid background in material science or hydrodynamics. A physics student on the other hand, has a very strong background in quantum mechanics or statistical mechanics but almost no background in hydrodynamics or material science. A second challenge is that HED science is so cross disciplinary that it is still an open question as to what constitutes a core curriculum. The implication is that there are gaps in many HED science programs.

To address these issues, course sharing is growing in popularity. Using modern conference technology such as WebEx or Zoom, national laboratories in the U.S. and university campuses are starting to share courses. The need to identify a core curriculum in HEDS and coordinate course sharing activities, led to a meeting of universities and national laboratories on the UCSD campus in December of 2019. Present were Professors Yasuhiko Sentoku and Yasuhiro Kuramitsu along with representatives from ten U.S. universities. Osaka University is a participating institution in the consortium of universities offering to share courses in HED science and laser technology.



Figure 1. Professor Shinsuke Fujioka from Osaka spent a sabbatical year at LLNL

Sabbatical opportunities for scientists from Japan and the United States are available. Professor Fujioka spent a sabbatical year at LLNL performing research on fast ignition. Professors Sentoku from Osaka and Arefiev from UCSD are coordinating and exchange of both short-term and long-term visitors between HED science institutions in Japan and the United States.

Student internship opportunities are also available. Dr. Hiroki Morita spent seven months at LLNL while working on his dissertation, consulting with scientists on transport properties in dense plasmas. He is now a postdoc at ILE in Osaka.



Figure 2. Dr. Hiroki Morita giving a presentation while a student

We believe mutual exchanges of students, postdocs and staff scientists, in both short-term and long-term efforts, would bring benefit to each side of community. People interacting in other cultures produces new ideas and advances the HEDS science and makes the ties of friendship stronger. Under the COVID-19 situation starting in spring 2020, both countries are facing difficult situations. Some efforts have had to be canceled such as visiting student and scientist programs. However, applying new technologies, e.g., online meetings and distance learning, we have managed to keep scientists engaged.

CHAPTER 4 Joint Institute for Fusion Theory (JIFT)

4.1 Objectives

The distinctive objectives of the JIFT program are (1) to advance the theoretical understanding of plasmas, with special emphasis on stability, equilibrium, heating, and transport in magnetic fusion systems; and (2) to develop fundamental theoretical and computational tools and concepts for predicting nonlinear plasma evolution. Both objectives are pursued through collaborations between U.S. and Japanese scientists by means of two types of exchange program activities namely, workshops and exchange visits.

4.2 Activities

Each year the JIFT program usually consists of four topical workshops (two in each country) and six exchange scientists (three from each country). So far, during its 40 years of successful operation, JIFT has sponsored 245 long-term visits by exchange scientists and 138 topical workshops.

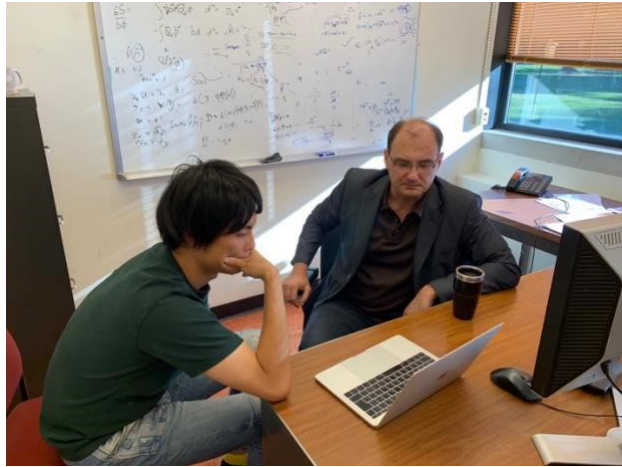
- The *workshops* typically have an attendance of 15–30 participants, of whom usually three to seven scientists (depending on the particular workshop) travel to the workshop from the non-host country. Scientists from countries other than the U.S. and Japan are also often invited to participate in JIFT workshops, either as observers or multi-laterals.
- Of the approximately three *exchange visitors* in each direction ever year, one (called the JIFT Visiting Professor) is supported by the host country, while the others (called Exchange Scientists) are supported by the sending country. The visits of the Exchange Scientists usually last from one to several weeks in duration, whereas the Visiting Professors normally stay for one month.

The topics and also the participating scientists for the JIFT exchange visits and workshops are selected so as to have a balanced representation of critical issues in magnetic fusion research, including both fundamental problems as well as questions of near-term significance, and also to take into account the specific capabilities and interests of both countries. The Japanese and US members of the JIFT Steering Committee agree together on the appropriateness of proposed topics before recommending them.



Participants at the JIFT Workshop on US-Japan collaborations on co-designs of fusion simulations for extreme scale computing (October 2019, RIKEN Center for Computational Science, Kobe)

Note that information about the JIFT program after 1992, including previous JIFT annual reports and JIFT meetings in Japan, may be found on the Japanese JIFT web site. Information on the JIFT program prior to 2008 including annual schedules of exchange activities, can be found on the US JIFT web site.



Ph.D. student, K. Yanagihara (left), of Nagoya University visited Princeton Plasma Physics Laboratory in May 2019 as an Exchange Scientist for collaboration with Dr. I. Y. Dodin (right) on Introduction of non-uniform dissipation to a quasi-monochromatic ray tracing

4.3 Administration

JIFT has a Steering Committee consisting of eight members, four from each country. Two of these members are the Japanese and US co-chairmen. Two other members of the Steering Committee, the US and Japanese co-executive secretaries, are responsible for the ongoing daily oversight of the progress of JIFT activities. The co-chairman and co-executive secretary on the US side are, respectively, the director at the Institute for Fusion Studies (IFS) of The University of Texas at Austin and a Professor at the University of California in San Diego. The Japanese co-chairman is the Leader of the Numerical Simulation Reactor Research Project at the National Institute for Fusion Science, and the Japanese co-executive secretary is the director of the Fundamental Physics Simulation Research Division in the Department of Helical Plasma Research at the National Institute for Fusion Science. Furthermore, on the Japanese side there is an Advisory Committee comprised of five members representing a spectrum of Japanese universities and the National Institutes for Quantum and Radiological Science and Technology; and on the US side there is an Advisory Committee comprised of five members representing a spectrum of US universities and national laboratories. The names of the persons on the Steering Committee and the names of the Advisors are listed below.

JIFT Steering Committee

US Members

- F. Waelbroeck (IFS) – Co-Chairman
A. Arefiev (UCSD) – Co-Exec. Secretary
D. Spong (ORNL)
J. Mandrekas (DOE)

Japanese Members

- H. Sugama (NIFS) – Co-Chairman
S. Ishiguro (NIFS) – Co-Exec. Secretary
S. Murakami (Kyoto)
Y. Sentoku (Osaka)

JIFT Advisors

Japanese Advisory Committee: Y. Todo (NIFS), Y. Kishimoto (Kyoto), Z. Yoshida (Tokyo), T.-H. Watanabe (Nagoya), M. Yagi (QST)

US Advisory Committee: J. Palastro (LLE/Univ. of Rochester), F. Graziani (LLNL), C. S. Chang (PPPL), and P. Terry (UWM)

The JIFT Steering Committee attempts to schedule workshops in such a way as to dovetail with other meetings. It also encourages participation at workshops by interested experimentalists and invites relevant available scientists from other countries to attend workshops.

As the principal program for fundamental theoretical exchanges in the US-Japan Fusion Research Collaboration, JIFT operates alongside the Fusion Physics Planning Committee (FPPC) and the Fusion Technology Planning Committee (FTPC). In particular, the JIFT activities are coordinated with the four FPPC areas of activity, viz., core plasma phenomena, edge behavior and control, heating and current drive, and new approaches and diagnostics.

4.4 Accomplishments and Highlights

A number of general benefits have resulted over the years from the JIFT program. In particular, the following may be cited: JIFT has provided efficient communication channels for the latest theoretical research results, techniques, and directions; JIFT activities have attracted serious participation from allied fields such as fluid turbulence, statistical physics, computational science, and space plasma physics, which brings new scientific tools into the fusion program and enhances the stature of fusion physics; JIFT exchanges have contributed to efficient utilization of international research facilities; and, JIFT emphasis on large-scale computational studies has reaped significant mutual benefits from the supercomputer resources and code-building expertise of both countries.

Through JIFT, close and long-lasting scientific connections have been established between the U.S. and Japanese fusion theory communities. Not only have senior scientists profited from these collaborations, but also young scientists and even, on occasion, advanced graduate students have had many opportunities to enhance their research careers. Some of highlights of achievements are shown hereafter.

JIFT Exascale Computing Workshops: Innovation and co-design of fusion simulations towards extreme scale computing

Category: JIFT

Name: CS Chang^{a)}, Jack Wells^{b)}, Tomo-Hiko Watanabe^{c)}, Yasuhiro Idomura^{d)}, Masanori Nunami^{e)}

Affiliation: ^{a)}PPPL, ^{b)}ORNL, ^{c)}Nagoya University, ^{d)}JAEA, ^{e)}NIFS,

During the Fusion Sciences session at the '2014 Smoky Mountains Computational Sciences and Engineering Conference and US/Japan Exascale Applications Workshop,' it was decided that the US/Japan fusion exascale workshop would continue on an annual basis. It was then later decided that the workshop would be held in the JIFT framework. The initial organizers chosen were T. Watanabe (Japanese Chair), Y. Idomura (Japanese Co-Chair), C.S. Chang (US Chair), and J. Wells (US Co-Chair). In 2019, the Japanese Chair was replaced by M. Nunami.

The purpose of the workshop was to promote a US-Japan collaboration on the co-design of magnetic fusion simulations towards extreme-scale computing of core-edge plasma physics and plasma-material interactions. Through the collaboration, US and Japan would share the status of fusion research enabled by high performance computers, identify gaps and challenging collaboration topics among scalable US and Japanese fusion codes in getting to exascale, and establish vision for paths.

The first meeting was held at Nagoya University on August 20 and 21, 2015. 12 Japanese and 11 US fusion and computational scientists made presentation. A wide range of extreme-scale topics were discussed: planning of next generation scientific computer hardware, status of full-f gyrokinetic simulations, scalable algorithms, tools, software engineering, data management and visualization, material simulations, performance prediction and optimization, MHD/fluid simulation, and particle-MHD hybrid simulation of energetic particles.

Toward the end of the meeting, the extended Japan and US organizing committee members met to discuss challenging collaboration problems related to exascale computing. The Japanese side suggested the full-f gyrokinetic simulations for tokamaks and stellarators as the most suitable and challenging exascale problems. The US side agreed to these problems.

The second meeting was held at ORNL on August 17-19, 2016. 17 US and 7 Japanese participants made presentation. In addition to covering the topics set in the 2015 workshop, two most active US-Japan collaboration activities were reported. One was the OpenACC based GPU performance portability analysis of the Japanese full-f continuum gyrokinetic code GT5D on ORNL's Titan by a US collaborator (S. Abbot, ORNL) and the other was the performance portability analysis of the US full-f gyrokinetic particle code XGC on NIFS's FX100 by a Japanese collaborator (M. Nunami, NIFS).

The third meeting was held at JAEA at Future Center Initiative, University of Tokyo on August 7-8, 2017. 13 Japanese and 12 US participants made presentation. The PostK hardware architecture was revealed at this meeting.

The fourth meeting was held at PPPL on July 30 and 31, 2018. 15 US and 9 Japanese participants made presentation (see Figure 1). From this meeting, the workshop topics focused on the continuum and particle gyrokinetic simulations as the strongest candidates for exascale computing. As a special feature, the US plans for the exascale computers were revealed. Also highlighted was the introduction of the US-Japan collaboration activity on the development of the stellarator version XGC.

The fifth meeting was held at RIKEN Center for Computational Science in Kobe, Japan on October 28-29, 2019. 13 Japanese and 12 US participants made presentation. The workshop topics were extended to include the Post-K and ECP collaboration, under the new title of the workshop 'Joint US-Japan Workshop on PostK-ECP Collaboration and JIFT Exascale Computing Collaboration.' The workshop was also extended to include machine learning application. The Japanese full-f gyrokinetic continuum code GT5D was given access to the then world's fastest US computer Summit, and the US full-f gyrokinetic particle-in-cell code was accepted to the Japanese Post-K Fugaku Early Science Program. Fugaku is now the world's fastest computer. A specific success story out of the close US-Japan collaboration was reported by T. Moritaka (NIFS): the birth of XGC-S that can simulate not only the Japanese LHD but also other stellarators such as German W7-X and PPPL's NCSX.

The five JIFT workshops on exascale computing have been highly rewarding, allowing for the open exchange of ideas, and learning of each other's successes. The workshop will advance to the next phase: joining the Workshops on US DOE and Japan MEXT Collaboration on Extreme Computing.

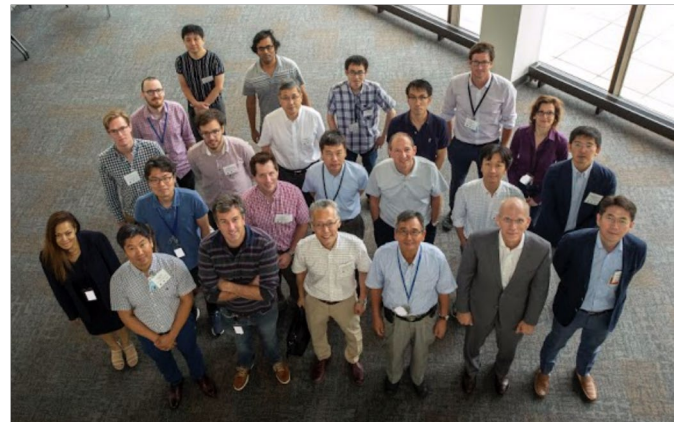


Figure 1. Participants of the fourth JIFT Exascale Computing Workshop at PPPL in 2018.

Progress on Advanced Optimization Concept and Modeling in Stellarator-Heliotrons

Category: JIFT

Name: S. Murakami / D.T. Anderson

Affiliation: Kyoto Univ. / Univ. of Wisconsin-Madison

LHD (NIFS) has been operated since 1998 and has extended the operation regions of plasma parameters, i.e., high temperature more (>10 keV) and high density($>1020\text{m}^{-3}$). Heliotron-J (Kyoto Univ.) has been operated since 2000. A first quasi-symmetric device HSX (UW-Madison) has been conducted since 1999. These devices have shown many interesting results about optimization effects on the confinement properties and the plasma confinement in the quasi-symmetric geometry.

Based on these experimental results, the activities of finding the next generation stellarator are progressed in both Japan and the US. This workshop aims to enhance the present recent progress on advanced optimization concepts and modeling in stellarator-heliotron configuration. We hope fruitful discussions and the starting of new collaborations between Japan and the US. We had two workshops in Japan (Kyoto University, 2018) and the US (University of Wisconsin-Madison, 2019).

The first workshop was held at the Uji Campus of Kyoto University on 22-23 March 2018. A total of 26 participants (US:4 and Japan:22) attended the workshop. Japanese participants presented the recent results of the LHD and Heliotron-J experiment results, and the development of the next-generation device. The US participants presented the HSX experiment results and the idea of next-generation device related to the turbulent transport, divertor configuration, and energetic particle confinement.

Confinement characteristics of ITB plasmas with deuterium in the LHD was presented by H. Takahashi (NIFS). The improvement of the energy confinement of the deuterium e-ITB plasmas was systematically confirmed. The statistical approach for thermal transport modeling in LHD based on the TASK3D-a database was presented by M. Yokoyama (NIFS). 3D transport modeling of peripheral plasmas, neutrals, and impurities in LHD with EMC3-EIRENE was presented by G. Kawamura (NIFS). Heliotron-J results in terms of the bumpy field were presented by S. Yamamoto (Kyoto Univ.). Effect of magnetic field structure on electron internal transport barrier and its role for the barrier formation in Heliotron J was presented by T. Minami (Kyoto Univ.)

A Next-Step in the UW-Madison Stellarator Program was presented by D.T. Anderson (UW-Madison). He discussed Wisconsin's interest to participate in designing and building a new mid-size quasi-helically symmetric stellarator in conjunction with a diverse team of national and international participants.

Turbulent transport optimization in stellarators was presented by C. Hegna (UW-Madison). A theoretical paradigm

for turbulence optimization is developing based on turbulent saturation processes. Turbulence research activities in LHD and Beyond was presented by M. Nakata (NIFS). Next Generation Stellarator Task Force is recently initiated at NIFS, and the new optimization concept is being explored.

The second workshop was held at University of Wisconsin-Madison on 19-21 June 2019. A total of 24 participants (US:17 and Japan:7) attended the workshop. US participants presented the results from the Simons Collaboration on stellarator optimization. Also, HSX experiment results and the turbulent transport, divertor configuration, and energetic particle confinement related to the next device. Japanese participants presented the plan of the next device of LHD and the progress of CFQA construction, and Heliotron-J experiment results.

Early results from the Simons Collaboration on stellarator optimization was presented by A. Cerfon (New York Univ.). The Simons collaboration on Hidden Symmetries and Fusion Energy aims to place on a more rigorous and firmer footing the optimal design principles of the stellarator class of toroidal magnetic confinement devices and to develop a new stellarator optimization strategy based on cutting-edge optimization algorithms and approaches. Adjoint methods for efficient stellarator optimization and sensitivity analysis were presented by E. Paul (Univ. of Maryland). Direct construction of stellarator shapes with good confinement was presented by M. Landreman (Univ. of Maryland).

Stellarator designs with permanent magnets were presented by C. Zhu (PPPL). He introduced the recent research work at PPPL on designing new stellarators using permanent magnets and simple coils.

A comparison of ITG turbulent transport in HSX and NCSX within the context of turbulence optimization was presented by I. McKinney (UW-Madison). They concluded that the consideration of nonlinear physics is necessary to accurately assess the heat flux due to ITG turbulence when comparing QS stellarator equilibria. Optimizing Stellarators for Reduced Turbulent Transport was presented by B. Faber (UW-Madison).

Progress of new device project in NIFS was presented by M. Nakata (NIFS). An extended turbulence proxy is constructed based on the simplified transport model with nonlinearity and ZF generation, which has been validated with LHD experiments. Built-in divertor configuration in an optimized stellarator by Y. Suzuki (NIFS). QH configuration with continuous helical coils was presented by H. Yamaguchi (NIFS). Integrated Transport Modeling for Helical Reactor was presented by S. Murakami (Kyoto Univ.).

Recent Status of NIFS-SJTU Joint Project for CFQS Quasi-axisymmetric Stellarator was presented by M. Isobe (NIFS). The CFQS first plasma will appear in FY2021.

JIFT Workshops on high-intensity laser-plasma interactions and high energy density physics

Category: JIFT

Name: Yasuhiko Sentoku / Alexey Arefiev

Affiliation: ILE / UCSD

Since 2014, seven workshops focused on theory and simulations of high-intensity laser-plasma interactions and related high energy density physics have taken place in Japan and in the US:

- 2014 JIFT Workshop (Austin, TX)
- 2016 JIFT Workshop (Fukui, Japan)
- 2016 JIFT Workshop (San Jose, Japan)
- 2017 JIFT Workshop (San Diego, CA)
- 2018 JIFT Workshop (Hiroshima, Japan)
- 2018 JIFT Workshop (Portland, US)
- 2019 JIFT Workshop (Osaka, Japan)

On the US side the workshops were organized by Prof. Arefiev (IFS/UCSD). On the Japanese sides the workshops were organized by Prof. Sentoku (Osaka University & ILE), Dr. Sunahara (ILE/Purdue University), and Prof. Johzaki (Hiroshima University).

The development of two multi-picosecond laser systems capable of achieving relativistic laser intensities, one in Japan (LFEX laser system) and one in the US (NIF ARC), has opened up new regimes of laser-plasma interactions to exploration. Previously, relativistic laser-plasma interactions were typically restricted to sub-ps durations. Due to the increased laser pulse duration at LFEX and NIF ARC, energetic electrons are able to perform many bounces along a laser-irradiated target. This enables stochastic electron heating, with electrons effectively getting a 'kick' every time they return to the laser-irradiated surface of the target. Another important aspect is the ion response in these multi-ps laser-plasma interactions. The ions have the time to respond to charge separation electric fields on a multi-ps time scale, so their motion must be explicitly included into electron heating models. Due to high electron energy, a kinetic description becomes a necessity, which introduces an extra level of complexity into already challenging multi-scale problems. These problems are of common interest for the US and Japanese scientific communities and that is why multi-ps laser-plasma interactions were one of the major topics covered by the workshops.

Results presented by LLNL and ILE scientists^{1,2)} showcased the described novel features of multi-ps relativistic laser-plasma interactions. Major results include a significant increase in energies of laser-heated electrons and

accelerated ions compared to previous studies for shorter laser pulses with the same laser intensities. Workshop presentations have also highlighted new approaches to modeling and theoretical analysis of these regimes.

Another subject of common interest is the utilization of a newly developed experimental capability to generate strong magnetic fields. It has been shown that capacitor-coil targets irradiated by a ns-long kJ laser pulse can generate magnetic fields that are hundreds of Tesla in strength³⁾. These fields persist on a ns time scale, so they are able to diffuse into targets used for studies of relativistic laser-plasma interactions. The presence of these quasi-static magnetic fields adds a new 'control knob' or an extra dimension to the parameter space that can be explored in laser-plasma interactions. The capability to generate strong laser-driven magnetic fields has been developed in parallel at high-energy laser facilities in Japan (ILE) and in the US (LLE and LLNL). The results presented at multiple workshops demonstrate that kT-level magnetic fields qualitatively alter laser-plasma interactions at relativistic laser intensities⁴⁾ and the resulting high energy density phenomena, such as laser-driven ion acceleration⁵⁾.

The workshops have also covered those phenomena that arise in plasmas irradiated by ultra-high-intensity lasers. There are several facilities in the US that are capable of reaching 1022 W/cm², e. g. TPW and Hercules, and, recently, J-KAREN laser system at KPSI, Japan has been upgraded to reach such an intensity as well. The regimes enabled by this capability have generated significant interest from both US and Japanese sides, with multiple results demonstrating novel particle⁶⁾ and radiation sources⁷⁾ presented.

The workshops were dedicated primarily to kinetic simulations and theoretical models of the described regimes, but some experimental results were also presented and discussed to provide context. These workshops served well their primary goal to bring together researchers from the US and Japan interested in laser-plasma interactions and to enable exchange of ideas. The workshops have served another important function, which is the integration of junior researchers and students into the high energy density community. Multiple students and postdoctoral fellows attended each workshop. Many of them are now research scientists and some are faculty members, with the JIFT workshops serving as an important stepping stone in their career development. The workshops have also generated several US-Japan collaborations, which demonstrates the advantage of the format with extended discussion segments.

¹⁾ D. Mariscal et al., Phys. of Plasmas 26, 043110 (2019).

²⁾ N. Iwata et al., Plasma Phys. Control. Fusion 62, 014011 (2020).

³⁾ S. Fujioka et al., Sci. Rep. 3, 1170 (2013).

⁴⁾ T. Sano et al., Phys. Rev. E 100, 053205 (2019).

⁵⁾ A. Arefiev et al., New J. Phys. 18, 105011 (2016).

⁶⁾ R. Matsui et al., Phys. Rev. Lett. 122, 014804 (2019).

⁷⁾ D. Stark et al., Phys. Rev. Lett. 116, 185003 (2016).

JIFT Workshop on Plasma Simulation Science

Category: JIFT

Name: Alexey Arefiev / Hiroaki Ohtani

Affiliation: IFS (Present: UCSD) / NIFS

Methods for simulating kinetic phenomena in plasmas have undergone significant advances since the early development of the particle-in-cell (PIC) method in the 1950s. The conventional PIC method is typically limited to simulating problems with high-frequency, small-scale phenomena because of the employed full-f formulation and explicit time-differencing. However, many modern-day plasma physics problems fall outside of that category, as they involve low-frequency, large-scale phenomena. Innovative methods that introduce techniques such as adaptive mesh refinement, implicit time-differencing, the Monte Carlo method, dela-f and gyrokinetic formulations, the variational principle, etc., allow us to successfully tackle the challenges posed by multi-scale problems.

Dr. Arefiev and Dr. Ohtani organized a series of seven workshops on plasma simulation science between 2008 and 2014. The workshop focused on the recent progress of simulation techniques, modeling, data analysis methods and so on for large-scale computer simulations in plasma physics and fusion science. In this paper, we report four workshops that took place between 2011 and 2014.

1. Workshop 2011 (NIFS, Toki, Japan)

A workshop entitled “The Next Stage in the Progress of Simulation Science in Plasma Physics” was held at NIFS, Japan on December 2-3, 2011. The workshop was attended by 28 participants. There were 19 oral presentations (7 from the US, 12 from Japan), which covered a range of subjects related to advanced simulation methods and modeling about gyrokinetic code, hybrid kinetic-MHD model, extended delta-f method, integrated modeling, full-f kinetic simulation, multi-scale simulation, adaptive mesh refinement for PIC simulation, application of GPGPU to PIC simulation, effective parallelization for PIC simulation, remote collaboration system by the internet and scientific visualization by VR system.

2. Workshop 2012 (Providence, RI, USA)

A workshop entitled “Innovative Methods in Plasma Particle Simulations” was held at Providence, RI, USA on November 2-3, 2012. The purpose of this workshop was to bring together US and Japanese researchers working on plasma kinetic simulations to exchange ideas and report recent research progress. The workshop was attended by 26 participants. There were 21 oral presentations (14 from the US, 7 from Japan). The workshop highlighted the development and applications of novel methods in the context of various plasma physics problems, including fusion, reconnection, and laser-plasma interactions. The workshop also included a discussion of using GPU in parallel algorithms to accelerate particle simulations.

3. Workshop 2013 (NIFS, Toki, Japan)

A workshop entitled “New Aspects of Plasma Kinetic Simulation” was held at NIFS, Japan on November 22-23, 2013. Innovative modeling and simulation techniques, such as adaptive mesh refinement, implicit time-differencing, the Monte Carlo method, dela-f and gyrokinetic formulations, the variational principle, multi-hierarchy model, etc., are developed to tackle the challenges posed by multi-scale problems in fusion plasma. The purpose of this workshop was to bring together US and Japanese researchers working on plasma kinetic simulations to exchange ideas and report recent research progress. The goal of the workshop was to highlight the development and application of novel methods in the context of various plasma physics problems, including fusion, reconnection, and laser-plasma interactions and so on. The workshop was attended by 33 participants. There were 19 oral presentations (six from US, one from Canada, and 12 from Japan), which covered a wide range of subjects related to radiation transport simulations with particle-in-cell (PIC) simulation, micro-scale physics in inertial confinement fusion implosions, a Fokker-Planck-Landau equation solver for both continuum and PIC kinetic codes, Accelerations of gyrokinetic and PIC models by OpenACC and CUDA, and optimization of load balance in PIC simulation, data compression methods of PIC simulation, and so on.

4. Workshop 2014 (New Orleans, LA, USA)

A workshop entitled “Progress in Kinetic Plasma Simulation” was held at New Orleans, LA, USA on October 31 and November 1, 2014. The three main goals of the workshop were 1) to highlight the progress in development of new algorithms and the improvements made to the existing ones; 2) to present new results obtained using kinetic plasma simulations; 3) to discuss the new physics aspects that need to be considered when performing kinetic plasma simulations. Plasma kinetic simulations are used to tackle a wide ranging of problems from fusion plasmas to plasmas irradiated by high intensity lasers. The diversity of these problems has stimulated development of novel yet very specific techniques to address the issues of interest. Typically, the discussion of these techniques is confined to a small community of researchers working on a specific topic. The purpose of this workshop was to bring different communities together for an exchange of ideas. The workshop was attended by 26 participants. There were 22 oral presentations (14 from the US, eight from Japan). The workshop covered a range of subjects related to an application of gyrokinetic model to Tokamak edge, Toroidal full-f GK code, an application of PIC code to laser-plasma acceleration phenomena, implicit scheme, multi-hierarchy model, PIC simulation on plasma periphery, VR visualization and so on.

Three-dimensional MHD Equilibrium Calculation by Simulated Annealing

Category: JIFT

Name: M. Furukawa / P. J. Morrison

Affiliation: Tottori University / University of Texas at Austin

The “Simulated Annealing (SA)” technique is a new method to calculate equilibria of ideal fluids, including ideal magnetohydrodynamics (MHD). M. Furukawa and Prof. P. J. Morrison have been developing the method for ideal MHD equilibria in three-dimensional torus geometry. The equilibria, to be obtained by SA, can in principle include plasma rotation and/or magnetic islands and stochasticity. Because we have found several issues worth studying, M. Furukawa visited Prof. P. J. Morrison at Institute for Fusion Studies, University of Texas at Austin during March 6–March 31, 2019 under the JIFT exchange program JF-9. The stay was followed by another one week for an extended collaboration outside the JIFT program.

Such an ideal fluid system is described by a Hamiltonian expressed via noncanonical variables and a corresponding Poisson bracket. The Poisson bracket can have degeneracy since the variables are noncanonical, which result in Casimir invariants. A set of phase points where each Casimir invariant takes a same value is a Casimir leaf. Then the ideal fluid system follows a trajectory with a constant Hamiltonian on a Casimir leaf in the phase space. An equilibrium of the system is given by an extremum of the Hamiltonian on the Casimir leaf. If an initial condition is chosen away from the equilibrium, the ideal dynamics never reaches the equilibrium.

The SA technique enables us to reach the equilibrium by solving an artificial dynamics that is derived from the Hamiltonian structure of the ideal fluid. The simplest way to construct such an artificial dynamics is to operate with the Poisson bracket twice; once would be the original dynamics. So far, we have demonstrated that SA generates low-beta reduced MHD equilibria in two-dimensional rectangular domains and in cylindrical geometry. Especially of note, MHD equilibria with magnetic islands were obtained in the cylindrical geometry¹⁾. Moreover, we have extended our development to high-beta reduced MHD in axisymmetric toroidal geometry²⁾. There, we have successfully obtained large-aspect-ratio and circular cross-section tokamak equilibria as well as toroidally-averaged heliotron equilibria.

During this visit to IFS, we focused our discussion on how to impose additional constraints other than the Casimir invariants that are built into the Poisson bracket. The Casimir invariants are quantities integrated over the volume. An example is the magnetic helicity for ideal MHD. SA obtains an equilibrium that is an energy extremum on a Casimir leaf. However, when we obtain a tokamak equilibrium by solving the

Grad-Shafranov (G-S) equation, we specify pressure and current density profiles that are local quantities. Therefore, the equilibrium obtained by solving the G-S equation may not be the energy extremum without local constraints on the profiles. In other words, we may find a lower energy state with the same values of the Casimir invariants by relaxing the local profile constraints. In fact, if we perform SA starting from a symmetric MHD equilibrium with a helical perturbation, the system does not return to the symmetric equilibrium even though it is MHD stable linearly. This means that SA searches for an energy extremum in a broader region on the Casimir leaf than we assume with the local profile constraints. Consequently, we need a method to restrict the phase space by the local constraints in which the SA searches for an energy extremum.

We found a nice formulation of a Dirac bracket that embeds additional constraints while preserving the original Casimir invariants. To verify the usefulness, we first examined dynamics of a heavy top written in noncanonical variables. This system has two Casimir invariants, although it is a six degrees of freedom system. Figure 1 shows the time evolution of three variables among six during SA, and one of them r was kept unchanged by the Dirac constraint.

We observed that the energy successfully decreased monotonically while two Casimir invariants did not change in this simulation.

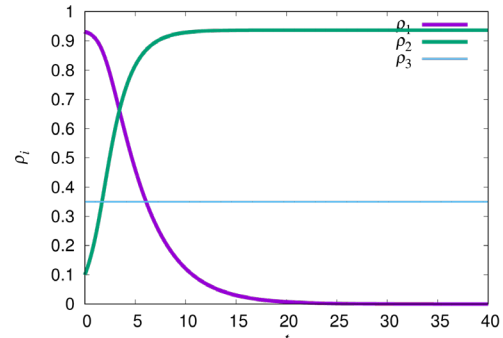


Figure 1. Time evolution of three variables among six for the heavy top. The Dirac constraint kept ρ_3 unchanged. The energy decreased monotonically by the SA, leading to an equilibrium that is not an equilibrium without the constraint.

We have also completed the formulation of a Dirac bracket to impose constraints on the current density profile for low-beta reduced MHD during this visit to IFS. We will examine if this works well for obtaining an equilibrium with a specified current density profile.

¹⁾ M. Furukawa and P. J. Morrison, Plasma Physics and Controlled Fusion 59, 054001 (11 pp) (2017).

²⁾ M. Furukawa, Takahiro Watanabe, P. J. Morrison, and K. Ichiguchi, Physics of Plasmas 25, 082506 (8 pp) (2018).

Quasioptical modeling of wave beams with mode conversion and non-uniform dissipation

Category: JIFT

Name: K. Yanagihara¹⁾, I. Y. Dodin²⁾, and S. Kubo³⁾
 Affiliation: 1)QST, 2)PPPL, 3)NIFS

Quasioptical propagation of wave beams with mode conversion and non-uniform dissipation in inhomogeneous anisotropic media was studied during I. Y. Dodin's visit to NIFS in 2017 and K. Yanagihara's visit to PPPL in 2019.

Electron Cyclotron Resonance Heating (ECRH) is one of the essential methods used to heat and control fusion plasmas so it is important to model ECRH with fidelity. Since an Electron Cyclotron Wave (ECW) beam generally consists of two (O and X) modes, and their relative contributions evolve as the beam propagates in inhomogeneous plasma, full-wave codes are usually considered necessary to simulate such beams. However, full-wave simulations are prohibitively slow for the mm waves of interest; thus, more efficient numerical tools are needed. The collaborative work by Yanagihara et al. sponsored by JIFT has recently yielded a such a tool, which is unique in its class¹⁻⁴⁾.

By extending the recent theory by Dodin and Ruiz for geometrical-optics waves with mode conversion, Yanagihara et al. developed a quasioptical formulation that can describe ECW beams with refraction, mode conversion, and diffraction taken into account simultaneously²⁾. Using this formulation, Yanagihara et al. also developed a new code PARADE (PArxial RAY DEscription) that can simulate ECW beams fast with minimal computational resources^{3,4)}. PARADE solves two coupled approximate Schrödinger-type equations for the appropriate projections of the wave envelope around a Reference Ray (RR), which is found using traditional ray tracing.

PARADE has two unique advantages. The first one is that unlike in other quasioptical codes, mode conversion is fully resolved. This is illustrated in Figure 1, which shows PARADE simulations of a beam that starts off as a pure-O wave but then evolves into a mixture of O and X waves. Figure 1(e) demonstrates the evolution of the mode-amplitude ratio. This effect is due to the rotation of the dc magnetic field along the beam propagation, which couples the O and X waves¹⁾.

PARADE's second unique advantage is that the transverse profile of the wave intensity is not assumed but calculated directly, so inhomogeneity of dissipation can also be modeled. This is illustrated in Figure 2, which shows PARADE simulations of O-wave partial absorption near the electron cyclotron resonance. The absorption rate varies strongly in the beam cross section, so the intensity profile is distorted. Then,

the beam experiences stronger diffraction and the beam "center of mass" gets shifted relative to the RR.

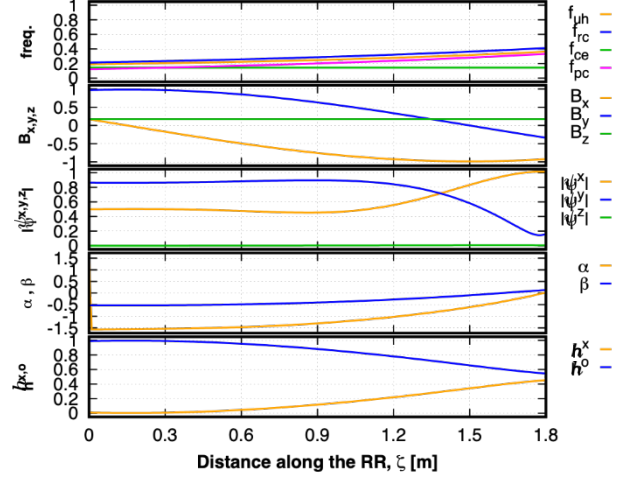


Figure 1. Results of PARADE simulation of an ECW beam that experiences O-X mode conversion due to the sheared dc magnetic field while propagating along the z-axis in low-density cold plasma. (a) The key frequencies on the RR trajectory: the upper-hybrid frequency, the right-cutoff frequency, the electron cyclotron frequency, and the plasma frequency (all normalized to the wave frequency). (b) The components of the dc magnetic field (normalized to the local $|\mathbf{B}|$). (c) The absolute values of the individual components of the vector wave amplitude on the RR. (in arbitrary units) (d) The polarization angles, namely, inclination angle α and ellipticity β [4]. (e) The relative intensities of the O and X components of the beam.

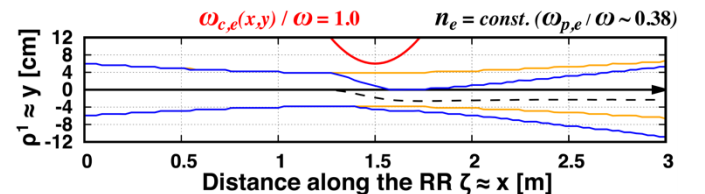


Figure 2. Results of PARADE simulation of an O-wave beam propagating along the x-axis and partially passing through the cyclotron resonance (red) in hot electron plasma. The black dashed line shows the beam center of mass. The blue lines show the beam width along the RR (black arrow). For a reference, the orange lines show the beam width without absorption.

¹⁾ I. Y. Dodin et al., Phys. Plasmas 24, 122116 (2017).

²⁾ I. Y. Dodin et al., Phys. Plasmas 26, 072110 (2019).

³⁾ K. Yanagihara et al., Phys. Plasmas 26, 072111 (2019).

⁴⁾ K. Yanagihara et al., Phys. Plasmas 26, 072112 (2019).

Molecular Dynamics Simulation for Tungsten Divertor

Category: JIFT

Name: S. Saito¹, S. I. Krasheninnikov², R. D. Smirnov², H. Nakamura³, K. Sawada⁴, M. Kobayashi³, G. Kawamura³, M. Hasuo⁵

Affiliation: ¹Yamagata University, ²University of California San Diego (UCSD), ³National Institute for Fusion Science (NIFS), ⁴Shinshu University, ⁵Kyoto University

Molecular dynamics (MD) simulations are widely used for investigation of the elementary processes of the plasma-material interactions (PMI). The accuracy of the interatomic potential function in MD calculations greatly affects the reliability of the calculations. Although, tungsten-hydrogen interaction is important in the investigation of PMI in fusion devices, it was difficult to perform the MD simulations because of the lack of accurate interatomic potential for tungsten-hydrogen system. With the help and expertise of the UCSD group of Prof. S. I. Krasheninnikov and Dr. R. Smirnov, the latest tungsten-hydrogen potential function ¹⁾was implemented to our MD code for the investigation of PMI through the JIFT program. The developed tungsten-hydrogen MD code led to the investigation of the contribution of thermal process in the formation of hydrogen platelet-like structure and the development of a hydrogen recycling model on tungsten divertor.

1. Contribution of thermal process in the formation of hydrogen platelet-like structure

The UCSD group found by MD simulations that hydrogen atoms absorbed in tungsten material at high concentrations form

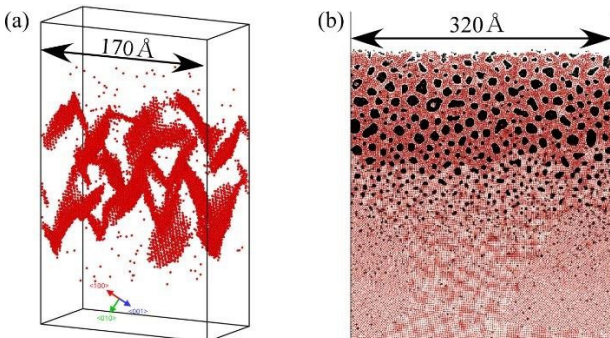


Figure 1. (a) Platelet-like structure of hydrogen in tungsten calculated by R. D. Smirnov and S. I. Krasheninnikov². (b) Helium bubble structure in tungsten calculated by S. Saito, et al.⁴⁾ (Figure 1(b): Copyright (2018) The Japan Society of Applied Physics)

a platelet-like structure ²). On the other hand, S. Saito (dispatched researcher) found that the helium bubbles are formed by energy minimization of the tungsten-helium potential ³). The fact that a structure forms by energy minimization means that the structure develops without thermal vibration or thermal diffusion.

A calculation was performed to reveal whether hydrogen platelet-like structures could be formed by the energy minimization process.

As a result of the calculation, no platelet-like structure is observed even after performing a sufficient energy minimization. Different from the formation of the helium bubbles, the result indicates that it is necessary to cross the potential maximum point by a thermal process for the formation of the platelet-like structure of hydrogen in tungsten.

2. Hydrogen recycling model on tungsten divertor

Most hydrogen ions impinging on plasma facing materials (PFMs) are recycled at the PFMs in fusion devices. For the boundary condition of analysis of the neutral transport in the edge plasma, it is important to estimate the parameters of recycled hydrogen atoms and molecules at PFMs such as the emission angle distribution and the translational, rotational and vibrational energy distributions. Japanese group had developed the hydrogen recycling model on carbon divertor^{5,6)}. The implementation of tungsten-hydrogen potential with advice from the UCSD group made it possible to extend the hydrogen recycle model to tungsten divertor.

Figure 2(a) shows an example simulation using the developed recycling model. In this model, trajectory of a hydrogen particle injected into the hydrogen contained tungsten material is simulated. From this simulation model, it is found that the hydrogen atom travels on the surface of the tungsten material and remains there for a while because it is trapped on the surface of the tungsten material as shown in Figure 2 (b). The obtained information about hydrogen dynamics will be used for neutral transport analysis in the fusion devices.

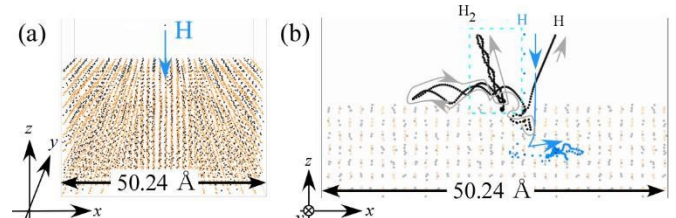


Figure 2. (a) Developed hydrogen recycling model on tungsten divertor. (b) One of the examples of hydrogen emission process calculated by the model.

¹⁾ Li-Fang Wang, et. al., J. Phys. Condens. Matter, 29 (2017) 435401

²⁾ R. D. Smirnov, and S. I. Krasheninnikov, Nucl. Fusion 58 (2018) 126016

³⁾ A. M. Ito, et. al., Phys. Scr., T159 (2014) 014062

⁴⁾ S. Saito, et. al., Jpn. J. Appl. Phys., 57 (2018) 01AB06

⁵⁾ S. Saito, et. al., Contrib. Plasma Phys., (2020) e201900152

⁶⁾ K. Sawada, et. al., Contrib. Plasma Phys., (2020) e201900153

A Fractal Hierarchy of Partial Barriers in the Chaotic Edge of Heliotrons

Category: JIFT

Name: S. R. Hudson, Y. Suzuki*

Affiliation: Princeton Plasma Physics Laboratory (PPPL), *National Institute for Fusion Science (NIFS)

The magnetic fields in the periphery of helical fusion devices such as heliotrons and stellarators and also in tokamaks with applied perturbation fields is invariably a fractal mix of invariant flux surfaces with irrational rotational-transform known as KAM surfaces and magnetic islands, which create irregular or chaotic field lines where they are sufficiently large so as to overlap. The KAM surfaces provide complete barriers to fieldline transport, and the irregular fields create regions of poor confinement.

Interspersed in the chaotic regions are cantori. A cantorus is like a leaky KAM surface, and magnetic field lines can escape through; but, their importance lies in the fact that fieldline transport across a cantorus can very, very low, even though it may not be exactly zero. The cantori can provide effective partial barriers to fieldline transport. The KAM surfaces and cantori have irrational rotation-transform, and the islands form where the rotational-transform is rational. Understanding how these structures of the magnetic field fit together and influence transport of heat and particles across the plasma edge requires an understanding of how irrational and rational numbers fit together on the number line.

To understand the structure of the magnetic field in the edge, we constructed a hierarchy of “ghost surfaces”¹⁾. Ghost surfaces are derived mathematically by exploiting an analogy between magnetic field line flow in toroidal magnetic fusion experiments and Hamiltonian dynamical systems, and then using the Lagrangian formulation to write the magnetic field line action, S , as the line integral of the magnetic vector potential, $S = \int \mathbf{A} \cdot d\mathbf{l}$.

The unstable (X) periodic fieldlines, for which the rotational transform is rational, e.g. $\iota p/q$ where p and q are integers, are closed periodic curves that minimize the action integral. The stable (O) periodic field lines are closed periodic curves that extremize the action. These curves are actually minimax points, or saddles. By constructing a family of periodic curves for each pair of p, q using the action gradient flow, $\partial \mathbf{x} / \partial \tau = -\delta S / \delta \mathbf{x}$ where \mathbf{x} describes position the curve and ϕ is the toroidal angle, $\delta S / \delta \mathbf{x}$ is the first variation of the action, and τ is a poloidal integration parameter, we construct a (p, q) ghost surface that connects the stable and unstable periodic orbits, and thus creates a rational almost-invariant surface. By taking limits so that p, q approximates an irrational number, we can construct the KAM surfaces when they exist. Where they

don’t exist, the irrational ghost surfaces “fill in the gaps” in the cantori and are irrational almost-invariant surfaces.

We can use a radial framework of ghost surfaces, which are guaranteed to not overlap, to construct “chaotic coordinates”. In Figure 1, we show what the magnetic field as computed using the HINT²⁾ code, looks like in chaotic coordinates. for the Large Helical Device (LHD), a heliotron in operation at NIFS.

Because the rational ghost surfaces, by construction, poloidally interpolate between the periodic fieldlines, both the O and X periodic fieldlines for a given pair (p, q) lie on the (p, q) ghost surface. Because the irrational ghost surfaces coincide with the KAM surfaces, the intact flux surfaces appear flat in chaotic coordinates. The irrational ghost surfaces that approximate the cantori, which are partial barriers to magnetic field line transport, serve to partition the chaotic regions into subregions with small fieldline flux from one subregion to another.

By constructing chaotic coordinates, we obtain a precise understanding of the fractal hierarchy of complete and partial barriers across the edge of fusion devices. Transport in fusion plasmas is highly anisotropic, i.e. transport along the fieldlines is much greater than transport across. So, to a very good approximation, the pressure and temperature are constant on the ghost surfaces.

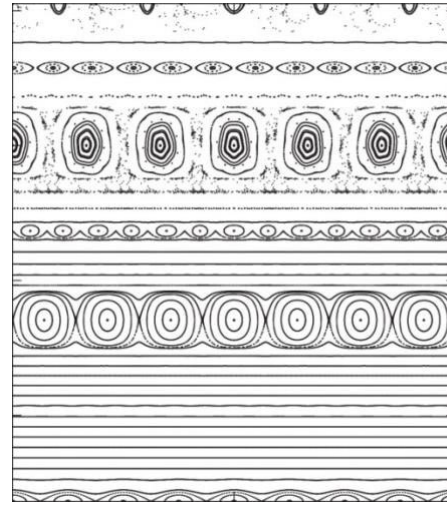


Figure 1. By transforming to “chaotic coordinates”, all the flux surfaces and cantori in LHD appear as straight lines, and the edge region is partitioned into regions of good-flux surfaces and regions of islands and irregular trajectories. The horizontal axis is the poloidal angle, and the vertical axis is a radial coordinate.

¹⁾ S. Hudson, Y. Suzuki, Phys. Plasmas 21, 102505 (2014); <https://doi.org/10.1063/1.4897390>

²⁾ Y. Suzuki, N. Nakajima et al., Nucl. Fusion 46, L19 (2006). <https://doi.org/10.1088/0029-5515/46/11/L01>

New simulation methods for energetic particle instabilities in stellarators

Category: JIFT

Name: D. A. Spong and Y. Todo

Affiliation: ORNL, NIFS

All toroidal magnetic fusion systems share a common interest in controlling instabilities driven by energetic particle (EP) components. These instabilities lead to a deterioration in heating efficiency, high localized wall heat loads, and lowered reactor ignition margins. The stellarator provides a unique environment for the study of EP-driven turbulence due to its long pulse lengths and direct control over the rotational transform level. In the future, the opportunities for 3D optimization of the stellarator are expected to provide a degree of control over these instabilities beyond what can be achieved in axisymmetric systems. The LHD stellarator project has for many years contributed to research on EP instabilities through excellent diagnostics, superb scientific staff, and generous allocations of experimental time. This work also can improve the understanding 3D effects on these instabilities in tokamaks.

For these reasons, the U.S.-Japan JIFT program has provided an ideal platform for the development and verification of new EP instability simulation methods. This originated with the development of Alfvén continuum analysis of 3D systems,¹⁾ followed by efficient methods to solve for the stable MHD global eigenmodes.²⁾ These tools coupled with our experience in Monte Carlo particle simulation methods then led to early perturbative, particle-based instability models³⁾ for Alfvén instabilities, which were applied to LHD and several other stellarators. The particle-based model allowed the first consistent treatment of finite orbit width stabilization effects on AE instabilities in stellarators and has indicated these effects can be significant in LHD. Regular JIFT visits have allowed the EP simulation methods to be shared with LHD scientists and resulted in many applications to LHD experimental data and collaborative publications.

These early efforts have formed a sound basis for our more recent work, which has been directed toward improving the tools for Alfvén instability analysis to take into account increasingly non-perturbative, kinetic, and nonlinear effects of these instabilities. In 2015 with assistance from Ihor Holod and Zhihong Lin we adapted the GTC global gyrokinetic particle-in-cell stability code to stellarators. The LHD device was our first application⁴⁾ of this new instability model (Figure 1) and it was demonstrated that Alfvén instabilities similar to those driven experimentally by neutral beam injection could be simulated for a range of toroidal mode number families

and for both monotonic and reversed shear rotational transform profiles. Nonlinear studies (Figure 2) based on this model were also reported in an invited talk given at the 2015 International Stellarator Heliotron Workshop in Greifswald, Germany.

In 2015 development also began on a new gyro-Landau closure model (FAR3d)⁵⁾ for Alfvén instabilities in stellarators.

This was an extension of an earlier model (TAEFL)⁶⁾ that had been extensively applied to tokamaks. This effort benefited from essential contributions by Luis Garcia of the Universidad Carlos III de Madrid and Jacobo Varela (at that time an ORNL post-doc). Such models incorporate the wave-particle resonance effects that drive EP instabilities into closure relations, resulting in a reduced description that can be very computationally efficient. Again, LHD provided the first application for the FAR3d model to a stellarator. Since then, it has been applied to a wide range of regimes in LHD, as well as other stellarators and tokamaks. Its inclusion of both EP instabilities and reduced MHD in an integrated framework has aided in guiding experimental interpretation in situations where there are transitions from MHD to more kinetic EP-driven instabilities. The most recent applications of FAR3d are addressing the EP nonlinear regime.

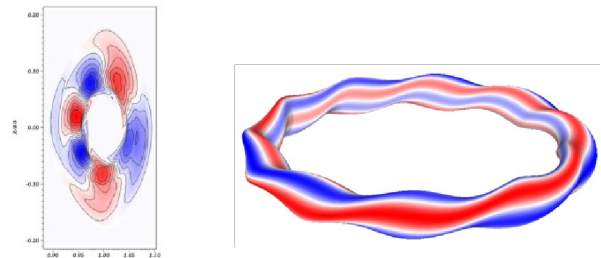


Figure 1. LHD $n = 2$ toroidal Alfvén instability obtained using the GTC global gyrokinetic particle-in-cell model.

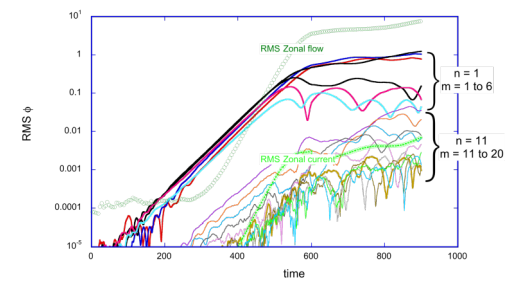


Figure 2. Nonlinear evolution of an $n = 1$ TAE instability in LHD using the GTC global gyrokinetic particle-in-cell model.

¹⁾ D. Spong, R. Sanchez, A. Weller, Phys. Plasmas, 10 (2003) 3217.

²⁾ D. A. Spong, E. D'Azevedo, and Y. Todo, Phys. Plasmas 17 (2010) 022106.

³⁾ D. A. Spong, B. N. Breizman, D. L. Brower, et al., Contrib. Plasma Phys. 50 (2010) 708.

⁴⁾ D. A. Spong, I. Holod, Y. Todo, Nuclear Fusion 57 (2017) 086018.

⁵⁾ J. Varela, D. A. Spong, L. Garcia, Nuclear Fusion 57 (2017) 046018.

⁶⁾ D. A. Spong, et al., Phys. Fluids B 4 (1992) 3316.

Global Gyrokinetic Simulation of Stellarators and Heliotrons

Category: JIFT

Name: M. D. J. Cole^{a)}, T. Moritaka^{b)}, R. Hager^{a)},
C.S. Chang^{a)}

Affiliation: ^{a)}Princeton Plasma Physics Laboratory
(PPPL), ^{b)}National Institute for Fusion Science (NIFS)

We developed a global gyrokinetic code for simulation of 3D toroidal magnetic confinement fusion plasmas, based on the XGC whole volume total-F gyrokinetic code for tokamaks. This code, XGC-S, was then applied to simulations of modern stellarators/heliotrons, including the Large Helical Device (LHD; NIFS), Wendelstein 7-X (W7-X; Max Planck Society), and the National Compact Stellarator eXperiment (NCSX; PPPL design).

This work involved the extension of the equilibrium model in XGC from 2D to 3D, including an interface with both the ideal MHD 3D equilibrium code VMEC, and the resistive equilibrium code HINT3D. The unstructured mesh technology of XGC, which permits whole volume simulation through the separatrix, was modified to account for toroidal variation in mesh node placement based on equilibrium information from the above equilibrium codes. A new tool was created to generate such meshes while enforcing the condition that node placement be field aligned. The charge deposition and scattering routines and equations of motion were modified for 3D toroidal simulation. A model of the stellarator/heliotron first wall was implemented and tested using engineering data for LHD, along with corresponding equilibrium extension into the edge region using the EXTENDER code.

To verify this new development, we performed simulations of energetic particle confinement and radial electric field evolution in LHD ¹⁾, and linear electrostatic ion temperature gradient-driven (ITG) modes in W7-X ²⁾ (see Figure 1). Good agreement was found between XGC-S and the BEAMS3D, GT5D and EUTERPE codes respectively in all these test cases. Good agreement in benchmark cases for a range of different physical phenomena, and in comparison with a number of different codes, gives good confidence in the correctness of the implementation.

Simulations have also been performed into the nonlinear phase for electrostatic ITG modes in the NCSX stellarator (see Figure 2). By extending into the turbulent phase this is a first-of-its-kind simulation with global gyrokinetic codes in stellarator geometry. The simulations showed that the highly localized linear ITG mode structure, characteristic in optimized stellarators (see e.g., Figure 1), can give way to a more broadly spread mode structure in the nonlinear phase. This has implications for predicting and optimizing turbulent heat

transport in stellarators, suggesting that tailoring geometry for mode localization may be less valuable.

A global gyrokinetic code for stellarators has broad application. In on-going work, the code is being used to investigate the turbulence properties of different stellarator/heliotron configurations. Developments also aim to model the effect of impurities in stellarators. Impurity accumulation is an important topic for stellarator reactors, potentially creating limiting conditions for their operational performance; it is an area where the behavior of stellarators is known to differ fundamentally from that of tokamaks.

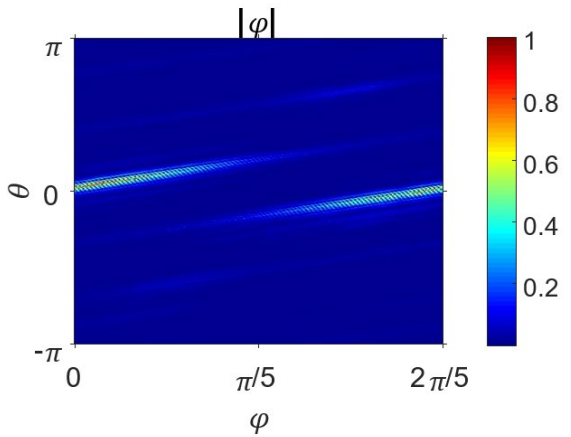


Figure 1. Fine-scale electrostatic potential mode structure on the central flux surface for linear electrostatic ITG mode, normalized to the surface maximum, in the W7-X stellarator

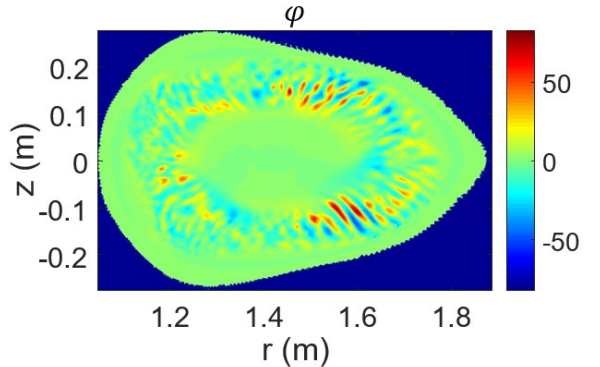


Figure 2. Cross-section of the perturbed electrostatic potential (V) for an electrostatic ITG mode during the nonlinear phase in the NCSX quasi-axisymmetric stellarator design.

¹⁾T. Moritaka, R. Hager, M. Cole et al., *Plasma*, 2 (2019) 179-200

²⁾M. D. J. Cole, R. Hager, T. Moritaka et al., *Phys. Plasmas*, 26 (2019) 082501

³⁾M. D. J. Cole, T. Moritaka, R. Hager et al., *Phys. Plasmas*, 27 (2020) 044501

ATEQ: Adaptive Tokamak EQuilibrium code

Category: JIFT

Name: Linjin Zheng, M. T. Kotschenreuther, F. L. Waelbroeck/Y. Todo
Affiliation: IFS, UT-Austin/NIFS, Japan

This collaboration is centered on the development of the ATEQ (Adaptive Tokamak EQuilibrium) code. It is motivated by the challenges of both the stability and equilibrium computations.

Due to the complexity related to the tokamak X-point, most of stability analyses are carried out with some portion of edge region being cut off. This leads the safety factor value to become finite, instead of infinity, at the boundary. The stability analyses in Ref. [1] shows that the critical wall position is sensitive to how the edge region is cut off as shown in Figure 1 for $n=3$ external kink modes. This is especially the case when the resulting edge q is close to a rational number. From the energy minimization for peeling modes one can also see that more energy can be tapped when the last closed flux surface is close to a rational value. This indicates that inclusion of the X-point effects is important for the stability analyses, especially for peeling-balloonning modes.

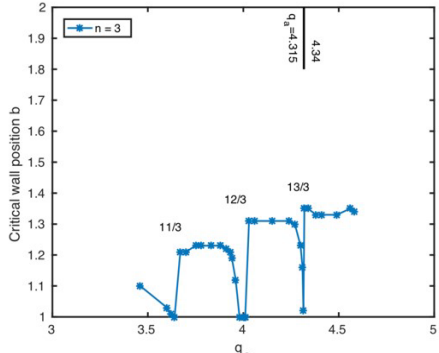


Figure 1. The critical wall position versus the safety factor at the tokamak edge [2]. The external kink modes are unstable when the wall position is larger than the critical wall position.

Most of equilibrium codes do converge poorly at tokamak edge with the X-point included. The wedge of magnetic surface at the X-point indicates a derivative discontinuity. This makes the equilibrium calculation challenging.

To meet these challenges, we have developed the ATEQ code. It is based on a radially adaptive numerical scheme and a multiple-region matching technique. The adaptive feature makes the ATEQ code more adaptable to a challenging equilibrium computation, especially for dealing with the region near the X-point.

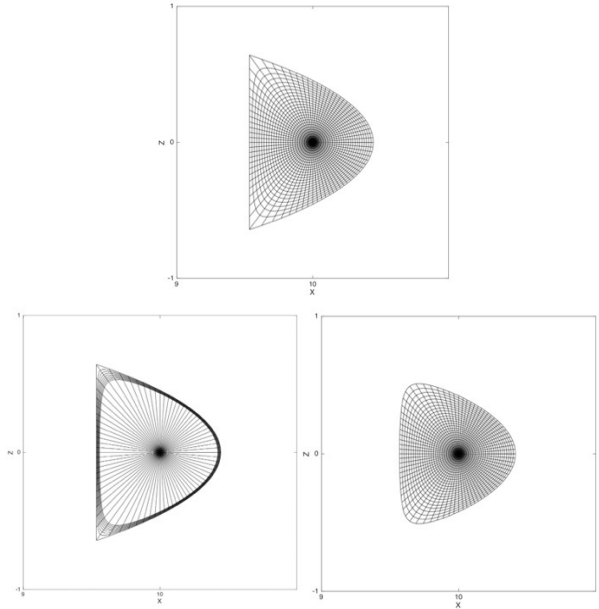


Figure 2. Edge region separation in the ATEQ numerical scheme.

Because the core and edge regions differ a lot, for example the edge region requires much more Fourier components to describe, the core and edge regions are treated separately as shown in the lower part of Figure 2. This allows the edge region with X point to be resolved better.

The code treats the core region as a fixed boundary equilibrium problem. The Fourier representation is used in the poloidal direction, while adaptive shooting with the independent solution decomposition is applied in the radial direction. The multiple region matching technique is used. The results are benchmarked with the Solovev solution and other MHD equilibrium codes. Actually, the lower right Figure in Figure 2 is the ATEQ shooting results for the Solovev equilibrium. Good agreement with the Solovev solution is achieved.

The edge region is treated as an initial value problem with the adaptive shooting. From the core solution, one obtains the magnetic flux and its derivative at the core region boundary. They can be used as the initial values for outward shooting for the edge region. There is possibility to shoot beyond the last closed flux surface, so that the vacuum region can be dealt with as well in this numerical scheme.

¹ L. J. Zheng, M. T. Kotschenreuther, and P. Valanju, Phys. Plasmas 24, 102503 (2017).

Study on Fast Ignition by Photon-Pressure Accelerated Ion Beam with Next Generation Ultra-Intense Laser

Category: JIFT

Year-Number: 2012-JF-4 I 2013-JF-9

Name: T. Johzaki / Y. Sentoku

Affiliation: Hiroshima Univ./Univ. Nevada, Reno
(present address; Osaka Univ.)

In fast ignition, an ultra-intense pico-second laser is irradiated to heat a pre-compressed fusion fuel up to the ignition temperature. When the laser-accelerated electron beam is used for core heating, the large beam divergence, the broad energy spectrum and the difficulty in generating fast electrons having suitable energy to the core heating inhibit the efficient core heating. One of the alternative core heating schemes is use of ion beam generated by the hole boring radiation pressure acceleration (HBRPA). The 1D theoretical and numerical predictions^{1,2)} showed that it is possible to accelerate ions to the energy suitable for the core heating with the small energy spread and the small angular divergence. However, the 20 PIC simulations^{2,3)} showed the broader energy spectrum, the larger angular divergence and the lower conversion than those obtained in the 1D predictions. In addition, there are no ignition requirement evaluations based on the integrated simulation including the ion acceleration, the core heating and the fusion burning. In the present collaboration research, we have evaluated the ignition requirement for HBRPA-Carbon-beam-driven fast ignition by the integrated simulations where the ion beam properties were evaluated with 20 PIC simulations using PICLS2D⁴⁾ developed by Y. Sentoku and the following core heating and fusion burn processes were simulated by a 20 hybrid code FIBMET⁵⁾ developed by T. Johzaki.

Figure 1 shows the energy conversion efficiencies for fast ion and electron beams from incident laser η_b (a) and the energy and angular distributions of the beams (b) and (c) evaluated by 20 PIC simulations for HBRPA where a solid density carbon target is irradiated with the circular-polarized intense lasers of which intensity is $I_L \sim 10^{23} \text{ W/cm}^2$. The target surface, that is initially flat, is bended due to the finite spot effect ($\phi = 20 \mu\text{m}$, Super Gaussian) and perturbed in the laser-wavelength scale due to the Rayleigh-Taylor instability. As the result, the C⁶⁺ beam qualities become poorer than the ideal theoretical prediction: C⁶⁺ acceleration efficiency decreases and the energy and angular spreads become larger with time. Alternatively, the electron acceleration becomes remarkable due to the heated plasma expansion and oblique irradiation resulting from the interaction surface perturbation.

Using the beam profiles obtained by the PIC simulations, we carried out hybrid simulations where the beam is injected

100 μm away from the center of a spherically compressed DT plasma ($\rho = 500 \text{ g/cm}^3$, $\rho R = 2 \text{ g/cm}^2$), and evaluated the ignition required laser energy. In Figure 2, fusion output energies E_F obtained for $I_L = 0.9, 1.0, 1.1 \times 10^{23} \text{ W/cm}^2$ are plotted as a function of laser energy E_L . It was found that the circular-polarized intense laser with $E_L \geq 170 \text{ kJ}$, $I_L \sim 10^{23} \text{ W/cm}^2$ and $r_L = 10 \mu\text{m}$ and the carbon target for beam generation with the density of $\rho \sim 2 \text{ g/cm}^3$ are required for ignition. Also, we found that not only C⁶⁺ beam but also simultaneously accelerated electrons plays important role for core heating.

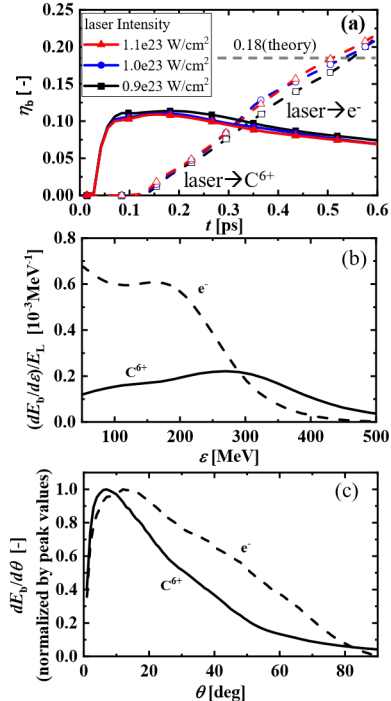


Figure 1. C⁶⁺ and electron (e⁻) beams properties; (a) temporal evolution of energy conversion efficiency and time-integrated energy and angular distributions ($L = 1023 \text{ W/cm}^2$) (b) and (c).

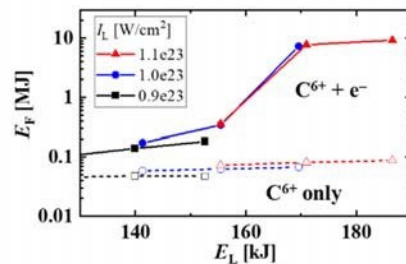


Figure 2. Fusion output energy E_F as a function of laser energy E_L .

¹⁾ Macchi et al. Phys. Rev. Lett. 94, 165003 (2005).

²⁾ N. Naumova et al.. Phys. Rev. Lett. 102, 025002 (2009)

³⁾ O. Klimo, et al.. Phys. Rev. ST Accel. Beams 11, 031301 (2008).

⁴⁾ Y. Sentoku and A. Kemp. J. Comput. Phys. 227, 6846 (2008).

⁵⁾ T. Johzaki, et al.. Proc. of IFSA 2003. ANS. 474 (2004).

CHAPTER 5 DIII-D

5.1 Objectives

Collaborative activities on the DIII-D program were extended to establish the scientific basis for the optimization of the tokamak for fusion energy, using a non-circular cross-section plasma with high triangularity, double-null divertor configuration, and various current drive systems. During the last decade these activities continued in a quest to understand the physics of steady and high-performance plasmas and determining methods of achieving and sustaining these scenarios.

5.2 Activities

The Japan Atomic Energy Research Institute (JAERI), from October 2005 Japan Atomic Energy Agency (JAEA), extended an agreement with the U.S. DOE to collaborate on the DIII-D tokamak at General Atomics (GA) in San Diego. This Agreement has provided close collaborative work on the research programs at JAERI (later JAEA and most recently QST) and GA for 40 years. Although the size of the collaboration has decreased in the last 10 years as QST focused on preparing JT-60SA, the two groups continue to value the close relationship and the progress made.

Joint research activities were carried out through participation in the DIII-D program and exchange of information. Progress has been made in several areas including advanced tokamak physics, divertor properties, ELM-free operation, high beta physics and control, electron cyclotron heating and current drive, diagnostics development, and tokamak stability. These collaborations also provided input for planning the research programs on JT-60SA. This experience built enduring mutual respect and friendships between QST and GA scientists and engineers. This collaboration has continued to lead to significant scientific achievements as well as contributing to Japan's JT-60 program and improving the world fusion program.

5.3 Administration

The Steering Committee Meeting is held at General Atomics, San Diego every year throughout the period of collaboration between the U.S.DOE and JAEA/QST to coordinate the collaborative work program. The committee comprises representatives of QST, DOE and GA. The steering Committee discussed the accomplishments of the collaboration and the potential benefits of the collaboration for advancing plasma physics in general, and for the ITER program in particular. The committee reviewed and recommended approval of the proposed exchanges from QST to DIII-D in each fiscal year. The meeting was sometimes organized in conjunction with the DIII-D Program Advisory Committee meeting. It emphasized technical discussions and closer collaborations.

5.4 Accomplishments and Highlights

The main subjects of collaboration in the last 10 years continued to emphasize progress towards physics understanding and optimization of higher-beta, higher confinement, and steady-state plasmas. During 2011-20, joint research supported both the DIII-D and QST program efforts in furthering Advanced Tokamak (AT) research in a broad set of area including transport, ELM stability, plasma control, advanced scenarios, and boundary control.

Transport studies have been a particular highlight. These studies developed new understanding of thermal and momentum transport in tokamak plasmas. One of the outstanding achievements in recent years has been

elucidation of the relationship of magnetic shear to transport, thereby providing techniques to improve confinement in future devices.

Stability has also been a major topic of the collaboration, with studies addressing energetic particle driven modes and avoidance of disruptive instabilities such as the Neoclassical Tearing Mode. Collaborative work also produced new understanding of the physics underlying the naturally ELM-free QH-mode. Other topics include the divertor and edge performance in an advanced divertor, and real-time control of high-performance plasmas.

A number of pioneering results have been achieved through the collaborative work between the DIII-D and JT-60 Teams. We look forward to continuing our fruitful collaboration in the next decade

Impact of Plasma Rotation on MHD Stability and Turbulence in QH-mode Pedestals

Category: DIII-D

Name: N. Aiba¹, Xi Chen², A. Garofalo², G. McKee³, M. Ono^{1,4}

Affiliation: ¹QST, ²GA, ³U. Wisconsin, ⁴NIFS/Sokendai

Quiescent H-mode (QH-mode) is a promising scenario that realizes ELM suppression and high confinement at reactor-relevant plasma parameters ¹). Edge Harmonics Oscillations (EHOs) arise and replace ELMs, driving transport and controlling density and are thought to be a current-driven MHD (kink/peeling) mode^{2,3)}. Experimentally, large toroidal rotation and/or edge ExB shear are required to access and maintain QH-mode. Thus various studies have investigated the impact of rotation on the EHO.

In QH-mode plasmas, the ion diamagnetic drift frequency ω_{*i} can be comparable to the plasma rotation frequency $\Omega_{v \times B}$. To identify the key mechanism explaining the role of rotation for triggering the EHOs, we analyze the impact of plasma rotation on kink/peeling mode stability in QH-mode plasmas by considering $\Omega_{v \times B}$ and ω_{*i} simultaneously with the linear extended MHD stability code MINERVA-DI⁴). The analyzed plasma, #153440@1.725 sec. had an $n=2$ dominant EHO (n is the toroidal mode number). The $\Omega_{v \times B}$ profile is determined with the measured rotation of carbon $\Omega_{v \times B,C}$, where the toroidal component of this rotation is counter- I_p . When analyzing the MHD stability without the ω_{*i} effect, the stability boundary on the $(j_{ped,max}, \alpha_{max})$ diagram indicates the kink/peeling mode is slightly destabilized by $\Omega_{v \times B,C}$ rotation, consistent with previous results⁵). However, when considering the ω_{*i} effect, the kink/peeling mode is stabilized by rotation [Figure 1(a)].

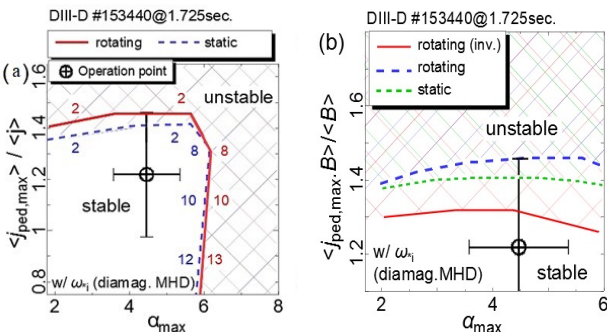


Figure 1. (a) MHD stability diagram on $(j_{ped,max}, \alpha_{max})$ plane; the stability was analyzed including the ω_{*i} effect. Numbers are the n number of the mode determining the stability boundary. (b) Inverted rotation destabilizes kink/peeling mode.

The physics mechanism stabilizing the kink/peeling mode was investigated with the energetics¹²⁸⁾. In the ideal MHD case, an MHD mode can be destabilized due to energy flow from a fast-rotating equilibrium to a slow-rotating mode.

When including the ω_{*i} effect, part of the energy flow from an equilibrium to a mode is proportional to the product of $\Omega_{v \times B}$ and ω_{*i} , and the modulation of dynamic pressure can stabilize the kink/peeling mode. When inverting the direction from $\Omega_{v \times B,C}$ to $-\Omega_{v \times B,C}$, the stability boundary on the stability diagram moves downward as shown in Figure 1(b).

Toroidal rotation impacts EHO stability, and pedestal turbulence and transport. As injected counter- I_p torque is gradually reduced, ExB shear is likewise reduced and

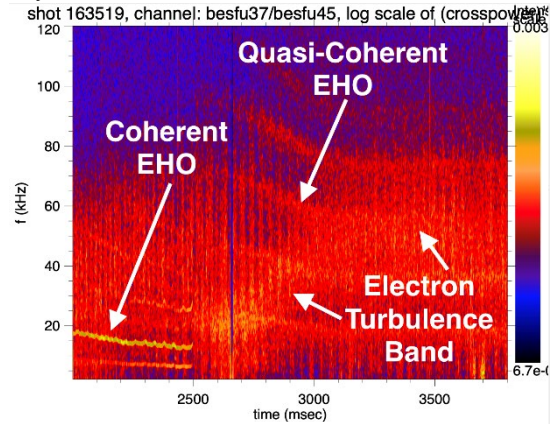


Figure 2. Density fluctuation spectrogram (BES) illustrating transition from Coherent EHO to Quasi-coherent EHO and strong turbulence as torque reduced at $\rho \approx 0.95$.

turbulence is found to increase, as illustrated in Figure 2. Between 2000 and 3500 ms, torque is reduced from 4 to 0 N-m. The coherent EHO disappears, while a Quasi-Coherent band appears along with a strong electron-diamagnetic-direction band of turbulence. The increased turbulence and resulting transport reduce pedestal pressure gradients, allowing the pedestal to widen, increasing global pedestal stability and allowing for a higher pedestal pressure and core confinement.

Based on these results, a hypothesis has been developed explaining why QH-mode discharges favor toroidal rotation in the counter- I_p direction. The plasma is assumed to be axisymmetric before the transition to QH-mode, but when a kink/peeling mode becomes unstable, the plasma has non-axisymmetric distortion. Such distortion can accelerate plasma rotation in the counter- I_p direction near the plasma surface⁶). The kink/peeling mode will stop growing due to rotational stabilization, and the non-axisymmetric distortion will be sustained, observable as EHOs.

¹⁾ K.H. Burrell et al., Phys. Rev. Lett. 102, 155003 (2009).

²⁾ K.H. Burrell et al., Phys. Plasmas 12, 056121 (2005).

³⁾ P.B. Snyder et al., Nucl. Fusion 47 961 (2007).

⁴⁾ N. Aiba et al., Nucl. Fusion 60, 092005 (2020).

⁵⁾ Xi Chen et al., Nucl. Fusion 56, 076011 (2016).

⁶⁾ A.M. Garofalo et al., Phys. Rev. Lett. 101, 195005 (2008).

Dynamics of energetic particle driven modes and MHD modes in wall-stabilized high beta plasmas on JT-60U and DIII-D

Category: DIII-D

Name: G. Matsunaga¹⁾, M. Okabayashi²⁾, N. Aiba¹⁾, J.A. Boedo³⁾, J.R. Furon⁴⁾, J.M. Hanson⁵⁾, G.Z. Hao⁶⁾, W.W. Heidbrink⁷⁾, C.T. Holcomb⁸⁾, Y. In⁹⁾, G.L. Jackson⁴⁾, Y.Q. Liu¹⁰⁾, T. C. Luce⁴⁾, G. R. McKee¹¹⁾, T.H. Osborne⁴⁾, D.C. Pace⁴⁾, K. Shinohara¹⁾, P.B. Snyder⁴⁾, W.M. Solomon²⁾, E.J. Strait⁴⁾, A.D. Turnbull⁴⁾, M.A. Van Zeeland⁴⁾, J.G. Watkins¹²⁾, L. Zeng¹³⁾, the DIII-D Team and the JT-60 Team

Affiliation: ¹⁾National Institutes for Quantum and Radiological Science and Technology, ²⁾Princeton Plasma Physics Laboratory, ³⁾Department of Aerospace and Mechanical Engineering, UCSD, ⁴⁾General Atomics, San Diego, ⁵⁾Department of Applied Physics and Applied Mathematics, Columbia University, ⁶⁾Southwestern Institute of Physics, ⁷⁾Department of Physics and Astronomy, UCI, ⁸⁾Lawrence Livermore National Laboratory, ⁹⁾FAR-TECH, Inc., ¹⁰⁾Euratom/CCFE Fusion Association, ¹¹⁾Department of Engineering Physics, University of Wisconsin at Madison, ¹²⁾Sandia National Laboratories, ¹³⁾UCLA, Los Angeles

In the wall-stabilized high- β plasmas in JT-60U and DIII-D, interactions between energetic particle (EP) driven modes and edge localized modes (ELMs) have been observed^{1, 2)}. The ELM pacing by the EP driven modes (EPdMs) occurs when the repetition frequency of the EPdMs is higher than the natural ELM frequency. The EPdMs have strong waveform distortion that is composed of higher toroidal harmonics. In particular, EP behavior seems to be sensitive to the waveform distortion, thus, stronger waveform distortion correlates with an intense increase of EP transport to the edge. According to statistical analysis, the ELM triggering by the EPdMs infrequently occurs just after the ELM crash. Namely, the ELM triggering by the EPdMs needs finite level of waveform distortion and pedestal recovery. Transported EPs by the EPdMs are thought to contribute to change the edge stability.

Figure 1 indicates typical discharges where the ELM triggering by the EPdMs are observed with $Bt/I_p = 1.7T/1.0MA$ on DIII-D and $Bt/I_p = 1.5T/0.9MA$ on JT-60U. These EPdMs appeared when β_N exceeded no-wall β_N limit. Here, β_N is normalized β -value. In these discharges, the no-wall β_N limits are roughly described as $3.5/i_l$ on DIII-D and $3.0/i_l$ on JT-60U by using the internal inductance i_l , respectively.

The waveform distortion of the EPdM seems to strongly affect EP transport. Figure 2 shows the relation between the fundamental and distortion components and beam emission spectroscopy (BES) amplitude. Large spikes corresponding to the intense increases of EP transport are synchronized with Mirnov signals. The EP density increases as the distortion

component increases. Figure 2(d) indicates that the BES amplitude has a linear dependence of the waveform distortion.

From these, it is found that the waveform distortion is considered to rapidly increase EP transport to the edge region.

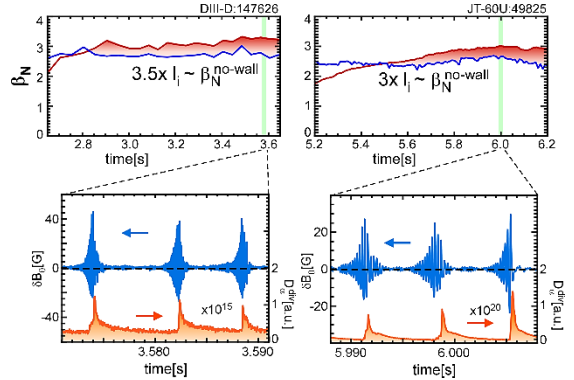


Figure 1. High- β_N discharges on (left) DIII-D and (right) JT-60U where ELM triggering by EPdMs: β_N with no-wall β_N limits, Mirnov signals and $\Delta\alpha$ emissions.

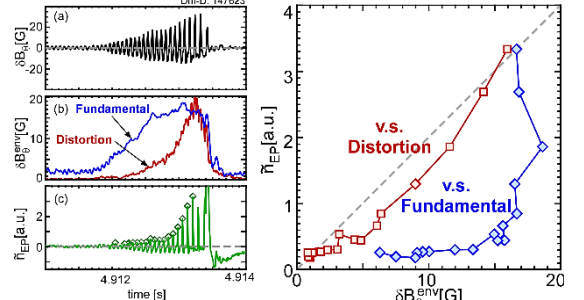


Figure 2. Dependence of BES amplitude on fundamental ($n = 1$) and distortion ($n > 1$) components of EPdM on DIII-D. (a) Integrated Mirnov signal, (b) decomposed fundamental and distortion components and (c) BES signal at edge. (d) BES amplitudes vs fundamental and distortion components.

In summary, we have observed that the ELM can be triggered by the EP driven modes on JT-60U and DIII-D. One of the distinctive features of the EPdMs is the waveform distortion. The waveform distortion is composed of higher harmonics $n = 2, 3, \dots$ in a synchronized manner and this behaves like a density snake near the plasma edge. EP diagnostics indicate that strong correlation between the waveform distortion and the EP transport to edge. Moreover, the ELM triggering by the EPdMs infrequently occurs just after ELM crash. This means that pedestal recovery, thus marginal stability condition on edge, is necessary for the ELM triggering by the EPdMs³⁾.

¹⁾G. Matsunaga *et al.*, Nucl. Fusion Vol.53 (2013) 073046

²⁾M. Okabayashi, G. Matsunaga *et al.*, Phys. Plasmas Vol.18 (2011) 056112

³⁾G. Matsunaga, M. Okabayashi *et al.*, Nucl. Fusion Vol.53 (2013) 123022

Exploring the avoidance of NTM-locking-induced disruption via rotating 3D magnetic perturbations

Category: DIII-D

Name: S. Inoue, M. Okabayashi*, E.J. Strait**

Affiliation: QST, *PPPL, **GA

Locked modes (LMs) destabilized by small error fields (EF) are frequently observed in tokamak experiments and are a major cause of plasma disruptions. In RFX-mod and DIII-D, stabilization effects of applied control fields (CF) have been explored, and the LM is avoided by the CF pre-emptively. Here, we have developed a nonlinear resistive MHD simulation code AEOLUS-IT¹³⁴⁾ to study the interaction between the CF and the magnetic island under realistic dissipation parameters. Simulations of LMs in a cylindrical plasma without a conducting wall are qualitatively consistent with results of LM entrainment experiments in DIII-D.

Screening (frequency range (II) & (IV) in Figure 1) and partial screening (frequency range (III) in Figure 1) hypothesis are numerically suggested under JT-60SA relevant dissipation parameters, where the static error fields are screened out by an extremely slowly rotating control field¹⁾. Figure 1 shows the CF frequency (ω_{cf}) dependence of (a) the island growth rate and (b) the plasma rotational frequency at the rational surface. The EF/CF amplitudes are 0.1/0.4G, and the ω_{cf} is scanned from 20 to 400Hz discretely. The island growth rate is evaluated at quasi-steady states ($t = 3 \times 10^5 t_A$), where the plasma rotation, which is driven by the CF, saturates. As shown in Figure 1, the ω_{cf} dependence of the plasma response can be classified into four ω_{cf} regions labeled by (I)-(IV). In the range (I), the plasma rotation linearly increases with increase of the ω_{cf} as shown in Figure 1(b), which indicates that the CF penetrates into the rational surface and drives the island growth. In the range (II), the plasma starts to slip from the CF and the remaining plasma rotation as seen in Figure 1(b) screens out the EF. However, for further increase of the ω_{cf} , the EF penetrates into the rational surface as seen in the range (III). For further high ω_{cf} , the LM is stabilized again as shown in the range (IV). Consequently, the extremely slowly rotating field (<100Hz) even can suppress the error field penetration.

We did cross-comparisons between our simulation and DIII-D experiments, where the partial screening regimes were obtained in DIII-D by changing the rotating field amplitude. As shown in Figure 2, two characteristic toroidal angle dependences of the $B_p(a)$ before/after the CF exceeds the EF were observed²⁾. First, when the amplitude of the CF is lower than that of the EF, the magnetic island is trapped by the EF, which results in the standing-wave like B_p response as shown in Figure 2(a1). Second, when the CF amplitude is above the EF amplitude, the B_p response coherently propagates as shown in

Figure 2(a2). In the experiment, by the increase of the CF current by a factor of 1.3, the corresponding B_p were observed as shown in Figures 2(b), which verifies our simulation results. On the other hand, radial mode profiles revealed qualitatively different behavior. This led to a revised hypothesis that in actual non-circular toroidal devices, a tearing layer in forced rotation induces a shielding process at other rational surfaces when we take into account multiple resonant Fourier components. The time evolution experiment of the radial penetration is supportive of the hypothesis³⁾. Cross-comparison including multi-helicity effects to prove our revised hypothesis is our future work.

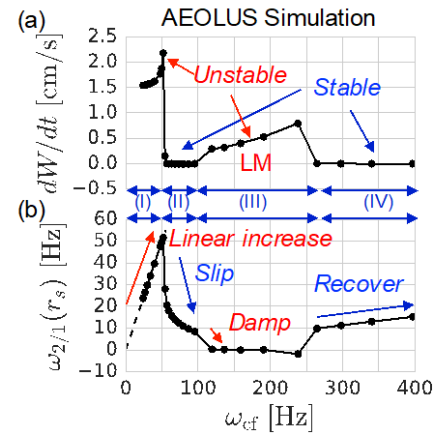


Figure 1. Dependence of (a) the island growth rate and (b) the plasma rotation on the CF frequency (ω_{cf}).

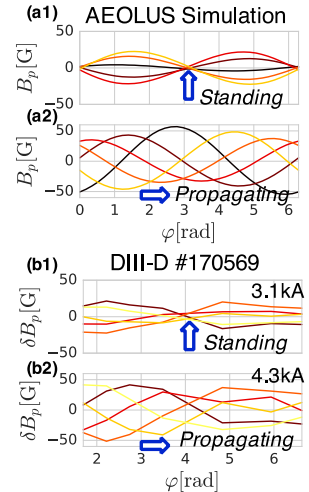


Figure 2. Temporal evolution of toroidal angle dependence of the poloidal magnetic field at the plasma surface in the case with (a) AEOLUS simulation and (b) DIII-D #170569. Time evolves from the heavy (black) to the light colors (yellow) of lines.

¹⁾ S. Inoue *et al.*, Nucl. Fus. **57**, 116020 (2017).

²⁾ S. Inoue *et al.*, in proceedings of IAEA FEC 2018.

³⁾ M. Okabayashi *et al.*, Nucl. Fus. **59**, 126015 (2019).

Magnetic shear and q profile effects on plasma transport with EC in DIII-D

Category: DIII-D

Name: M. Yoshida¹, G. R. McKee², C. C. Petty³, B. A. Grierson⁴, M. Nakata⁵, C. Rost⁶, T. L. Rhodes⁷, D. R. Ernst⁶, A. M. Garofalo³

Affiliation: ¹*QST*, ²*UW*, ³*GA*, ⁴*PPPL*, ⁵*NIFS*, ⁶*MIT*, ⁷*UCLA*

Electron heating by alpha particles will be dominant in ITER and DEMO. Confinement degradation has been observed as the electron to ion temperature ratio (T_e/T_i) approaches unity with application of electron cyclotron heating (ECH) to neutral beam heated discharges^{1,2)}. Magnetic shear is key to moderate the confinement degradation. In JT-60U, the negative magnetic shear (NCS) prevented the increase in thermal and particle transport as T_e/T_i approached unity²⁾. A physics understanding of the underlying mechanisms, however, was not identified due to the lack of fluctuation measurements.

In this study, the negative magnetic shear effect on plasma transport as $T_e/T_i \sim 1$ has been demonstrated in DIII-D steady-state scenario plasmas to mitigate confinement degradation, and the physics mechanisms have been assessed using a set of fluctuation measurements and gyrokinetic simulations. A systematic comparison of core turbulence and transport at high T_e/T_i with different magnetic shears allows for a better physics understanding of the transport processes.

Figure 1(a) shows radial profiles of the change in the power balance ion heat diffusivity (χ_i) with ECH in the DIII-D positive shear (PS) and NCS plasmas. The ion heat diffusivity significantly increased over all radii in the PS plasma with increased electron heating. On the other hand, in the NCS plasma, the increase in χ_i was smaller. The results reflect to global plasma confinement as shown in Figure 1(b). A higher improved global confinement factor was achieved in the NCS plasma at $T_e/T_i \sim 1$. The transport dependence on ECH in DIII-D is consistent with that observed in JT-60U as shown in Figure 1(c). The ion thermal diffusivity remained roughly constant in the negative shear region but increased in the positive shear region with increased T_e/T_i by ECH heating. The fluctuation measurements showed a consistency with the transport responses. A comparison of the changes in the low-wavenumber density fluctuation spectra from BES between the PS and the NCS plasmas as shown in Figure 2. The modest increase in fluctuations in the NCS plasma correlated with the modest increase in the ion and electron thermal transport in the NCS plasma. A stability analysis was performed using a gyrokinetic simulation code. The linear growth rates of low and higher- k modes increased less in the NCS plasmas compared to those in the PS plasmas as shown in Figure 3. The smaller increase in the growth rate in the NCS

plasmas compared with that in the PS plasmas correlates with the thermal transport and turbulent fluctuations in the experiments. These results demonstrate a technique to improve confinement with controlled magnetic shear in ITER and DEMO.

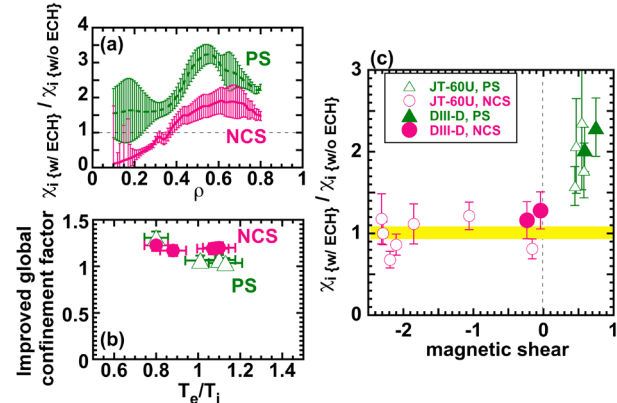


Figure 1. Radial profiles of (a) the change in the ion heat diffusivity (χ_i) with ECH in the PS and NCS plasmas. (b) The improved confinement factor as a function of T_e/T_i . (c) The change in χ_i with ECH around T_i -ITB region as functions of magnetic shear in DIII-D and JT-60U.

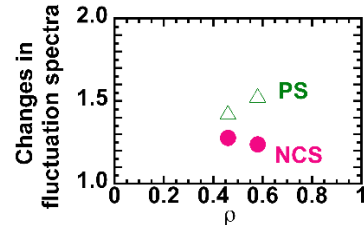


Figure 2. Increase in frequency-integrated fluctuations with ECH in the PS and NCS plasmas.

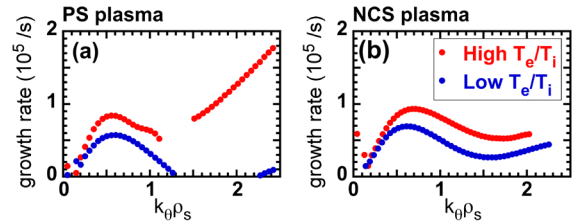


Figure 3. The poloidal wavenumber spectra of the linear growth rates calculated by the GKV code at low T_e/T_i (blue) and high T_e/T_i (red) in (a) the PS and (b) NCS DIII-D plasmas.

¹⁾ McKee G. R. et al 2014 Turbulence behavior and transport response approaching burning plasma relevant parameters 25th IAEA Int. Conf. on Fusion Energy (St Petersburg, Russia, 2014) EX-2/2

²⁾ Yoshida M. et al 2015 Nucl. Fusion **55** 073014

³⁾ Yoshida M. et al 2017 Nucl. Fusion **57** 056027

CHAPTER 6 US-Japan Joint Research Projects Overview

The US-Japan Joint Research Projects have decades of rich and successful history contributing to advancing fusion materials science and enabling technologies, with FRONTIER as the latest, ongoing project. These projects are defined and approved by the Coordinating Committee on Fusion Energy (CCFE) under the “Agreement between the Government of the United States of America and the Government of Japan on Cooperation in Research and Development in Energy and Related Fields” signed in 1979. Since the first project, RTNS-II that started in 1981, the core research subjects have evolved from fundamental radiation materials science focusing on the effects of fusion spectrum neutrons to increasingly include applied science and enabling technologies for magnetic confinement fusion energy (Table 1); however, the effects of neutron irradiation in fusion materials and components has remained the undeviating technical backbone. The use of unique US experimental capabilities and key facilities has been among the principles of collaboration.

Table 1. History of the US-Japan Joint Research Projects on fusion materials and technologies.

Project Title	Period*	Key Facility	Core Subject
RTNS-II	1981-1986	RTNS-II	Low-dose D-T neutron irradiation
FFTF/ MOTA	1987-1994	FFTF, EBR-II	High-fluence neutron irradiation
JUPITER	1995-2000	HFIR, ATR, HFBR	Non-steady and transient radiation effects
JUPITER-II	2001-2006	HFIR, STAR, MTOR	Key issues for advanced blanket concepts
TITAN	2007-2012	HFIR, TPE, MTOR, PISCES	Thermofluid, n-T synergism, coating, and joining
PHENIX	2013-2018	HFIR, PAL, TPE	Tungsten-based, helium-cooled PFC technologies
FRONTIER	2019-2024	HFIR, TPE	Interface elements in PFC

*Japanese fiscal year.

6.1 Objectives, Research Subjects, and Facilities

During the last decade, the US-Japan Joint Research Projects evolved the TITAN (Tritium, Irradiation and Thermofluid for America and Nippon) that concluded in JFY-2012, PHENIX (Technological Assessment of Plasma Facing Components for DEMO Reactors) that started in JFY-2013 and concluded in JFY-2018, and FRONTIER (Fusion Research Oriented to Neutron Irradiation Effects and Tritium Behavior at Material Interfaces) that is currently in its early phase after starting in JFY-2019. Each of these projects had/has a performance period of six years.

Highlights from the technical accomplishments in each task and the irradiation program are given in the following subsections.

TITAN – The TITAN project focused on advancing scientific understanding of the effects of complex operating environments of fusion reactors on the behaviors of hydrogen isotopes and (magneto-) thermofluid dynamics in the blanket, first wall, and fuel recovery systems. The TITAN project contributors were from NIFS, INL, ORNL, and a number of universities including UCLA and UCSD in USA and nine different universities in Japan. The project was unique in integrating these fusion fuel cycle and liquid metal and salt blanket technology issues with the effects of neutron irradiation on properties and interfacial behaviors of the blanket and first wall materials [1]. This was a pioneering effort of an integrated multi-scale, multi-physics approach in understanding the performance of material systems in environments that couple extreme operating conditions. It pioneered

today's trend in performance modeling of nuclear energy systems. A dedicated overview of the TITAN project is given later in this Section.

PHENIX – The acronym PHENIX stands for PFC Evaluation by Tritium Plasma, Heat and Neutron Irradiation Experiments. The main project goal was to evaluate the technical feasibility of helium-cooled, tungsten-armored divertor concepts, which include several high technical risks, high pay-off options for fusion DEMO divertors with outstanding safety characteristics [2]. Understanding the effects of neutrons, heat loading, and plasma exposure is the overarching goal of PFC materials science. Among the various technical issues for PFCs, the PHENIX project examined the heat transfer and high-heat-load responses, effects of neutron irradiation, and the hydrogen isotope behaviors.

The PHENIX project consisted of three technical tasks: Task 1, Heat Flow Response; Task 2, Neutron Effects in Materials; and Task 3, Tritium Behavior. As depicted in Figure 1, Task 1 dealt with issues related to heat load and flux, including the high heat load in armor materials, heat transfer from the armor through a structural cartridge to the helium coolant, and the high-pressure/high-temperature helium flow in the multi-jet impingement cooling. The main experimental facilities for Task 1 were the High Heat Flux Test Station at the Plasma Arc Lamp (PAL) facility at ORNL and the helium loop facility at the Georgia Institute of Technology.

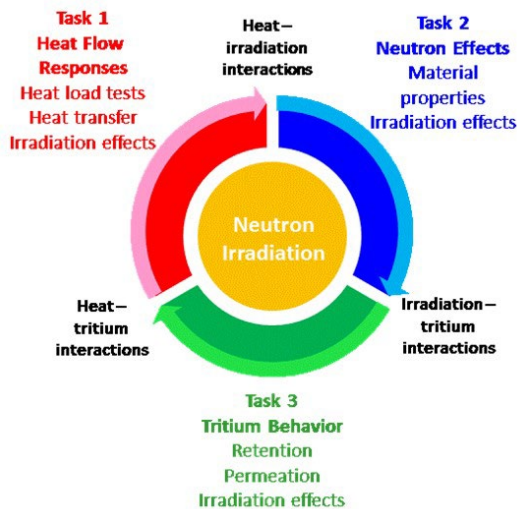


Figure 1. Task structure and inter-relations in PHENIX project.

Task 2 on Neutron Effects determined the effects of neutron irradiation at PFC-relevant temperatures on the thermal, mechanical, and physical properties of tungsten materials, in response to the critical demands for reliable data for properties of neutron-irradiated tungsten. The outcome from this task enabled greatly improved fidelity of modeling and integrity assessment for PFC structures. This task mainly used the 3025E hot cell facility, the Low Activation Materials Development and Analysis (LAMDA) Laboratory, and the associated microscopy center at ORNL (Figure 2).



Figure 2. Visiting researcher from Osaka Prefectural University, Japan, conducting post-irradiation examination at Oak Ridge National Laboratory.

Task 3 on Tritium Behavior focused on the retention and permeation of hydrogen isotopes in neutron-irradiated tungsten. The Tritium Plasma Experiment (TPE) facility located at Idaho National Laboratory (INL) served as the primary experimental capability (Figure 3). In addition, various additional facilities in US and Japan were used for measurements of deuterium permeation, thermal desorption, and depth profiling.



Figure 3. Visiting researcher from Hokkaido University, Japan, participating an experiment at Idaho National Laboratory with US research scientist.

Neutron irradiation program served as a core function of the PHENIX project as it provided all three technical tasks with a consistent and systematic set of irradiated test specimens. The planning for the irradiation program, test matrix development, capsule development and construction, and execution of irradiation were conducted in collaboration with all tasks.

FRONTIER – with the successful conclusion of the PHENIX project, a great deal of critical knowledge was developed in areas of heat flow and removal, baseline properties and hydrogen isotope interactions of tungsten materials, and the effects of neutron irradiation on all of these. The FRONTIER project, building upon and complementing the preceding project, will address the scientific questions related to the neutron and hydrogen isotope interactions with the interfacial and transition elements in advanced PFCs. Such elements include the solid-solid interfaces within the plasma-facing materials and components, the solid-solid transitions in advanced PFCs, the solid-liquid interfaces in the liquid metal PFC systems, and the PFC-oxidant-tritium interactions in liquid cooled and liquid surface concepts. Interface effects in the materials integration enabled by advanced manufacturing and accident events are included. The FRONTIER research addresses the evolving research needs arising from the rapid PFC innovations.

6.2 Administration and Operations Management

In coordinating these six-year projects with funding uncertainties and evolving availability/functionality of the key resources, the annual Steering Committee Meetings (SCMs) played a critical role (Figure 4). In each project, a total of seven SCMs were held with participation by the Representative, Program Coordinator, Task Coordinators and additional key people from both the US and Japan. The administration structures of PHENIX and FRONTIER projects are given in Tables 2 and 3. The TITAN project administration is found in the next subsection. In addition to the SCMs, topical workshops were organized typically a few times a year across multiple tasks. These workshops served as the venue to discuss; detailed technical planning, integration of technical tasks and irradiation plans, discussion of the experimental results, and exchange of other relevant information.

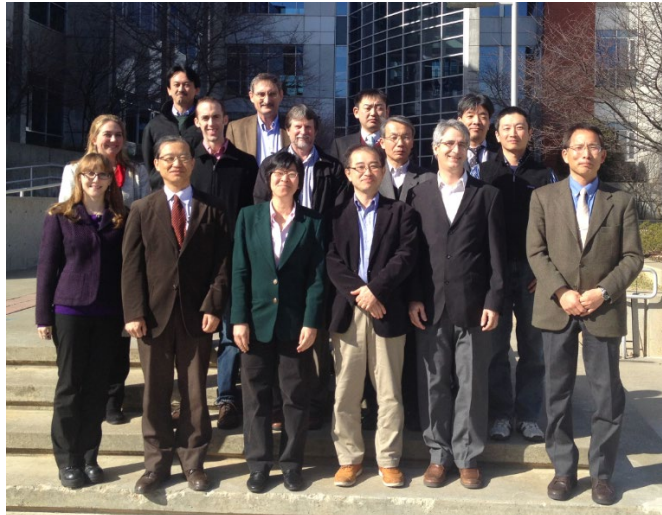


Figure 4. Photo from the 3rd PHENIX Steering Committee Meeting, held in 2015 at Georgia Institute of Technology.

Table 2. Administrative structure of PHENIX project.

Steering Committee

	Japan	USA
Representative	Y. Ueda (Osaka U.)	P. Pappano / D. Clark (DOE)
Program Coordinator	Y. Hatano (U. Toyama)	P. Pappano / D. Clark (DOE)

Task Coordinators and Deputies

	Japan	USA
Task 1 Heat Flow Responses	T. Yokomine (Kyoto U.) Y. Ueda (Osaka U.)	M. Yoda (GA Tech) A. Sabau (ORNL)
Task 2 Neutron Effects	T. Hinoki (Kyoto U.) A. Hasegawa (Tohoku U.)	Y. Katoh / L. Garrison / J.W. Geringer (ORNL)
Task 3 Tritium Behavior	Y. Oya (Shizuoka U.) Y. Hatano (U. Toyama)	B. Merrill / M. Shimada (INL) D. Buchenauer (SNL)

Table 3. Administrative structure of FRONTIER project.
Steering Committee

	Japan	USA
Representative	Y. Hatano (U. Toyama)	D. Clark (DOE)
Program Coordinator	T. Yokomine (Kyoto U.)	Y. Katoh (ORNL)

Task Coordinators and Deputies

	Japan	USA
Task 1 Solid-Solid Interfaces	T. Hinoki (Kyoto U.) N. Hashimoto (Hokkaido U.)	L. Garrison / X. Hu / W. Geringer (ORNL)
Task 2 Tritium Transport Accident Safety	Y. Oya (Shizuoka U.) T. Otsuka (Kindai U.)	M. Shimada (INL) R. Kolasinski (SNL)
Task 3 Solid-Liquid Interfaces	M. Kondo (TITECH) J. Miyazawa (NIFS)	B. Pint / J. Jun (ORNL)
Task 4 Divertor Systems Analysis	T. Yokomine (Kyoto U.)	C. Kessel (ORNL)

References

- [1] T. Muroga, D.K. Sze, K. Okuno, T. Terai, A. Kimura, R.J. Kurtz, A. Sagara, R. Nygren, Y. Ueda, R.P. Doerner, B.J. Merrill, T. Kunugi, S. Smolentsev, Y. Hatano, T. Yamamoto, A. Hasegawa, Y. Katoh, Research on Tritium/Heat Transfer and Irradiation Synergism for First Wall and Blanket in the TITAN Project, in: 24th IAEA Fusion Energy Conf., International Atomic Energy Agency, San Diego, 2012.
- [2] Y. Katoh, D. Clark, Y. Ueda, Y. Hatano, M. Yoda, A.S. Sabau, T. Yokomine, L.M. Garrison, J.W. Geringer, A. Hasegawa, T. Hinoki, M. Shimada, D. Buchenauer, Y. Oya, T. Muroga, Progress in the U.S./Japan PHENIX project for the technological assessment of plasma facing components for DEMO reactors, *Fusion Sci. Technol.* 72 (2017) 222–232. doi:10.1080/15361055.2017.1333868

TITAN Overview

Category: TITAN/PHENIX/FRONTIER

Name: T. Muroga

Affiliation: NIFS

1. Introduction

The joint projects by Japan (NIFS and Universities) and USA under the Fusion Cooperation Program have a history of almost 40 years. The TITAN project (Tritium, Irradiation and Thermofluid for America and Nippon) was carried out through six years (FY 2007-2012). Before TITAN, four joint projects have been carried out. The initial three projects (RTNS-II, FFTF/MOTA, and JUPITER) focused on neutron irradiation effects on fusion materials using neutron irradiation and post irradiation examination (PIE) facilities in the US. The next project (JUPITER-II) extended the subject of the initial projects to include key issues for advanced blankets using facilities for tritium and thermofluid tests in the US, in addition to those for neutron irradiation [1].

The use of unique US facilities is the major incentive in this collaboration. The contributions of the Japanese side include the supply of high-quality test materials and characterization technologies for microstructures, mechanical properties, tritium distribution, thermofluid performance, and others.

2. Objective and task structure

The TITAN project has a broader scope than the JUPITER-II project by including first wall issues and interface issues among the first wall, blanket, and recovery system. Particular emphasis was placed on obtaining fundamental understanding for establishing tritium and thermofluid control. The experiments were designed for testing under conditions specific to fusion, such as intense irradiation, high heat/particle flux, and circulation in a high magnetic field. The results were applied using integrated modeling to advance the design of tritium and heat control in MFE and IFE systems.

Table 1 summarizes the tasks, subtasks, facilities, and research subjects. The project has three tasks and seven subtasks. Task 1 is about transport phenomena that consider mass and heat flow in the first wall, blanket, and recovery system. Special emphasis is placed on mass transfer during the interaction of mixed plasma of D/He/Be with the first wall, tritium transfer in liquid breeders, and the thermofluid control in liquid breeders in a magnetic field. Task 2 focuses on the irradiation effects of materials with an emphasis on the synergistic effects of irradiation and tritium or other impurities including transmutation-induced helium. The common task is a unique group organized by those who are engaged in other tasks and take care of the modeling. This task performs integration modeling of materials performance, thermofluids in magnetic fields, tritium and mass transfer for the enhancement of reactor system design, including the evaluation of the available modeling codes and the enhancement of reactor system designs.

Table 1. Organization of the TITAN project as of April 2011

Representatives Coordinators		JP : K. Okuno (Sizuoka U.) JP : T. Muroga (NIFS)		US : G. Nardella (USDOE) US : D. Sze (UCSD)		
Task	Subtask	Facility	TC (JP)	STC/Deputy (JP)	TC (US)	STC/Deputy (US)
Task 1 Transport phenomena	1-1 Tritium and mass transfer in first wall <i>(concluded March 2010)</i>	TPE PISCES	T. Terai (U.Tokyo)	Y. Ueda (Osaka U.)/ N. Ohno (Nagoya U.) K. Tokunaga (Kyushu U.)	D. Sze (UCSD)	R. Doerner (UCSD)
	1-2 Tritium behavior in blanket systems	STAR		T. Terai (U. Tokyo)/ S. Fukada (Kyushu U.) S. Konishi (Kyoto U.)		P. Calderoni(INL)
	1-3 Flow control and thermofluid modeling	MTOR		T. Kunugui (Kyoto U.)/ T. Yokomine (Kyoto U.)		S. Smolentsev (UCLA)/ K. Messadek (UCLA)
Task 2 Irradiation synergism	2-1 Irradiation-tritium synergism	HFIR STAR	A.Kimura (Kyoto U.)	Y. Hatano (Toyama U.)/ Y. Oya (Shizuoka U.)	R. Kurtz (PNNL)	M. Sokolov (ORNL)/ Y. Katoh (ORNL) P. Calderoni (INL)
	2-2 Joining and coating integrity	HFIR ORNL-HL (incl. T-test)		A. Kimura (Kyoto U.)/ N. Hashimoto (Hokkaido U.) T. Nagasaki (NIFS)		T. Yamamoto (UCSB)/ M. Sokolov (ORNL)
	2-3 Dynamic deformation			A. Hasegawa (Tohoku U.)/ T. Hinoki (kyoto U.)		Y. Katoh (ORNL)
Common Task System integration modeling	MFE/IFE system integration modeling		A.Sagara (NIFS)	A. Sagara (NIFS)/ H. Hashizume (Tohoku U) T. Norimatsu (Osaka U.)	R. Nygren (SNL)	R. Nygren (SNL)
Laboratory Liaisons	ORNL : INL : IMR-Oarai (Tohoku) :	R. Stoller (ORNL) B. Merrill (INL) T. Shikama (Tohoku U.)				
IFE Liaisons		K. Tanaka (Osaka U.)	Kodama(Osaka U.) Yoneda(UTC)	M. Tillack (UCSD)		

3. Facilities used

The following US facilities are used.

(a) STAR (Safety and Tritium Applied Research) [INL]

Established at the Idaho National Laboratory in 2001, with an allowable tritium inventory of 16,000 Ci, STAR includes the Tritium Plasma Experiment (TPE) and various facilities for testing tritium behavior in blanket conditions. Unique features of the facility include use of Be and neutron-irradiated materials.

(b) HFIR (High Flux Isotope Reactor) [ORNL] HFIR is a

100MW mixed spectrum research reactor, currently operated at 85MW, which is planned to remain in operation until 2035. The HFIR is a unique irradiation facility with the potential for high environmental and temperature control during irradiation, and very low to high flux irradiation. Some of the HFIR-irradiated specimens were shipped to Oarai Center of Tohoku University for PIE.

(c) MTOR (Magneto-Thermofluid Omnibus Research Facility) [UCLA]

The facility includes a magnet of homogeneous field to 2T in an area 15cm wide and 1m long, which can be used for testing the fluid dynamics of liquid metals and MHD flow for high Prandtl number simulant fluids using electrolytes.

(d) PISCES (Plasma Interactive Surface Component Experimental Station) [UCSD]

A linear plasma simulator which can produce high-density plasmas with H, D, He and Be. Pulsed lasers are equipped for synergistic plasma exposure and pulse heating studies. Plasma diagnostics and surface characterization systems are furnished.

A quite unique effort initiated in the TITAN project is to send radioactive samples from ORNL to INL allowing tritium tests and plasma exposure for neutron irradiate materials. This activity is continuing throughout TITAN, PHENIX and FRONTIER projects.

4. Project progress

The TITAN project started in April 2007. The budget available for the project (~1.0 M\$ from each side) was almost steady in the first three years with a minor decline. However, sizable budget reduction occurred in FY2010 (down to ~0.74 M\$ each). Re-planning of the project, including downsizing of test matrices and tasks restructuring, was made to accommodate the budget cuts. Task 1-1 was decided to be concluded as of March 2010. The TPE part of the task was merged to Task 2-1, and some of the research projects in PISCES continued outside the TITAN budget by Japanese scientists assigned to UCSD.

5. Summary of the achievements

The research highlights were published in refs. [2,3]. They are outlined as follows.

(1) Tritium diffusion into bulk for PFM was evaluated using T plasma. Effects of mixed plasma by He/Be/D was elucidated.

(2) Basic data for tritium solubility in Li-Pb and tritium permeation barrier performance were obtained.

(3) It was demonstrated that MHD pressure drop of Li-Pb can be mitigated by three-sided insulation wall.

(4) Irradiation effects on deuterium inventory and diffusion was evaluated by D plasma exposure of neutron-irradiated samples.

(5) Neutron irradiation effects on advanced coating and joining for blanket application were investigated.

(6) Radiation creep of ceramics materials was evaluated using a newly developed method.

(7) System integration modeling was carried out to enhance the contribution of the present results to reactor and blanket design.

References

[1] K. Abe, A. Kohyama, S. Tanaka, C. Namba, T. Terai, T. Kunugi, T. Muroga, A. Hasegawa, A. Sagara, S. Berk, S.J. Zinkle, D.K. Sze, D.A. Petti, M.A. Abdou, N.B. Morley, R.J. Kurtz, L.L. Snead, N.M. Ghoniem, Fusion Engineering and Design, 83 (2008) 842-849.

[2] T. Muroga, D.K. Sze, K. Okuno et al., Fusion Science and Technology, 60 (2011) 321-328.

[3] T. Muroga, D.K. Sze, K. Okuno, Fusion Engineering and Design, 87 (2012) 61

Task 1: Heat Transfer Tests

Category: PHENIX

Name: M. Yoda, S.I. Abdel-Khalik / T. Yokomine

Affiliation: Georgia Tech / Kyoto University

(a) Task 1a: Understanding Heat Transfer and Fluid Flow

The objective of this task was to perform experimental studies of a tungsten-alloy test section modeling the helium-cooled divertor with multiple-jet cooling (HEMJ). A helium (He) test loop pressurized to 10 MPa was built at Georgia Tech (GT) with a maximum He mass flow rate $\dot{m} = 10$ g/s and a maximum He inlet temperature T_i of 350 °C.

A HEMJ test section consisting of a WL10 outer shell and AISI 304 stainless inner shell (Figure 1 inset) was fabricated based on the J1c design, heated by a 10 kW radio-frequency induction heater from the Idaho National Laboratory via a water-cooled copper coil. The data, obtained at incident heat fluxes as great as 8 MW/m² (based on an energy balance on the He)¹⁾ agree with our earlier correlation for the dimensionless heat transfer coefficient (HTC) or Nusselt number $Nu = 0.045 Re^{0.67} \kappa^{0.19}$ (Figure 1)²⁾ where the Reynolds number Re is the dimensionless \dot{m} and κ is the ratio of the thermal conductivities of the WL10 and He. The dimensionless pressure drop across the HEMJ test section $K_L \approx 3.2$ for $T_i \geq 300$ °C, and is essentially independent of Re .

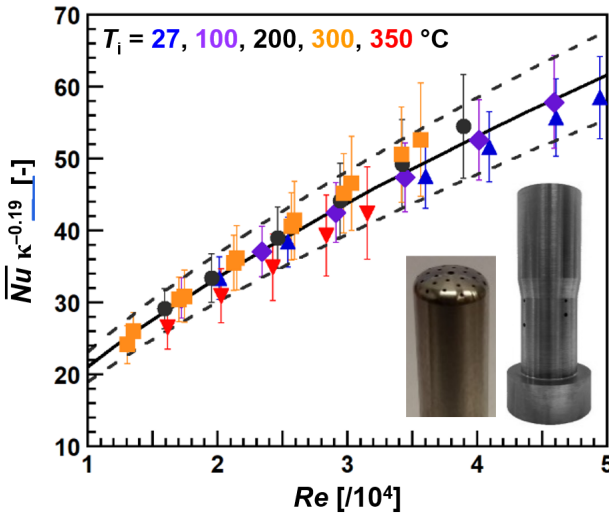


Figure 1. Experimental data (points) and correlation (solid line; dashed lines $\pm 10\%$ error bounds) for Nusselt number Nu as a function of Reynolds number and thermal conductivity ratio κ . The insets show the inner jets cartridge and outer shell

The Nu correlations and K_L results were extrapolated to prototypical conditions to estimate the thermal performance of the HEMJ. These extrapolations suggest that the hexagonal tile (*i.e.*, plasma-facing surface) of the HEMJ can, for a maximum pressure boundary temperature of 1200°C, accommodate

maximum steady-state heat fluxes of 11.5 MW/m² and 9.9 MW/m² at $T_i = 600$ °C and 700 °C, respectively, at a pumping power fraction β of the total incident thermal power of 10% and 18%, respectively.

(b) Task 1b: Optimization of Cooling Configuration

The objective of this task was to simplify the complex geometry of the HEMJ, which involves 25 jets issuing from holes of two different diameters issuing from and impinging on a curved surface (Figure 1 inset), without compromising thermal performance. Coupled computational fluid dynamics and thermal stress simulations were used to model various configurations of fewer jets issuing from holes of the same diameter on a flat surface. The total cross-sectional area of the jets was constrained to be the same as that for the HEMJ.

The simulations suggested that the most promising candidate, the “flat design,” with seven jets issuing from 1.18 mm diameter holes on a flat surface (Figure 2 inset), had a somewhat higher average HTC and slightly lower maximum von Mises stress on the cooled (WL10) surface.³⁾ Very recent experimental studies of this configuration in the GT He loop suggest that this design has Nu that are about 10% higher than those predicted by the HEMJ correlation at the prototypical $Re = 2.1 \times 10^4$ (Figure 3). These results suggest that simpler finger-type modular divertor designs that can withstand ITER-like steady-state heat fluxes are feasible with suitable development.

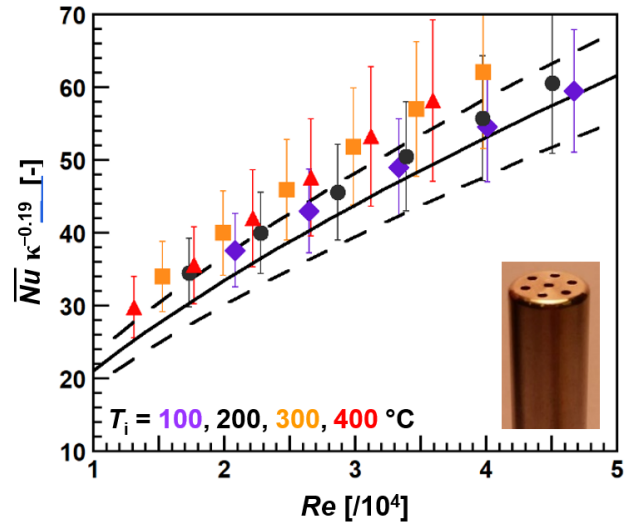


Figure 2. Experimental data (points) for the flat design compared with the correlation (solid line; dashed lines $\pm 10\%$ error bounds) for the HEMJ for $Nu(Re, \kappa)$. The inset shows the inner jets cartridge of the flat design.

¹⁾ D. S. Lee *et al.*, Fusion Sci. & Tech., 75 (2019) 873

²⁾ B. H. Mills *et al.*, Fusion Sci. & Tech., 68 (2015), 541

³⁾ B. Zhao *et al.*, Fusion Eng. & Des., 136 (2018), 67

High Heat Flux Testing of Plasma-Facing Materials for Fusion

Category: PHENIX

Name: A. Sabau/L. Garrison/K. Tokunaga/K. Ibane

Affiliation: ORNL/Kyushu University/Osaka University

Task 1 of the six-year US-Japan PHENIX collaboration included high-heat flux (HFF) testing of neutron-irradiated W materials. The objective of the HHF effort was to determine how changes in material properties due to neutron irradiation will affect the performance of plasma-facing components, especially tungsten (W). The HHF plasma-arc lamp (PAL) facility at ORNL was used for this study. The experiments were complemented by finite-element simulation of thermal loads and stresses.

Assessing the effect of neutron irradiation on plasma-facing materials is difficult due both to technical and radiological challenges. In an effort to address the radiological challenges, a new HHF facility based on water-wall plasma-arc lamps was developed at ORNL [1] and upgraded recently [2]. *The first accomplishment* was the successful demonstration of safe HHF testing of low radioactivity level irradiated materials using unbolted W neutron-irradiated specimens at 1.6 MW/m² absorbed heat flux (incident 3.5 MW/m²) in a low-vacuum controlled atmosphere [3]. *The second accomplishment* was the design of specimen holders to bolt the so-called “small-and-thin material specimens” (STMS) specimen onto actively cooled Cu modules. Six vacuum plasma-sprayed (VPS) W-on-F82H low activation steel [4] STMS were successfully HHF tested at 1.6 MW/m² on the bolted mounting [5, 6]. *The third accomplishment* was the development of a simplified 3D thermo-mechanical Finite Element Analysis (FEA) model that was used to understand the complex deformation of the bimetallic F82H/W specimens during HHF [5, 6]. Numerical simulation results for one HHF cycle, which were obtained with a FEA model that considers the specimen bolting effect in the VPS-W and F82H, were found to qualitatively reproduce the experimentally observed deformation of the specimen [5]. The predicted stress levels using the FEA model during one HHF cycle in the VPS-W, were found to exceed the failure stress of the brittle VPS-W layer near the clamped edges of the specimen and this explains the observed cracking of a W/F82H specimen during HHF. *The fourth accomplishment* was the design, fabrication, and testing of a new PAL reflector to attain fusion-prototypical steady-state absorbed heat fluxes in W of 6 MW/m² (incident 12 MW/m²) over a 2 cm wide strip [2]. The new reflector was designed with side ports to allow the external mounting of a pyrometer with direct line-of-sight to the specimen, enabling the direct measurement the specimen temperature using pyrometers. *The fifth accomplishment* was the upgrade of the bolting specimen holder to withstand 6 MW/m² (incident 12 MW/m²) heat fluxes provided by the new reflector while enabling (a) the highest thermal gradient through the specimen and (b) the use of thermocouples underneath the sample to measure back-side temperatures (Figure 1a) [2].

To simulate on/off cycling of normal operating plasma, target temperatures of 950 to 1,150°C were sought for the top surface of the specimen while actively cooling the specimen on its back surface to attain a high thermal gradient. Target sample surface temperatures were obtained by employing 4.7/5.1 MW/m² (incident 11.0/11.9 MW/m²) HHF cycles of 2–3 s duration with 60–80 s cooling time between cycles. The measured temperature data indicate that the target surface temperature was attained (Figure 1b). Moreover, surface examination indicated that the back surface of the specimen was in good thermal contact with the actively cooled Cu during HHFT.

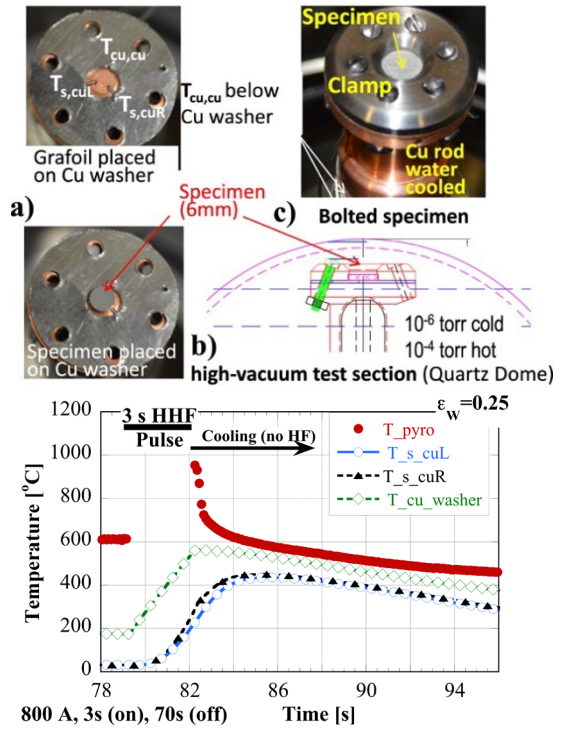


Figure 1. (a) Thermocouple placement, specimen mounting, and confined test section, and (b) Measured temperatures for a 3s heat flux pulse of 4.7 MW/m². The PAL was immediately shutdown after the HHF pulse.

The sixth accomplishment was the successful HHF exposure of 7 W-based samples, including two neutron-irradiated samples [7]. The tested materials were thick plate “ITER type” W produced by ALMT and K-doped W-3%Re. Both materials had samples prepared in two orientations: with the grains elongated perpendicular to or parallel to the sample surface. These 6 mm diameter and 2 mm thick samples were irradiated in the HFIR RB*19J capsule that used thermal neutron shielding to better approximate the transmutation rates of a fusion reactor.

To simulate on/off cycling of a normal operating plasma, samples were exposed to approximately 800–900 cycles at

4.7 MW/m² absorbed heat flux (incident heat fluxes of 11.0 MW/m²) [7]. After PAL exposure, scanning electron microscopy examination showed slight changes on the surfaces of the pure W samples. The samples showed some annealing in the near surface polished region, but all eight samples tested were below the damage threshold for cracking or other destructive changes [7]. While these HHF conditions do not exactly replicate the conditions of a particular fusion reactor, they serve as baseline experimental data for future modeling and simulation. The ultimate goal is the modeling-based design of plasma-facing components.

- [1] A.S. Sabau, E.K. Ohriner, J.O. Kiggans, et al., *Phys. Scripta* T159, 014007 (2014)
- [2] Sabau, A. S., Tokunaga, K., Littleton, M. et al., *Fusion Sci. Tech* 75 no 7 (2019): 690-701.
- [3] A.S. Sabau, E.K. Ohriner, J.O. Kiggans, et al., *Fusion Sci. Tech* 66, 394 (2014)
- [4] K. Tokunaga, T. Hotta, K. Araki, et al., *J. Nucl. Mat* 438, S905 (2013)
- [5] Ibano, K., A. S. Sabau, K. Tokunaga, et al., *Nucl. Mater. and Energy* 16 (2018): 128-132.
- [6] A.S. Sabau, K. Tokunaga, S. Gorti, et al., To be submitted to *Fusion Sci. Tech.* (April 2021).
- [7] Garrison, L. M., Sabau, A. S., Gregory, B., et al. *Phys. Scripta* T171, 014077 (2020).

Task 1: Investigation of Overall Heat Flow Response in Plasma-Facing Components

Category: PHENIX

Name: T. Yokomine¹, Y. Ueda², K. Yuki³, K. Tokunaga⁴, M. Akiyoshi⁵, K. Ibano², M. Yoda⁶, A. Sabau⁷

Affiliation: ¹Kyoto Univ., ²Osaka Univ., ³Sanyo-Onoda City Univ., ⁴Kyushu Univ., ⁵Osaka Pref. Univ., ⁶GIT, ⁷ORNL

Plasma Facing Components (PFC) are subject to steady/unsteady heat load and particle load at the same time. As a result, the effects of thermal stress, thermal fatigue, hydrogen/He, etc. are additive on the plasma facing material, and there is concern that the integrity of the PFC may deteriorate due to damage or embrittlement of the materials. The flow of heat and particles is regarded as a primary safety phenomenon in PFC where robust design is required. Ideally, the overall heat flow in PFC should be simulated experimentally, but in addition to the difficulty of reproducing nuclear heat generation, it is almost impossible to carry out simultaneous material and cooling performance tests for safety analysis. Therefore, in this task, the material heat load test and heat transfer experiment on the plasma facing material under high heat flux are performed separately. By combining the results, we aimed to provide safety evaluation criteria for plasma facing materials under overall heat flow conditions of PFC. Heat transfer experiments and heat load experiments were conducted at Georgia Institute of Technology and Oak Ridge National Laboratory, respectively, in cooperation with researchers from Japan. Since those results are described in Sections 6.3 and 6.4, here we introduce an example of the results of research conducted in Japan for the purpose of supplementing the experimental results in the United States.

In conventional research on impinging jet heat transfer, the heat transfer increases as the ratio (H/D) between the nozzle-heat transfer surface distance (H) and the nozzle diameter (D) decreases. Therefore, using the experimental apparatus at GIT, with the aim of further improving the heat transfer performance, a heat transfer experiments were performed with an H/D value smaller than the HEMJ reference design value ($H/D=1.0$). Figure 1 shows the changes in the Reynolds number and the average Nusselt number with respect to the helium temperature when $H/D=0.25$ and 0.5. When $H/D=0.5$, the average Nusselt number increases with increasing temperature or Reynolds number. This is in agreement with the results of conventional experiments conducted at 100°C or lower. On the other hand, when $H/D=0.25$, when the helium temperature is 100°C or less, it exceeds the average Nusselt number when $H/D=0.5$, which is consistent with the previous research results. However, in the temperature range 200°C or higher, the heat transfer coefficient was lower than in the case of $H/D=0.5$. Furthermore, when the same $H/D=0.25$ was compared, there was a phenomenon that the heat transfer coefficient decreased compared to the low temperature range,

which was not seen in the conventional papers. Re-laminarization is considered to be the cause of this.

Figure 2 shows the numerical simulation results of the HEMJ flow field. Focusing on the two jets on the outer circumference, when $H/D=0.5$, the jet structure is maintained, while when $H/D=0.25$, a region is formed where the symmetrical jet structure collapses and strong acceleration downstream of the jet occurs. At the outer periphery of multiple jet impingement, there may be synergistic laminarization caused by rapid acceleration and laminarization caused by property change of helium gas which is strongly heated near the impingement surface. This problem cannot be avoided unless the H/D value is small. It is possible to form a high acceleration region even under high temperature conditions alone, so it is important to confirm the conditions under which re-laminarization occurs and to establish the turbulence model to predict re-laminarization to realize a successful gas-cooled divertor.

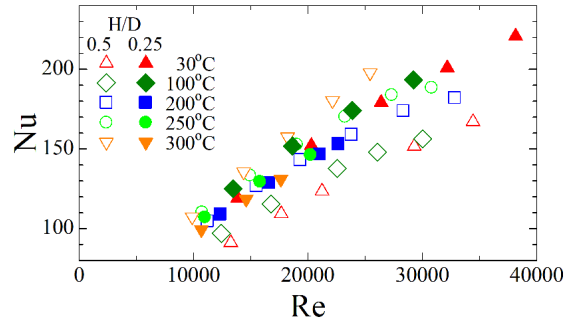


Figure 1. Heat transfer performance degradation depending on H/D and gas temperature

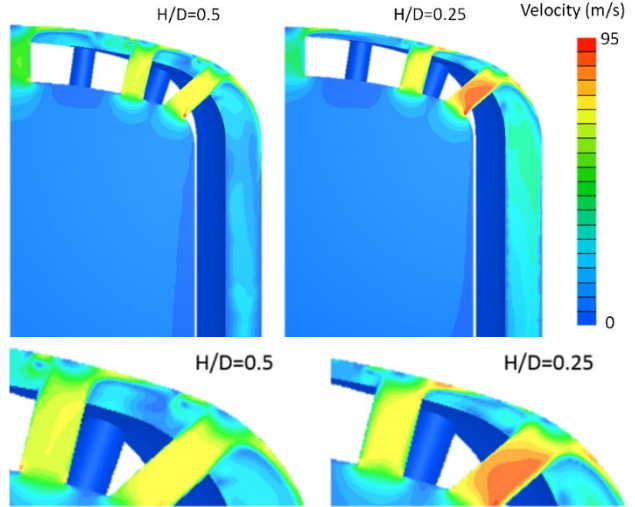


Figure 2. Results of CFD simulation: $H/D = 0.5$ (left row); $H/D = 0.25$ (right row).

Task 2: Material Performance - Evaluation and Irradiation

Category: PHENIX

Name: T. Hinoki/A. Hasegawa/L. Garrison/Y. Katoh

Affiliation: Kyoto Univ./Tohoku Univ./ORNL

Plasma facing materials in fusion systems are exposed to very severe conditions, and neutron fluence for DEMO will be much greater than for ITER. No current commercialized materials have adequate properties to survive these conditions, especially the effects of neutron irradiation. Improved or new materials are required. Japan, the US, and other countries are devoting significant effort to material development and improvement, including increasing the fracture toughness of tungsten and other materials for use in plasma facing components (PFC). The feasibility of PFC significantly depends on material performance under thermal loads, as discussed in Task 1, among other factors. It is necessary to establish the potential and limitation of candidate materials to develop a robust design. Advanced candidate tungsten-based plasma facing materials with improved performance were selected for study in this Task. The performance of these materials under neutron irradiation was evaluated. In order to clarify displacement damage effects under lower transmutation conditions, a thermal neutron shield made of Gadolinium (Gd) was used for these irradiations in the RB*19J capsule in the High Flux Isotope Reactor (HFIR). The objective was to clarify the potential and limitations of plasma facing materials and establish a design window for a DEMO relevant divertor.

One set of materials included in the PHENIX irradiation focused on the effects of tungsten grain size, with grain size ranging from single crystal tungsten with very large grains, powder metallurgy produced tungsten with medium grains, and rolled tungsten foil with very small grains. This irradiation of unalloyed tungsten concentrated on gathering baseline irradiation data on tungsten at transmutation rate to dpa ratio that is relevant for fusion. Only very limited data existed previously on neutron irradiated tungsten at conditions similar to those expected in fusion reactors. The PHENIX collaboration collected a wide range of microstructural, thermal, and mechanical properties data for the materials¹⁾.

Single crystal tungsten samples were included in the RB*19J capsule irradiation for direct comparison with previous irradiation of single crystal tungsten without shielding. It was noted that tungsten irradiated in HFIR without shielding undergoes high rates of transmutation to Re and Os, which leads to the precipitation of Re and Os rich clusters, with severe consequences on mechanical properties^{2,3)}. The single crystal tungsten irradiated in the RB*19J shielded capsule had noticeably lower hardness after irradiation than the irradiated unshielded tungsten, which is attributed primarily to the reduced transmutation in the shielded samples. Additionally, the single crystal tungsten irradiated in the shielded capsule at the highest temperature of ~994°C has the complimentary effects of lower transmutation and higher irradiation

temperature and thus more dynamic annealing of irradiation defects, leading to a lower hardness.

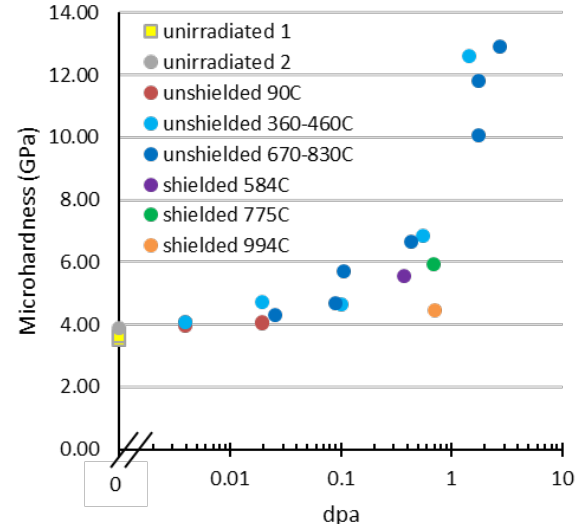


Figure 1. Microhardness of single crystal tungsten irradiated in HFIR. Temperatures listed in the legend are the average irradiation temperature of the specimens tested.

ITER W diverter tiles are fabricated by powder metallurgy, to give homogeneity to the material and limit the manufacturing cost. One feature of W or W alloy materials manufactured by powder metallurgy is control of the working ratio and the grain size. In particular, a layered structure of pancake-shaped grains is formed by rolling during the manufacture. The elastic strain due to the rolling is moderated by a stress relief heat treatment (SR) where the worked dislocations are partially recovered to form a dislocation cell structure in the grain^{4,5)}. These microstructure controls can be effective in suppressing the low temperature embrittlement. In addition, potassium (K)-doping or the combination of K-doping and 3%Re addition can increase the recrystallization temperature and the high temperature strength at 1000 °C or higher^{6,7)}. Grain refinement by K-doping and 3%Re addition is also expected to improve the low temperature embrittlement. Effects of Re addition are known to decrease the DBTT and increase high temperature strength by the solid solution strengthening mechanism⁸⁾.

Figure 2 shows engineering stress-strain curves from 700°C tensile tests of unirradiated and irradiated pure W (SR) and its alloys (SR). HFIR irradiations were at ~800°C⁹⁾. All irradiated W materials (SR) showed yielding stress about twice that of unirradiated materials. All W materials (SR) exhibited yielding but irradiated pure W (SR) and irradiated W-3%Re (SR) fractured without necking whereas irradiated K-doped W (SR) and irradiated K-doped W-3%Re (SR) fractured after a significant amount of necking. Irradiated pure W (SR) showed yielding but the elongation was reduced after irradiation compared to the unirradiated materials. The rupture surface

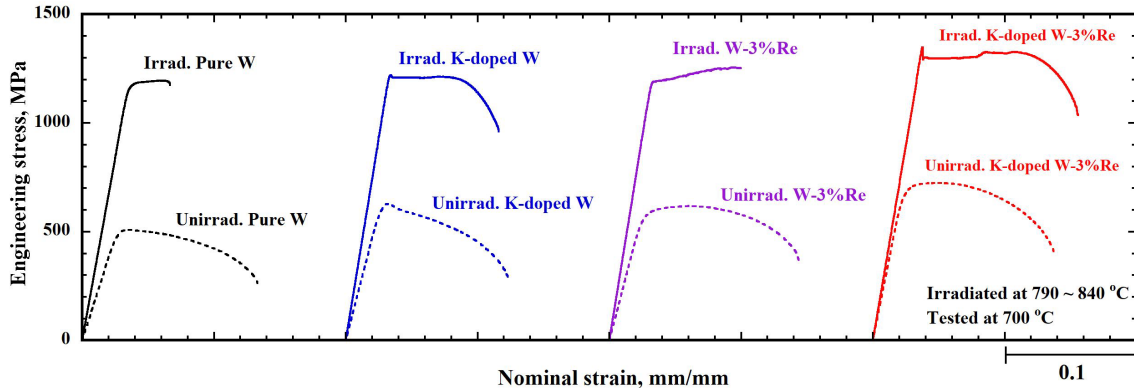


Figure 2. Engineering stress-strain curves from 700 °C tensile tests of unirradiated and irradiated stress relieved pure W (SR) and its alloys (SR) at 800 °C

showed no necking, with a cleavage fracture. Irradiated W-3%Re (SR) also showed the same tensile and fracture behavior as irradiated pure W (SR). Irradiated pure W (SR) and W-3%Re (SR) both showed the loss of ductility and a brittle fracture mode. On the other hand, elongation of K-doped W (SR) and K-doped W-3%Re (SR) after irradiation was almost the same as the unirradiated materials. The ruptured surfaces showed necking and dimples. Delamination of the layered structure was also observed. The results showed that K-doped W (SR) and K-doped W-3%Re (SR) had good ductility after irradiation. All W materials (SR) irradiated at 550 °C and evaluated at 500 °C also showed yield stress about twice that of unirradiated material. The irradiated pure W (SR) showed irradiation hardening and was ruptured in the elastic region without yielding. K-doped W (SR) showed yielding but a small elongation of 0.4%. However, W alloys with the addition of 3% Re (W-3%Re (SR) and K-doped W-3%Re (SR)) showed some elongation. The relevant fractographs showed necking and dimples, evidence of a ductile fracture. Delamination of the layered structure was also observed in the fracture surface in K-doped W-3%Re (SR). W alloys with the addition of 3% Re also showed irradiation hardening, but they exhibited ductility and plastic instability.

The thermal properties of tungsten are critical to its use in fusion reactors, so this was another experimental focus of the PHENIX collaboration. A special effort was devoted to developing a reliable technique for measuring the thermal diffusivity of 3 mm diameter, 0.5 mm thick miniature irradiated samples. Specimens with this geometry are more sensitive to surface condition and the fixture in the thermal diffusivity measurement device than more standard 10 mm diameter samples¹⁰⁾. This effort was coordinated with the Task 1 high heat flux exposure of irradiated samples, which compared unalloyed tungsten with K-doped W-3%Re material. Thermal diffusivity was measured from room temperature to 800°C. At all temperatures the unalloyed tungsten had significantly higher thermal diffusivity than the K-doped W-3%Re, however that difference became less at higher temperatures. After irradiation

in the RB*19J capsule, both materials had decreased thermal diffusivity, but the unalloyed and irradiated tungsten values still remained higher than the unirradiated K-doped W-3%Re. This confirms that the transmutation in the shielded capsule was less than 3% Re.

References

- 1) L.M. Garrison, et al., Fusion Science & Technology, 75 (2019) 499-509
- 2) L.M. Garrison, et al., Journal of Nuclear Materials, 518 (2019) 208-225
- 3) T. Koyanagi, et al., Journal of Nuclear Materials, 490 (2017) 66-74
- 4) K. Sasaki, et al., Journal of Nuclear Materials, 461 (2015) 357-364
- 5) K. Sasaki, et al., Fusion Engineering and Design, 88-9-10 (2013) 1735-1738
- 6) K. Tsuchida, et al., Nuclear Materials and Energy, 15 (2018) 158-163
- 7) M. Fukuda, et al., Fusion Engineering and Design, 89 (2014) 1033-1036
- 8) E.M. Savitskii, et al., Metal Science and Heat Treatment of Metals, 2 (1960) 483-486
- 9) T. Miyazawa, et al., Journal of Nuclear Materials, 529 (2020)
- 10) M. Akiyoshi, et al., Fusion Engineering and Design, 136-Part A (2018) 513-517

Task 3: Irradiation Response on Deuterium Retention in Unshielded Neutron-Irradiated Tungsten

Category: PHENIX Task 3

Name: M. Shimada^{a,*}, D.A. Buchenauer^b, Y. Hatano^c, and Y. Oya^d,

Affiliation: ^aINL, ^bSNL-CA, ^cUniv.of Toyama, and ^dShizuoka Univ.

One of the critical challenges during long-term operations of the fusion pilot plant and demonstration (DEMO) reactors is the development of fusion materials that can withstand the extreme conditions created by high plasma/neutrons particle fluxes and high heat-flux, while minimizing in-vessel inventories and ex-vessel permeation of tritium. Understanding irradiation effects on heat transfer, thermo-mechanical properties, and tritium retention/permeation in PFCs determines the feasibility and safety of divertor components under severe conditions from plasma/neutron particle fluxes and heat-flux. During the previous US-Japan TITAN program, polycrystalline tungsten (PCW) was irradiated in unshielded capsules at *low temperature* (<373K) to understand the fundamental deuterium migration and trapping mechanisms in irradiated tungsten [1]. The scope of US-Japan PHENIX Task 3 was to improve understanding of tritium behavior (retention and permeation) in tungsten and tungsten alloys under divertor-relevant high-flux plasma and *elevated temperature* regions (>873K). Approximately 300 tungsten discs (6 or 10 mm OD, and 0.25, 0.5, or 1.0 mm thickness) were irradiated at three temperature zones, nominally 773, 1073, and 1373K, to radiation level of approximately 0.5 dpa in HFIR-RB* with gadolinium neutron shielding under the PHENIX program. The Tritium Plasma Experiment (TPE) at INL offers a radiological capability to investigate irradiation effects on deuterium retention in low-activity samples. The following are highlights of irradiation response on deuterium retention in unshielded tungsten under the PHENIX program.

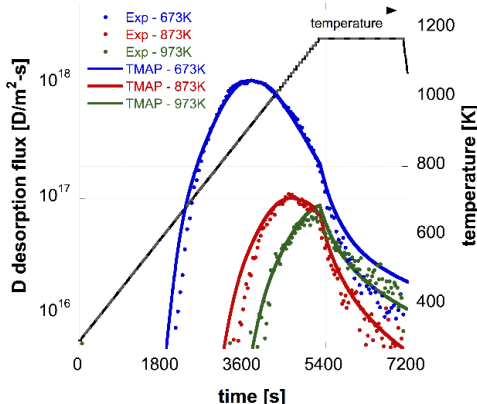


Figure 1: The experimental TDS spectrum (in dotted line) and the TMAP-simulated TDS spectrum (in solid line) of 673 K (in blue), 873 K (in red), and 973 K (in green).

For the unshielded PHENIX program neutron irradiations, single crystal tungsten (SCW) was irradiated at elevated temperatures (633 K, 963 K, and 1073 K) to approximately 0.1 dpa in unshielded capsules to study the irradiation response. A pair of neutron-irradiated tungsten specimens was then exposed to a deuterium (D) plasma to ion fluence of $5.0 \times 10^{25} \text{ m}^{-2}$ at three different exposure temperatures (673 K, 873 K, and 973 K) at the TPE [2-3]. A combination of thermal desorption spectroscopy, nuclear reaction analysis, and rate-diffusion modeling code (Tritium Migration Analysis Program, TMAP) were used to understand D behavior in neutron-irradiated tungsten [2-3]. Figure 1 shows the experimental TDS spectra of 673 K (in blue), 873 K (in red), and 973 K (in green) along with the TMAP-simulated TDS spectra for three temperature cases. Total D retention was approximately $1.9 \times 10^{21} \text{ m}^{-2}$ for 0.1 dpa, 673 K. A broad D desorption spectrum from the plasma-exposure temperature up to 1173 K was observed. Trap density up to $2.0 \times 10^{-3} \text{ Traps/W}$ and detrapping energy from 1.80 to 2.60 eV were obtained from the TMAP modelling [2-3]. Figure 2 compares total D retention in 0.1 dpa neutron-irradiated SCW (solid triangles) [2] with the previous results from 0.025 dpa (solid circles) and 0.3 dpa irradiated SCW (solid squares) [1].

Although the near-surface D concentrations decreased at elevated temperatures, the deep migration and trapping of D resulted in non-negligible D retention in unshielded 0.1 dpa SCW due to D trapping in vacancy clusters and voids. FRONTIER program tritium permeation and retention experiments in TPE with the thermal neutron-shielded tungsten discs will be reported in future work.

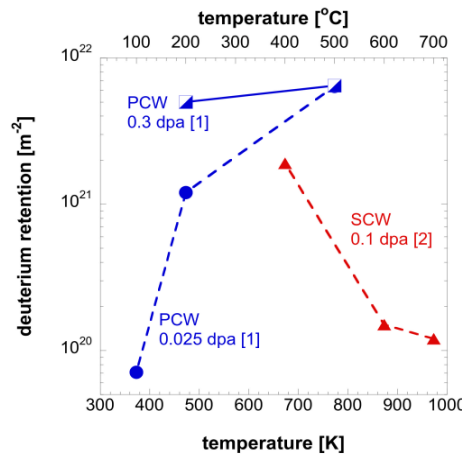


Figure 2: Total deuterium retention from 0.1 dpa neutron-irradiated SCW (in solid triangles), and 0.025 dpa (in solid circles) and 0.3 dpa neutron-irradiated SCW (in solid square).

References:

- [1] M. Shimada *et al.*, *Nucl. Fusion* **55** (2015) 013008.
- [2] M. Shimada *et al.*, *Fus. Eng. Des.* **136** (2018) 1161
- [3] Y. Oya *et al.*, *J. Nucl. Mater.* **539** (2020) 152323.

Task 3: Hydrogen Isotope Behavior in Irradiated Tungsten

Category: PHENIX Task 3

Name: Y. Oya, M. Shimada, Y. Hatano, D. Buchenauer

Affiliation: Shizuoka Univ., INL, Univ. Toyama, SNL

Due to the high tritium solubility in graphite, tungsten (W) is now the primary candidate material for fusion plasma-facing components. Recent studies show that tritium dynamics will be clearly controlled by the characteristics of W material, the damage profiles introduced by neutrons and other energetic particles, accumulation of impurities like He and/or C on the W surface, and transmutation of W by neutrons. The interaction of irradiation-induced defects and hydrogen isotopes is envisioned to be one of the most prominent problems for plasma-facing materials, particularly because the neutron damage will be distributed throughout the material.

In this study, damage level dependence of D retention for 0.0003 dpa to 1.0 dpa Fe^{2+} ion irradiated W samples was initially studied. For the undamaged W, D₂ desorption stages were concentrated at lower temperatures, below 500 K. However, as displacement damage was introduced, a second desorption stage (Stage 2) was found at temperatures between 500 K and 700 K. Above 0.03 dpa, an additional desorption stage (Stage 3) was found at a temperature above 700 K. The desorption temperatures for both Stages 2 and 3 shifted upward as damage was accumulated. The hydrogen isotope diffusion and trapping (HIDT) simulation revealed that the D₂ desorption behavior can be accurately simulated using three trapping sites with energies of 0.65 eV, 1.25 eV and 1.55 eV, corresponding to the desorption of D trapped by dislocation loops, vacancies and voids, respectively. Figure 1 shows the comparison of D₂ TDS spectra for W samples damaged by Fe^{2+}

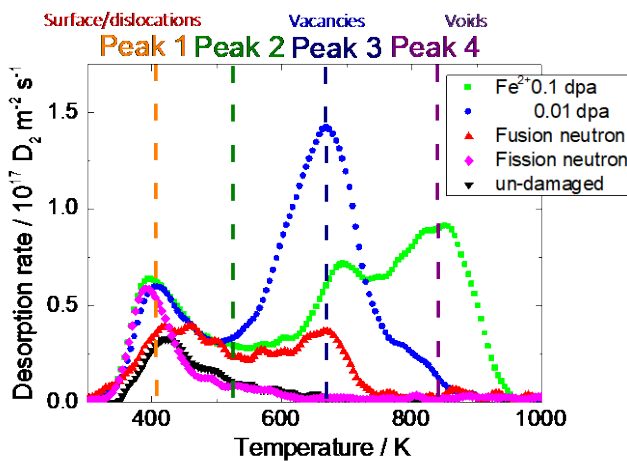


Figure 1. Comparison of D₂ TDS spectra for irradiated W after 1 keV D₂⁺ implantation with $1.0 \times 10^{22} \text{ D m}^{-2}$. (Fusion neutron: $\sim 2 \times 10^{-7} \text{ dpa}$, Fission neutron: $\sim 4 \times 10^{-4} \text{ dpa}$). irradiation, by fusion neutron irradiation or by fission neutron irradiation. Although high vacancy and void concentrations

within the shallow region near the surface were introduced by Fe^{2+} irradiation, single vacancies with low concentrations were distributed throughout the sample for 14 MeV neutron irradiated W. Only dislocation loops were introduced by fission neutron irradiation at low neutron fluence. The desorption peak of D for fission neutron irradiated W was concentrated in a low temperature region below 550 K, but that for 14 MeV neutron irradiated W was extended toward the higher temperature side due to D trapping by vacancies.

The effect of damage introduction at higher temperature on D retention in Fe^{2+} -irradiated W was also studied. Figure 2 shows D₂ TDS spectra for W Fe^{2+} -irradiated W at various temperatures to 0.1 dpa with Fe^{2+} and for material irradiated at room temperature then annealed at elevated temperatures. A clear reduction of D desorption at ~ 800 K after higher temperature irradiation was found compared to with W post-irradiation-annealed at that same temperature. In addition, D₂ desorption temperatures shifted toward lower temperatures for peaks at 573 K and 873 K. These results show that dynamic recovery of damage is enhanced by higher temperature irradiation, and modification of trapping sites reduces the associated trapping strength of voids.

It can be seen that the type of trapping sites and their distributions clearly controls the D desorption behavior. Accumulation of damage in W creates stable trapping sites (vacancy and voids) for hydrogen isotopes, leading to the D desorption at higher temperatures.

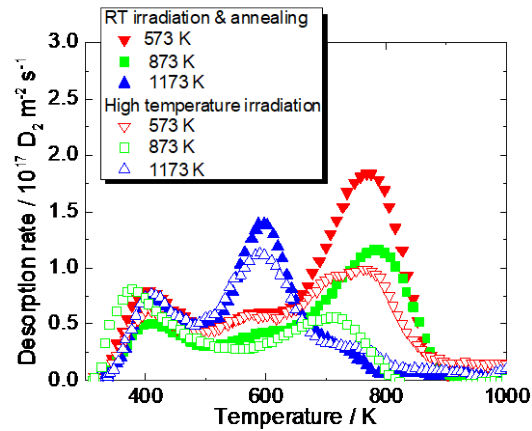


Figure 2. D₂ TDS spectra for 0.1 dpa Fe^{2+} -irradiated W at various annealing temperatures. (1 keV D₂⁺ with $1.0 \times 10^{22} \text{ D m}^{-2}$).

The PHENIX Instrumented HFIR RB 19J Experiment

Category: PHENIX

Name: J.W. Geringer¹, J.M McDuffee¹, T. Hinoki²

Affiliation: ¹ORNL, ²Kyoto University

The HFIR RB19J irradiation experiment was a shared collaborative effort between the US and Japan Fusion Materials programs to evaluate neutron irradiation effects in tungsten (W) for plasma facing components under divertor conditions and in blanket structural materials for DEMO and other fusion reactors. The focus of the PHENIX program was to establish effects in tungsten of fusion-relevant transmutation-to-dpa ratio to enable comparison with previous unshielded irradiations.

The experiment was designed to irradiate tungsten and RAFM (F82H) steel specimens at controlled temperatures of 300°C, 500°C, 800°C and 1200°C in the Removable Beryllium (RB) position of the High Flux Isotope Reactor (HFIR), shown in Figure 1. The RB region is part of the reflector which is the concentric ring surrounding the control plates and outer fuel element.

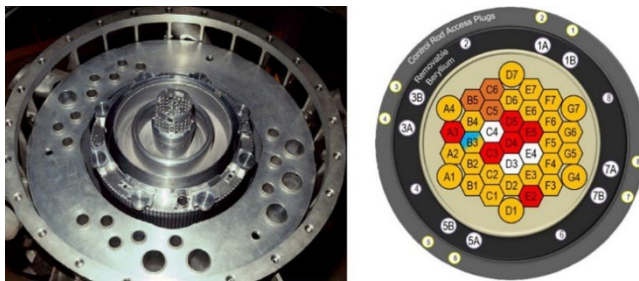


Figure 1. The HFIR core with the beryllium reflector (left) and schematic of the RB layout (right)

The RB19J capsule contained a 1 mm thick gadolinium (Gd) metal liner, located on the inside of the capsule housing, surrounding the specimen holders. It served as a thermal neutron shield to modify the fast/thermal neutron ratio over the life of the experiment, thus controlling the W to rhenium (Re) and osmium (Os) transmutations. This was the first use of a Gd shield in the HFIR for this purpose.

The experiment contained six cylindrical holders (four temperature zones) which housed ~1300 tungsten and steel specimens. Three of the six holders were made of graphite with target temperatures of 800°C, 1200°C and 500°C and contained a variety of tungsten material specimens, including tensile, fracture toughness, torsion, various disc type specimens and even some fiber specimens. The remaining three holders were made of aluminum for a 300°C target temperature and housed the steel specimens. The effective total internal sub-capsule length was 480 mm with a mean diameter of ~30 mm.

Temperatures inside the capsule were controlled by a combination of gas gap thickness and gas composition (helium and argon) and monitored by thermocouples as shown in Figure 2. Temperature control was performed by purging the

capsule with helium and then changing with a controlled gas ratio (argon-helium mixture). Passive SiC temperature monitors were included in each holder and neutron dosimetry monitors were inserted in the spacer regions between the holders.

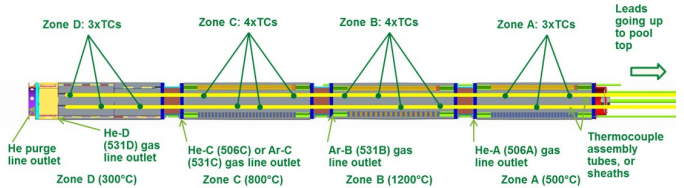


Figure 2. Schematic of the RB19J capsule layout showing the four temperature zones and gas lines.

Assembly of the RB19J capsule was completed in May 2016 and its first HFIR irradiation cycle, 466, started in June 2016. Starting temperatures stabilized within design ranges for the 500°C and the 800°C holders. The 1200°C and the 300°C were lower and higher than designed by about 50°C and 100°C respectively. The fourth and last irradiation cycle, 469, was completed in December 2016.

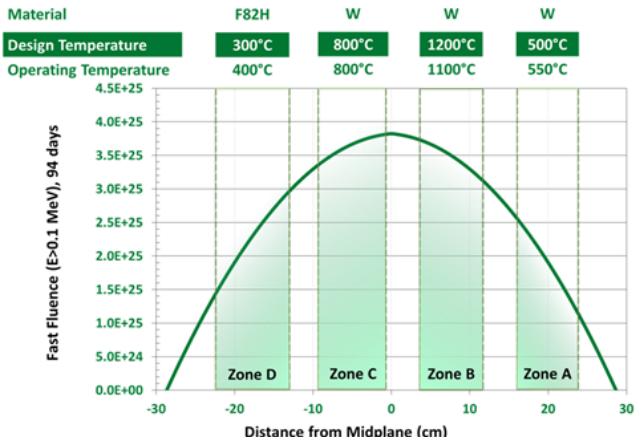


Figure 3. Calculated fluence distribution and temperature zones over the length of the capsule.

The experiment completed a total of 8001 MWD of neutron irradiation over a period of 94 days during 4 HFIR cycles. Analysis indicated that the Gd-shield was effective during the irradiation period. Figure 3 shows the calculated fast fluence ($E > 0.1$ MeV) over the four temperature zones and labels give the average temperature performance during operation.

Calculations based on post irradiation evaluation of flux monitors determined that a maximum dose of 0.586 dpa was achieved for the tungsten specimens. Analysis of the temperature monitors concluded mean temperatures of ~568°C, 848°C and 974°C for the applicable zones in the final irradiation cycle.

FRONTIER Project

Category: FRONTIER

Name: Y. Hatano¹, D. Clark², T. Yokomine³, Y. Katoh⁴

Affiliation: ¹Univ. Toyama, ²USDOE, ³Kyoto Univ.,

⁴ORNL

FRONTIER is the abbreviation of Fusion Research Oriented to Neutron Irradiation Effects and Tritium Behavior at Material Interfaces. This six year project started in April 2019 with the goal of providing the scientific foundations for reaction dynamics in interfaces of plasma facing components (PFCs) for DEMO reactors.

In the TITAN (2007-2012) and PHENIX (2013-2018) projects, extensive efforts were made for the development of materials resistant to neutron irradiation and plasma exposure, joining techniques for those materials and the evaluation of hydrogen isotope retention and permeation. However, the effects of neutron irradiation on the properties of joining interfaces and hydrogen isotope transport through the interfaces have been scarcely studied. Performance and robustness of plasma-facing components might be limited by properties of those of interfaces if the properties are poorer than those of the bulk materials.

Liquid divertors may have larger heat removal capacity than W-armored solid divertors and hence that is one of the alternative options for the DEMO divertor. The compatibility of liquid metals and structural materials is an issue for liquid divertor and has been studied under static and flowing conditions. However, the effects of neutron irradiation on the compatibility have not been evaluated.

Based on these considerations this project will tackle the issues listed below:

- (1) Reactions at the interface between plasma-facing materials and structural materials, the neutron irradiation effects on the reactions, and the influence of reaction layers on the mechanical properties and heat transfer of the interface;
- (2) Tritium transport through the interfaces and the neutron irradiation effects;
- (3) Oxidation of neutron-irradiated plasma-facing materials and subsequent tritium release; and
- (4) Compatibility of liquid metals with structural materials, surface oxide films and coating materials, and neutron irradiation effects on this compatibility.

To reach these goals, four tasks were defined for the project, and are shown in Figure 1.

The objectives of Task 1, Irradiation Effects on Reaction Dynamics at Plasma-Facing Material/Structural Material Interfaces, are to understand neutron-induced microstructure modifications and the consequent changes in mechanical and heat transfer properties of interfaces between plasma-facing material and structural material (Figure 2). This task performs neutron-irradiation in the High Flux Isotope Reactor (HFIR) and post-irradiation examinations in the Low

Activation Materials Development and Analysis laboratory (LAMDA) at Oak Ridge National Laboratory (ORNL). Task 1 has prepared a variety of layered and joined materials using state-of-the-art joining techniques such as diffusion bonding of W materials with reduced activation ferritic/martensitic steels (RAFS), Cu alloys, SiC, oxide dispersion strengthened (ODS) alloys and vanadium alloys. Direct diffusion bonding of SiC to W was successfully developed and additional focus is now on developing K-doped W laminated composites. Direct brazing between W and ODS-Cu alloy was developed. Additional underwater explosive welding and vacuum plasma spraying with friction stir processing are being explored. Composite laminates and particle reinforced W alloys are also under development. Spark plasma sintering (SPS) processing, used to develop the dispersion-strengthened W materials, was found to be useful to fabricate dense and fine-grained samples of various compositions. Based on these results, the task has established a test matrix for neutron-irradiation campaign. The design of irradiation capsules is nearly complete, and neutron irradiations will start Japanese fiscal year 2020.

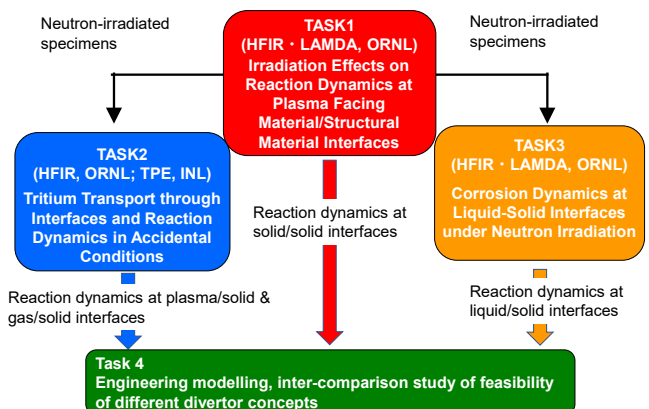
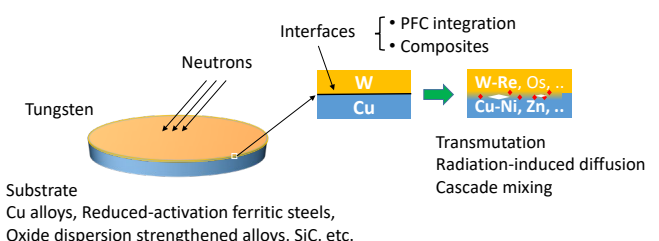


Figure 1. Task structure of the FRONTIER project.



Issues: integrity, thermal conductivity, tritium transport, etc.
Figure 2. Schematic description of neutron irradiation effects on interface between plasma-facing and structural materials.

Task 2 (Tritium Transport through Interfaces and Reaction Dynamics in Accidental Conditions) aims to measure retention and permeation of hydrogen isotopes including tritium in layered materials using the linear plasma machine Tritium Plasma Experiment (TPE) at Idaho National Laboratory (INL) (Figure 3). In these experiments, the hydrogen isotope transport through the interface between plasma-facing material and structural material before and after neutron irradiation will be studied together with the effects of He seeding and isotope mixing in the plasma. The task also investigates the oxidation of neutron-irradiated W materials by steam, air etc. after exposure to tritium plasma. This will help construct a fundamental database on radioisotope emission from W under accidental conditions. The mobilization device built in the Safety and Tritium Applied Research (STAR) facility, INL during the JUPITER-II project (2001-2006) is available for this purpose.

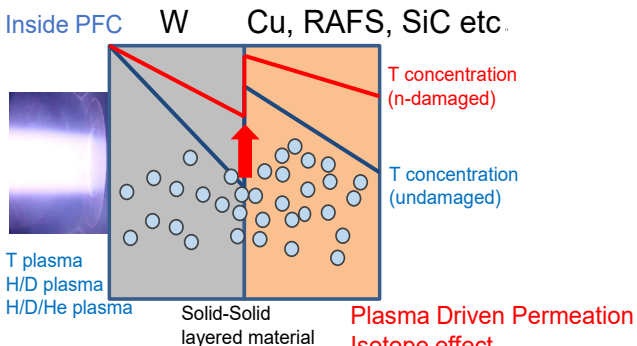


Figure 3. Schematic diagram of tritium transport through layered materials under plasma exposure

The objective of Task 3 (Corrosion Dynamics at Liquid-Solid Interfaces under Neutron Irradiation for Liquid Divertor Concepts) is to study the corrosion characteristics of liquid Sn as a divertor coolant with and without neutron irradiation. Liquid Sn has been selected as a candidate liquid metal for divertor applications due to the acceptably low vapor pressures at expected service temperatures. Material issues for the liquid Sn divertor concept are summarized in Figure 4. The preliminary corrosion tests of unirradiated materials under static conditions performed by the task partners revealed that Al-rich steels (e.g. Fe-15Cr-6Al steel and its ODS steel) have excellent corrosion resistance against liquid Sn. Hence, the task plans to investigate the corrosion resistance under non-isothermal conditions using a thermal convection loop at ORNL. The tube material of the thermal convection loop is AMPT steel (Fe-21Al-5Al-3Mo) and the contamination of liquid Sn by the corrosion of loop tubes is suppressed. The material compatibility test under neutron irradiation in HFIR is also under planning. In the current capsule design, two SSJ specimens are installed in a single capsule together with a small amount of liquid Sn.

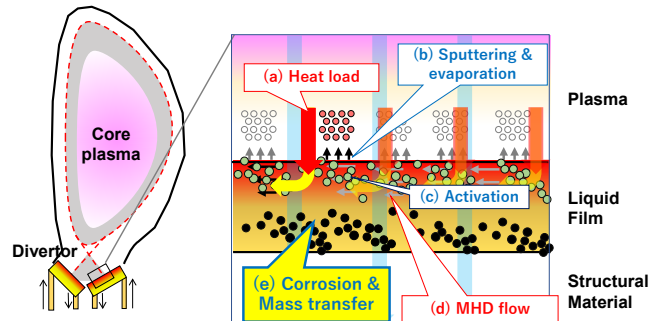


Figure 4. Schematic diagram of a liquid divertor.

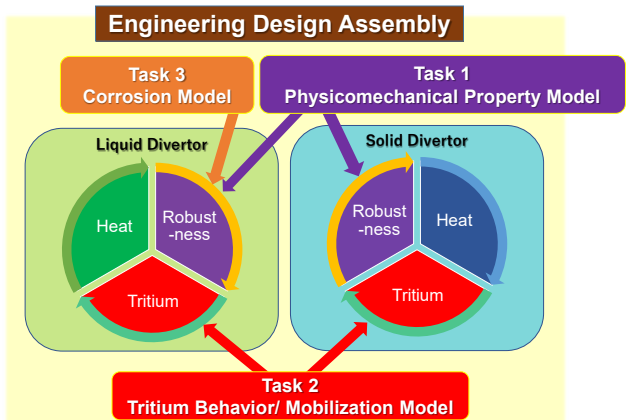


Figure 5. Contribution of tasks in engineering modeling performed in Task 4.

Task 4 (Engineering Modeling) will consolidate the results of each task focusing on hetero-phase/interphase interfacial dynamics interdisciplinary, link them organically as a phenomenon acting in the PFCs, and apply to an engineering model that can correspond to the PFC system (Figure 5). At present, a system with water cooling and W material is the main candidate divertor concept, but resistance to unexpected large heat loads is low. Against this backdrop, the task conducts an engineering inter-comparison study of gas-cooled solid divertor and liquid divertor to evaluate their relative feasibilities.

CHAPTER 7 HFIR Collaborative Research

Japan and the United States have worked together for 36 years on a Project between JAERI, JAEA, then QST, MEXT of Japan, and U.S. DOE. This Collaboration is now under the Cooperation in Research and Development in Energy and Related Fields. Both partners note with satisfaction the steady progress and high productivity of this partnership and look forward to the continuation and growth of this collaboration.

7.1 Objectives

The goal of this collaboration is to jointly design, conduct, and evaluate irradiation experiments in the High Flux Isotope Reactor (HFIR) at Oak Ridge National Laboratory to investigate the irradiation response of structural materials that are of interest to Japan and U.S. The final objective of this collaboration is to develop and qualify structural materials for use in fusion reactors.

Two classes of properties are evaluated to establish the performance limits of materials – (1) the basic properties needed to identify the mechanisms that control the degradation of performance under irradiation, and (2) the engineering properties that contribute to the database needed for DEMO reactor design. This knowledge of the material behavior is combined with the available comprehensive modeling efforts to extrapolate behavior beyond the database to reactor operating conditions and to identify promising paths for compositional or microstructural modifications that will lead to improved material systems.

7.2 Accomplishments and Highlights

The collaborative testing program for fusion first wall and blanket structural materials (FSM) has completed seven phases, each of five-year terms, in the program starting in 1983. The current Phase VIII of this collaborative program (FSM-P8) started in April 2019.

In the last 10 years, HFIR target position experiments JP-28, -29, -30, and -31 completed irradiation, reaching DEMO-relevant goal maximum exposures of 80 and 20 dpa at the irradiation temperature from 300 to 500°C on Japanese RAFM steel F82H variations, including Ni-doped F82H to simulate transmutation formed He production under fusion neutron irradiation, and U.S. advanced nanostructured ferrite alloys. The companion HFIR target position rabbit capsules also achieve the goal fluences of 50 and 20 dpa on F82H variations at 300°C. The tensile properties after these high dose irradiations at a lower temperature (~300°C) show the largest hardening and loss of total elongation compared to the lower dose (<30dpa) results but did not show complete embrittlement. Fracture toughness of ~70dpa irradiated F82H, and its variation is the world's first toughness data of Reduced Activation Ferritic/Martensitic (RAFM) steel. It revealed that F82H MOD3, the toughness-improved version of F82H, shows it has better toughness, preserved even after irradiation. Results on irradiated 58Ni-doped F82H, which contained ~770 appm He, might indicate a potential detrimental He effect on fracture toughness.

Several rabbit capsules with SiC specimens have completed irradiation in HFIR to 40, 70, and 100 dpa, while other high fluence capsules continue irradiation in the reactor to target fluences up to 200 dpa. The results obtained to date indicate no evidence of irradiation-induced mechanical property degradation or progressive radiation damage in high purity SiC in stoichiometric and polycrystalline form. This indicates there is significant room for improvement in high dose radiation tolerance of the commercial SiC-based nanocrystalline fibers and pyrolytic carbon interphases used in the current generation nuclear grade SiC/SiC composites. These very high dose neutron irradiation campaigns for SiC ceramics and composites are unique to this DOE-QST HFIR collaboration, making it a world-leading program that is generating the data required in evaluating these materials for use in fusion power reactor in-vessel components.

Two HFIR removable beryllium (RB*) position experiments, capsules designed with instrumentation and sweep gas flow for temperature control, have completed irradiation. RB15J, which had a europium thermal neutron shield for neutron spectrum tailoring, achieved 6 dpa exposure of F82H, F82H weld joints, and B-doped F82H at 300 and 400°C. The results of specimen evaluation indicated that the tendency for localized deformation at the heat-affected zone (HAZ) of weldment became significant after irradiation, but that this tendency does not appear if the volume fraction of HAZ is near zero or very small. Irradiation creep was evaluated using pressurized creep tubes; and ^{10}B -doped F82H, which generated ~300 appm He, showed a slightly larger creep strain compared to that of ^{11}B -doped F82H, and the estimated swelling level expected from the formation of small helium bubbles in the ^{10}B -doped material is consistent with the difference measured in creep strain.

A shared HFIR irradiation experiment, the RB19J with a gadolinium thermal neutron shield, has completed irradiation and achieved a maximum of 2.5 dpa exposure on F82H alloy variations. The SiC temperature monitors indicated that most of the specimen were irradiated at a higher temperature than the design temperature, but the bottom section specimens indicated the smallest deviation. Those specimens will be tested in the near future.

A new program of collaborative HFIR irradiation and examination of fusion reactor structural materials for DEMO design activities (DDA) was started in April 2018, and Phase I of the collaborative program (DDA-P1) is now underway. The first campaign of HFIR rabbit capsule irradiation of Cu alloys, candidate structural material for divertors, was completed in 2020. The results will contribute to the expansion of the DEMO irradiation effects database.

During the period 2010 to 2019, 24 Japanese scientists visited ORNL for direct collaboration on post-irradiation experiments and to assist in preparing irradiation experiments in collaboration with U.S. scientists. In that same period 30 papers based on the collaborative work were published. The results and direction of this collaboration, including the personnel and technical exchanges, continue to be of value to both Japan and the U.S. and of interest and value to the international fusion community. Steady progress in improving material performance and in understanding the effects of the fusion environment on material properties can be seen throughout this long and productive collaboration.

Effect of High-Dose Neutron Irradiation on the F82H RAFM Steel

Category: HFIR

Name: T. Hirose, H. Tanigawa, H. Sakasegawa,
M. Ando, / Y. Katoh, X. Chen, J.W. Geringer, L. Tan,
B.K. Kim, K.G. Field, L.L. Snead

Affiliation: QST/ORNL

The reduced activation ferritic/martensitic (RAFM) steel F82H was irradiated up to 87 dpa at 573, 673 and 773 K in the High Flux Isotope Reactor (HFIR) at Oak Ridge National Laboratory, which took seven years to complete irradiation. The materials examined in this work are reduced activation ferritic/martensitic steel, F82H-IEA (0.1C-8Cr-2W-0.2V-0.04Ta) and F82H with additional tantalum added for toughness improvement, F82H-MOD3 (0.1C-8Cr-2W-0.2V-0.09Ta)¹⁾. Preliminary analysis of the passive thermometry demonstrated it was possible the irradiation temperature was lower than the design temperature, especially for specimen holders intended for 673 and 773 K²⁾.

Tensile tests of the irradiated miniature dog bone specimen, SS-J3, were conducted at the nominal irradiation temperatures³⁾. Tensile properties of F82H-MOD3 were comparable with those of F82H-IEA, and showed obvious irradiation hardening even above 673 K for all specimens. Most irradiated specimens had poor elongation less than 10 % at the test temperature.

The dose dependence of hardening as the 0.2% proof stress and total elongation are given in Figure 1 and Figure 2, respectively. These figures include previous results from material irradiated in the Fast Breeder Reactors (FBRs) Fast Flux Test Facility (FFTF)⁴⁾ and BOR-60⁵⁾. Irradiation hardening at 573 K asymptotically increases to 500 MPa, and seems to be consistent with the previous work in FBRs. In contrast, the hardening gradually increased with increasing dose for HFIR irradiation at temperature above 663 K where softening was observed in FBRs experiments. It is noted that F82H irradiated in the FFTF tended to show increased hardening to doses from 40 to 60 dpa. Therefore, hardening at higher temperature might have an incubation dose for hardening to start.

As shown in Figure 2, the dose dependence of ductility changes seems to be strongly affected by specimen geometry. Specimen with lower aspect ratio demonstrated a tendency for saturation of total elongation around 7%. In contrast, modified specimens with larger aspect ratio, SS-J3, successfully evaluated a gradual decrease of total elongation. We did not see

any obvious tendency for saturation in loss of ductility in this work.

Irradiation conditions in HFIR and FFTF experiments are different in damage rate, but normalized by megawatt day (MWD) are within a factor of two. Moreover, the irradiation periods are too short to demonstrate mechanical property changes due to thermal aging. Therefore, these facts imply that hardening behavior is affected by the difference in the irradiation conditions.

Calculations show that HFIR introduces 30 times larger transmutation of tungsten than does FFTF. This is due to the three order of magnitude difference in neutron flux near neutron energy of 20 eV where tungsten has a giant resonance⁶⁾. Although it is reported that osmium and rhenium have no significant effects in martensitic steel, precipitates such as Laves phase include these elements and have strong impact on the mechanical properties⁷⁾. This ductility loss at 673 and 773 K should be monitored as well as embrittlement since these properties might limit the use of these steels.

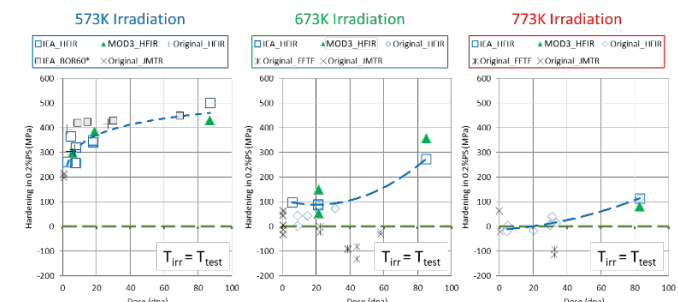


Figure 1. Dose dependence of irradiation hardening in F82H

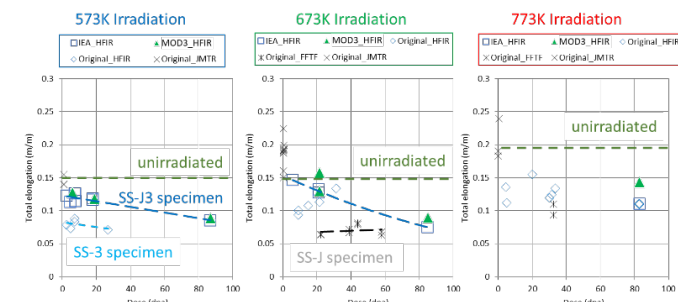


Figure 2. Dose dependence of irradiation induced ductility loss in F82H

¹⁾ K. Shiba, H. Tanigawa, T. Hirose, T. Nakata, Fusion Sci. Tech., 62 (2012) 145.

²⁾ H. Sakasegawa, H. Tanigawa et al., DOE/ER-0313 Semi-Annual Progress Reports, 59 (2015) 22

³⁾ T. Hirose, H. Tanigawa et al., DOE/ER-0313 Semi-Annual Progress Reports, 62 (2017) 8

⁴⁾ Y. Kohno, A. Kohyama, et al., J. Nucl. Mater. 271&272 (1999) 145

⁵⁾ E. Gaganidze, J. Aktaa, Fusion Eng. Des. 88 (2013) 118

⁶⁾ R.E. Stoller and L.R. Greenwood, J. Nucl. Mater. 271-272 (1999) 57

⁷⁾ R.L. Klueh, D.J. Alexander, M.A. Sokolov, J. Nucl. Mater. 279 (2000) 91

Fracture Toughness of F82H Irradiated in HFIR-JP28/JP29

Category: HFIR

Name: X. Chen

Affiliation: ORNL

F82H is the reference reduced-activation ferritic-martensitic (RAFM) steel in Japan as the candidate structural material for fusion blanket applications. It has favorable properties for fusion applications such as lower radioactivity, superior swelling resistance, good thermal conductivity, and sufficient fracture toughness in the normalized and tempered condition. However, the harsh environment of a fusion reactor, such as neutron irradiation and He/H damage, can result in significant degradation of materials fracture toughness. Therefore, understanding the fracture toughness behavior of F82H in the fusion environment is critical to ensure the long-term safe operation of the fusion reactor. To address the effects of high dose irradiation and He on fracture toughness of F82H, standard and Ni-doped F82H were irradiated in the JP28 and JP29 irradiation campaigns at the High Flux Isotope Reactor (HFIR) of Oak Ridge National Laboratory (ORNL). The irradiation covered an irradiation temperature range of 300–500°C with the peak dose up to ~70 displacements per atom (dpa). This report presents the post irradiation examination (PIE) of F82H fracture toughness after 300°C irradiation.

The irradiation conditions are summarized in Table 1. Four variants of F82H, including F82H IEA, F82H Mod3, F82H doped with 1.4% ^{58}Ni , and F82H doped with 1.4% ^{60}Ni , were irradiated. Vickers microhardness and Master Curve fracture toughness testing was performed on the M3CVN miniature multi-notch bend bar specimens machined in the T-S orientation of each material.

Table 1. Irradiation conditions of F82H

Materials	Target irradiation temperature (°C)	SiC thermometry temperature (°C)	Dose (dpa)
F82H IEA	300	341	68
F82H Mod3	300	341	68
F82H+1.4% ^{58}Ni	300	307	70
F82H+1.4% ^{60}Ni	300	307	70

The post-irradiation hardness followed the order of F82H Mod3 < F82H IEA < F82H+1.4% ^{60}Ni < F82H+1.4% ^{58}Ni as shown in Figure 1. The hardness results were in general agreement with the upper shift in the Master Curve transition temperature T_0 shown in Figure 2 with an exception that F82H+1.4% ^{60}Ni had less embrittlement than what would have been expected from hardness measurements. Nonetheless, no detrimental effect of 1.4% ^{60}Ni doping on F82H fracture toughness was observed after neutron irradiation. F82H Mod3 was developed as a toughness-improved F82H and its better toughness was preserved even after irradiation. Significant

embrittlement in irradiated F82H+1.4% ^{58}Ni which contained ~770 appm transmutation He may indicate a potential detrimental He effect on fracture toughness, but further study is needed to confirm this observation.

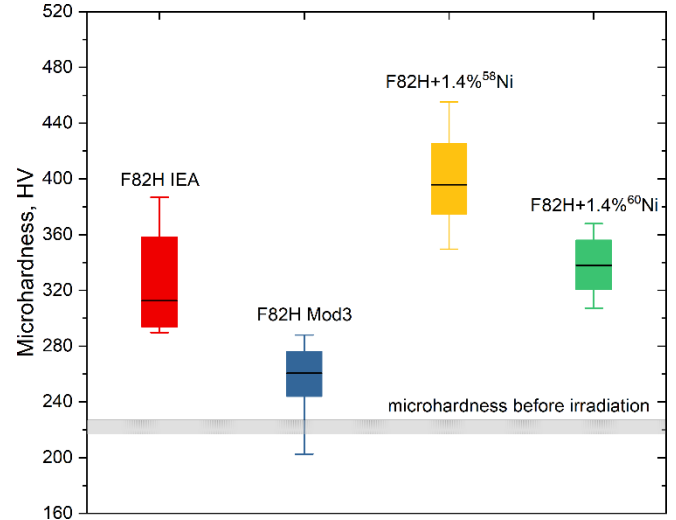


Figure 1. Vickers microhardness of four F82H steels after irradiation. The median, \pm one standard deviation, and min-max hardness measurements are shown as the horizontal line, the box, and the whisker, respectively.

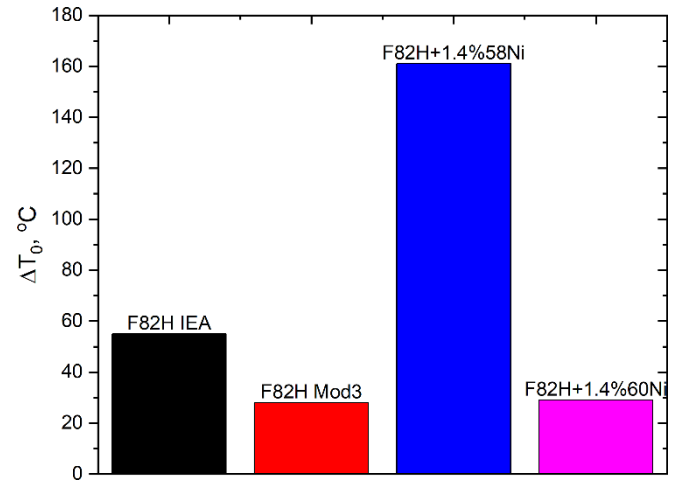


Figure 2. Upper shift in the Master Curve transition temperature T_0 of four F82H steels after irradiation.

The JP28 and JP29 irradiation campaigns for F82H steels represent the highest dose irradiation on such materials to date. Fracture toughness PIE is critical for addressing burning questions for the irradiation embrittlement behavior of F82H, e.g., the high dose embrittlement saturation behavior and the He effect on fracture toughness.

Irradiation Response of Weldments and HIP Joints in RAFM Steel, F82H

Category: HFIR

Name: T. Hirose, M. Ando, H. Tanigawa, K. Shiba/
M.A. Sokolov, R.E. Stoller / G.R. Odette
Affiliation: QST/ ORNL / UCSB

The fusion breeding blanket is an in-vessel component located around the fusion plasma that will be exposed to high heat load and neutron flux. In the Japanese reference design for DEMO, the first wall (FW) of the blanket, which faces the fusion plasma, has built-in cooling channels made by hot-isostatic-pressing (HIP). The FW is welded to the side walls (SWs) and back wall to form a box structure of the blanket. Therefore, the joints are exposed to a high neutron flux and it is necessary to investigate their response to irradiation. The objective of this work is to investigate irradiation response of the F82H joints. These sample joints were prepared by tungsten-inert-gas (TIG) welding, electron beam (EB) welding, and HIP¹⁾.

The weld joints investigated in this work were produced from plate of 15 mm thick F82H-IEA (Fe-8Cr-2W-0.2V-0.04Ta-0.1C LN) which was hot-rolled at 1473 K and then normalized at 1313 K for 0.63 h and tempered at 1023 K for 1 h. TIG and EB weldments were annealed at 993 K for 1 h as a post-weld heat treatment (PWHT). The chemical compositions of F82H TIG weld wire was Fe-7.4Cr-2W-0.22V-0.03Ta-0.07C-LN. The specimens tested were SS-J3 sheet tensile specimens with gauge section 5 x 0.76 x 1.2 mm. In the case of the TIG welded joints the fine-grained HAZ (FG-HAZ) is defined as the HAZ heated above the AC₃ transformation temperature during the TIG welding process. Over-tempered HAZ (OT-HAZ) is defined as the zone heated below the AC₃ temperature. The HIP joint was prepared from 25 mm-thick F82H-IEA plates. HIP was conducted at 1373 K with 150 MPa for 2h using a KOBELCO O2-Dr. HIP. The HIP joint was heat treated at 1233 K for 0.5 h and 1023 K for 1 h to optimize the microstructure²⁾.

Neutron irradiation was conducted in the High Flux Isotope Reactor (HFIR) at the Oak Ridge National Laboratory (ORNL). The specimens were irradiated in liquid lithium in the instrumented capsule MFE-RB-15J, which used a europium thermal neutron shield for neutron spectrum tailoring. The nominal irradiation conditions were 3 and 4.5 dpa at 573 K³⁾. All post irradiation tensile and Charpy impact tests, were conducted in the Irradiated Materials Examination and Testing (IMET) hot cell facility at ORNL

Post irradiation tensile tests conducted at the irradiation temperature indicated that irradiation hardening in TIG weldment and base metal was greater than 300 MPa. However, the TIG weld joint, which included a HAZ region, exhibited

about half that of the F82H-IEA (equivalent to base metal: BM) after irradiation at 573 K (Figure 1). It was also revealed that the deformation tended to be localized in the HAZ section and this tendency was enhanced after irradiation. This indicates that the neutron irradiation significantly decreases the strength of the HAZ, because the HAZ is the weakest part of the joint even before irradiation.

On the other hand, the irradiation response of the HIP joint was similar to that of the base metal. Post tensile properties of the HIP joint were almost equivalent to those of base metal. Charpy impact test indicated that there was no significant drop of upper shelf impact absorbed energy in fracture behavior of the HIP interface, even though the irradiation caused embrittlement of the matrix material.

These results suggested that the weld joints could be in danger of local deformation at the HAZ, which could be found in the joint between the FW and the SWs. Thus, it would be better if the weld joint can be shifted as far away as possible from the plasma side to reduce the impact of neutron irradiation. HIP joints, which will be located in the FW, could be expected not to increase the possibility of failure, as long as the initial soundness of HIP joints can be guaranteed.

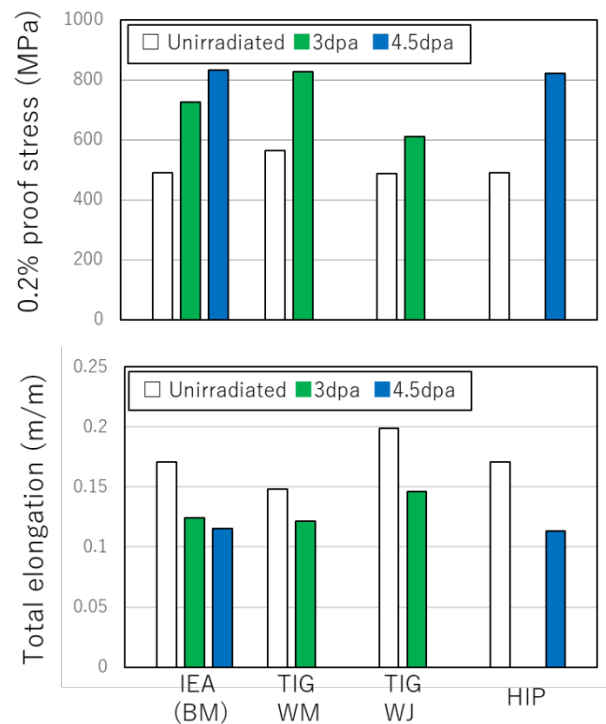


Figure 1. Tensile properties of F82H-IEA base metal and joints irradiated at 573K. (Top) 0.2% proof stress, and (lower) total elongation

¹⁾ T. Hirose *et al.*, J. Nucl. Mater. 442 (2013) S557

²⁾ T. Hirose *et al.*, J. Nucl. Mater. 329-333 (2004) 324

³⁾ T. Hirose *et al.*, DOE/ER-0313 46 (2009) 72-78

Irradiation Creep of B-doped F82H Irradiated in the HFIR RB15J Capsule

Category: HFIR

Name: M. Ando, T. Nozawa, T. Hirose, H. Tanigawa /

Y. Katoh

Affiliation: QST/ ORNL

Reduced activation ferritic/martensitic steels (RAFM) are the most promising candidates for blanket structural materials of fusion reactors. Irradiation creep has been recognized as one of the important properties for engineering data required for the blanket structural design. Specifically, it is anticipated that irradiation creep of RAFM at lower temperatures (<573K) could be significant for fusion reactors. Furthermore, some transmutation products (mainly helium atoms) will also be produced by high-energy neutrons in the first wall of a fusion reactor. In this research, irradiation creep data at 573-673K up to 6 dpa was successfully obtained using a liquid metal filled capsule, and the effect of helium (~300 appm) on irradiation creep behavior was examined by comparing pressurized creep tubes (PCT) of F82H and B-doped F82H.

The materials studied were F82H IEA heat (8Cr-2WVTa) and boron-doped F82H steels. The ¹⁰B-doped F82H was provided to investigate the effect of helium on mechanical properties. In this experiment, two types of boron-doped F82H were prepared by a co-doping with boron and nitrogen in F82H steel¹⁾. The ¹⁰BN-F82H produced helium atoms during irradiation by the reaction ¹⁰B (n, α) ⁷Li.; the ¹¹BN-F82H did not produce helium. The tube specimens had dimensions of 4.5 mm outside diameter and 25.4 mm length with a 0.2 mm wall thickness as shown in Figure 1.

End caps were electron beam welded to the tube segments, and the specimens were pressurized with high purity helium to obtain the desired hoop stresses at the irradiation temperatures. The hoop stresses ranged from 0 to 380 MPa at the irradiation temperature. Irradiation was performed in the HFIR to atomic displacement levels up to 5.8 dpa in the removable beryllium (RB) position. This capsule was equipped with a thermal neutron shield. As a result, ¹⁰B was slowly transmuted to helium during irradiation. Nominal irradiation temperatures were 573 and 673K. Each tube was measured using a laser profilometer system in the ORNL hot cell. Irradiation creep strain was calculated from tube diameter measured before and after irradiation.

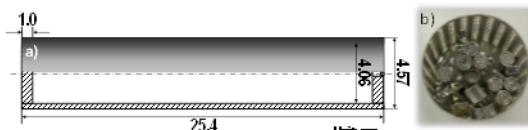


Figure 1. a) Geometry of the PCT specimen, b) PCT specimens inside RB-15J specimen holder basket.

Figure 2a shows the relationship between the effective creep strain (ϵ_{eff}) and the effective stress (σ_{eff}) for F82H IEA and BN-F82H irradiated at 573K. The F82H IEA and BN-F82H exhibit similar irradiation creep behavior at 573K up to ~4 dpa. The irradiation creep strain in F82H was nearly linearly dependent on the effective stress for stresses up to ~260 MPa. However, the creep strain becomes nonlinear at higher stress levels. Figure 2b shows the results for 673K irradiation. In this case, the irradiation creep strain of F82H is linear below ~170 MPa. The effect of helium on irradiation creep of F82H was also examined by comparing ¹⁰BN and ¹¹BN-F82H. Helium production during irradiation was estimated to be about 300 appm and its production rate was controlled in this thermal neutron shielded capsule. The creep strain of ¹⁰BN-F82H was similar to that of F82H IEA at each effective stress level except for ~290 MPa at 573K irradiation. For 673K irradiation, the creep strain of some ¹⁰BN-F82H tubes was larger than that of ¹¹BN-F82H tubes. It is suggested that a limited amount of swelling may be induced in ¹⁰BN-F82H because of small helium bubbles arising from the production of helium by the ¹⁰B(n, α) ⁷Li reaction. An estimated 0.06% swelling was obtained based on the volume increase of tube. This result is consistent with the swelling expected from formation of small helium bubbles.

In this research, the effect of helium on irradiation creep behavior up to 300 appm, ~6 dpa was examined using F82H and BN-doped F82H in the HFIR RB capsule. At 573K and 4.2 dpa, the irradiation creep behavior of F82H and ¹⁰BN-doped F82H was similar. On the other hand, at 673K, and 5.8 dpa, the irradiation hardening and creep strain in ¹⁰BN-doped F82H was slightly higher. However, they did not cause a large difference in irradiation creep behavior.

Recently, some new rabbit capsule creep experiments using PCT specimens are being developed at ORNL²⁾. They will contribute to the difficult task of obtaining irradiation creep data at higher dose levels.

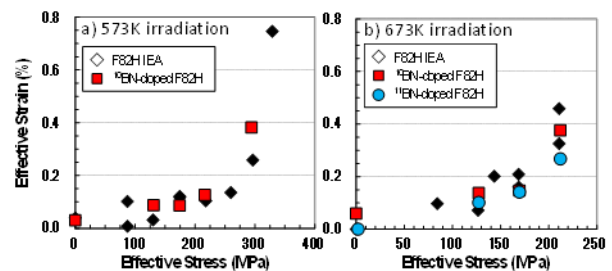


Figure 2. Summary of irradiation creep behavior for F82H. a) 573K irradiation, b) 673K irradiation.

¹⁾ E. Wakai et al., et al., J. Nucl. Mater., 398, 64-67 (2010).

²⁾ A. A. Campbell et al., DOE/ER-0313/67 (2019) 147-153.

Impact of Inclusions on Fracture of Irradiated RAFM Steels

Category: HFIR

Name: H. Tanigawa, M. Ando, T. Hirose, T. Kato, H. Sakasegawa / N. Okubo / Y. Katoh
Affiliation: QST / JAEA / ORNL

Inclusions in steels, mostly oxides or sulfide formed during melting, are expected to have no significant impact on most mechanical properties as long as inclusions are controlled to low number density and do not agglomerate in a narrow region. This is because steels have enough plasticity and work-hardenability to blunt any cracks formed around inclusions and prevent further crack propagation. On the other hand, it is well known that those impacts become significant in high strength steels or high yield-tensile ratio (YR) steel. In high YR steel, the fatigue properties are sensitive to inclusions, but the tensile fracture process is also affected by the inclusions.

The reduced activation ferritic/martensitic (RAFM) F82H (Fe-8Cr-2W, V, Ta), is a relatively high YR steel ($YR \sim 0.85$), developed with an emphasis on high-temperature properties. Significant issues for RAFM steels are irradiation-induced hardening, loss of uniform elongation, and embrittlement observed after irradiation at low irradiation temperature, where YR becomes about 1 as a consequence. This suggests that the impact of inclusions on the fracture process could become significant after irradiation. This study investigates these possible impacts of inclusion on the fracture process through fractography of mechanical-tested F82H.

Typical inclusions observed in F82H were Al_2O_3 , Ta_2O_5 , MnS, and inclusion a mix of these 3 types. It was reported that Ta_2O_5 , tends to form a large composite oxide with Al_2O_3 and tend to agglomerate at mid positions of plates, if the steel was fabricated with insufficient deoxidation¹⁾. For unirradiated F82H, those inclusions affect the Charpy impact properties, but have no significant effect on tensile properties.

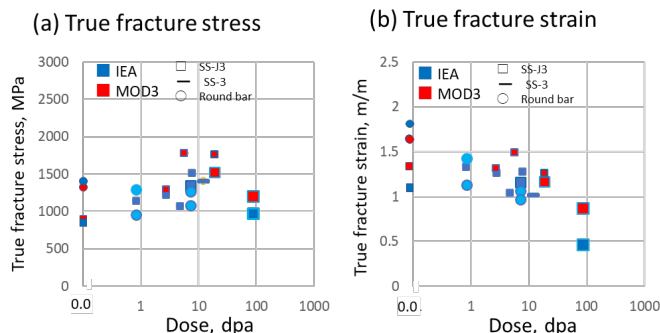


Figure 1. Irradiation dose dependence of (a) true fracture stress and (b) true fracture strain of irradiated F82H-IEA and F82H-MOD3

Tensile properties were evaluated at irradiated temperatures on F82H-IEA (Fe-8Cr-2W-0.2V-0.04Ta-0.1C LN) and F82H-MOD3 (Fe-8Cr-2W-0.2V-0.1Ta-0.1C LN) irradiated up to 84 dpa at 300°C²⁾. In these F82H variations, the large inclusions, typically composite oxides, tend to be observed in IEA, but not in MOD3. It was observed that the yield stress kept increasing, and the total elongation decreasing as the irradiation dose increase in both F82H-IEA and MOD3. The true fracture stress and strain were evaluated based on the reduction in area data, analyzed through fracture surface observation. The data suggested that the true fracture stress was not significantly affected by irradiation dose, but the true fracture strain degraded as the dose increased, and this tendency was more significant in F82H-IEA (Figure 1).

Fracture surface details were analyzed by scanning electron microscope (SEM) followed by 3D surface generation using three tilted images (Figure 2), in order to understand the mechanisms that caused the different true fracture strain degradation. These details indicated that shallower and smaller equiaxed dimples were observed on the fracture surface of heavily irradiated MOD3, but a few deep dimples with a large inclusion at the bottom were observed in irradiated F82H-IEA. These morphologies suggest that the extensive degradation of true fracture strain might be caused by the presence of larger inclusions observed in F82H-IEA, while those of MOD3 were not comparably significant.

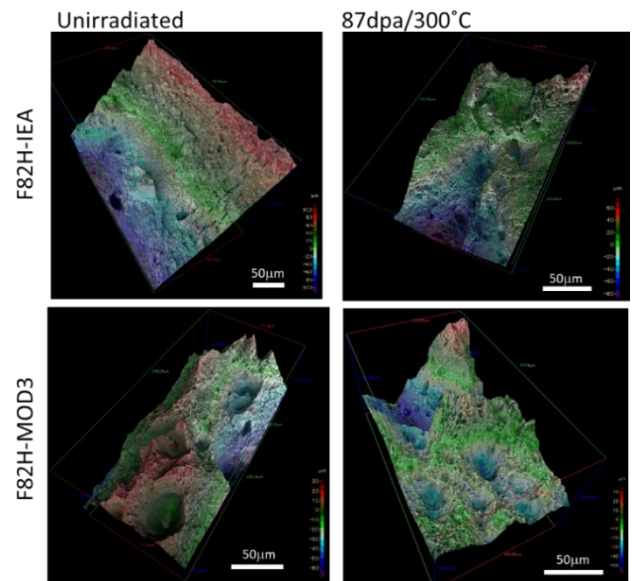


Figure 2. Generated 3D tensile fracture surfaces of unirradiated and irradiated F82H-IEA and MOD3

¹⁾H. Tanigawa, H. Sakasegawa, T. Hirose, Fusion Eng. & Des., 88 (2013) 2611

²⁾H. Tanigawa, M. Ando *et al.*, Presented in ICFRM-17 Aachen, Germany, 11-16 October 2015

Microstructures of RAFM Steels Irradiated to 72 dpa

Category: HFIR

Name: K. Wang*, C.M. Parish, K.G. Field, L. Tan,

Y. Katoh, H. Tanigawa^{**}

Affiliation: ORNL (*: Now at Alfred University), **QST

A reduced activation ferritic/martensitic steel, Eurofer97, was neutron irradiated up to 72 dpa near 300°C in the High Flux Isotope Reactor (HFIR). Electron microscopy was applied to investigate the radiation-induced segregation and phase instability that occurred during the neutron irradiation. Amorphization was observed in M₂₃C₆ carbides. Cr-rich clusters were seen within the matrix, near the lath boundaries and close to the M₂₃C₆ carbides. Cr enrichment and Fe depletion were detected at both prior austenite grain boundaries and lath boundaries, but differed in segregation magnitude. In addition, the enrichment of Ni, the depletion of V, and tiny cavities (presumably helium bubbles) are also found at lath boundaries. This work interrogates the evolution of microstructures during neutron irradiation, which provides detailed understanding of the microstructural aspects controlling the mechanical integrity of Eurofer97 under high-dose neutron damage.

The material used in this study was a European reduced activation ferritic/martensitic (RAF/M) steel, Eurofer97. The as-received material had a tempered martensitic steel structure, with typical lath microstructures arranged in packets within the prior austenitic grains (PAGs). The specimens were irradiated in the JP28 & 29 full-length target capsules in HFIR. The irradiation temperature was designed to be 300 °C, which was estimated to be ≈284°C based on SiC temperature monitors. The total irradiation time was 58 HFIR cycles (26,824 h), in calendar years 2005-2013. The estimated neutron fluence was $9.4 \times 10^{22} \text{ n} \cdot \text{cm}^{-2}$ ($E > 0.1 \text{ MeV}$) or ≈72 dpa with the neutron flux of $9.7 \times 10^{14} \text{ n} \cdot \text{cm}^{-2} \text{s}^{-1}$ (equivalent to $7.5 \times 10^{-7} \text{ dpa} \cdot \text{s}^{-1}$).

The unirradiated archive material (Figure 1) consists of a typical F/M microstructure. Although the 72 dpa microstructure (Figure 2) is overall similar, important differences are seen. Most significantly, large amounts of Os (a W neutron-transmutation product) are visible in the Cr-W carbides after 72 dpa but not in the archive material.

Irradiation caused significant segregation along boundaries. Both prior-austenite grain (PAG) and lath boundaries showed Fe depletion and Cr enrichment. Ni enrichment was also observed, despite very low bulk Ni content.

Further, the M₂₃C₆ precipitates were observed to have amorphized by 72 dpa, and small clusters of Cr were observed to have formed in halos around the M₂₃C₆ particles, perhaps due to a combination of diffusional kinetics and ballistic dissolution over the time to accumulate 72 dpa. Matrix Cr-rich clusters, possibly α', were also observed. Tiny cavities, presumably helium bubbles, sit at the lath boundary.

Overall, this work showed matrix phase instability and elemental segregation at the boundaries in Eurofer97 after

neutron irradiation up to 72 dpa at 300 °C. PAG boundaries and lath boundaries show large elemental segregation.

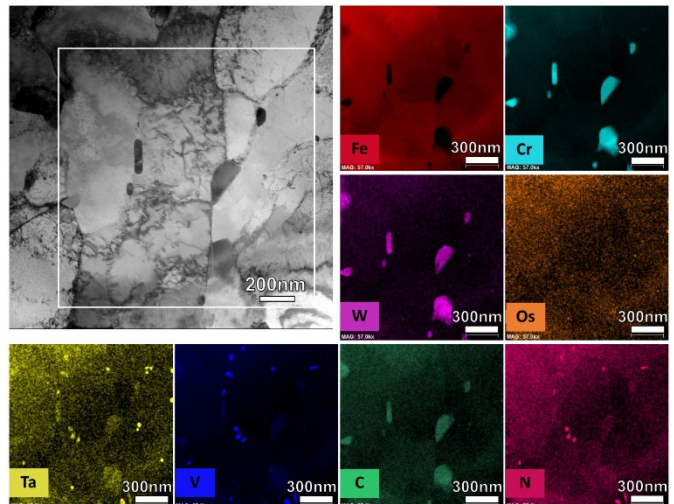


Figure 1. Bright field (BF) TEM image of typical martensite structure of unirradiated Eurofer97 and the corresponding STEM-EDS elemental mapping results of the white rectangle region in BF TEM image. 3×3 pixel smoothing applied.

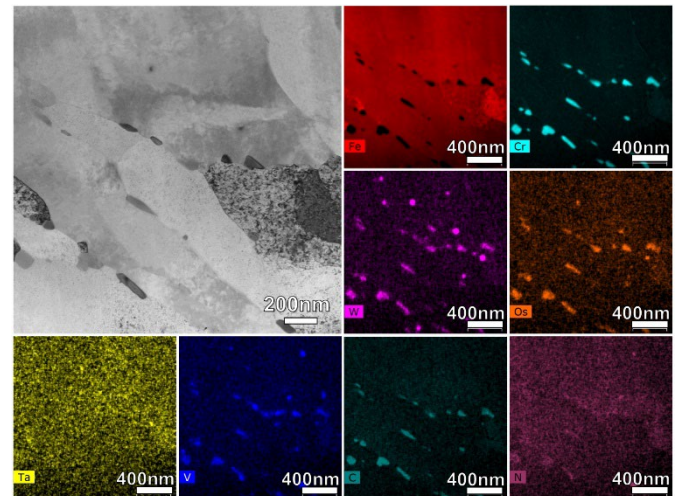


Figure 2. Bright field (BF) TEM image of 72 dpa irradiated Eurofer97 and the corresponding STEM-EDS elemental mapping results of BF TEM image. 3×3 pixel smoothing applied.

High Dose Neutron Irradiation of Silicon Carbide Composites

Category: HFIR

Name: T. Koyanagi, Y. Katoh/T. Nozawa

Affiliation: ORNL/QST

For the development of silicon carbide (SiC) fiber reinforced SiC matrix (SiC/SiC) composites for fusion reactor structural applications, degradation of material properties due to intense neutron irradiation is a critical feasibility issue. The objective of this task is to obtain better understanding of the effects of high neutron fluence irradiation on the thermo-mechanical properties and microstructures.

This collaboration has achieved the milestone of neutron irradiation up to ~ 100 displacements per atom (dpa) with an equibalance of $1 \text{ dpa} = 1 \times 10^{25} \text{ n/m}^2$ ($E > 0.1 \text{ MeV}$). Neutron irradiation was conducted in the HFIR at ORNL. The total duration of the irradiation was 1000–1150 days. The material investigated was chemical vapor infiltrated SiC/SiC with Hi-Nicalon Type-S (HNS) fiber coated with a multi-layer pyrolytic carbon (PyC)/SiC interphase. Key physical and mechanical properties investigated included irradiation-induced swelling, thermal conductivity, proportional limit stress, and ultimate strength. For these properties, strength reductions predominantly determine the limitations of the materials at high neutron doses, whereas positive results have been reported for the other properties.

The length change of the specimens found that the SiC/SiC composites were dimensionally very stable at high neutron doses; swelling of SiC/SiC composites saturated at nominal neutron damage of ~ 1 dpa at elevated temperatures. This saturation behavior has been confirmed at up to 100 dpa at 300 and 600°C and up to 70 dpa at 800°C. Similar to swelling, changes in the thermal conductivity saturate at ~ 1 dpa. Although reduction of the thermal conductivity following irradiation is significant at low irradiation temperatures, the stable thermal conductivity at high doses is favorable for fusion applications.

Degradation of the mechanical properties at high neutron doses was irradiation-temperature dependent. The degradation of proportional limit stress and ultimate flexural strength was moderate at an irradiation temperature of 800°C. However, the proportional limit stress and ultimate flexural strength were significantly degraded due to irradiation at lower temperatures as shown in Figure 1. In case of the irradiation at 320°C, the quasi-ductile fracture behavior of the unirradiated composite became brittle after irradiation, which was explained by loss of functionality of the fiber/matrix interface associated with disappearance of interphase by irradiation (Figure 2). The specimens irradiated at 630°C showed increased apparent failure strain because of the fiber/matrix interphase weakened by irradiation-induced partial debonding based on fractography. The fractography also suggested a loss of the fiber strength irradiated at 320°C.

In summary, this study provided critical experimental data on the effects of high-dose neutron irradiation on the composite properties. Improvement of the irradiation resistance has been pursued under this collaboration.

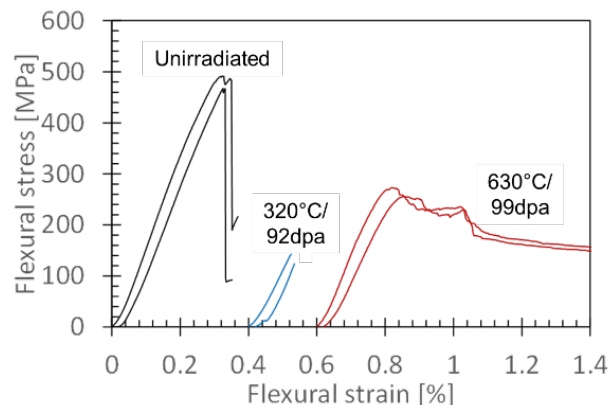


Figure 1. Flexural behavior of unirradiated and irradiated SiC/SiC composites.

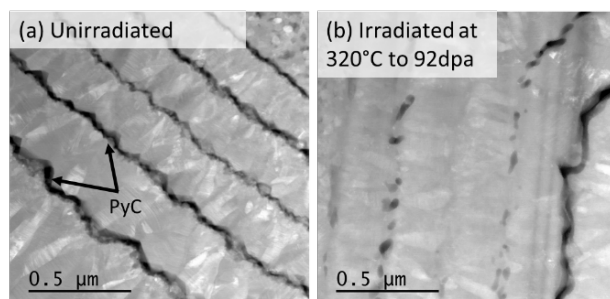


Figure 2. STEM-HAADF micrographs of PyC/SiC multi-layer interphase: (a) unirradiated and (b) irradiated.

HFIR Irradiation Campaigns in Support of the DOE/QST Fusion Materials Collaboration

Category: HFIR

Name: Y. Katoh, J.W. Geringer / H. Tanigawa, T. Nozawa
Affiliation: ORNL/QST

The Project Arrangement between JAERI, JAEA, now QST, MEXT of Japan and U.S. DOE, under the Cooperation in Research and Development in Energy and Related Fields, has been in effect for more than 37 years. The basis of this collaboration is the shared use of irradiation experiments in ORNL mixed spectrum fission reactors, first the ORR, then the HFIR reactor.

The objective of this collaboration is to design, conduct and evaluate joint irradiation experiments that partially simulate DT fusion irradiation conditions for the purpose of investigating the irradiation response of Japanese and U.S. structural and special purpose materials. The experiments target high levels of atomic displacement and helium content in order to establish the database on the properties and behavior of such materials and to evaluate their performance for the use in future fusion reactors.

During the last decade, HFIR has achieved 6 to 7 operating cycles per year, each lasting approximately 24 days at an operating power of 85 MW. It has remained operational and available for most of the period, except for the nearly year-long shutdown period that started in November 2018 and ended in October 2019, followed by another 6-month downtime period that started in August 2020 and ended February 2021, both due to issues related to fuel quality.

There have been a large number of collaboration irradiation campaigns, mostly exclusively for DOE/JAEA (now QST). The few exceptions include the RB-19J that was a three-party collaboration including the PHENIX Project. Table 1 lists the current ongoing campaigns supporting this collaboration, with 18 rabbit capsules now in reactor. Several ongoing PIE activities continue generating materials data and developing technology using the specimens from these campaigns.

The future plan for HFIR is to continue operation at least until 2035, when the potential renovations planned include replacing the reactor pressure vessel and converting to low enriched uranium (LEU). In the near-term future, HFIR plans replacement of the permanent beryllium reflector. Given the current schedule, this outage is planned for early 2024.

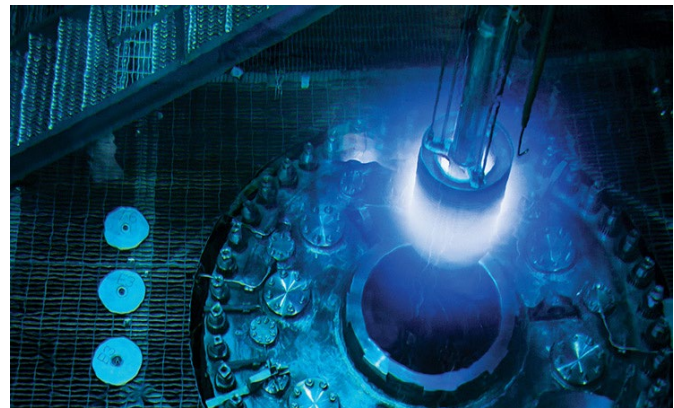


Figure 1 HFIR top plate and fuel element shown during a refueling operation in 2015. (credit G. Martin/ORNL)

Table 1. Irradiation campaigns conducted in the HFIR reactor in support of the DOE-QST collaboration on fusion materials research and development.

Campaign	Years	Program	Facility	Material	Temperature (°C)	Max. Fluence ($\times 10^{25}$ n/m ² , E>0.1MeV)
JP-26/27	2004-2008	DOE/JAEA	Target	RAFMS	300/400	~20
JP-28/29	2005-2013	DOE/JAEA	Target	RAFMS	300/400/500	~80
RB-15J	2008-2009	DOE/JAEA	RB*	RAFMS	300/400	~6
JP-30/31	2011-2013	DOE/JAEA	Target	RAFMS	300/400/650	~20
RB-19J	2016	DOE/NIFS/JAEA	RB*	RAFMS, W	300-1200	~4
F8 Rabbits	2009-2013	DOE/JAEA	Target	RAFMS	300	~60
F11 Rabbits	2011-2013	DOE/JAEA	Target	RAFMS	300	~25
JCR11 Rabbits	2012-	DOE/JAEA	Target	SiC	950	10/30/50/100/200
J12 Rabbits	2013	DOE/JAEA	Target	RAFMS	300	1.5/6
F13 Rabbits	2014-2018	DOE/JAEA	Target	RAFMS	300	15/30
SCF Rabbits	2014-	DOE/JAEA	Target	SiC	600/950	10/30/100/200
FHC Rabbits	2018	DOE/QST	Target	RAFMS	300	~5
FMP Rabbits	2020	DOE/QST	Target	Cu	100 -350	5
FH Rabbits	2020-2021	DOE/QST	Target	RAFM	300	5

